

Dopaminergic enhancement of cognition in old age

Rumana Chowdhury, BMedSci MBBS MRCP

Institute of Cognitive Neuroscience,

University College London

Dissertation submitted for the degree of Doctor of Philosophy (PhD) of

University College London

December 2012

Primary supervisor: Professor Emrah Düzel

Secondary supervisor: Professor Raymond J Dolan

Declaration

I, Rumana Chowdhury, confirm that the work presented in this thesis is my own.

Where information has been derived from other sources, I confirm that this has been indicated in the thesis.

Signature:

Abstract

As humans age, the brain undergoes many changes. This includes loss of the neurotransmitter dopamine, which forms a bridging link between age and the ensuing changes in cognition. However many questions about the precise nature of this relationship with regards to brain structure and function remain unanswered. These questions are important given our expanding aging population, and the answers may help the discovery of new therapeutic interventions for age-related impairments as well as identify mechanisms to promote successful aging. Old age also provides a model for understanding the role of dopamine in many fundamental human behaviours.

The aim of my research was to use a multimodal approach to explore the contribution of dopamine to learning and memory in healthy older age. In this thesis I present four studies in which I used a combination of behavioural testing, pharmacological manipulation, structural and functional magnetic resonance imaging in older adults. I show that dopamine boosts delayed episodic memory in a non-linear dose-dependent manner. Using functional MRI, I show this effect is mediated through consolidation rather than encoding by the hippocampus. In two further imaging studies conducted to explore the role of dopamine in reward-based learning, I show that the flexibility of learning depends on the structural integrity of the substantia nigra/ventral tegmental area (the origin of dopamine projections) and that pharmacological enhancement of dopamine levels can remediate abnormal reward processing in the ventral striatum. Individual differences in neural activity associated with reward prediction also relate to anatomical nigro-striatal connectivity, identified using

diffusion tensor imaging. Finally, I show that in old age, valence influences decision-making in relation to ones own beliefs about the future, mediated by volume of the anterior cingulate cortex. I conclude this thesis with a brief discussion of the implications of these findings, study limitations and potential future studies.

Acknowledgments

I am grateful to both my primary supervisor Emrah Düzel and second supervisor Ray Dolan; it has been a true privilege to work with them both. Emrah has been a constant source of inspiration and remains the kind of scientist I aspire to be – a brilliant mind coupled with kindness and a healthy dash of good humour. Thanks to Ray for his generous support, for helping me to expand my horizons during my research years and get some welcome fresh air outside of the office.

Next my thanks go to my fantastic partner-in-crime Marc Guitart-Masip, whose scientific rigueur I have the utmost respect for. With Marc I have laughed until I've cried on many, many occasions. Long may our friendship (unintelligible to the outside world) continue! I would also like to thank FILm club co-creator Christian Lambert, who has been a cherished source of knowledge, code and entertainment over the past years. Many others, too many to mention, have helped me along the way, including: Tamara Shiner, Nico Bunzeck, John Ashburner, Peter Dayan, Antoine Lutti, Ged Ridgeway, Nik Weiskopf, Karl Friston, Aidan Horner, Rosalyn Moran, Nick Wright, Anna Jafarpour, Tali Sharot, my students, and the support staff at the ICN and the FIL. Thanks also to all the volunteers who took part in my studies for showing me the brighter side of growing older.

I would like to thank my wonderful mother and father to whom I dedicate this work and the rest of my family for their never-ending support. Most of all, I'd like to thank my husband Adam Wagstaff who has accompanied me on the rollercoaster ride of research. Without his love, understanding and hot dinners, this work would not have been accomplished.

Contributions

The work in this thesis is entirely my own unless otherwise indicated. I carried out the data collection and behavioural and imaging analysis for all studies. My supervisor Professor Emrah Düzel has guided me on every study presented here and both Professors Düzel and Dolan have overseen my work.

The task in Chapter 4 was designed by Emrah Düzel, Nico Bunzeck and myself. The experimental tasks in Chapters 5 and 6 were designed by Marc Guitart-Masip and Peter Dayan, the former in collaboration with myself. The task in Chapter 7 was designed by Tali Sharot and Christoph Korn and modified by myself to be applicable to an elderly population. The ideas for the analysis of diffusion tensor imaging data were my own and implemented using methods created partly by Christian Lambert. The analysis of modelling data in Chapter 5 was performed in collaboration with Marc Guitart-Masip and Peter Dayan.

My students Jasmine Medhora and Laura Sasse assisted with data collection for the studies in Chapters 4 & 5 and used the behavioural data from Chapter 4 for their BSc and Masters dissertations respectively. My students Thomas Wolfe and Elin van Duin assisted with data collection for the study in Chapter 7 and Thomas used the behavioural data for his BSc thesis.

I was awarded a Wellcome Trust clinical research fellowship which has funded the work in this thesis.

Publications arising from this work

Chapter 4 has been published in the Journal of Neuroscience (Chowdhury et al., 2012) and has received commentary in the same journal and also Nature Reviews Neuroscience (Lewis, 2012). Chapters 5, 6 and 7 are under review for publication.

Table of Contents

Chapter 1	18
Introduction	18
Chapter 2	20
Literature Review	20
2.1. Dopamine	20
2.1.1 Anatomy of dopamine	21
2.1.1.1 Regions and pathways	21
2.1.1.2 Receptors and firing	23
2.1.1.3 Functional dopamine circuits: action and valence	24
2.1.1.4 Functional dopamine circuits: memory	26
2.1.2 Biochemistry of dopamine	28
2.1.2.1 Dopamine synthesis	28
2.1.2.2 Pharmacological manipulation of dopamine	28
2.1.2.3 Non-linear dose-dependent effects of dopamine	29
2.1.3 Functions of dopamine	33
2.1.3.1 Reinforcement learning	33
2.1.3.2 Novelty and exploration	35
2.1.3.3 Memory consolidation	37
2.2. Aging.....	39
2.2.1 Age-related changes in cognition	39
2.2.1.1 Long-term memory	39
2.2.1.2 Reward processing.....	41
2.2.1.3 Valence processing	42
2.2.2 Age-related structural brain changes.....	45
2.2.3 Interpretation of functional brain activity in old age	46
2.2.4 Age-related changes in dopamine.....	48
2.3. Outstanding questions	51
Chapter 3.....	53

Methods	53
3.1. Principles of MRI	53
3.1.1 Nuclear magnetism	53
3.1.2 Contrasts	55
3.2. BOLD fMRI	55
3.3. fMRI preprocessing	59
3.3.1 Realignment and unwarping	60
3.3.2 Normalisation	60
3.3.3 DARTEL	61
3.3.4 Smoothing	62
3.4. Statistical testing	62
3.4.1 General Linear Model	63
3.4.2 Group analyses	64
3.4.3 Multiple comparisons and Random Field Theory	64
3.4.4 Model-based fMRI	66
3.5. Quantitative structural neuroimaging	67
3.5.1 Magnetization transfer	69
3.5.2 Diffusion tensor imaging	72
3.6. Analysis of structural neuroimaging	75
3.6.1 Voxel-based morphometry	75
3.6.1.1 Segmentation	75
3.6.1.2 Modulation	76
3.6.1.3 Statistical analysis	77
3.6.2 Voxel-based quantification	78
3.7. Neuropsychological tests	79
3.7.1 Mini-Mental State Examination	79
3.7.2 Beck Depression Inventory	79
3.7.3 Geriatric Depression Scale	80
3.7.4 Rey Auditory Verbal Learning Test	80
3.7.5 Trail-Making Test	81
3.7.6 Forward and Backward Digit Span	81
3.7.7 Visual Object and Space Perception	81
3.7.8 Digit Symbol Substitution Test	82

3.7.9	Controlled Oral Word Association Test	82
3.7.10	Tridimensional Personality Questionnaire	82
3.7.11	National Adult Reading Test	83
3.7.12	Bond and Lader Visual Analogue Scales	83
Chapter 4		85
Dopamine and episodic memory		85
4.1.	Introduction	85
4.2.	Methods	89
4.3.	Results	104
4.3.1	Encoding performance	104
4.3.2	Dose-dependent enhancement of memory by L-DOPA	105
4.3.3	Order effects	114
4.3.4	Subsequent memory effects on fMRI data	114
4.3.5	Dose-dependent modulation of encoding activity	121
4.4.	Discussion	123
Chapter 5		130
Dopamine and reward prediction		130
5.1.	Introduction	130
5.2.	Methods	135
5.3.	Results	154
5.3.1	Behavioural performance in young and older adults	154
5.3.2	Reinforcement learning behaviour	154
5.3.3	L-DOPA and striatal prediction errors in older adults	157
5.3.4	Relationship between anatomical connectivity and prediction errors in older adults	161
5.3.5	Baseline individual differences	164
5.3.6	Post-hoc tests: performance in older adult subgroups	166
5.4.	Discussion	170
Chapter 6		175
Midbrain structural integrity and flexible learning		175

6.1. Introduction	175
6.2. Methods	178
6.3. Results	194
6.3.1 Go/no-go task performance in older adults	194
6.3.2 Structural neuroimaging in older adults	197
6.3.3 Voxel-based quantification	204
6.3.4 Age-comparison of task performance.....	206
6.3.5 Age differences of SN/VTA structural integrity and relationship with performance	209
6.3.6 Instrumental learning and novelty seeking in older adults	210
6.4. Discussion	212
Chapter 7	218
Optimism in older age	218
7.1. Introduction	218
7.2. Methods	223
7.3. Results.....	236
7.3.1 Age-comparison of optimistic behaviour.....	236
7.3.2 Structural neuroimaging: ACC and biased updating.....	241
7.3.3 SN/VTA integrity and trait optimism.....	248
7.4. Discussion	254
Chapter 8	258
Discussion	258
8.1. Memory	258
8.2. Reinforcement learning.....	261
8.3. Optimism.....	267
8.4. Other considerations.....	269
8.4.1 Aging as a model of dopamine decline.....	269
8.4.2 Generalisability.....	270
8.4.3 Final remarks	270
References.....	272

Tables

Table 1. Demographic details.	104
Table 2. Mean hit rates and false alarms for the conditions of interest.	106
Table 3. Mean d' and response bias.	107
Table 4. Regression analyses between remember and know responses and weight-adjusted dose of L-DOPA.	110
Table 5. Remembered versus forgotten neutral items.	119
Table 6. Interaction between memory for neutral items (remember > forgotten) and drug.	120
Table 7. Demographic details of 32 older adults.	136
Table 8. Quality of behavioural fits in older adults for four models.	143
Table 9. Individual differences on task performance and computation model and functional neuroimaging parameters.	165
Table 10. Neuropsychological test scores in older adults.	179
Table 11. Co-variance between neuroimaging parameters.	191
Table 12. Separate correlations between neuroimaging parameters and no-go to win.	191
Table 13. Co-variance between performance in different task conditions.	193
Table 14. Multiple regression results for each predictor variable for no-go to win performance.	198
Table 15. Multiple regression models relating imaging parameter values to go/no-go performance in each of the four task conditions.	199
Table 16. Voxel-based quantification results for no-go to win positive correlation with grey matter MT images.	205

Table 17. Demographic details.	224
Table 18. List of 45 stimuli presented to participants.	228
Table 19. Optimism task reaction times.	229
Table 20. Subjective ratings and memory performance.	239
Table 21. Correlation between ACC subregions and update bias.	243
Table 22. Correlation between dorsal ACC volume and update.	246
Table 23. Positive correlation with desirable update across all participants.	249
Table 24. Correlations with undesirable update across all participants.	250
Table 25. Correlations with update bias across all participants.	251
Table 26. Age-comparison of update bias (desirable update > undesirable update).....	252
Table 27. Conjunction analysis.	253

Figures

Figure 1. Network of connections between the SN/VTA, striatum and prefrontal cortex.	22
Figure 2 Hippocampal-VTA loop links reward and novelty processing with long-term memory.	27
Figure 3. Schematic of the inverted U-shape relationship between dopamine and cognitive function.	31
Figure 4. Converging evidence of dopamine loss in older age.	50
Figure 5. The typical BOLD response.	58
Figure 6. fMRI preprocessing.	59
Figure 7. Single subject example of multiparameter maps at 1mm isotropic resolution.	68
Figure 8. Magnetization transfer.	71
Figure 9. Experimental timeline.	88
Figure 10. Delayed test results for recollection of neutral items.	109
Figure 11. Difference between L-DOPA and placebo remember hits and false alarms for neutral items at delayed test.	113
Figure 12. Medial temporal lobe activation for subsequent memory.	116
Figure 13. Dose-dependent 'U-shaped' modulation of hippocampal activity by L-DOPA.	118
Figure 14. Task design and performance in young and older adults	133
Figure 15. Reinforcement learning model and behaviour.	156
Figure 16. Reward prediction in the nucleus accumbens in 32 older adults ...	159
Figure 17. Anatomical connectivity and baseline functional prediction errors .	163

Figure 18. Probabilistic monetary go/no-go task	182
Figure 19. Manually-defined regions of interest. Single-subject example of right substantia nigra/ventral tegmental area (red) and subthalamic nucleus (green).	186
Figure 20. Go/no-go task performance in older and younger adults	195
Figure 21. Higher no-go to win performance is associated with higher structural integrity of SN/VTA and STN	200
Figure 22. Relationship between SN/VTA structural integrity and flexibility of instrumental learning.....	202
Figure 23. Illustration of performance in older subgroups (low/high MT) and younger subgroups (leaners/non-learners)	208
Figure 24. Correlation between novelty seeking and the interaction in go/no-go task performance.	211
Figure 25. Optimism task design.....	221
Figure 26. Older adults are even more optimistic than younger adults	237
Figure 27. Region of interest analysis of the anterior cingulate cortex (ACC). ..	244
Figure 28. Dorsal ACC volume and update.	245

Abbreviations

ACC	anterior cingulate cortex
BDI	Beck depression inventory
BOLD	blood-oxygen-level dependent
DTI	diffusion tensor imaging
FA	fractional anisotropy
fMRI	functional magnetic resonance imaging
FWE	family wise error
GDS	geriatric depression scale
GLM	general linear model
L-DOPA	levodopa
LOTR	Life orientation test-revised
LTP	long-term potentiation
MD	mean diffusivity
MMSE	mini-mental state examination
MNI	Montreal Neurological Institute
MRI	magnetic resonance imaging
MT	magnetization transfer

PET	positron emission tomography
RAVLT	Rey auditory verbal learning test
ROI	region of interest
RT	reaction time
SEM	standard error of mean
SN/VTA	substantia nigra/ventral tegmental area
SPM	statistical parametric mapping
STN	subthalamic nucleus
TE	echo time
TR	repetition time
VBM	voxel-based morphometry
VBQ	voxel-based quantification

Chapter 1

Introduction

We live in an aging society. Consequently there has been a shift towards trying to understand why some adults age successfully and other do not, in a bid to improve the quality of life as we grow older. This in part requires understanding the basis of individual differences in cognition and behaviour amongst healthy older adults. Current research on the neuroscience of aging therefore focuses on some major themes. First, better characterisation of the cognitive profile in older adults, achieved through the use of well-designed experimental paradigms. Second, identifying the associated neural correlates. Here a broad approach that encompasses age-related differences in neurotransmitter systems together with changes in brain structure and function can be achieved through the use of different neuroimaging techniques coupled with pharmacological manipulations.

In this thesis, I will present a series of studies which examine cognition in healthy older adults, with an emphasis on the neurotransmitter dopamine. In these studies I sought to define the effects of dopaminergic modulation of episodic memory (Chapter 4), to better characterise the interplay between dopamine and reward-based decision-making (Chapters 5 & 6), and to explore affective processing (Chapter 7). I have employed a multimodal approach,

combining behavioural and pharmacological manipulation with structural and functional MRI, to reveal new insights into learning and memory in older age.

First, I provide a literature review pertaining to the relevant topics in this thesis (Chapter 2) and an overview of the methodological techniques used in the experimental chapters (Chapter 3). This is followed by four experimental chapters (Chapters 4 - 7) and finishes with a general discussion about study implications, limitations and ideas for future work (Chapter 8).

Chapter 2

Literature Review

2.1. Dopamine

The catecholamine dopamine is a neurotransmitter that plays an important role in a wide range of cognitive processes including motivation, novelty and reward processing and memory. Dopamine neurons in the midbrain project to different brain regions, act on different types of receptors that vary in their expression across the brain and have different modes of firing. Dopamine acts a neuromodulator in the central nervous system, where a neuromodulator may be defined as 'neurotransmission that is not directly excitatory or inhibitory and causes a change in the response state of a neuron(s)' (Picciotto et al., 2012). Moreover, dopamine neurons decline as a function of normal aging. Thus the differential degeneration of dopaminergic pathways and receptors with increasing age has been implicated in the inter-individual variability in age-associated cognitive changes. Given this link between dopamine and cognition in aging, I will provide a brief overview of dopamine anatomical pathways and the role of dopamine pertaining to the cognitive systems that I will present in this thesis.

2.1.1 Anatomy of dopamine

2.1.1.1 Regions and pathways

Dopamine neurons in the substantia nigra/ventral tegmental (SN/VTA) area of the midbrain project to different regions in the brain. Dopamine neurons consist of three cell groups: the retrorubral field (termed cell group A8 in rats), the SN pars compacta (SNc, A9) and the VTA (A10). Major projections from the SNc to the dorsal striatum (caudate and putamen) are termed the *nigrostriatal* pathway; neurons from the VTA projecting to the ventral striatum, hippocampus, septum and amygdala are termed the *mesolimbic* pathway and dopamine neurons projecting to the prefrontal, cingulate and perirhinal cortex form the *mesocortical* pathway. Whilst this parcellation of the dopaminergic midbrain holds true for rodents, it is an oversimplification when considering primates where these cell groups are more contiguous (Duzel et al., 2009b). An alternative approach is to divide the SN/VTA complex into ventral and dorsal tiers, where the dorsal tier consists of the dorsal SNc and contiguous VTA (Figure 1). The influential work of Alexander (Alexander et al., 1986) and later Haber et al. (Haber et al., 2000; Haber and Knutson, 2009) describe a topography of spiral interconnecting loops between the midbrain, basal ganglia and cortex such that dopamine neurons from the ventral tier of the SN/VTA project to the dorsal striatum, and those from the dorsal tier of the SN/VTA project to the ventral striatum. In such a way, the ventral striatum can influence the dorsal striatum via the dopaminergic midbrain. Dopamine neurons from the dorsal tier also project more diffusely to the frontal cortex as well as amygdala and hippocampus. In addition to the massive striatal projections to the SN/VTA, there are also projections from the amygdala mainly to the dorsal tier of the

SN/VTA. The SN/VTA also receives glutamatergic afferent inputs from the pedunculo pontine nucleus, serotonergic inputs from the dorsal raphe nucleus and sensory inputs from the superior colliculus. There is also a direct, albeit small, projection from the prefrontal cortex to the dopaminergic midbrain.

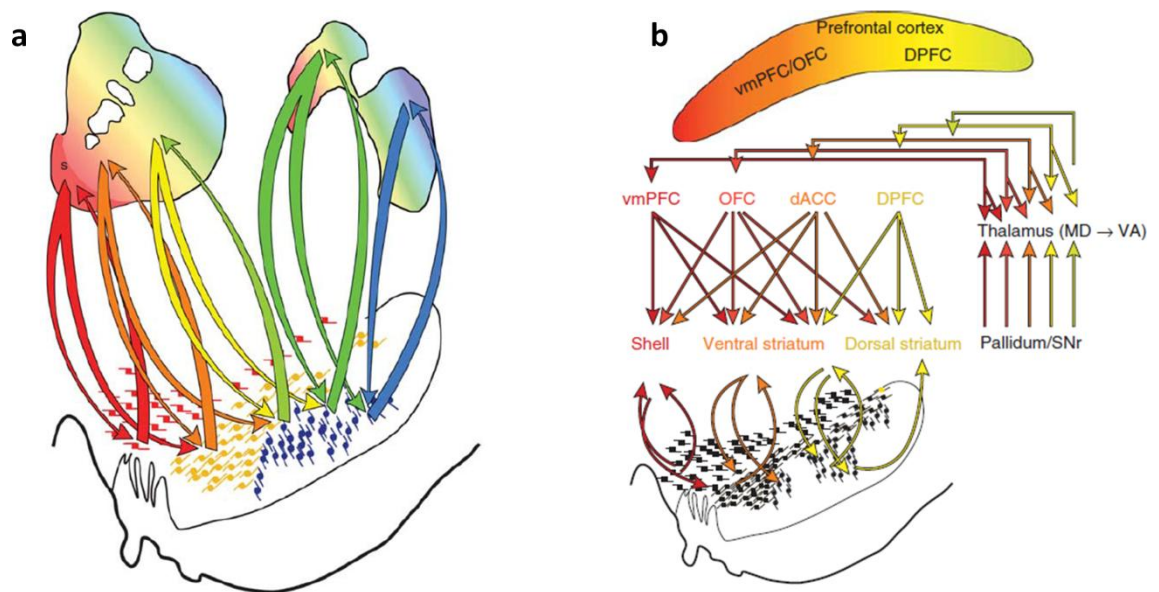


Figure 1. Network of connections between the SN/VTA, striatum and prefrontal cortex.

Adapted from Haber and Knutson (2010).

(a) Organisation of midbrain dopaminergic cells (red = dorsal tier; blue = ventral tier) and their connections with the striatum.

(b) Further illustration of the topography of spiral interconnecting loops incorporating SN/VTA, basal ganglia, thalamus and cortex.

2.1.1.2 Receptors and firing

Five dopamine receptor subtypes often grouped into D1-like (D1 and D5) and D2-like (D2, D3, D4) have been described (Missale et al., 1998). D1-like receptors have excitatory effects, whereas D2-like receptors are inhibitory. Unlike D1, D2 receptors are also located pre-synaptically and therefore can act as autoreceptors, thus excessive D2 stimulation can inhibit neuronal firing.

D1 is most widespread and expressed in the striatum, olfactory tubercle, limbic system including the hippocampus and the SN pars reticulata. D5 is the main dopamine receptor type in the hippocampus, and is also expressed in the thalamus, cortex and striatum. D2 receptors are also expressed in the dorsal and ventral striatum as well as the limbic system (hippocampus and amygdala) and frontal regions (prefrontal and cingulate), hypothalamus and SN/VTA. There is a higher concentration of D2 receptors in the striatum than in the prefrontal cortex. D3 is more restricted to the ventral rather than dorsal striatum. D4 is expressed less in the striatum and more-so in the frontal and limbic systems.

Changes in dopamine levels may be phasic or tonic. Phasic (i.e. synaptic) changes are mainly mediated by burst firing of dopamine neurons, which can be triggered by unpredicted rewards, reward-predicting cues and novel stimuli (Schultz et al., 1997). Tonic (i.e. extrasynaptic) changes also depend on dopamine firing but are additionally modulated by cortical and limbic glutamatergic inputs and change over a slower timescale than phasic levels (Floresco et al., 2003). Phasic and tonic levels mediate different aspects of behaviour, for example the former has been linked to reward processing (Schultz, 1998).

2.1.1.3 Functional dopamine circuits: action and valence

Influential functional models of dopaminergic circuitry liken the basal ganglia to 'gating' structures, filtering the flow of information between the frontal cortex and motor system (Cohen and Frank, 2009). In relation to motor activity, two key pathways have been described: a direct 'go' circuit (D1-receptor dependent) and an indirect 'no-go' circuit (D2-receptor dependent). In the direct pathway striatal dopamine neurons inhibit the internal globus pallidum (GPi) which through disinhibition of the thalamus allows representations of actions in the frontal cortex to be enabled. In the indirect pathway, D2 receptor activation inhibits the external GP (GPe) which via the GPi inhibits the thalamus and thus blocks action representations in the frontal cortex from being realised. This functional system also incorporates the subthalamic nucleus (STN) which sends a 'no-go' signal via its excitatory effect on the GPi. In this model, high levels of dopamine facilitate the go pathway whereas low dopamine levels promote the no-go pathway. Recent work using optogenetic techniques has shown that indirect pathway stimulation in mice resulted in reduced motor activity which could be rescued by direct pathway stimulation (Kravitz et al., 2010). Frank et al further hypothesised that phasic bursts of dopamine from positive feedback (e.g. reward) would promote 'go' learning and dips in dopamine firing from negative feedback (e.g. punishment) would promote 'no-go' learning. This was tested in patients with Parkinson's disease using a reinforcement learning task and indeed revealed that patients on dopaminergic medication were better at choosing the most rewarding stimulus ('go' learning from positive feedback)

and patients off medication were better at avoiding the least rewarding stimulus ('no-go' learning from negative feedback) (Frank et al., 2004).

It is worth noting that the model described above does not disentangle action processing (go/no-go) from valence (win/lose). Further studies have explored this relationship using a task that orthogonalises action and valence (Guitart-Masip et al., 2011; Guitart-Masip et al., 2012a). With regards to learning these action-valence contingencies, a striking asymmetry has been demonstrated whereby when participants are required to perform an action, they are better at learning to do this to obtain reward ('go to win', GW) than to avoid punishment ('go to avoid loss', GAL) (Guitart-Masip et al., 2012a). The opposite is seen when participants are required to inhibit an action in that they are better at learning to do this to avoid punishment ('no-go to avoid loss', NGAL) than to obtain a reward ('no-go to win', NGW). In these studies, GW and NGAL performance may represent Pavlovian biases in behaviour, whereas GAL and NGW require instrumental learning to overcome these biases (Guitart-Masip et al., 2012a). With regards to action anticipation, neuroimaging of this task revealed dissociable roles of the lateral and medial SN/VTA for representing action over valence and valence dependent on action respectively (Guitart-Masip et al., 2011). Functional neuroimaging performed during the learning phase of this task also showed that the inferior frontal gyrus was required for instrumental learning (Guitart-Masip et al., 2012a).

Dopaminergic activity has been inferred from fMRI studies showing activation in dopamine target regions such as the striatum using tasks that probe dopamine-related behaviours, such as reinforcement learning. More recently studies have also reported midbrain activation in response to motivational and reward-

predicting cues (Wittmann et al., 2005; Adcock et al., 2006) and novelty (Bunzeck and Duzel, 2006).

2.1.1.4 Functional dopamine circuits: memory

There is accumulating evidence for an influential model linking the VTA and hippocampus, with novelty, reward processing and long-term memory formation (Lisman and Grace, 2005) (Lisman et al., 2011). As illustrated in Figure 2, there is evidence that the CA1 region of the hippocampus detects novelty, perhaps by comparing predictions computed by CA3 to actual information from layer 3 of the entorhinal cortex. These novelty signals are conveyed to the VTA by a polysynaptic pathway via the nucleus accumbens and ventral pallidum, forming the downward arc of this loop. Regarding the upward arc, there probably are direct dopamine projections from the SN and VTA to the hippocampus, whereby the anterior hippocampus receives projections from the VTA and the posterior hippocampus receives projections from both SNc (A9) and the VTA (Scatton et al., 1980). Thus stimulation of this pathway by novel items may lead to dopamine release and long-term potentiation (LTP) in the hippocampus, resulting in protein synthesis and consolidation of these novel items in long-term memory. In this way, dopamine may act as a filter for information that enters long-term memory. Additional components of this circuit include a pathway from dorsal CA3 projecting to the VTA via the lateral septum, which has been shown to modulate reward-seeking behaviour (Luo et al., 2011).

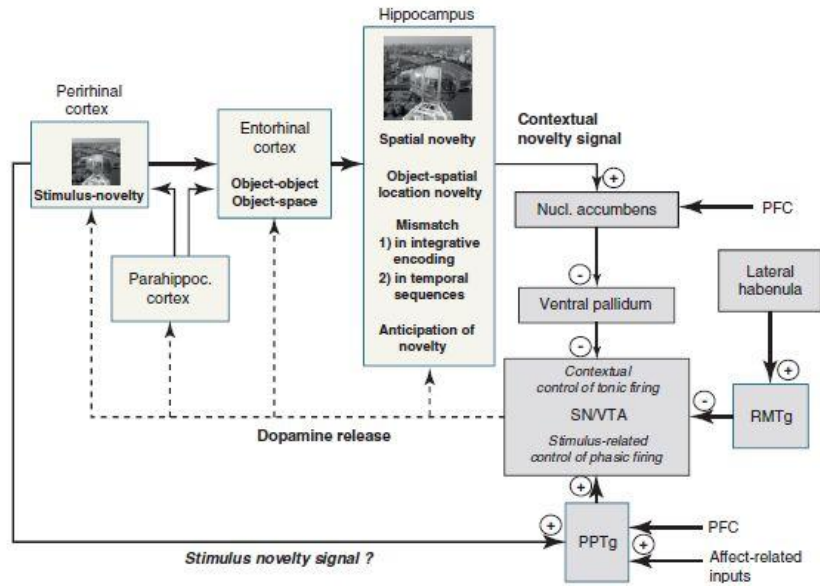


Figure 2 Hippocampal-VTA loop links reward and novelty processing with long-term memory.

Adapted from (Lisman et al., 2011)

2.1.2 Biochemistry of dopamine

2.1.2.1 Dopamine synthesis

Levodopa, derived from the substrate L-Tyrosine, is the amino acid precursor for the catecholamine dopamine. Dopamine itself is a precursor for two other catecholamines in the brain – noradrenaline and adrenaline. Dopamine is synthesized in nerve terminals and stored in presynaptic vesicles. The duration of action of dopamine depends partly on the amount released, partly on its removal from the synaptic cleft by dopamine transporters (DAT) and partly on the function of presynaptic autoreceptors which inhibit the release of dopamine when activated (Koller and Melamed, 2007). Dopamine metabolism is regulated by the enzymes monoamine oxidase (MAO) and catechol-O-methyltransferase (COMT).

2.1.2.2 Pharmacological manipulation of dopamine

Levodopa (L-DOPA) was introduced in the 1960s as a replacement therapy for Parkinson's disease. Oral administration of L-DOPA, unlike dopamine, readily crosses the blood brain barrier and increases striatal dopamine levels (Koller and Rueda, 1998). It is administered with a peripheral aromatic-amino-acid decarboxylase inhibitor (AADI), carbidopa or benserazide, to reduce extracerebral degradation. L-DOPA has a half-life of approximately 60-90 minutes (Koller and Melamed, 2007) (Nutt, 2008). A common side-effect of L-DOPA is nausea and vomiting which is reduced by concurrent administration with AADIs and by pre-administration of an anti-emetic such as the peripheral D2-antagonist domperidone. In my studies I used 187.5 mg of Madopar dispersible, which

contains 150mg of levodopa and 37.5mg of benserazide, administered 60-90 minutes before behavioural testing.

2.1.2.3 Non-linear dose-dependent effects of dopamine

Since dopamine is implicated in a range of cognitive processes, a natural hypothesis to test is whether cognition can be improved by elevating dopamine levels. The results of such studies reveal a complex pattern, with some evidence that dopamine improves verbal learning (Knecht et al., 2004), motor memory (Floel et al., 2008), cognitive flexibility and working memory (Robbins and Arnsten, 2009) whereas other studies report a decline in learning and memory (Breitenstein et al., 2006) (Morcom et al., 2009). The reasons for this complexity are multifactorial and include: differences in baseline performance, differential changes in the underlying integrity of the dopamine system depending on the study cohort (e.g. Parkinson's disease, young adults, older adults), different techniques used as a marker of the dopamine system (e.g. genetics, structural imaging, functional imaging), different modes of action of dopaminergic pharmacological manipulations on tonic and phasic dopamine levels, and non-linear dose-dependent effects of dopamine (see (Cools and D'Esposito, 2011) for a review). These non-linear effects are characterised by an inverted 'U-shape' dose-dependent relationship between dopamine and cognition (see Figure 3 for a schematic diagram of this effect).

Many studies have focussed on the effects of dopamine on working memory since there is a high concentration of dopamine receptors in the prefrontal cortex, a region of the brain that plays a critical role in working memory. One

way of exploring the non-linear effects of dopamine here is to compare performance on tasks tapping into different dopaminergic pathways in patients with Parkinson's disease who predominantly lose dopamine projections from ventrolateral SN/VTA to dorsal striatum (Cools et al., 2001). Here, patients withdrawn from their dopamine medication were impaired on a task-set switching task, which depends on dorsal striatal dopamine, but performed better on a probabilistic learning task which required a ventral striatal circuit likely to be more intact in patients. Another approach has been to use baseline performance as a marker of starting dopamine levels. For example task performance in participants with a lower baseline working memory capacity can improve with dopamine, whereas performance deteriorates in those with higher baseline performance (Kimberg et al., 1997). A further approach is to use genotype as a marker of baseline dopamine levels. The gene catechol-O-methyltransferase (COMT) breaks down dopamine, thus higher COMT activity is associated with lower dopamine levels. Individuals homozygous for the Val allele have higher COMT activity and thus lower dopamine levels, whereas the converse is true for individuals with the Met allele. Individuals homozygous for the Met allele respond differently to drugs manipulating dopamine levels in comparison to individuals homozygous for the Val allele in line with non-linear effects of dopamine (Cools and D'Esposito, 2011).

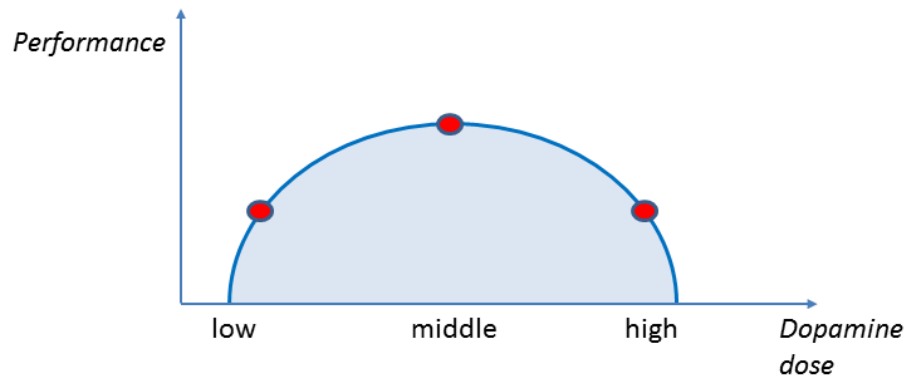


Figure 3. Schematic of the inverted U-shape relationship between dopamine and cognitive function.

A certain optimal ('middle') level of dopamine may boost cognitive function but too little ('low') or too much ('high') may be ineffective or detrimental respectively.

Possible dose-dependent effects of dopamine were elicited in a study showing enhanced verbal learning following administration of the dopamine precursor levodopa (L-DOPA), whereby learning was higher in participants of lower body-weight who effectively received higher relative doses of the drug (Knecht et al., 2004). A more direct test of the non-linear dose-dependent effects of dopamine was examined using a range of doses of L-DOPA in combination with transcranial direct current stimulation (Monte-Silva et al., 2010). Here, low and high doses impaired motor plasticity whereas the medium dosage prolonged plasticity. Similar findings relating to a more focal type of plasticity have been found in a study using transcranial magnetic stimulation (Thirugnanasambandam et al., 2011).

This non-linear 'inverted U-shape' relationship between dopamine and cognition provides an explanation as to why studies show both improvements and

impairments of cognitive function when dopamine levels are enhanced and why the effects may differ across populations (e.g. young adults versus healthy older adults versus patients with Parkinson's disease). Importantly, this descriptive inverted U-shape account of dopamine does not shed light on the underlying physiological reasons as to why excessive levels of dopamine would have unfavourable consequences. This may differ depending on which brain regions are being tested, due to different regional concentrations of D1- and D2-like receptors which will respond differently to enhanced dopamine levels. Also, pharmacological agents differ with respect to their effect on tonic and phasic dopamine transmission which may have differential effects on behaviour. For example, the dopamine precursor levodopa, which increases presynaptic dopamine availability and thus modifies tonic and phasic dopamine transmission, improves learning in younger adults (Knecht et al., 2004). In contrast, administration of a dopamine agonist which acts on post-synaptic dopamine receptors and thus affects tonic dopamine transmission, impairs learning in younger adults (Breitenstein et al., 2006) and enhances forgetting effects in the medial temporal lobes in older adults (Morcom et al., 2009).

An important outstanding question is whether non-linear effects of dopamine extend to cognitive domains other than working memory. Simulated data from a computational model suggest this to be the case (Li et al., 2005). This is based on an important theoretical account of impaired dopaminergic modulation, for example in old age, resulting in less distinct neural representations by altering the signal-to-noise ratio of neural processing (Li and Sikström, 2002). We provide empirical data for a non-linear dose-dependent effect of dopamine on

episodic memory in Chapter 4 and discuss the possible underlying neurobiological mechanisms.

2.1.3 Functions of dopamine

2.1.3.1 Reinforcement learning

A dominant theory in neuroscience is the role of dopamine in reward-processing. The seminal studies of Schultz et al. in monkeys describe how dopamine neurons in the SN/VTA show phasic activations to unexpected rewards and reward-predicting cues and dips in firing when rewards are omitted (Schultz et al., 1997). Such observations can be characterised in terms of computational models of reinforcement learning, where learning occurs when outcomes violate expectations (Rescorla and Wagner, 1972). This difference between expected and actual outcomes is termed the *prediction error*. Prediction errors can be calculated on a trial by trial basis using the following classical reinforcement learning model:

$$\begin{aligned} Q_{a(t)}(t+1) &= Q_{a(t)}(t) + \alpha\delta(t) \\ \delta(t) &= R(t) - Q_{a(t)}(t) \end{aligned}$$

Here $\delta(t)$ is the reward prediction error which represents the difference between the actual reward $R(t)$ and expected reward $Q_{a(t)}(t)$. α denotes the subjects' learning rate. A Softmax rule is typically used to determine the probability of choices, in which the inverse temperature parameter β indicates how deterministic choices are:

$$P(a(t) = a) = \frac{\exp(\beta m_a(t))}{\exp(\beta m_0(t)) + \exp(\beta m_1(t))}$$

In this model, the prediction error acts as a teaching signal which updates the expected value on each subsequent trial; when there is no difference between the actual and expected outcome, that is when the prediction error is zero, learning has occurred. In the studies by Schultz et al., a key finding was that firing of dopamine neurons shifted from the time of reward presentation to the time of presentation of the conditioned (i.e. reward-predicting) stimulus over the course of learning, which has been formalised in a 'temporal difference' learning model (Sutton and Barton, 1998).

Reinforcement learning models can be used in humans in combination with fMRI to examine target projection areas of dopamine neurons for prediction error signals. A temporal difference learning-like prediction error signal has been demonstrated in humans in the ventral striatum (O'Doherty et al., 2003) (O'Doherty et al., 2004). Furthermore, dissociation between prediction error signals reported by the ventral and dorsal striatum have been described using the 'actor-critic' model. In this model, the actor component selects actions based on modifying stimulus-responses relationships such that actions associated with rewards are strengthened, whereas the critic estimates a temporal difference error which is used to update expected values (Sutton and Barton, 1998). Accordingly, in humans undergoing fMRI, ventral striatal (nucleus accumbens) activity correlated with prediction errors during both an instrumental and Pavlovian task corresponding with the critic component of the model, and dorsal striatal (caudate) activity correlated with prediction errors in

the instrumental versus the Pavlovian task supporting its role as the actor (O'Doherty et al., 2004).

This temporal difference reinforcement learning model is described as a 'model-free' system that underlies habitual control, where behaviour depends on previous reinforcement of actions. In contrast a 'model-based' reinforcement learning system has been proposed to underlie goal-directed learning in which there is a representation of the overall task structure (Daw et al., 2011). Prefrontal cortex and ventral striatum are thought to serve the model-based and model-free systems respectively although there is evidence for an overlap between the neural substrates underlying these two systems (Daw et al., 2005; Daw et al., 2011). It has recently been shown that older adults underperform on model-free tasks and outperform on model-based tasks in comparison to younger adults (Worthy et al., 2011).

2.1.3.2 Novelty and exploration

Reinforcement learning models can be extended to understand the 'explore-exploit' dilemma, in which an organism must make decisions that balance maximising rewards ('exploit') and learning new information that may lead to future rewards ('explore'). So-called 'bandit' tasks can be used to assess exploration and exploitation, whereby participants must choose from different slot machines ('bandits') and choose the optimal bandit to obtain reward (exploit). By varying the underlying probability or magnitude of reward associated with each bandit, optimal performance requires a combination of exploration and exploitation. In one study, humans performing such a task

showed striatal and ventromedial prefrontal cortex activation for exploitation and frontopolar cortex and intraparietal sulcus activity for exploration (Daw et al., 2006). This explore-exploit trade-off may be linked to motivation and dopamine. Exploration allows an organism to encounter novel and potentially rewarding stimuli. Computationally, this role of dopamine signalling novelty to encourage exploration is termed the 'exploration bonus' (Kakade and Dayan, 2002). In humans, novelty has been shown to enhance exploration in a reinforcement learning task and such a novelty bonus was associated with ventral striatal activation, similar to reward prediction error signalling (Wittmann et al., 2008). Novelty signalling in contrast to other salient features such as negativity or rareness has been identified in the SN/VTA (Bunzeck and Duzel, 2006), more specifically in a rostral subregion of the medial SN/VTA that differed from a more caudal subregion of the SN/VTA associated with reward anticipation (Krebs et al., 2011), suggesting some functional segregation underlies these processes.

Taken together, converging evidence suggest dopamine has a fundamental role in motivating behaviours, in the context of reward, novelty, action and arbitrating between exploratory and exploitative behaviour. A framework linking such behaviours has been proposed: NOvelty-related Motivation of Anticipation and exploration by Dopamine (NOMAD) (Duzel et al., 2009a). The NOMAD model has two important consequences for the research presented here. First, it provides a link between the motivational properties of dopamine and long-term memory formation in the hippocampus which could serve to guide future successful behaviour (Shohamy and Adcock, 2010). Second, the model makes the prediction that age-related dopamine decline will impact upon motivational

behaviours which may relate to learning and memory impairments in older adults.

2.1.3.3 Memory consolidation

Donald Hebb proposed the theory that the synaptic connection between two cell groups will be strengthened if the cells are active together (Hebb, 1949), encapsulated in the adage that '*cells that fire together wire together*'. This influential theory informs studies of the cellular mechanisms of learning and memory. Experimental evidence for synaptic plasticity from studies on long-term potentiation (LTP) and long-term depression (LTD) provide support for Hebb's rule. LTP has been defined as 'an activity-dependent increase in synaptic strength' (Bliss and Gardner-Medwin, 1973). In the hippocampus, it has been suggested that LTP is the model underlying cellular consolidation and stabilisation of memories. LTP can be divided into an early phase (protein synthesis-independent), lasting less than 3 hours, and a late phase (protein synthesis-dependent) occurring 4-6 hours post-encoding (Frey and Morris, 1997). Dopamine is critical for the late-phase of LTP (O'Carroll et al., 2006) and for the persistence of memories over longer but not shorter periods (Bethus et al., 2010). The synaptic tagging and capture hypothesis provides a model for the role of late-LTP in the cellular consolidation of memories (Frey and Morris, 1997) (Redondo and Morris, 2011). This is a dual-step process in which early-LTP, induced by coactivation of AMPA and NMDA receptors by glutamate, and the setting of a synaptic 'tag' establishes the potential for a long-term memory. In the other step, a series of other biochemical interactions convert this synaptic potentiation ("tag") into a stabilised trace at those synapses at which tags have

been set (Wang and Morris, 2010). These biochemical processes include calcium entry into the post-synaptic neuron with subsequent activation of cyclic adenosine monophosphate (cAMP) which activates further molecules leading to an increase in the number of post-synaptic AMPA receptors and so increasing its response to subsequent stimulation. cAMP also activates other molecules that leads to protein synthesis. Thus both a 'tag' and so-called plasticity related proteins are required to convert early-LTP to late-LTP. Dopamine is required for the late-phase of LTP to enable hippocampal protein synthesis (Smith et al., 2005; Bethus et al., 2010). Bethus et al. demonstrated the impact of dopamine on memory persistence in a series of elegant experiments using a hippocampal-dependent paradigm which used tests at different time-points to dissociate between encoding, storage and retrieval of episodic-like memory (Bethus et al., 2010). In these experiments, rats were taught paired flavour-location associates. New information was then presented in the form of novel pairings together with an infusion of either a D1/D5 dopamine antagonist into the hippocampus or a placebo. Memory for these novel pairings was tested after a short (30 mins) and long (24 hours) delay. The authors found that memory tested after a short interval remained intact whereas memory tested after a longer delay was impaired, suggesting that dopamine is necessary when encoding new events in order for memory for those events to persist long-term but not necessary for encoding *per se*. Furthermore, the authors were able to exclude the possibility that the results were confounded by different state-dependent effects during retrieval after short and long delays by comparing the effects of the dopamine antagonist and saline administration at encoding only and at both encoding and retrieval.

An overall framework incorporating the above ideas was recently proposed as an update to Hebb's rule, providing key evidence for the critical role of dopamine in late-LTP and thus episodic memory consolidation (Lisman et al., 2011) . Such a framework provides a bridge between the fields of reward, motivation and novelty processing, and episodic memory via dopaminergic neuromodulation.

2.2. Aging

The UK Office for National Statistics report that as birth and death rates have fallen over the past 150 years, the size of our elderly population has increased (<http://www.statistics.gov.uk/hub/population/ageing/older-people>). By 2010, 17% of the population was aged >65 years and this is projected to expand to 23% by 2035. With increasing age comes a multitude of changes in cognition, brain structure and function which I will briefly describe here.

2.2.1 Age-related changes in cognition

2.2.1.1 Long-term memory

The most common and well-recognised cognitive impairment in aging is a decline in episodic memory (Light, 1991). Episodic memories are both full of contextual details and are relational, that is they incorporate the 'what', 'where' and 'when' aspects of an event (Clayton and Dickinson, 1998). Episodic memory can be viewed as having three key stages: encoding, storage and retrieval. Encoding is defined as 'the set of processes involved in transforming

external events and internal thoughts into both temporary and long-lasting neural representations' (Craik and Rose, 2012). Storage entails structural and neurobiological changes which occur after acquiring new information in order to stabilise memories, underpinned by the process of consolidation. Consolidation, defined as a 'time-dependent stabilisation process leading to the permanent storage of newly acquired memories' (Nader and Hardt, 2009), comprises cellular and systems-level processes reflecting molecular changes over a shorter time frame and interplay between the hippocampus and neocortex over a longer time period respectively (McKenzie and Eichenbaum, 2011). A further extension is the concept of reconsolidation, whereby memories become labile following retrieval and thus require further consolidation ('reconsolidation') to become stabilised again (Nader and Hardt, 2009).

Studies have suggested deficits in older adults at all of these stages. However, the majority of studies to date have focussed on encoding and retrieval deficits since storage has no easily testable behavioural correlate (Craik and Rose, 2012). Studies are required in which memory performance is tested after various time intervals to explore consolidation deficits. Encoding deficits have been supported by differences in functional activation between young and older adults, such as reduced left prefrontal cortex and medial temporal lobe activity at encoding (Craik and Rose, 2012). Interestingly, older adults who perform as well as younger adults on memory tasks show bilateral prefrontal cortex activation at encoding, suggesting that the loss of lateralisation with increasing age may serve as a compensatory mechanism for asymmetrical age-related structural and functional changes (Cabeza et al., 2002) (Buckner, 2004).

Older adults are generally thought to have greater impairment of recollection abilities with a relative sparing of familiarity (Yonelinas, 2002), studied using the remember/know procedure (Tulving, 1985). Here, remember responses reflect hippocampal-dependent episodic memory. This may be because older adults encode information less deeply with less contextual information resulting in less distinctive memory representations (Craik and Rose, 2012). This links in with computational data suggesting the decline in neural representations is associated with the age-dependent loss of dopamine (Li and Sikström, 2002). However deficits in familiarity judgements have also been identified in older adults as well as higher rates of false alarms (incorrect 'old' judgements for new items) (Duarte et al., 2010). In this study, dorsomedial and inferior frontal activations mediated age-related familiarity deficits, in keeping with known frontal lobe changes with age.

2.2.1.2 Reward processing

Reinforcement learning (learning through trial and error to maximise rewards) is affected by the aging process. Older adults are slower at learning stimulus-responses associations (Mell et al., 2009; Mohr et al., 2010) and exhibit valence asymmetries such as better learning from negative feedback (Frank and Kong, 2008) and impaired learning from positive feedback (Mell et al., 2005). 'Win-stay' behaviour (choosing the same stimulus again after it has delivered a rewarding outcome) reduces with increasing age, suggesting reduced trial-by-trial learning from rewards (Frank and Kong, 2008). Age-related neural differences in reward based learning have also been shown whereby older adults have absent mesolimbic activation to reward-predicting cues, but intact

activation for reward feedback which may result from reduced dopamine causing a reduction in the ability to estimate rewards (Schott et al., 2007). Older adults performing a financial risk task show increased temporal variability in the nucleus accumbens, which was associated with increased risk-seeking mistakes (Samanez-Larkin et al., 2010). This measure of temporal variability may reflect noisier rather than reduced processing in the nucleus accumbens. Together, these findings suggest that although outcome representations may be maintained, older adults are unable to use this feedback to make optimal decisions. Indeed in a study in which older adults were presented with expected value information, decision-making improved to match that of younger adults (Samanez-Larkin et al., 2011). Age-related decline of the structural integrity of white matter pathways from dorso-medial thalamus to medial prefrontal cortex, and medial prefrontal cortex to nucleus accumbens, indexed using DTI (mean fractional anisotropy values of tracts), have been linked to worse reward-learning (Samanez-Larkin et al., 2012), suggesting that variability in anatomical connectivity between these regions as a function of age mediates reward processing. We build on this body of evidence of impaired probabilistic reward learning in old age in Chapter 5 by analysing the effect of enhancing dopamine levels on components of the prediction error signal.

2.2.1.3 Valence processing

In contrast to reinforcement learning studies, a different asymmetry when processing positive and negative stimuli independent of probabilistic learning has been described. Here, older adults tend to display a 'positivity bias', which is a greater sensitivity to positive rather than negative stimuli (Mather and Carstensen, 2005). Older adults remember faces displaying positive emotions

more than negative emotions (Mather and Carstensen, 2003), remember positive images more than negative images (Mather and Carstensen, 2005), have less rich autobiographical memory for negative events (Comblain et al., 2005) and experience less negative arousal when anticipating monetary loss in comparison to younger adults (Samanez-Larkin et al., 2007). Samanez-Larkin et al., (2007) performed a study in which older adults underwent functional MRI whilst performing an incentive processing task called the monetary incentive delay task. In this task, subjects are shown cues which indicate whether they will win or avoid losing money if they respond quickly enough to a target. Neural activation in older adults differed from younger adults for loss anticipation (reduced striatal and insular activation) whereas both groups showed similar activation patterns for gain anticipation, identifying an age-related neural basis for this asymmetry in valence processing (Samanez-Larkin et al., 2007).

Brassen et al., (2012) studied neural responses to regret in young and healthy older adults, and older adults with depression (Brassen et al., 2012). Participants performed a task in which successive boxes could be opened revealing monetary gain unless a 'devil' was encountered resulting in a loss of winnings. Participants were shown how much more they could have gained if they stopped early thus providing the opportunity to study missed chances (i.e. regret). Healthy older adults differed from young adults and old adults with depression by showing increased anterior cingulate activation (ACC) for missed opportunities than wins and increased ventral striatal activity for non-optimal gains compared to actual losses. Behaviourally, healthy older adults did not show subsequent risk-taking behaviour after missed chances whereas younger and older depressed adults did. These findings suggest that healthy older adults

have reduced neural responses to regret by employing cognitive control strategies. ACC activity has also been linked to greater emotional stability and processing of positive information in old age (Brassen et al., 2011).

This apparent paradox in older age between studies of reinforcement learning and valence processing showing biases towards negative and positive stimuli respectively has been raised in a recent review (Eppinger et al., 2011). Here the authors suggest that in the context of reinforcement learning when the outcome is probabilistic and important for guiding subsequent behaviour, older adults are more sensitive to negative or punishing outcomes. In contrast, studies in which the outcome does not affect behaviour, for example in the monetary incentive delay task described above, or in psychosocial studies examining emotional processing, older adults tend to place greater emphasis on positive outcomes. The reasons underlying these differences in the effects of valence remain unknown.

An interesting consideration is whether greater emotional regulation with increasing age is a positive phenomenon whereby older adults have additional resources to employ during emotional processing, as the socioemotional selectivity theory would suggest, or rather a negative 'side-effect' of age-related neurodegeneration. The greater activation in the ACC identified in the aforementioned studies would support the former hypothesis. An extensive body of literature indicates the ACC plays a critical role at the cognitive-emotional interface (for reviews see (Bush et al., 2000) and (Ochsner and Gross, 2005)) and encodes an age by valence interaction during socio-emotional tasks (Leclerc and Kensinger, 2008). Previous studies also argue against the emergence of a positivity bias as a consequence of age-related

neural degeneration, since this bias can be minimised in older adults by modifying task parameters (for a review see (Samanez-Larkin and Carstensen, 2011)). This debate assumes importance when considering the concept of successful aging. The term successful aging relates to the phenomenon of greater heterogeneity amongst older individuals which in turn influences behaviour (Buckner, 2004), such that a subset of older adults have less impairments in physical and mental health than the usual aging process entails (Rowe and Kahn, 1987). If greater emotional regulation is related to greater well-being and health in old age and the underlying mechanisms and direction of effect can be elucidated, this may be harnessed in order to promote successful aging.

2.2.2 Age-related structural brain changes

Gross changes in the elderly brain include reduced brain volume and weight, enlargement of the ventricles and expansion of the sulci (Raz and Rodrigue, 2006). The trajectory of change over time varies between different brain regions. Regional reduction in volume is found predominantly in the prefrontal cortex (PFC) and medial temporal lobe structures with relatively sparing of other regions such as occipital cortex (Hedden and Gabrieli, 2004). Age-related volume reduction has also been identified in the cingulate sulci (Good et al., 2001), amygdala and cerebellum (Raz and Rodrigue, 2006). Striatal volume also decreases with age, with a greater decline in the caudate and putamen than the globus pallidus (Raz et al., 2003).

Volumetric MRI studies demonstrate a decline in hippocampal size with age in the region of 2-3% per decade, increasing above the age of 70 years (Hedden and Gabrieli, 2004). Interestingly, one study found subiculum atrophy in healthy older subjects versus CA1 atrophy in patients with Alzheimer's disease, although the authors note their study may have been at risk of bias due to its cross-sectional design plus the inclusion of only a small number of very elderly subjects (Chételat et al., 2008). The relationship between hippocampal size and memory performance in healthy aging is inconsistent, in contrast to the positive correlation between hippocampal size and memory in patients with Alzheimer's disease (Van Petten, 2004). This may partly be due to the paucity of longitudinal studies in normal aging although even in such studies, the results are conflicting (Raz and Rodrigue, 2006).

Gross white matter volume stays relatively stable across the lifespan but microstructural white matter changes occur. This has been inferred from neuroimaging techniques such as diffusion tensor imaging (DTI), which provides a semi-quantitative measure of the integrity of white matter tracts. DTI reveals a general pattern of greater decrease of fibre integrity in the frontal white matter compared to temporal, parietal and occipital white matter (Raz and Rodrigue, 2006) (Head et al., 2004).

2.2.3 Interpretation of functional brain activity in old age

A key feature of aging research is recognising and understanding the increasing variability in performance with age, which is presumed to be partly due to the diversity of experiences between individuals (Carstensen, 2006) alongside reorganisation of brain pathways and recruitment patterns (Buckner, 2004), and

the interaction between these external and internal factors. More generally, this links to the concept of 'successful' and normal or 'usual' aging, whereby usual aging entails various declines in cognition but a subgroup of individuals exist who are less affected (Rowe and Kahn, 1987). Individuals who age successfully may have greater 'cognitive reserve', that is greater cognitive processing resources allowing individuals to cope with age-related impairments (Buckner, 2004). More recently the idea of 'brain maintenance' has been proposed, which suggests that preserved brain structure and function may underlie successful cognitive performance (Nyberg et al., 2012) (Düzel et al., 2011). The importance of this idea is that identifying mechanisms which delay or prevent the onset of pathology in the brain could predict successful aging. This also has implications regarding training programmes in old age.

Older adults often show decreased functional brain activity in comparison to younger individuals but paradoxically may also show increased activation. Whilst a decrease in activity may represent an age-related deficit (that is, under-recruitment of a brain region associated with poor performance), increases in activity can be interpreted as either compensation or impairment, depending on the associated behaviour (Reuter-Lorenz and Lustig, 2005). Compensation is inferred in older adults showing high levels of performance, or similar performance to younger individuals. This may explain why some older adults with high performance levels have less neural asymmetry (Cabeza et al., 2002). For example, left-frontal activity in younger adults is related to verbal learning whereas older adults are reported to show bilateral activation (Morcom et al., 2003). Impairment is suggested when increased activity correlates with poor

performance, where greater activity is thought to reflect less efficient neural processing and dedifferentiation.

It is important to acknowledge that physiological changes, such as changes in cerebral blood flow and the cerebral metabolic rate of oxygen consumption (Small et al., 2011), in the aging brain may account for some of the age-related differences in functional MRI activity. Thus the comparison of BOLD signal changes between younger and older adults can be problematic (Ances et al., 2009). An advantage of the fMRI studies in this thesis is that we used a within-subject design to determine the effects of pharmacological manipulation, so taking into account inter-individual variability in neurovascular coupling. We also screened participants for a history of cerebrovascular disease and vascular risk factors, since conditions such as diabetes and hypertension could also affect neurovascular coupling and the BOLD signal (D'Esposito et al., 2003).

2.2.4 Age-related changes in dopamine

Autopsy data has shown there is a decline in post-synaptic dopamine (D1 and D2) receptors with age of approximately 10% per decade as well as loss of the presynaptic dopamine transporter, DAT (Bäckman et al., 2006). There is loss of both striatal and extrastriatal dopamine receptors with age, demonstrated both in post-mortem studies and with PET (Inoue et al., 2001). There is a 5-10% loss per decade of post-synaptic D1 and D2 receptors across the brain with advancing age, with a greater rate of loss of D2 receptors from the frontal cortex, and a comparable loss of presynaptic DAT (Kaasinen and Rinne, 2002). There is an average loss of dopaminergic neurones in the SN of 4.7% per

decade (Fearnley and Lees, 1991) which correlates with a decrease in striatal dopamine availability (Düzel et al., 2008). Using PET, age-related loss of dopamine receptors has been associated with hypometabolism particularly in frontal and cingulate regions (Volkow et al., 2000) and D2 binding in the striatum predicts cognitive performance (Bäckman et al., 2000). Increased segregation between dopaminergic pathways in older adults has also been described, as determined by PET D1 binding potentials in key regions of the nigrostriatal, mesolimbic and mesocortical pathways, relating to differences in the speed of task performance (Rieckmann et al., 2011).

With advancing age, there is a greater loss of dopamine neurons from the dorsal tier than medial ventral than lateral ventral tier of the SN/VTA. This pattern of loss differs from Parkinson's disease (Fearnley and Lees, 1991). DTI data complements this histological data by showing changes in DTI metrics (reduced fractional anisotropy, increased radial diffusivity) in the dorsal but not ventral SN/VTA in healthy older adults (Vaillancourt et al., 2012). Figure 4 summarises these changes.

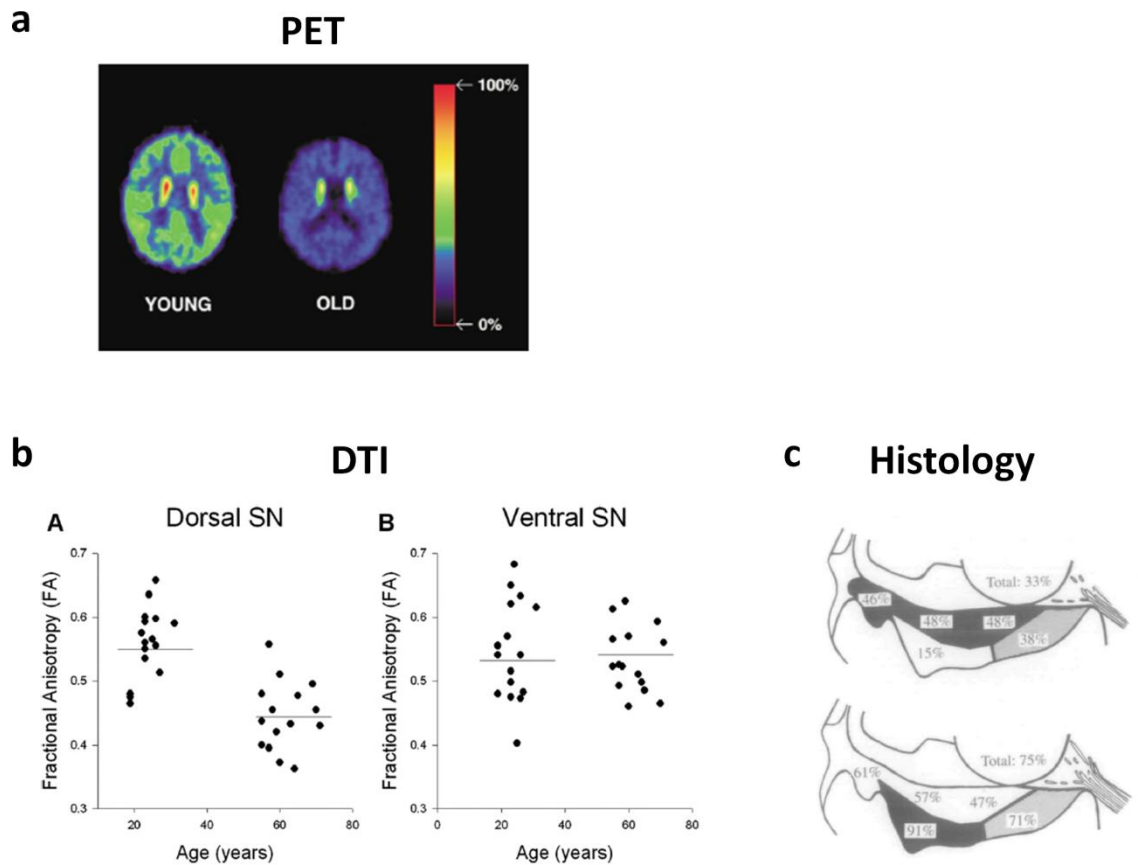


Figure 4. Converging evidence of dopamine loss in older age.

(a) Functional imaging using positron emission tomography (PET) shows widespread loss of dopamine receptors with age. Image shows relative uptake of the D2-like receptor ligand [^{11}C]FLB 457.

(b) There is a typical pattern of loss of dopamine neurons in aging, with greater age-related loss from the dorsal than ventral substantia nigra, evidenced by structural diffusion tensor imaging (DTI) and histological data.

(c) This pattern of dopamine loss as a function of aging (c, top) also distinguishes healthy older adults from patients with Parkinson's disease which is a disease characterised by marked dopamine loss but more so from the ventral than dorsal substantia nigra (c, bottom).

a: adapted from Kaasinen et al (2002); b: adapted from Vaillancourt et al (2012); c: adapted from Fearnley and Lees (1991).

2.3. Outstanding questions

The studies presented in this thesis build on this review of the literature and present a multi-modal approach to exploring learning and memory in older age and how this relates to changes in dopamine, brain structure and brain function.

These studies are based on the following questions:

1. Given that both memory decline (Section 2.2.1.1) and dopamine decline (Section 2.2.4) are part of the normal aging process, a key outstanding question is whether enhancing dopamine levels may improve episodic memory in older adults. As outlined in Section 2.1.3.3, empirical evidence for the role of dopamine in memory consolidation is largely based on animal literature, in which only episodic-like memory paradigms can be used. In Chapter 4 I study the role of dopamine in human episodic memory consolidation in a pharmacological study in healthy older adults performing a functional MRI episodic memory task.

2. As discussed in Section 2.2.1.2, the precise nature of the deficit underlying abnormal reward processing in old age remains unclear. In Chapter 5 I use a reinforcement learning model-based approach with pharmacological manipulation to better characterise the reward-based learning deficit in old age and the role of dopamine. I also used DTI in this study to explore individual differences in the relationship between nigro-striatal structural connectivity and

functional reward signalling in the striatum. In Chapter 6 I use a different structural imaging technique (MT imaging) to relate structural changes in the dopaminergic midbrain to the flexibility of reward-based learning.

3. Section 2.2.1.3 reviews the literature suggesting that cognitive processes in old age may be modulated by a 'positivity bias'. Processes that bias cognition may impact upon decision-making in old age. It has also been suggested that a positivity bias is linked to better emotional regulation and successful aging. I therefore explore how age influences the bias for updating beliefs about the future following desirable and undesirable information, and the associated structural neural correlates in Chapter 7.

Chapter 3

Methods

Magnetic resonance imaging (MRI) is a powerful non-invasive tool for exploring the neural correlates of human behaviour. This chapter outlines the principles underlying structural and functional MRI which are the neuroimaging tools I used in the studies presented in this thesis. In addition, studying healthy aging requires a broad cognitive screening process. In this chapter I therefore also include an overview of the neuropsychological tests I administered to elderly participants.

3.1. Principles of MRI

3.1.1 Nuclear magnetism

Our body tissue is composed of approximately 80% water consisting of hydrogen atoms. The nucleus of the hydrogen atom contains a single proton which possesses a fundamental property known as spin. When protons are placed in a magnetic field (B_0) the axes of their spins aligns with the static magnetic field. In a static magnetic field, an MR signal cannot be detected. However if a strong radiofrequency signal (B_1) is applied at right angles to the static magnetic field, this excites some of the nuclear spins into a higher energy spin state (spin flip) such that the axis of the proton spin now precesses about

the B1 field. The frequency of the precession of the proton spins is proportional to the strength of the magnetic field, known as Larmor frequency. When the radiofrequency signal is switched off there is a relaxation of spins from the higher energy state to the lower energy state which produces a measurable amount of radiofrequency signal at the Larmor frequency associated with that field and forms the basis of MRI (Huettel, 2004). Proton relaxation occurs longitudinally (T1 relaxation) and transversely (T2 relaxation), both of which differ depending on tissue type resulting in different MRI contrasts from grey and white matter. T1 provides better contrast between tissue types and is commonly used for structural images. T2 and T2* decay are quicker and are therefore used for functional MRI. T2* is the apparent transverse relaxation which is a combination of T2 and inhomogeneities in the magnetic field.

Following proton excitation, additional magnetic fields containing spatial gradients are applied to determine the location of proton spins and thus localise the MR signal in 3D. These fields are aligned orthogonally on the X axis (left-to-right), Y axis (posterior-to-anterior) and Z axis (superior-to-inferior) and are known as the frequency-encoding or readout gradient, phase-encoding gradient and slice-select gradient respectively. The signal emitted by relaxing protons is then detected by a radiofrequency receiver coil as a function of time in k-space, which may then be converted to signal strength as a function of frequency using a Fourier transformation to form an image (Huettel, 2004).

3.1.2 Contrasts

Tissues vary in their proton relaxation rates (T1 and T2 values). MRI scanning parameters can be optimised to generate images where the contrast between tissues emphasises the differences in the T1 or T2 values depending on the type of data required. Typically the repetition time (TR), the amount of time between successive pulses applied to the same pulse, and the echo time (TE), the time interval between an excitation pulse and measurement of the signal, can be altered. T1-weighted images (i.e. images sensitive to the relative T1 values of tissues) are acquired using a pulse sequence with short TE (<30ms) and intermediate TR (<500ms). T2-weighted and T2*-weighted images (i.e. images sensitive to the relative T2 and T2* values of tissues respectively) are generated from pulse sequences with an intermediate TE (>80ms) and longer TR (>2000ms) (Huettel, 2004). Gradient-echo sequences are most commonly used to generate T2*-weighted images. For functional MRI, T2*-weighted images need to be acquired more rapidly than for structural neuroimaging in order to reflect physiological changes in the brain and generally have a TR of 1-3s. A technique known as echo-planar imaging is used for such purposes.

Motion-weighted contrasts such as diffusion-weighted images can also be acquired which exploit the direction of movement of water molecules within tissues.

3.2. BOLD fMRI

Functional MRI measures the blood oxygenation level-dependent (BOLD) signal which reflects the changes in magnetic properties of haemoglobin. Oxygen is

carried by haemoglobin in the blood. When haemoglobin is oxygenated (oxyhaemoglobin) it is diamagnetic and does not cause local inhomogeneities in the magnetic field. When haemoglobin is not oxygenated (deoxyhaemoglobin) it is paramagnetic due to the presence of unbound-iron containing haem-groups and thus causes local inhomogeneities. These inhomogeneities cause dephasing of protons, whereby higher levels of deoxyhaemoglobin lower the $T2^*$ signal whereas lower levels of deoxyhaemoglobin increase the $T2^*$ signal. Importantly, levels of deoxyhaemoglobin are influenced by different factors including the cerebral metabolic rate of oxygen, cerebral blood flow and cerebral blood volume (Huettel, 2004). Changes in blood oxygenation reflect changes in brain activity by neurons requiring oxygen (Heeger and Ress, 2002). The time-course of the MRI BOLD signal in response to increased neuronal activity is known as the haemodynamic response function (HRF) and is well characterised (Heeger and Ress, 2002). The HRF shows an initial dip due to oxygen consumption, followed by a large increase due to the oversupply of oxygenated blood (peak 4-6 seconds after stimulus onset) and then another dip below baseline whereby cerebral blood flow returns to normal before cerebral blood volume causing a relative increase in deoxyhaemoglobin (Figure 5). Hence the BOLD signal is an indirect measurement of oxygen usage by the brain which can be measured using gradient-echo sequences employed in fMRI (Ogawa et al., 1990; Ogawa et al., 1992). The increase in the HRF reflects the relative decrease of deoxyhaemoglobin in relation to oxyhaemoglobin as a result of increased blood flow. It has been suggested that the initial dip in the HRF may be a better marker of neuronal activity since it reflects changes in neuronal oxygen consumption prior to changes in cerebral blood flow, but this

remains a matter of debate since the 'dip' has not been demonstrated consistently across fMRI studies (Heeger and Ress, 2002).

Which component of neuronal activity elicits the BOLD response is unclear. There remains debate as to whether BOLD reflects changes in local field potentials, that is, synchronized dendritic currents averaged over a large volume of tissue reflecting inputs to an area, or neuronal firing reflecting outputs, although there is some evidence that BOLD activity is more tightly coupled to the former (Logothetis et al., 2001; Heeger and Ress, 2002).

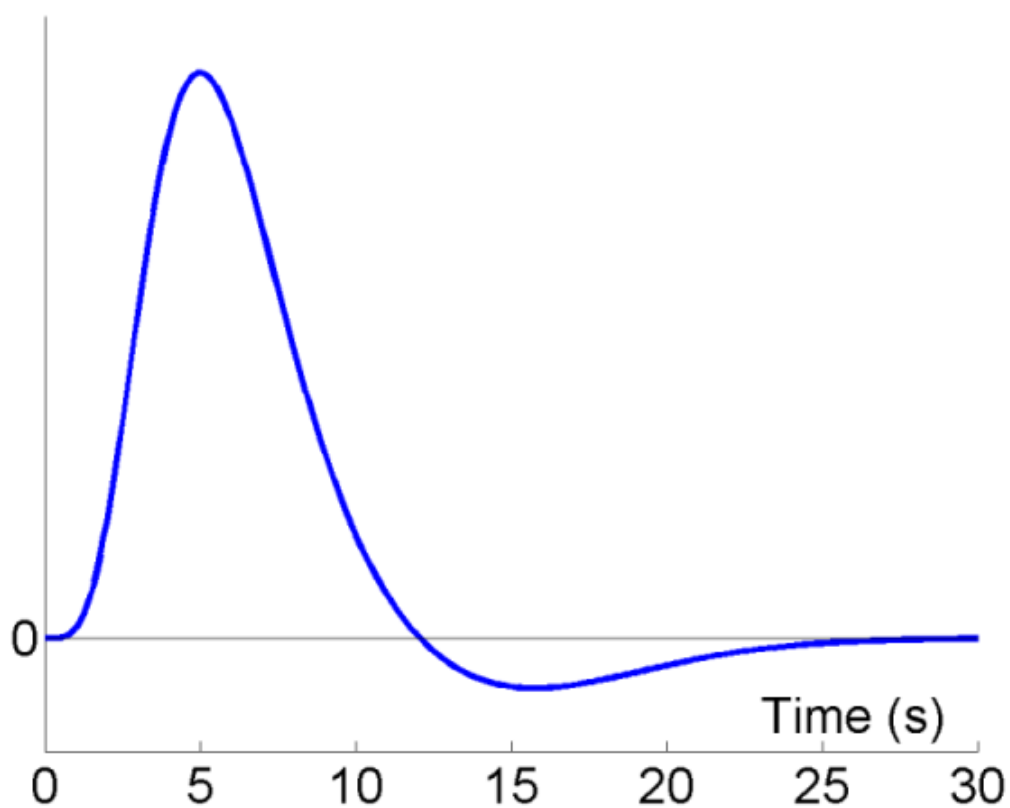


Figure 5. The typical BOLD response.

Y-axis represents percentage signal change. Adapted from Henson 2008

(<http://imaging.mrc-cbu.cam.ac.uk/imaging/DesignEfficiency>).

3.3. fMRI preprocessing

Preprocessing of functional images is performed before statistical analysis to reduce variability in the data not associated with the experimental task. The standard preprocessing steps used in the fMRI experiments in this thesis are described below (summarised in Figure 6) and have been implemented using SPM8 (Wellcome Trust Centre for Neuroimaging, London, www.fil.ion.ucl.ac.uk/spm). Note the initial six images acquired during each fMRI time series have been discarded in keeping with standard practice to allow longitudinal magnetization to reach a steady state.

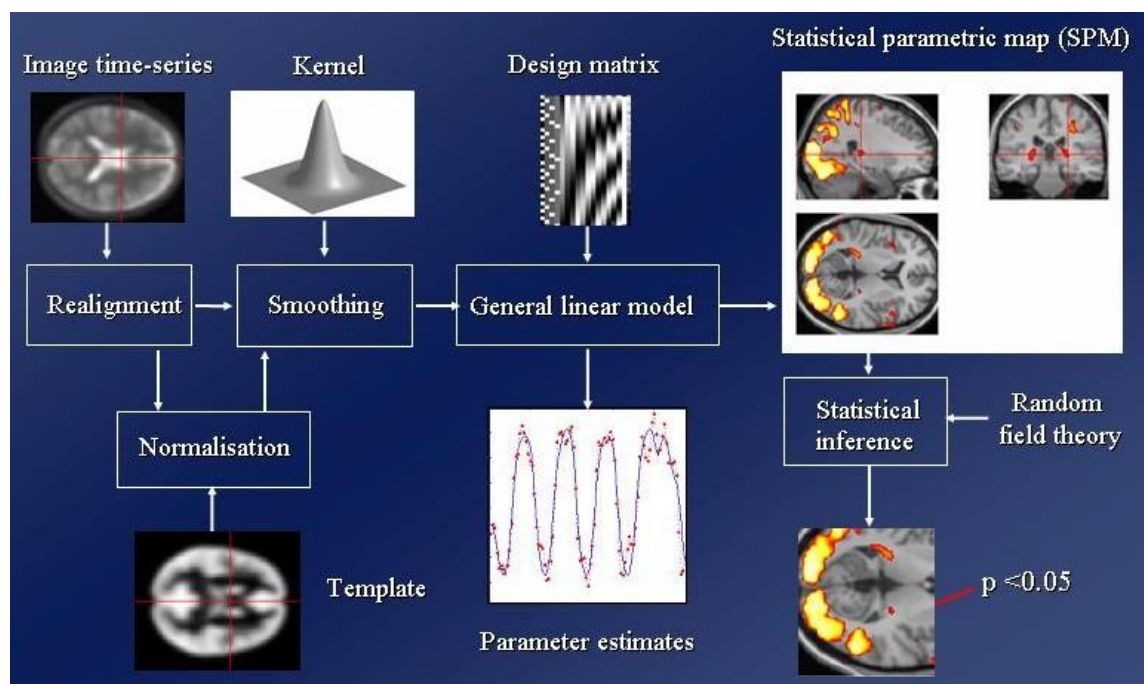


Figure 6. fMRI preprocessing.

Outline of the stages of processing beginning with raw MRI data and ending with a statistical parametric map. Reproduced from (Flandin and Friston, 2008).

3.3.1 Realignment and unwarping

A large source of variance in fMRI data comes from head movement and therefore realignment is performed to align a time-series of images acquired from the same subject so that the brain is in the same position in every image. The initial step of registration determines the six parameters of the rigid body transformation (three translations and three rotations) between each source image and a reference image, which is the first image in the acquired time-series, followed by transformation. Inhomogeneities in the magnetic field distort images in a non-linear manner which interacts with subject movement within the scanner. Thus a further step of unwarping is performed to correct for non-rigid deformations. This requires a field map image to be collected which explicitly measures the magnetic field inhomogeneities and is used to calculate a static deformation field (i.e. local deflections throughout the magnetic field). Unwarping then uses a forward model to estimate and correct for changes in the deformation field due to subject movement at each time point (Andersson et al., 2001).

3.3.2 Normalisation

To align images between subjects to a standard space, normalisation is performed. This allows findings to be generalised to the population level and reported using a standard co-ordinate system, facilitating cross-study comparisons. In this thesis, the Montreal Neurological Institute (MNI) standard space is used. SPM uses an intensity based approach to perform normalisation. This is first achieved by within-subject coregistration of the mean

realigned/unwarped functional image to their structural T1-weighted image using a rigid-body transformation, estimated by maximising the mutual information between the two images. Next, segmentation is performed to classify the structural T1-weighted image into grey matter, white matter and cerebrospinal fluid (Ashburner and Friston, 2005) and a nonlinear deformation field is used to map this onto template tissue probability maps. This map is then applied to spatially normalise both the structural and functional images. In this thesis, information encoded within the ‘flowfields’ generated by the diffeomorphic registration algorithm (DARTEL) are used to warp images to MNI space (Ashburner, 2007).

3.3.3 DARTEL

Diffeomorphic Anatomical Registration using Exponentiated Lie algebra (DARTEL) is a method developed by John Ashburner (Ashburner, 2007) to achieve more accurate inter-subject registration. Prior to applying DARTEL, image segmentation is performed to produce grey and white matter images, followed by rigid transformation of these maps to produce images that are closely aligned to tissue probability. The first step of DARTEL involves creation of a cohort-specific initial template (an average of the aligned maps), followed by an iterative process whereby the nonlinear deformations from the template to the individual images are calculated and then a new template is formed from the images after applying the inverse transformation of the deformations. The deformation for each individual is stored as a ‘flow field’ which can be applied to both structural and functional MRI data and used to normalise images to MNI

space. DARTEL is highly accurate and performs particularly well for registration of the brainstem, striatum and hippocampus in comparison to older SPM methods and some other automated registration packages (Klein et al., 2009). DARTEL is used in the normalisation step for both functional and structural data in all studies in this thesis.

3.3.4 Smoothing

Smoothing is performed to both improve the signal-to-noise ratio and to perform analysis under the assumptions of the Gaussian Random Field Theory thus reducing the effective number of statistical tests (Huettel, 2004). In the experiments presented in Chapters 4, 5 and 6, smoothing is done by convolving images with a Gaussian kernel with full-width at half-maximum (FWHM) of 6mm and in Chapter 7 with a Gaussian kernel with FWHM of 8mm.

3.4. Statistical testing

fMRI analysis employs a mass-univariate approach whereby a statistical test is performed at every voxel, within the framework of the General Linear Model. An image of these statistical tests called a statistical parametric map (SPM) can then be generated. In this thesis, all statistical tests were carried out using SPM8.

3.4.1 General Linear Model

The General Linear Model relates a matrix Y containing the data (e.g. BOLD signal observations) to the design matrix X which is a linear combination of all predictor variables (Friston et al., 2006). β is a vector of the parameters to be estimated, to quantify how much each predictor variable in X influences the dependent variable Y .

$$Y = \beta X + \varepsilon$$

β is estimated using Restricted Maximum Likelihood (ReML). ε is a residual error term which encapsulates variance in the data not explained by X , whereby errors are assumed under the GLM framework to be independent and identically distributed (IID). Since this is often not the case, corrections to impose sphericity must be applied. A process of ‘whitening’ can be used, which is an autoregressive model which effectively calculates the degree of correlation between the residuals and applies a correction to remove this from the GLM.

The design matrix contains all experimentally controlled factors, potential confounding factors and covariates of no interest. Each factor is convolved with the haemodynamic response function before being entered as a regressor in the design matrix. Regressors may be categorical, for example coded as 1 or 0 to indicate when a stimulus is presented or not, or parametric whereby the height of the regressor is modulated by the quantity associated with the current trial. A parametric design thus allows the contribution of different dimensions of a stimulus to be quantified. Both categorical and parametric regressors are used in this thesis.

T-tests or F-tests are applied to every voxel to make statistical inferences, resulting in a map of T- or F- statistics across the whole brain (the SPM). T-tests are directional as they test whether estimates are significantly different from zero. F-tests test the null hypothesis that the parameter is zero and are therefore not directional (Friston et al., 2006).

3.4.2 Group analyses

These methods describe conducting analysis at the single subject level. In order to make group comparisons, a between-subjects analysis must be performed. This approach of generalising results from the subject level to the population can be implemented using a two-stage summary statistics approach (Friston et al., 2005). At the 1st-level (within-subject), parameters are estimated for each subject using a fixed-effects model which assumes that the experimental effect is equal across subjects. These contrast estimates are then brought to the 2nd - level (between-subjects) where a random-effects analysis is performed which treats the experimental manipulation as variable across subjects.

3.4.3 Multiple comparisons and Random Field Theory

Since statistical analysis of fMRI data involves a mass-univariate approach of performing statistical tests over a very large number of voxels, there is a high risk of Type 1 errors (incorrectly rejecting the null hypothesis). One approach to this multiple comparison problem is to control the probability of making false positives by using a family-wise error (FWE) correction. Classically this is achieved by performing a Bonferroni correction where the significance level (i.e.

the acceptable level for Type 1 errors) is adjusted according to the number of statistical tests performed. This stringent approach assumes each statistical test is independent. However, in neuroimaging, each voxel in an image is not independent due to a variety of factors, such as the underlying physiological properties and smoothing during preprocessing. Since there are fewer independent observations than there are voxels, a Bonferroni correction may be too conservative. Therefore an alternative approach is to account for this topographical nature of the data. Random field theory considers a static image as a continuous random field with a multivariate Gaussian distribution and continuous error fields. Within this framework, an acceptable Type 1 error rate can be calculated by estimating smoothness in the data to derive the number of independent comparisons ('resolution elements' or resels) and by calculating the expected Euler Characteristic (an estimate of the number of clusters expected to be found by chance at a given statistical threshold) (Huettel, 2004).

Treating the data as co-varying clusters of voxels rather than independent observations means that statistical inferences can be made at the peak level, dependent on the height of the local maxima, or at the cluster level depending on the number of activated voxels in a particular region. Although cluster-level inference has greater sensitivity, it has less spatial localising power. Since many of the studies in this thesis focus on relatively small regions (e.g. SN/VTA), a high degree of anatomical precision is preferred thus I have used peak level inferences.

An alternative to the mass-univariate approach described above are region of interest (ROI) analyses (see Chapters 6 & 7). This targeted approach takes advantage of a priori knowledge about brain regions expected to be involved in

a task. A ROI can be defined manually for each subject (as in Chapter 6), or using an atlas-derived mask (as in Chapter 7) or using automated software (as used in Chapters 4 & 5). An advantage of this approach over whole-brain voxel-based analyses is that each ROI is treated as a single region as opposed to many voxels, thus the number of statistical tests performed and the need to correct for multiple comparisons is reduced. ROI analyses can minimise the need for preprocessing if ROI's are defined in native subject space thus minimising inaccuracies that may be made to the data during steps such as warping. I adopted this approach in Chapter 6 to allow a more precise analysis of relatively small regions (the SN/VTA and STN) such that I could determine inter-individual variability with greater accuracy.

3.4.4 Model-based fMRI

Beyond measuring brain responses to experimental factors, a deeper analysis of fMRI data can be obtained through the use of computational modelling. The principle underlying model-based fMRI is that different models of the same observed data, where the model embodies how the data was generated, are compared (Friston and Dolan, 2010). Such models are formed on the assumption that the brain works to optimise processing, for example minimising prediction errors. Model components from the best fitting model can then be regressed against fMRI data (O'Doherty et al., 2007).

In Chapter 5 I use a standard reinforcement learning model to predict subjects' actual behaviour. This model resides on the hypothesis that dopamine quantitatively codes a prediction of expected value and how this deviates from

the observed reward (the prediction error), and the product of this prediction error and learning rate are used to update future expectations (Behrens et al., 2009). The model parameters are optimised to find the model which best fits the observed data. The trial-by-trial components of the reward prediction error (reward and expected value) predicted by the winning model were then used as parametric modulators of the BOLD response at the time of the outcome in the fMRI analysis. This approach allows identification of regions where the model-predicted time series for reward-prediction errors correlates with the fMRI BOLD signal over time (O'Doherty et al., 2007). Model comparison is integral to this process. To address how good our model predictions were, we plotted the predicted and observed choices which showed a close match and also performing formal model comparison using Bayesian Information Criteria which included penalising for the number of model parameters.

3.5. Quantitative structural neuroimaging

Quantitative MRI mapping can be used to derive imaging parameters that reflect tissue micro-structural architecture and different underlying biophysical properties of structures (Tofts, 2003). These measures include magnetization transfer (MT) imaging which provides an *in vivo* semi-quantitative measurement of underlying structural integrity (Helms et al., 2008a), R1 images which measure longitudinal relaxation and are sensitive to myelin content (Draganski et al., 2011), and R2* images which measure proton transverse relaxation rate and reflect iron content (Martin et al., 2008) (Martin, 2009). I used a dedicated MRI sequence designed at the host institute termed 'multiparameter mapping'

to acquire MT-weighted, proton density and R1-weighted ($1/T_1$) images, and used in-house code to generate quantitative MT, R_2^* ($1/T_2^*$) and R1 maps (Figure 7). In Chapters 4, 5 and 6 I acquired 1mm isotropic multiparameter maps and in Chapter 7, I acquired 0.8mm isotropic multiparameter maps.

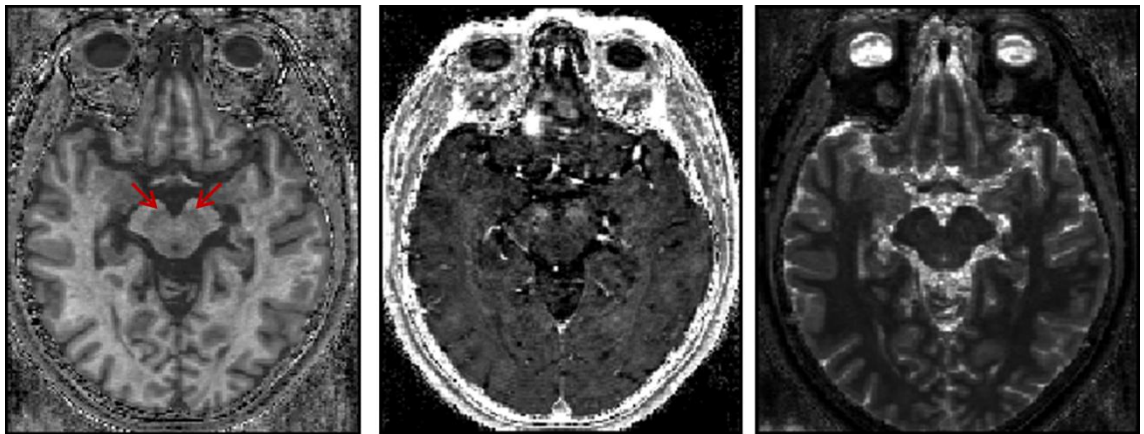


Figure 7. Single subject example of multiparameter maps at 1mm isotropic resolution.

From left to right – MT image, R_2^* image and R1 image. The substantia nigra/ventral tegmental area can be clearly seen on the MT image (arrows). See section 3.5.1 for details of how MT images are generated. R_2^* images are the gradient echo transverse relaxation rate ($1/T_2^*$). The T1 contrast generated from the exponential longitudinal relaxation is used to form R1 ($1/T_1$) images.

3.5.1 Magnetization transfer

MT imaging reflects the properties of protons bound to macromolecules (Wolff and Balaban, 1989) (Figure 8). Conventional T1w sequences measure mobile protons in free water which have longer T2 relaxation times (50-100ms), using *on resonance* radiofrequency pulses. Bound protons associated with macromolecules have a very short T2 relaxation time (microseconds) in comparison to free protons and are therefore 'invisible' to standard MRI (Henkelman et al., 2001). However, the coupling between free and bound protons can be exploited using *off resonance* radiofrequency pulses. Off resonance pulses lead to saturation of magnetization of the bound proton pool and subsequent transfer of magnetization between free and bound protons to re-establish equilibrium. An on resonance pulse can then be applied which now reflects both pools of protons. A consequence of MT is suppression of signal from tissues, which only tissues rich in macromolecular proteins demonstrate. Furthermore, the difference in saturation can be quantified on a voxel-by-voxel basis resulting in semi-quantitative MT imaging parameters (Helms et al., 2008a). MT imaging is sensitive to the properties of the radiofrequency pulse used to saturate the bound pool and therefore is vulnerable to differences between MRI scanners and sequence acquisition, thus limiting multi-centre comparisons.

MT imaging (MTI) reflects the properties of bound protons in structures such as myelin (Tofts, 2003), axons (Klistorner et al., 2011), cell membrane proteins and phospholipids (Bruno et al., 2004). MTI has been used extensively in diseases such as multiple sclerosis to reveal deficits in 'normal appearing white matter' (Filippi et al., 1995) and grey matter (Hayton et al., 2009), in Alzheimer's

disease to show reduced hippocampal MT values (Hanyu et al., 2000) (Ridha et al., 2007) and in temporal lobe epilepsy to demonstrate reduced MT values in the absence of temporal lobe volumetric differences between patients and controls (Flugel et al., 2006). MTI is particularly suited to visualising brainstem structures as it provides better grey/white matter contrast (Helms et al., 2009). In Parkinson's disease, where there is a dramatic decline in nigro-striatal dopamine neurons, there is a decrease in MT signal in the SN/VTA possibly reflecting disruption of the neuromelanin scaffolding (Eckert et al., 2004; Düzel et al., 2008; Tambasco et al., 2011).

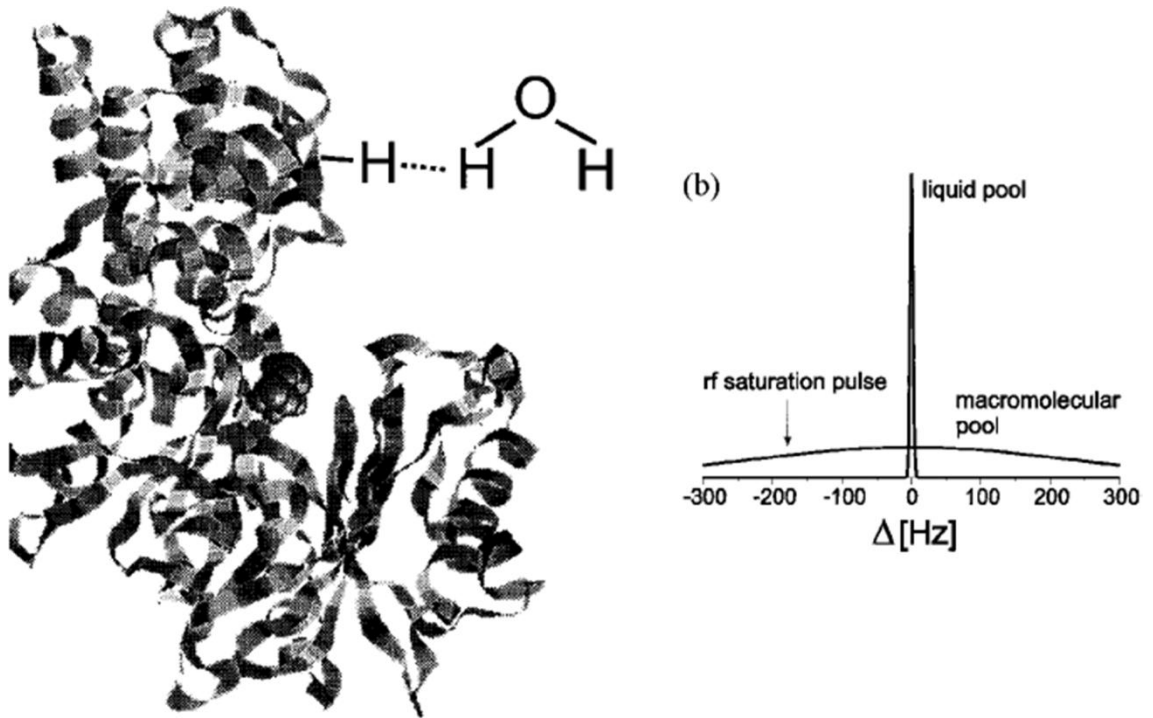


Figure 8. Magnetization transfer.

Magnetization is transferred between bound macromolecules and free water protons. An off-resonance radiofrequency pulse can be applied to saturate the bound 'macromolecular' pool (right, broader shape), with subsequent transfer of magnetization between free protons in the 'liquid pool' (right, narrower shape) and bound protons. Adapted from (Henkelman et al., 2001).

3.5.2 Diffusion tensor imaging

Diffusion tensor imaging (DTI) is a structural imaging technique which provides a marker of tissue organization and is based on the principle that water diffuses more readily along the principle axis of an axon than perpendicular to it. Thus although both DTI and MTI reflect tissue integrity, measurements from the former are based on directionality. Additionally, probabilistic diffusion tractography can be used to generate connectivity profiles from individual voxels within grey matter 'seed' regions to different target regions (Behrens and Johansen-Berg, 2005). These connectivity profiles are markers of the relative strength of white matter fiber connections between subregions of the seed structure and target regions. These maps have close correspondence to the results of histological tract tracing studies (Seehaus et al., 2012) (Klein et al., 2007) (Dyrby et al., 2007) and relate to inter-individual differences in cognition and behaviour (Cohen et al., 2009) (Forstmann et al., 2011; Forstmann et al., 2012).

The random movement of molecules over time through a medium due to thermodynamic effects is called diffusion. In a homogenous medium, diffusion is the same in every direction ('isotropic'). In contrast, in a non-homogeneous medium, diffusion is restricted in certain directions ('anisotropic'). Such is the case in axons, whereby diffusion occurs primarily along one axis. Thus in white matter fiber tracts, water principally diffuses along the length of the fiber rather than across the width of it and hence diffusion is largely anisotropic, whereas in grey matter structures, diffusion is less anisotropic.

MRI can be used to exploit this directionality in tissue by applying magnetic gradients that allow the MR signal to be sensitive to the direction of diffusion in tissues, thus generating a diffusion-weighted MRI contrast. In anisotropic diffusion, the motion of molecules resembles an ellipsoid in comparison to when diffusion is isotropic and resembles a sphere. An ellipsoid has three principle directions which can be described mathematically as a three-by-three tensor by extending Fick's law which describes diffusion in one direction. The tensor is characterised by three orthogonal directions or 'eigenvectors' each of which has an associated length or 'eigenvalue'. To determine the values of the six unique tensor elements, a minimum of six directionally-sensitized and one non-diffusion-sensitized measurements ('b0' image) are required. The aim of the DTI pulse sequence is therefore to apply controlled gradients in many different directions to allow the best fit of the diffusion tensor at every voxel. The higher the intensity of the gradient, known as the 'b-value', the higher the sensitivity to the diffusion effect. However, this is limited by MRI hardware and lower signal-to-noise.

Fractional anisotropy (FA) is a commonly used DTI metric calculated from the eigenvalues of the tensor and may represent, amongst other things, directionality-based structural integrity (Johansen-Berg, 2010). FA values characterise the extent of water diffusion every voxel with values ranging from zero (full isotropy) to one (full anisotropy). Mathematically, FA values represent the standard deviation of the eigenvalues normalised by the tensor magnitude. Mean diffusivity (MD) is another DTI metric which quantifies the average diffusion (average of the three eigenvalues) at every voxel and therefore, in contrast to FA, is independent of direction. FA and MD maps can be analysed

by various different techniques including voxel-based quantification (Draganski et al., 2011).

DTI tractography is a technique based on estimating the likelihood of a pathway existing between brain regions. Tractography can be performed using a deterministic or probabilistic model (the latter is used in Chapter 6). Deterministic tractography assumes there is one principle direction per voxel. Probabilistic tractography takes into account that there is a degree of uncertainty with regards to the determination of the principle eigenvectors' orientation by instead estimating the probability distribution of the principle direction of diffusion at every voxel (Behrens et al., 2003). This probability field is then sampled thousands of times to build a connectivity distribution that reflects the probability of connection with the seed voxel. The benefit of this method is that tracking can be performed in regions with high uncertainty, allowing tracking closer to grey matter targets. This method is also quantitative, thus the probability ('strength') of connectivity between regions can be calculated and related to other behavioural and functional measures, providing a more in-depth analysis of structure-function relationships. There are some methodological limitations of DTI tractography. For example, tractography is less accurate in regions where fibres cross or 'kiss'. DTI is less able to recognise smaller white matter bundles, an issue which may be addressed by improving spatial resolution and gradient strength.

DTI is performed using echo-planar imaging and therefore, like fMRI, is susceptible to B0 inhomogeneities. DTI also employs the application of strong gradients which can introduce another artefact called 'eddy current distortions'

which must be corrected during preprocessing. Other preprocessing steps are described in Chapter 5.

3.6. Analysis of structural neuroimaging

3.6.1 Voxel-based morphometry

Voxel-based morphometry (VBM) is a voxel-wise analysis of the local concentration of grey matter (Ashburner and Friston, 2000). This technique allows whole-brain structural changes to be related to performance. The preprocessing steps are as follows (some of which overlap with fMRI preprocessing and have already been described): segmentation of images into different tissue classes, inter-subject registration using DARTEL (Section 3.3.3), normalisation to a common template (Section 3.3.2) and smoothing (Section 3.3.4). Voxel-wise statistical tests can then be performed using the GLM framework. Two preprocessing steps, segmentation and modulation are described here in more detail.

3.6.1.1 Segmentation

To analyse structural differences in grey matter using VBM, images must first be segmented. The studies in this thesis used the New Segment toolbox in SPM8 to achieve this. This unified segmentation routine combines tissue classification, bias correction for image inhomogeneities and image registration into a single generative model (Ashburner and Friston, 2005). A modified mixture of Gaussians model is used to assign voxels to one of four tissue

classes (grey matter, white matter, cerebrospinal fluid and everything else) depending on voxel intensities. This also requires tissue probability maps which contain prior knowledge of the tissue types at different locations in the image and a Bayesian approach of combining these prior probabilities with the model given the data.

One limitation of segmentation algorithms such as this is that each voxel is assumed to contain one tissue type only. Therefore some voxels, such as those at the interface between white matter and ventricles, may be misclassified as grey matter. These so-called partial volume effects are greater with larger voxel sizes and following smoothing. A smoothing/weighting averaging procedure can be used to try to minimise partial volume effects (see VBQ section 3.6.2).

3.6.1.2 Modulation

As previously described, DARTEL is used to perform high-dimensional warps to achieve highly accurate inter-subject registration and normalisation to MNI space. However, if registration is exact then there would be no inter-subject volume differences left to identify. In order therefore to retain individual subject information about the actual amounts of gray matter within structures, modulation can be applied. This involves multiplying warped images by the Jacobian determinants of the deformation field (i.e. the relative voxel volumes). The result is that the signal from a region of a modulated image represents the tissue volume per unit of spatially normalised image. For example, as described in Ashburner and Friston (2001), if a subjects' temporal lobe is half the volume of that in the template, the volume will be doubled during normalisation thus the

doubling the number of voxels labelled as grey matter resulting in loss of the original absolute volume information (Ashburner and Friston, 2001). Modulation accounts for this confound by multiplying the volume in this region by its relative volume before and after warping. Thus modulated VBM compares the absolute volume of grey and white matter.

3.6.1.3 Statistical analysis

Statistical analysis of smooth, warped, modulated grey and white matter maps is performed using the GLM framework, as described for fMRI analysis. Thus one image per subject can be entered into a multiple regression model. The experimental manipulation(s) of interest is entered into the design matrix, along with other nuisance covariates such as age and gender. To adjust for differences in global volume, total intracranial volume can be entered as a nuisance covariate or used to perform proportional scaling to adjust the original voxel values (the former method is used in this thesis). As already described, corrections for multiple comparisons across the brain can be addressed using Random Field Theory. For VBM, voxel-level inferences (as used in this thesis) rather than cluster-level statistics should be applied since structural data is highly 'non-stationary' (Ashburner and Friston, 2000). This is in contrast to fMRI data where 'stationarity' of the smoothness is assumed across the whole image. However methods have been developed which correct for non-stationarity which may allow cluster-level statistics to be applied to structural data (Hayasaka et al., 2004). Explicit masking can be used to ensure the same number of voxels per subject are included in the analysis.

VBM results are thought to reflect differences in grey matter volume or concentration, although the translation to underlying cytoarchitectonic differences is less clear. A multimodal approach of combining VBM with other measures such as different quantitative imaging parameters (MT, $R2^*$ etc), PET, fMRI and actual histology will help to enhance the interpretation of findings. It should also be noted that problems with preprocessing such as misregistration or misclassification, as well as differences in cortical folding and thickness may result in VBM differences.

3.6.2 Voxel-based quantification

Voxel-wise analysis of quantitative multiparameter maps (VBQ) proceeds along similar lines to the VBM preprocessing and analysis steps described above. One improvement is the use of MT images for segmentation since these images have a better grey/white matter contrast particularly for subcortical regions. Another is to use a weighting/smoothing procedure to optimise the assignment of voxels to the appropriate tissue class for each of the parameter maps and thus account for partial volume effects (Draganski et al., 2011). This is performed by dividing smooth warped unmodulated parameter maps by the corresponding smooth warped modulated tissue class maps. This process effectively projects the Gaussian smoothing kernel from warped space to native space whilst preserving the weighted average of the parameter value over a region the size of the smoothing kernel (Hutton et al., 2009).

3.7. Neuropsychological tests

For all studies reported in this thesis involving older adults, I administrated a range of standardised neuropsychological tests to elderly participants to ensure they did not have significant cognitive impairments. Both young and old participants also completed questionnaires relating to mood and personality. Here I will briefly describe these tests.

3.7.1 Mini-Mental State Examination

The MMSE is a widely used brief screening instrument for dementia that tests a restricted range of cognitive functions (Folstein et al., 1975). Out of a maximum possible score of 30, scores above 27 are considered normal and scores less than 24 suggest dementia. The MMSE is most effective at discriminating moderate and severe dementia rather than milder cognitive changes from normal subjects. Therefore I used a cut-off score of <28 as an exclusion criteria, but participants were additionally required to perform within the normal range on a range of neuropsychological tests to ensure normal cognitive function.

3.7.2 Beck Depression Inventory

The BDI is a 21 item self-report rating scale measures current depressive symptoms (Beck et al., 1961). For each item, participants rate themselves on a scale from 0 to 3, where an increasing scores represents greater severity of the depressive symptom. Total scores less than 11 are considered within the normal range, scores of 11-16 indicative of mild mood disturbance and scores

>16 suggest clinical depression. This scale was used in Chapter 7 whereby participants scoring >10 were excluded.

3.7.3 Geriatric Depression Scale

The GDS is another self-report measure of current depressive symptoms for use in the elderly, consisting of 30 yes/no questions (Yesavage et al., 1982). A cut-off score of 11 is used to indicate depression. I used the GDS in studies in which only older adults participated (Chapters 4, 5 and 6).

3.7.4 Rey Auditory Verbal Learning Test

This RAVLT is a test of verbal learning and memory (Lezak et al., 2004). A list of 15 nouns (List A) is read aloud to the participant at a rate of one per second. The subject is then asked to repeat back as many words as they can remember in any order. The words are recorded in order of recall. This procedure is repeated for a further four trials. A second word list consisting of 15 different nouns (List B) is then read aloud and participants must recall as many words from the new list as possible. Immediately afterwards, participants are asked to recall as many words as possible from the first list without hearing them again (Trial 6). Finally, after a delay of 15 minutes, participants are asked to recall as many words from List A as possible without hearing them again (Trial 7). The total score from Trials 1-5 was used as a measure of immediate recall, and the number of words on Trial 7 as a measure of delayed recall. A recognition component of the task was also administered but is not reported here. Trial 7 (delayed free recall) is particularly sensitive at differentiating between Alzheimer's disease and normal aging (Estévez-González et al., 2003) and thus

I excluded participants who scored outside of the of the age-related norm for this measure.

3.7.5 Trail-Making Test

This is a test of attention, speed and mental flexibility (Reitan, 1955) (Lezak et al., 2004). Part A consists of 25 encircled numbers which participants are required to join in ascending order. Part B requires participants to alternate between numbers and letters thus also testing attentional shift. The time taken to complete each part and the number of errors made was recorded.

3.7.6 Forward and Backward Digit Span

These are both subtests from the Wechsler Adult Intelligence Scale and are considered to be tests of working memory (Lezak et al., 2004). Participants hear a sequence of digits read by the examiner at a rate of one digit per second and are then instructed to repeat the sequence in the same order (Forward Digit Span) or reverse order (Backward Digit Span). There were two items for each sequence and if the subject failed both the next trial was not attempted. The highest number of digits correctly recalled in their serial order was used to define digit span.

3.7.7 Visual Object and Space Perception

I used Test 7 (Number Location) (Warrington and James, 1991) to test space perception. Participants see a card containing two squares. The upper square contains randomly arranged numbers and the lower square contains one black

dot. Participants are required to indicate which number in the upper square corresponds to the position of the dot in the lower square. The number correctly located (out of 10) is recorded.

3.7.8 Digit Symbol Substitution Test

This test of attention is also part of the Wechsler Adult Intelligence Scale (Lezak et al., 2004). This pencil-and-paper task consists of the numbers 0-9, each paired with a nonsense symbol. A blank grid of 100 unpaired randomly ordered numbers is presented to the participant, where they are required to fill in the appropriate symbols for each number consecutively within 90 seconds. The score is determined by the number of correct substitutions.

3.7.9 Controlled Oral Word Association Test

This is a test of verbal fluency (Benton, 1967). To assess phonemic fluency, participants are asked to generate as many words as possible in 60 seconds beginning with the letter 'F'. This is repeated for the letters 'A' and 'S'. The total number of words and perseverative errors are recorded. Proper nouns and repetitions were excluded. To test for semantic fluency, participants are asked to generate the names of many animals as possible in 60 seconds.

3.7.10 Tridimensional Personality Questionnaire

The Tridimensional Personality Questionnaire (TPQ) is a 100 item questionnaire which measures three personality dimensions: Novelty Seeking, Reward Dependence and Harm Avoidance, each of which contains four

subscales (Cloninger, 1987a). These personality traits are thought to be heritable and stable over time. Reward dependence has been linked to the noradrenergic system, novelty seeking to the dopaminergic system and harm avoidance to the serotonergic system (Gardini et al., 2009). High novelty seeking personality scores reflect a trait towards 'frequent exploratory activity in pursuit of potential rewards as well as active avoidance of monotony and potential punishment' (Cloninger, 1987b). An inverse association between D2 receptor binding in the ventral midbrain and novelty seeking suggesting a heightened dopaminergic response to novelty in those scoring higher on this subscale (Zald et al., 2008), and a positive relationship between fMRI activation in the nucleus accumbens signalling positive prediction errors in high novelty seeking individuals (Abler et al., 2006) have been reported.

3.7.11 National Adult Reading Test

The NART provides an estimate of intellectual ability (Nelson, 1982). The test consists of a list of 50 phonetically irregular words which the subject must read aloud. The number of correct words is recorded and converted to an estimate of pre-morbid IQ. Words can only be pronounced correctly if the subject is familiar with them and so is independent of current cognitive capacity. Since minimal effort is required to read the words, it is also relatively resistant to poor concentration or motivation.

3.7.12 Bond and Lader Visual Analogue Scales

This test of subjective affect consists of 16 100mm visual analogue scales, for example ranging from alert to drowsy, and withdrawn to sociable (Bond and

Lader, 1974). Participants indicate with a vertical mark on each scale how they are feeling at the moment of the test. The scales load onto three factors: how alert, calm and content people feel, derived from a factor analysis. These scales were used in Chapters 4 & 5 to measure effects of pharmacological manipulation on subjective mood in comparison to placebo.

Chapter 4

Dopamine and episodic memory

4.1. Introduction

Converging evidence from animal studies suggests that dopamine critically contributes to the cellular consolidation of hippocampal-dependent memories by inducing protein-synthesis in hippocampal neurons (Frey and Morris, 1997; O'Carroll et al., 2006). Behavioural evidence from episodic-like memory paradigms in animals show that the availability of dopamine within the hippocampus during encoding is necessary for long-lasting memories (four to six hours and longer), but does not influence memory across short delays (30 minutes) (Bethus et al., 2010). Consequently, weakly encoded events not leading to dopamine release in the hippocampus can be recollected after short-delays but are forgotten after delays of six hours and longer (O'Carroll et al., 2006; Bethus et al., 2010). Testing for a similar role in human episodic memory requires manipulation of dopamine levels at encoding with subsequent testing of memory after both short and long retention intervals (Wang and Morris, 2010; Lisman et al., 2011).

A key prerequisite for characterizing the role of dopamine in human episodic memory consolidation is to relate the effects of dopamine to the strength of hippocampal activation at encoding. This is because the hippocampal release of

dopamine can be enhanced by strong hippocampal activation (for a review see (Lisman et al., 2011)). If increasing dopamine levels in humans improves memory performance after long delays through similar mechanisms to that seen in animal studies (O'Carroll et al., 2006; Bethus et al., 2010), dopamine administration should improve long-term memory for events that elicit only weak hippocampal activity at encoding, events that normally would be associated with low levels of hippocampal dopamine. This predicts that increasing availability of dopamine would decrease the influence of hippocampal activation at encoding, measured using functional MRI (fMRI), on delayed memory.

Here I tested these hypotheses amongst healthy older adults in a pharmacological fMRI study. I chose an elderly population as my target group for two reasons. Firstly, understanding the role of dopamine in episodic memory is of particular relevance in old age where a decline in episodic memory is well recognised (Light, 1991; Hedden and Gabrieli, 2004; Randy L, 2004). Secondly, there is known age-dependent degeneration of substantia nigra/ventral tegmental area (SN/VTA) dopamine neurons (Fearnley and Lees, 1991; Bäckman et al., 2006). Consequently, I recruited 32 healthy older adults who participated in a double-blind crossover study with the dopamine-precursor levodopa (L-DOPA) and placebo. Participants performed an fMRI encoding task in which they viewed indoor and outdoor scenes and episodic memory for these scenes was tested after two hours ('early test') or six hours ('delayed test') (Figure 9). I used an additional manipulation of reward as a way of manipulating endogenous mechanisms of dopamine-related memory enhancement and to compare its effect on memory consolidation to the exogenous manipulation through the administration of L-DOPA. Thus half the stimuli were

probabilistically associated with reward and half with no reward. In order to account for the possibility that the effect of L-DOPA may depend on the structural integrity of the SN/VTA in older participants, I used a semi-quantitative MR imaging technique called magnetization transfer (MT) imaging (Wolff and Balaban, 1989; Helms et al., 2009). It is known that the cognitive effects of dopamine are dose-dependent (Knecht et al., 2004), often showing a non-linear dose-response curve (Goldman-Rakic et al., 2000; Cools et al., 2001; Li and Sikström, 2002; Takahashi et al., 2008). To account for such a possibility also in episodic memory, I conducted planned correlations between body-weight adjusted relative doses of L-DOPA and behavioural and encoding-related functional outcomes measures.

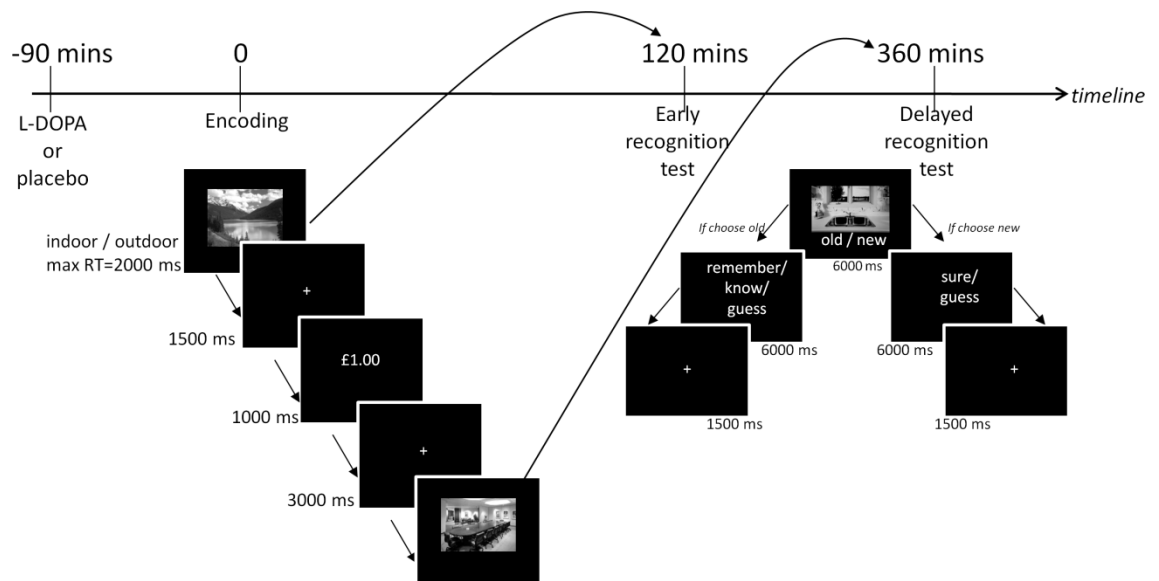


Figure 9. Experimental timeline.

In the fMRI scanner, participants viewed randomly presented images of scenes and were required to indicate whether they were indoor or outdoor scenes with a button press. 80% of correct responses for one category were followed by a reward (£1.00) and for the other category was followed by a neutral outcome (£0.00), thereby the images served as reward-predicting and neutral cues respectively. Following this outside the scanner, memory for half the scenes were tested two hours after encoding ('early') and the remaining scenes six hours after encoding ('delayed') using a remember/know paradigm.

4.2. Methods

Participants: I recruited participants via our departmental website, advertisement in local public buildings and word of mouth. To ensure participants were healthy, volunteers were initially screened by telephone and excluded if they had any of the following: current or past history of neurological, psychiatric or endocrinological disorders (including diabetes mellitus and thyroid dysfunction), metallic implants, tinnitus, major visual impairment, history of drug addiction. To control for vascular risk factors, individuals known to have had a stroke or transient ischemic attack, myocardial infarction or require more than one anti-hypertensive medication were not eligible for participation. All participants had a Mini-Mental State Examination score ≥ 28 and a Geriatric Depression Scale score ≤ 7 (a score > 11 would indicate depression). All participants performed within 1.5 SD of age-related norms on a range of neuropsychological tests, ensuring they were cognitively intact as follows: Rey Auditory and Verbal Learning Test (RAVLT) trials 1-5 (mean 50.2, SD 8.3), RAVLT trial 7 (mean 9.5, SD 2.3), D2 cancellation test of attention (mean 152.3, SD 33.5), Digit Span Forward (median 8, range 4 – 9), Digit Span Backward (median 5, range 3 – 8), Controlled Oral Word Association test (COWA) phonemic fluency (mean 58.0, SD 14.0), COWA semantic fluency (mean 26.5, SD 6.6) and Visual and Object Space Perception number location (median 10, range 8-10). All subjects had a normal neurological examination (performed by a neurologist R.C.) ensuring participants did not have concurrent undiagnosed neurological conditions. Written informed consent was obtained from all participants. The study received ethical approval from the North West London Research Ethics Committee 2.

Participants in the current study ($n = 32$) were selected from a larger sample of 42 healthy older adults aged 65 – 75 years who had participated in a previous study within the preceding six months. Preselection was based on an assessment of magnetization transfer (MT) values of the SN/VTA. MT imaging is a semi-quantitative MR imaging technique that reflects structural integrity (Wolff and Balaban, 1989) where lower MT values suggest less structural integrity (Eckert et al., 2004; Düzel et al., 2008; Tambasco et al., 2011). 10 individuals with MT values of the SN/VTA scattered around the mean MT values of the group were excluded to increase the variance in the sample, resulting in 16 participants with higher MT values ('high integrity' group) and 16 with lower MT values ('low integrity' group). Note that the current cohort still had a normal distribution of midbrain integrity in both the final subset of participants for the behavioural analysis ($n=29$: Kolmogorov-Smirnov test statistic = 0.11, $p = .200$) and the fMRI analysis ($n=23$: Kolmogorov-Smirnov test statistic = 0.093, $p = .200$). The two MT groups were matched for age (independent t-test, $p = .208$) and closely matched for gender (low group 12 females, high group 9 females; Mann Whitney U test, $p = .272$).

Three subjects were excluded from all analyses. Of these, two were excluded due to poor performance in the encoding task (<60% correct indoor/outdoor judgement) consequent upon side-effects of L-DOPA (vomiting during the encoding task) or misunderstanding the task instructions. One other participant misunderstood the instructions for the first remember/know test and was excluded from all analyses. With regards to side-effects of L-DOPA, four subjects vomited of whom one was excluded as noted above. For the other three participants, this brief side-effect occurred after the encoding task had

been completed and their encoding performance was >98% correct, thus I did not exclude them from my analyses.

Study procedure: I used a double-blind placebo controlled crossover design. Participants attended on two occasions, one week apart and performed the same task on both days, 90 minutes after ingestion of either levodopa (150mg levodopa + 37.5mg benserazide mixed in orange juice; L-DOPA) or placebo (orange juice alone), the order of which was counterbalanced. Benserazide promotes higher levels of dopamine in the brain whilst minimising peripheral side-effects such as nausea and vomiting. I chose a dose of 150mg as a previous study has shown that although 100mg can improve verbal learning in younger adults, those with a lower body-weight who effectively received higher doses showed a greater effect (Knecht et al., 2004). To achieve comparable drug absorption across individuals, subjects were instructed not to eat for up to two hours before commencing the study. Repeated physiological measurements were recorded on both days before and after the pharmacological manipulation, which showed a reduction in blood pressure from baseline to 90 minutes after L-DOPA (from average 148/82 to 142/80; paired t-tests systolic $t = 3.12$, $p = .004$; diastolic $t = 2.46$, $p = .020$) but no change in heart rate. Subjective mood rating scales were also recorded. This series of 16 visual analogue scales collapsed down to measure three factors: how alert, content and calm participants felt (Bond and Lader, 1974). When baseline levels were taken into account, there was no significant difference in these subjective mood rating scales at encoding after receiving L-DOPA compared to placebo. For the early and delayed memory tests, the only

significant difference was at early test where participants felt more content on the day they received L-DOPA compared to placebo (mean difference in scores 5.06, SD 11.1, paired t-test $t = 2.37$, $p = .027$).

fMRI encoding task : I presented participants with 120 grey-scale images of indoor ($n=60$) and outdoor ($n=60$) scenes in a randomised fashion (Figure 9). Different images were used on each of the two test days. Participants were required to indicate with a button press whether the image was of an indoor or outdoor scene (response required within 2s). After a brief delay (fixation cross, 1.5s), this was followed by either a reward (indicated by £1.00) or neutral outcome (indicated by £0.00) (outcome, 1s) and finally a further fixation cross (3s). 80% of correct responses for each category of scenes predicted either a reward or no reward. For each participant, which category predicted reward (indoor or outdoor) was different on the two test days and this order was counterbalanced across subjects.

Prior to pharmacological administration, participants were familiarized with the encoding task through ten practice trials using different images. During this practice task the outcome was not probabilistic. Participants were told which category (indoor or outdoor) would be rewarded, with this category remaining the same for the study task. The purpose of this was to ensure by the time participants performed the task in the scanner, they would anticipate a reward when they saw images in the rewarded category (thus serving as reward predicting cues) and vice versa for the unrewarded category (serving as neutral cues).

Participants were given written and verbal task instructions that included the following: 'pay attention to all the images presented as we may return to some of them later in the day'. This same instruction was given on both days without being explicitly told on the second day that they would be performing memory recognition tasks again to minimise practice effects. After completion of the encoding task, participants immediately went on to have further scanning to acquire diffusion tensor images on one day (not reported here) or were asked to sit alone in a room for an equivalent amount of time and not perform any activities on the other day. All participants also completed a brief unrelated decision-making task prior to performing the encoding task on both days (not reported here).

Behavioural recognition tasks: I tested memory for scenes shown during the fMRI encoding task behaviourally two hours and six hours after encoding (henceforth referred to as the early and delayed test respectively) using a remember/know paradigm. For the early test, participants were shown a random selection of half of the scenes they had previously viewed during the encoding task (30 indoor and 30 outdoor scenes) and 30 new distractor scenes (15 indoor and 15 outdoor). Memory for the remaining scenes intermixed with another set of 30 new distractor images was tested at the delayed test. For both tests, whilst the scene was displayed participants indicated with a button press whether the image was old (seen before during the encoding task) or new (never seen before) (maximum reaction time 6s). I also asked for a second decision in relation to the stimuli (maximum reaction time 6s): if they chose 'old' then participants had to commit to one of three further options: remember, know

or guess, where 'remember' indicated they could recollect something specific about the study episode. If the image was confidently familiar, but they had no recollective experience they were instructed to choose 'know'. Guess responses were given when unsure that the image was old. If participants indicated the picture was 'new' then a further decision was made of whether they were sure or had guessed. Remember responses are thought to reflect hippocampal-dependent episodic memory recollection, whereas know responses index familiarity (Yonelinas et al., 2002).

I chose to perform the early test of memory two hours after encoding (3.5 hours after L-DOPA/placebo administration) to minimise the potential confounding factor of persisting drug effects at early but not delayed test. Thus I was able to test participants' memory on two occasions after a short and long interval, ensuring they were not under the peak effects of L-DOPA on both occasions, whilst still allowing a sufficient time window between the tests to investigate my hypothesis that L-DOPA modulated consolidation (four to six hours post-encoding). I acknowledge that by performing the early test of memory after a two hour delay, the consolidation process may have already begun, but I would expect the effects to be less pronounced than at delayed test.

Behavioural analysis: For the encoding task I calculated the percentage of correct indoor and outdoor responses and reaction times for these responses. For the early and delayed memory tests, hit rates were calculated as a proportion of correctly encoded items for the condition of interest. Corrected hits were calculated as correct old responses minus old responses for new items

(false alarms). I then separated this into corrected remember hits (remember responses for correct old items minus remember responses for false alarms) and corrected know hits (know responses for correct old items minus know responses for false alarms). Corrected hit rates were calculated for the following conditions: reward-predicting scenes at early test on placebo, neutral scenes at early test on placebo, reward-predicting scenes at early test on L-DOPA, neutral scenes at early test on L-DOPA, reward-predicting scenes at delayed test on placebo, neutral scenes at delayed test on placebo, reward-predicting scenes at delayed test on L-DOPA and neutral scenes at delayed test on L-DOPA. Although all analyses were performed using corrected hit rates, I also report uncorrected hit rates and false alarms, d' and response bias for completeness. D' and response bias were calculated using standard Excel formula (Stanislaw H and N., 1999). I analysed hit rates using a 2 x 2 x 2 mixed ANOVA with drug (L-DOPA/placebo), time of test (early/delay) and reward (reward-predicting scenes/neutral scenes) as the within-subjects factors, and SN/MTA integrity group indexed by MT values (low integrity/high integrity) as a between-subjects factor.

Given evidence of an inverted U-shape relationship between dopamine and working memory, I hypothesised a similar relationship for episodic memory. Since the effective dose of L-DOPA is dependent on body-weight (Zappia et al., 2002), I calculated the weight-adjusted dose for each participant (150/body-weight, mg/kg). I then performed regression analyses using both linear and quadratic models, where corrected remember and know hit rates were the dependent variable and the weight-adjusted dose of L-DOPA was the independent variable.

I also grouped participants into three 'dose groups' (referred to as low, middle and high dose groups). I note that within these groupings, there were no significant differences in health-related variables or neuropsychological test performance as follows: years of education (one-way ANOVA, $F = 0.364$, $p = .698$), blood pressure ($F = 2.120$, $p = .139$), smoking status ($F = 0.225$, $p = .800$), cholesterol status ($F = 1.465$, $p = .250$), IQ ($F = 0.316$, $p = .732$), RAVLT trials 1-5 ($F = 0.352$, $p = .707$), RAVLT trial 7 ($F = 1.302$, $p = .290$), D2 cancellation test of attention ($F = 0.738$, $p = .488$), Forward Digit Span ($F = 3.17$, $p = .066$), Backward Digit Span ($F = 2.096$, $p = .143$), phonemic fluency ($F = 0.045$, $p = .956$), semantic fluency ($F = 0.023$, $p = .977$) and Visual and Object Space Perception ($F = 0.379$, $p = .689$).

I report results significant at the threshold $p < 0.05$. All significance tests are two-tailed.

Neuroimaging

All imaging was acquired using a 3.0T Trio MRI scanner (Siemens) with a 32-channel head coil.

Anatomical MRI data acquisition: A structural multi-parameter map protocol employing a 3D multi-echo fast low angle shot (FLASH) sequence at 1mm isotropic resolution (Helms et al., 2008b) was used to acquire MT weighted images (echo time, TE, 2.2-14.70ms, repetition time, TR, 23.7ms, flip angle, FA, 6 degrees), T1 weighted images (TE 2.2-14.7ms, TR 18.7ms, FA 20 degrees) and proton density weighted images (TE 2.2-19.7ms, TR 23.7ms, FA 6

degrees) (Helms et al., 2008b). B1 mapping (TE 37.06 and 55.59ms, TR 500ms, FA 230:-10:130 degrees, 4mm³ isotropic resolution) was acquired to correct the T1 maps for inhomogeneities in the transmit radiofrequency field (Lutti et al., 2010). A double-echo FLASH sequence (TE1 10ms, TE2 12.46ms, 3 x 3 x 2 mm resolution and 1mm gap) was used to measure local field inhomogeneities and correct for the image distortions in the B1 mapping data. Using in-house code, quantitative MT maps were extracted for each subject (Helms et al., 2008a).

fMRI data acquisition: Functional data was acquired for each subject on both test days. On each day, two fMRI time series were acquired containing 148 volumes (matrix size = 64 x 74; 48 slices; image resolution= 3 x 3 x 3mm; FOV=192 x 222mm; TR=70ms; TE=30ms). The fMRI acquisition protocol was optimised to minimise susceptibility-induced BOLD signal losses in inferior frontal and temporal lobe regions (Weiskopf et al., 2006b). Six additional volumes at the beginning of each series were acquired to allow for steady state magnetization and were subsequently discarded. Individual field maps were recorded using a double echo FLASH sequence (matrix size = 64 x 64; 64 slices; spatial resolution = 3 x 3 x 3 mm; gap = 1 mm; short TE=10 ms; long TE=12.46 ms; TR=1020 ms) for distortion correction of the acquired EPI images. Using the FieldMap toolbox, field maps were estimated from the phase difference between the images acquired at the short and long TE.

fMRI data preprocessing: Data were analysed using Statistical Parametric Mapping software (SPM8, Wellcome Trust Centre for Neuroimaging, www.fil.ion.ucl.ac.uk/spm). Bias correction (part of the Segmentation step in SPM8) was performed as fMRI data acquired with a 32-channel head coil may be prone to strong intensity inhomogeneities. Pre-processing then included realignment, unwarping using individual fieldmaps, co-registration and spatial normalization to the Montreal Neurology Institute (MNI) space. For normalisation, I used unified segmentation to classify anatomical T1w images into grey matter, white matter and cerebrospinal fluid (Ashburner and Friston, 2005), followed by the diffeomorphic registration algorithm (DARTEL) to generate flowfields to warp EPI images to MNI space (Ashburner, 2007). Finally, data were smoothed with a 6mm FWHM Gaussian kernel. The fMRI time series data were high-pass filtered (cut-off = 128 s) and whitened using an AR (1)-model. For each subject a statistical model was computed by applying a canonical hemodynamic response function (HRF) combined with time and dispersion derivatives.

fMRI data analysis: Statistical analysis was performed using the general linear model (GLM) approach. I used a subsequent memory analysis whereby neural activity at encoding was contrasted for items that were subsequently remembered or forgotten. I built two different GLMs at the first level, the first of which was to determine the overall subsequent memory effect for all 'recognised' items and a second model, more specific to my behavioural results, to determine the subsequent memory effect for items later 'remembered', in particular for neutral items. I collapsed together responses at early and delayed

recall to increase statistical power. For the same reason I excluded participants who had less than 10% of trials in either the remember plus know, remember or forget categories to ensure analyses were statistically robust. Thus whilst GLM 1 involved all 29 participants, GLM 2 included data from 23 participants (note the order of L-DOPA/placebo administration remained counterbalanced for this subset, where 11 participants received L-DOPA on day one and 12 participants on L-DOPA on day two). At the first level analysis, separate design matrices for L-DOPA and placebo were constructed.

GLM 1: Recognised (remember plus know) versus forgotten: At the first level, the design matrix consisted of regressors at the onset of the image presentation for reward-predicting scenes and neutral scenes. These encoding-related responses were modelled separately for items subsequently recognised (correct 'old' responses, thus collapsing both remember and know responses together) and forgotten (incorrect 'new' responses). Thus the following were the main regressors of interest:

- Correct old response for neutral scenes ('recognised')
- Correct old response for reward-predicting scenes ('recognised')
- Incorrect new response for neutral scenes ('forgotten')
- Incorrect new response for reward-predicting scenes ('forgotten')

Separate regressors at the time of the outcome for a win (where participants saw £1.00 on the screen) and no win (where participants saw £0.00) outcomes were included. I included a regressor of no interest for errors when participants failed to press the correct button to indicate whether the image was of an indoor

or outdoor scene. To capture residual movement-related artefacts, six covariates (the three rigid-body translation and three rotations resulting from realignment) were also included as regressors of no interest. Finally I also included 18 regressors for cardiac and respiratory phases in order to correct for physiological noise (Glover et al., 2000; Birn et al., 2006). At the first level, I implemented a contrast for the main effect of memory (recognised > forgotten).

GLM 2: Remember versus forgotten: My behavioural results identified a specific effect of L-DOPA on episodic memory indexed by remember responses. On this basis I performed another analysis where I divided correct 'old' responses into 'remember' and 'know' responses and modelled them as separate regressors.

- Thus, the following constituted the main regressors of interest:
- Correct remember response for neutral scenes ('remember')
- Correct remember response for reward-predicting scenes ('remember')
- Correct know response for neutral scenes ('know')
- Correct know response for reward-predicting scenes ('know')
- Incorrect new response for neutral scenes ('forgotten')
- Incorrect new response for reward-predicting scenes ('forgotten')

All other regressors of no interest used in the previous design were also included in this model. I was then able to contrast remember > forgotten responses at the first level for both rewarded and neutral items together and for neutral items alone.

Since I was predominantly interested in the effect of L-DOPA on memory, for both GLM 1 and 2, contrast images were entered into a paired t-test design at the second level. I was then able to examine the main effect of memory and the interaction between memory and drug (L-DOPA > placebo, and placebo > L-DOPA) using T-contrasts.

Based on an a priori hypothesis that dopamine promotes hippocampal consolidation, I built a functional ROI that included those voxels within the hippocampus that were more active for remembered when compared to forgotten items. I extracted parameter estimates within these voxels using the MarsBaR toolbox (Brett, 2002) and entered them in a two (remember/forget) by two (L-DOPA/placebo) ANOVA. With this approach I was able to test for the effects of drug on the selected voxels. Note that the drug effects are orthogonal to the main effect of memory used to define the functional ROI.

Anatomical masks: I created anatomical masks averaged across my study participants to use for small volume correction and to anatomically constrain functional ROIs from which parameter estimates were extracted. My motivation for this was to account for age-related structural brain changes to try to lend greater accuracy to my analyses. Freesurfer's (version 4.5.0, <http://surfer.nmr.mgh.harvard.edu/>) automated recon-all pipeline was used to parcellate the hippocampus (Fischl et al., 2004). The high level of grey/white matter contrast on MT images was exploited to manually segment the SN/VTA for each subject, performed by a trained individual (R.C) as per Düzel et al (Düzel et al., 2008) using MRICro (Rorden C, 2000). Individual subjects'

hippocampal and SN/VTA masks were warped to MNI space using DARTEL as previously described. A group-averaged mask was made from these warped images. For the bilateral hippocampus, I used 22 subjects' masks, where subjects were excluded due to preprocessing errors (n=6) or inaccurate segmentation after visual inspection (n=1). For the bilateral SN/VTA, all subjects' masks were used.

Statistics: Clusters were defined using a threshold of $p < 0.001$ and > 10 voxels. I report results corrected for multiple comparisons across the whole brain or after small volume correction (SVC) for the bilateral hippocampus and bilateral SN/VTA using family-wise error correction (FWE) at a threshold of $p < 0.05$. I selected the hippocampus and SN/VTA a priori for small volume correction given evidence for a functional SN/VTA-hippocampal circuit underlying the dopaminergic modulation of episodic memory (Lisman and Grace, 2005; Lisman et al., 2011). Imaging results are overlaid on a group-average MT image as the high level of grey/white matter allows good visualisation of both of my main regions of interest (hippocampus and SN/VTA).

Non-linear modulation of neural activity by dopamine: I tested if neural activity was also modulated in a non-linear (i.e. quadratic) manner by L-DOPA. I performed regression analyses using the parameter estimates from functionally activated clusters found in the hippocampus. In these models, parameter estimates were the dependent variable and the weight-adjusted dose of L-

DOPA was the independent variable. A similar regression analysis was performed using MT values of the SN/VTA rather than L-DOPA dose.

4.3. Results

4.3.1 Encoding performance

Demographic data for 29 of the 32 healthy older adults who participated are shown in Table 1. Accuracy for button presses for indoor and outdoor images during encoding was high (mean correct responses 97.6%, SD 2.99). Accuracy was not affected by L-DOPA and reward (main effect of reward: $F(1,29)=3.67$, $p=.07$; main effect of drug: $F(1,29) = 3.62$, $p=.07$; reward*drug interaction: $F(1,29) = 0.15$, $p=.71$), nor was reaction time (main effect of reward: $F(1,29) = 2.44$, $p=.13$; main effect of drug: $F(1,29) = 0.58$, $p=.45$; reward*drug interaction: $F(1,29) = 0.012$, $p=.91$).

Age (yrs)	70.31 (3.22)
Gender M:F	10: 19
Education (yrs)	16.00 (2.63)
National Adults Reading Test IQ	121.38 (6.58)
Body mass index	26.8(4.45)
Non-smoker	28 (96.6%)
Normotensive	27 (93.1%)
Mini-Mental State Examination	30 (28-30)
Geriatric Depression Scale	1 (0-7)

Table 1. Demographic details.

Results are mean (SD), number (%) or median (range).

4.3.2 Dose-dependent enhancement of memory by L-DOPA

All analyses were performed using corrected hit rates (hits minus false alarms as a proportion of correctly encoded trials, for the condition of interest). A summary of uncorrected hit rates and false alarms, d' and response bias are provided in Table 2 and Table 3 respectively.

The ability to recognize old (i.e. previously encoded) items and reject new items was better at early compared to delayed test as shown by a main effect of time ($F(1,27) = 9.505, p = .005$) in a two (drug: L-DOPA/placebo) by two (time of test: early/delay) by two (reward: reward-predicting scenes/neutral scenes) repeated measures ANOVA with structural integrity of the SN/VTA (low integrity/ high integrity) as a between-subjects factor. There was also a time by reward interaction ($F(1,27) = 48.289, p = .000$). Here post hoc tests showed that for reward-predicting images, corrected hit rates were higher at early compared to delayed test (paired t-test, $t(28)=7.178, p=.000$) with no difference evident for neutral items ($t(28) = 1.201, p=.240$). There was no main effect of drug ($p=.530$) and no interactions with drug (drug*time: $p=.797$; drug*reward: $p=.250$; drug*time*reward: $p=.254$). Furthermore there were no significant interactions with SN/VTA structural integrity (integrity group*drug: $p=.169$; integrity group*reward $p=.780$; integrity group*time of test $p=.664$).

	Remember reward hits	neutral hits	reward false alarms	neutral false alarms	Know reward hits	neutral hits	reward false alarms	neutral false alarms
ALL								
Placebo								
early	0.32(0.23)	0.27(0.22)	0.12(0.15)	0.07(0.10)	0.19(0.17)	0.14(0.15)	0.13(0.11)	0.08(0.13)
delay	0.22(0.17)	0.24(0.17)	0.06(0.08)	0.08(0.12)	0.16(0.14)	0.15(0.13)	0.12(0.13)	0.08(0.09)
L-DOPA								
early	0.36(0.22)	0.31(0.19)	0.10(0.13)	0.11(0.11)	0.18(0.14)	0.20(0.16)	0.14(0.15)	0.11(0.12)
delay	0.23(0.23)	0.23(0.16)	0.06(0.09)	0.07(0.11)	0.16(0.13)	0.17(0.13)	0.14(0.13)	0.11(0.11)
LOW								
Placebo								
early	0.22(0.16)	0.25(0.24)	0.10(0.16)	0.07(0.11)	0.28(0.18)	0.19(0.21)	0.17(0.15)	0.15(0.18)
delay	0.15(0.13)	0.19(0.12)	0.04(0.06)	0.04(0.05)	0.22(0.19)	0.20(0.17)	0.13(0.16)	0.11(0.09)
L-DOPA								
early	0.29(0.24)	0.18(0.16)	0.09(0.09)	0.15(0.14)	0.20(0.12)	0.25(0.16)	0.19(0.18)	0.15(0.13)
delay	0.18(0.20)	0.17(0.15)	0.03(0.03)	0.08(0.13)	0.19(0.15)	0.17(0.11)	0.13(0.09)	0.10(0.08)
MIDDLE								
Placebo								
early	0.41(0.27)	0.30(0.22)	0.17(0.15)	0.09(0.12)	0.13(0.13)	0.12(0.13)	0.13(0.12)	0.02(0.03)
delay	0.24(0.14)	0.24(0.16)	0.09(0.09)	0.11(0.13)	0.12(0.10)	0.06(0.06)	0.11(0.12)	0.07(0.11)
L-DOPA								
early	0.45(0.18)	0.43(0.15)	0.16(0.15)	0.11(0.11)	0.16(0.11)	0.18(0.19)	0.14(0.15)	0.12(0.15)
delay	0.35(0.30)	0.37(0.18)	0.10(0.13)	0.08(0.13)	0.13(0.10)	0.17(0.16)	0.11(0.10)	0.13(0.09)
HIGH								
Placebo								
early	0.35(0.22)	0.27(0.21)	0.09(0.13)	0.05(0.08)	0.16(0.16)	0.13(0.08)	0.09(0.34)	0.07(0.09)
delay	0.27(0.22)	0.29(0.22)	0.05(0.07)	0.09(0.15)	0.13(0.09)	0.16(0.12)	0.11(0.09)	0.05(0.06)
L-DOPA								
early	0.34(0.23)	0.31(0.17)	0.06(0.12)	0.06(0.07)	0.18(0.18)	0.17(0.13)	0.10(0.12)	0.07(0.05)
delay	0.17(0.16)	0.18(0.08)	0.07(0.08)	0.05(0.04)	0.16(0.15)	0.15(0.11)	0.19(0.17)	0.11(0.15)

Table 2. Mean hit rates and false alarms for the conditions of interest.

ALL = all participants, n = 29; LOW = low-dose L-DOPA group, n = 10; MIDDLE = middle-dose L-DOPA group, n = 9; HIGH = high-dose L-DOPA group, n = 10. SD in parentheses.

	d'		Response bias	
	reward	neutral	reward	neutral
ALL				
Placebo				
early	0.77 (0.62)	0.88 (0.70)	1.41 (1.48)	1.83 (2.19)
delay	0.66 (0.63)	0.83 (0.68)	1.29 (0.45)	1.86 (2.19)
L-DOPA				
early	0.77 (0.71)	0.81 (0.60)	1.45 (1.68)	1.39 (1.61)
delay	0.56 (0.48)	0.62 (0.59)	1.27 (0.50)	1.49 (1.60)
LOW				
Placebo				
early	0.73 (0.82)	0.55 (0.56)	2.08 (2.43)	1.04 (0.26)
delay	0.79 (0.63)	0.75 (0.78)	1.17 (0.29)	1.25 (0.68)
L-DOPA				
early	0.43 (0.66)	0.43 (0.61)	0.96 (0.24)	1.15 (0.33)
delay	0.56 (0.41)	0.39 (0.48)	1.15 (0.30)	1.18 (0.57)
MIDDLE				
Placebo				
early	0.69 (0.58)	1.19 (0.82)	1.05 (0.29)	3.21 (3.62)
delay	0.68 (0.46)	0.75 (0.71)	1.37 (0.36)	2.41 (2.71)
L-DOPA				
early	0.98 (0.64)	1.04 (0.60)	1.29 (0.84)	1.96 (2.89)
delay	0.87 (0.35)	1.01 (0.70)	1.37 (0.76)	1.96 (2.81)
HIGH				
Placebo				
early	0.89 (0.47)	0.92 (0.64)	1.10 (0.34)	1.38 (0.59)
delay	0.52 (0.77)	0.99 (0.60)	1.34 (0.64)	1.97 (2.69)
L-DOPA				
early	0.91 (0.77)	0.97 (0.44)	2.09 (2.71)	1.12 (0.27)
delay	0.28 (0.50)	0.50 (0.43)	1.30 (0.38)	1.39 (0.58)

Table 3. Mean d' and response bias.

ALL = all participants, n = 29; LOW = low-dose L-DOPA group, n = 10; MIDDLE = middle-dose L-DOPA group, n = 9; HIGH = high-dose L-DOPA group, n = 10. SD in parentheses.

I next performed a planned assessment of the potential dose-dependent effect of L-DOPA using regression analyses with the weight-adjusted dose of L-DOPA (150 mg / body-weight, mg/kg) and corrected remember and know hit rates for each condition separately (Table 4). Remember hit rates for neutral images at early test showed a significant quadratic and linear regression, explaining 28% ($p = .014$) and 22% ($p = .011$) of the variance respectively. At delayed test there was a significant quadratic regression alone, where the weight-adjusted dose of L-DOPA explained 29% ($p = .013$) of variance in an inverted 'U-shape' pattern (Figure 10a). In contrast, L-DOPA dose did not predict remember hit rates for the rewarded scene category, nor did it predict know hit rates for any condition. This points to a modulatory effect of L-DOPA on episodic memory for neutral items.

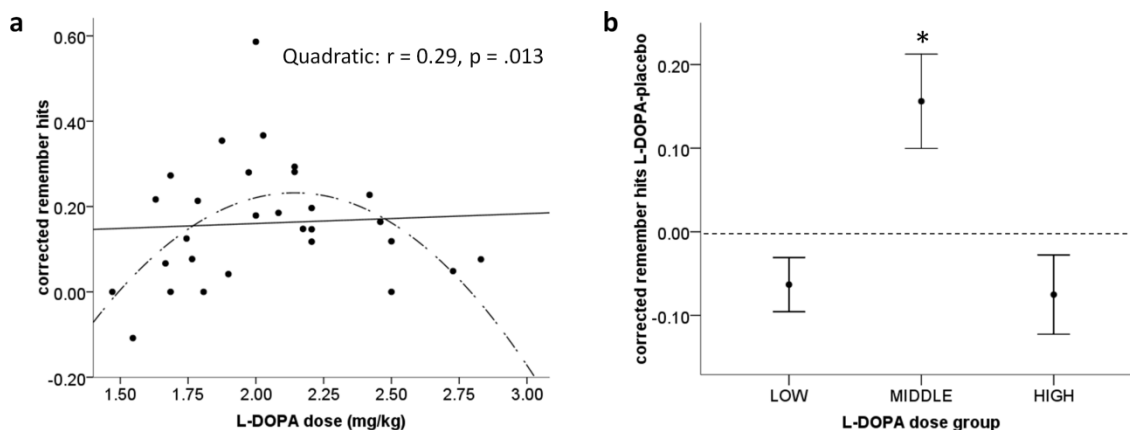


Figure 10. Delayed test results for recollection of neutral items.

(a) Significant quadratic correlation (indicated by the dashed inverted U-shape line) between the weight-adjusted dose of L-DOPA and corrected remember hits for neutral items at delayed test.

(b) Corrected remember hits on L-DOPA minus placebo for participants divided into three groups based on the amount of L-DOPA they received. Performance was significantly different between all three groups and better recollection on L-DOPA than placebo (indicated by performance above the dashed line) was seen for participants receiving the middle dose (average 2mg/kg).

Bars represent mean \pm 1 SEM. * two-tailed $p < 0.05$

Corrected hit rate	Quadratic			Linear		
	F	p	R ²	F	p	R ²
Early test						
Remember Reward	0.587	.563	.043	0.170	.683	.006
Remember No Reward	5.028	.014*	.279	7.463	.011*	.217
Know Reward	1.498	.242	.103	2.986	.095	.100
Know No Reward	0.652	.529	.048	0.950	.338	.034
Delayed test						
Remember Reward	0.365	.698	.027	0.620	.438	.022
Remember No Reward	5.205	.013*	.286	0.088	.769	.003
Know Reward	0.330	.722	.025	0.663	.423	.024
Know No Reward	1.490	.244	.103	0.094	.762	.003

Table 4. Regression analyses between remember and know responses and weight-adjusted dose of L-DOPA.

There was a significant quadratic relationship between dose and early and delayed remember responses for neutral items. A linear relationship was also seen for early remember responses for neutral items. * $p < 0.05$

To further assess whether L-DOPA enhanced memory recollection for neutral scenes, I subtracted hit rates on placebo from those on L-DOPA. To visualise this memory performance difference between L-DOPA and placebo, and to quantify the dose of L-DOPA that boosted memory, I ranked subjects based on the weight-adjusted L-DOPA dose they received and divided my cohort into three groups as follows: 'low' dose group (n=10), who received an average of 1.7 mg/kg L-DOPA, 'middle' dose group (n=9), who received an average of 2.0mg/kg and the 'high' dose group (n=10) who received an average of 2.5mg/kg. Here I saw that for delayed recall of neutral items, memory performance in the middle dose group was higher on L-DOPA than on placebo (one-sample t-test, $t(8)=2.767$, $p=.024$) (Figure 10b). Performance in the low and high dose groups did not differ between drug or placebo ($p = .083$ & $p = .147$ respectively). Performance was significantly different between all three groups (one-way ANOVA $F(2,26) = 7.803$, $p = .002$; low versus middle group, $p=.007$; middle versus high group $p=.005$). This demonstrates that within the 'inverted U-shape' relationship between L-DOPA and episodic memory, L-DOPA significantly enhanced memory performance within a relatively narrow dose range. I note that individual drug-minus-placebo difference scores did not show a significant quadratic correlation with L-DOPA weight-adjusted dose ($F(2,26)=2.518$, $p=.100$), presumably because the difference scores were more noisy than the behavioural scores under the drug.

In contrast, at early test performance did not differ between L-DOPA and placebo for the middle and high dose-groups and participants in the low dose group performed better on placebo than L-DOPA (one-sample t-test, two-tailed: low $t(9) = -3.097$, $p = .013$; middle $t(8) = 1.356$, $p=.212$; high $t(9) = 0.429$,

$p=.678$). There was no significant between-group differences either (one-way ANOVA $F(2,28) = 3.027$, $p=.066$). Overall these results demonstrate that the beneficial effect of L-DOPA on episodic memory was more robust at delayed than early testing.

Modulation of memory performance for neutral items at delayed test by L-DOPA was due to an effect on hits rather than false alarms. This was demonstrated by a significant 3-way interaction between drug (L-DOPA/placebo), memory performance (remember hits/false alarms) and dose group (low/middle/high) ($F(1,26) = 7.80$, $p = .002$). As shown in Figure 11, post hoc tests showed a selective increase in remember hits in the middle dose group compared to the high dose group ($t = 2.36$, $p = .031$) and a trends towards increased remember hits in the middle dose group compared to the low dose group ($t = 1.97$, $p = .065$), with no difference in false alarm rates between groups.

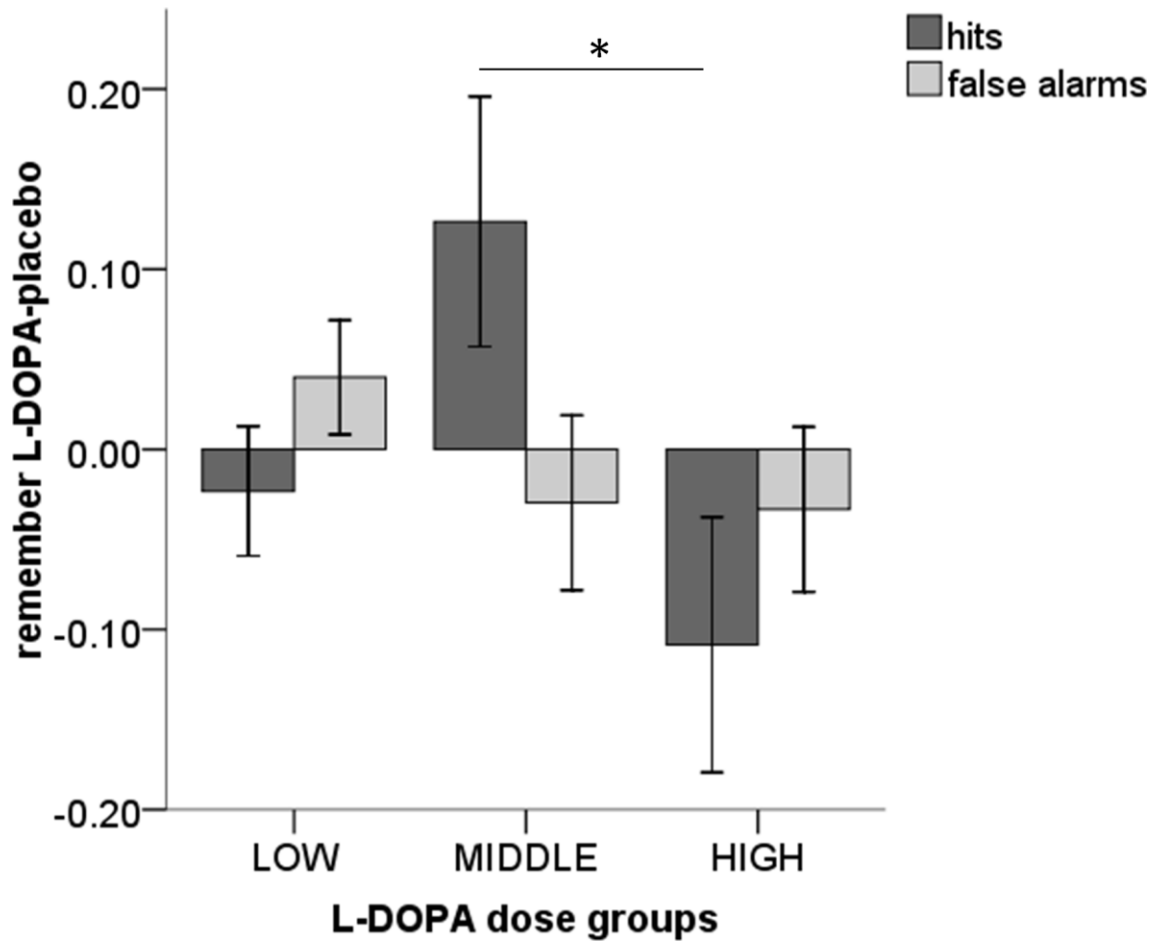


Figure 11. Difference between L-DOPA and placebo remember hits and false alarms for neutral items at delayed test.

The behavioural enhancement of memory by L-DOPA compared to placebo in the middle dose group was due to an increase in remember hits with no change in false alarms. Bars represent mean \pm 1 SEM. * $p < 0.05$

4.3.3 Order effects

To assess for order effects, I performed a repeated measures ANOVA across all responses (remember plus know corrected hit rates) with drug (L-DOPA/placebo), time of test (early/delayed), reward (reward-predicting scenes/neutral scenes) as within-subjects factors, and L-DOPA dose-group (low/middle/high) and order (L-DOPA day 1/ L-DOPA day 2) as between-subject factors. This showed no significant interactions with order (drug*order $p = .183$, drug*dose-group*order $p = .975$, time*order $p = .248$, time*dose-group*order $p = .519$, reward*dose*group*order $p = .962$, drug*time*order $p = .270$, drug*time*dose-group*order $p = .709$, drug*reward*order $p = .723$, drug*reward*dose-group*order $p = .438$, drug*time*reward*order $p = .642$, drug*time*reward*dose-group*order $p = .585$). As a follow-up, to determine if an order effect interacted with the key observation (that L-DOPA modulated corrected remember hits for neutral items), I performed a post hoc ANOVA for these responses only. This also showed no interactions with drug order (drug*time of test*dose-group*order $F = 1.121$, $p = .343$), confirming order effects were not present.

4.3.4 Subsequent memory effects on fMRI data

To analyse subsequent memory effects of the fMRI data acquired during encoding, I contrasted activation for items at encoding that were subsequently recognized (both remember and know responses) with items that were subsequently forgotten (classified as new during test). I collapsed over early and delayed tests and excluded participants with less than 10% of trials in a

category of interest to ensure analyses were statistically robust (where participants are excluded, I report the number of subjects for that particular analysis). The contrast 'remember and know > forget' revealed subsequent memory activation in the left parahippocampal gyrus [Montreal Neurological Institute (MNI) space coordinates (x,y,z) -30,-38,-14; peak Z = 5.02; $p < 0.05$ whole brain FWE] and left mid-occipital gyrus [MNI -44,-72,26; peak Z = 5.27; $p < 0.05$ whole brain FWE] (Figure 12a). This contrast did not reveal activation in the hippocampus or SN/VTA, nor was activity seen in these regions when examining for an interaction between memory and pharmacological manipulation (results at the uncorrected threshold $p < 0.001$ are available on request).

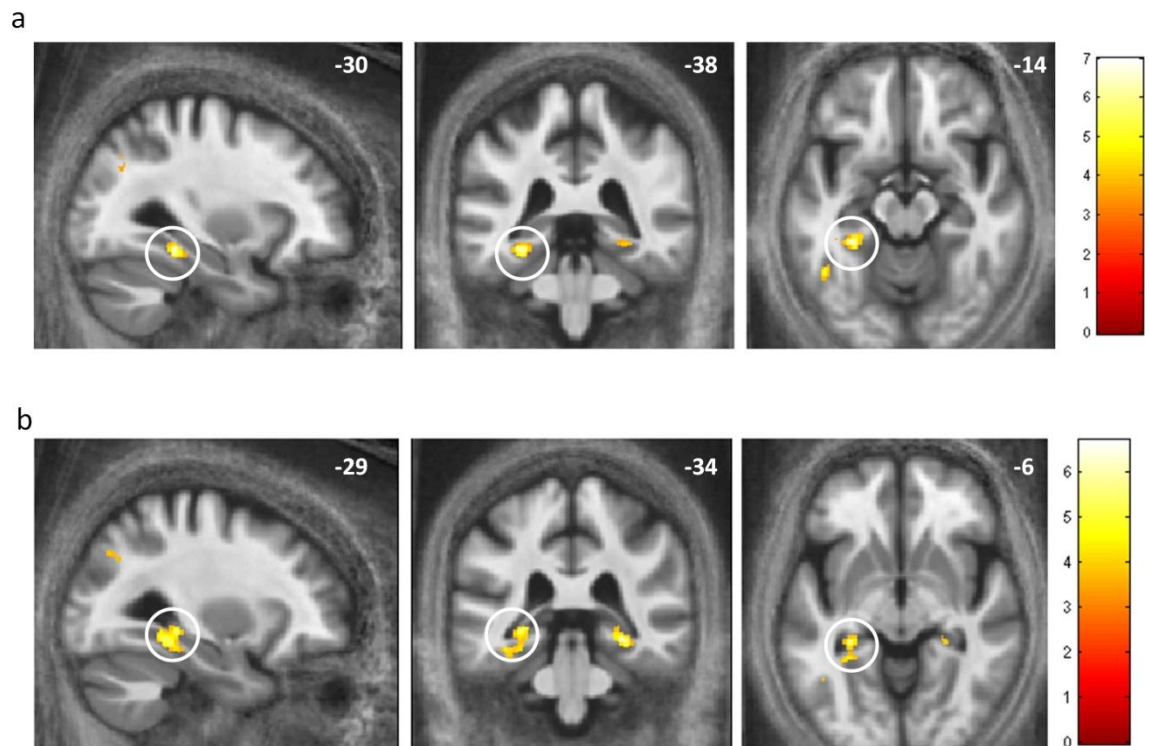


Figure 12. Medial temporal lobe activation for subsequent memory.

(a) Difference in activation for subsequently recognised (remember and know) versus forgotten items in the left parahippocampal gyrus (n=29).

(b) Activation in both left and right hippocampi, extending into parahippocampal gyri for remembered versus forgotten items (n=23). Displayed at the level of peak activation in the left hippocampus (circled).

Images displayed at the uncorrected threshold $p < 0.001$ on a group-averaged magnetization transfer image.

The behavioural effect I demonstrated of L-DOPA on episodic memory (indexed by remember responses) was restricted to neutral items. This motivated a further analysis to identify areas of activation that showed a subsequent memory effect for recollection of neutral items alone (n=23 participants that fulfilled the 10% correct criteria described above). This revealed activation in a cluster extending into the left hippocampus [MNI -26,-33,-11; peak Z = 4.01, $p < 0.05$ FWE SVC for bilateral hippocampus ROI] (Figure 13a; see Table 5 for all uncorrected results). Here there was no main effect of drug using a functional ROI approach ($F(1,22) = 1.952$, $p = .176$) (Figure 13b). For this contrast, I found an interaction between memory (remember > forget) and drug (L-DOPA > placebo) in the SN/VTA [MNI 5,-18,-18; peak Z = 4.15, $p < 0.01$ FWE SVC for bilateral SN/VTA ROI], whereby greater activation for forgotten compared to remembered neutral scenes on placebo was reversed by L-DOPA (see Table 6 for full uncorrected results). Another cluster with a peak in the right ventricle [MNI 20,-37,9; peak Z = 5.07, $p < 0.05$ whole brain FWE; 214 voxels], of which only a small part extended into the right hippocampus [MNI 18,-36,7; peak Z = 4.01, $p < 0.05$ FWE SVC for bilateral hippocampus ROI; 16 voxels] will not be considered further. I did not find any regions of activation for the interaction between memory and placebo > L-DOPA.

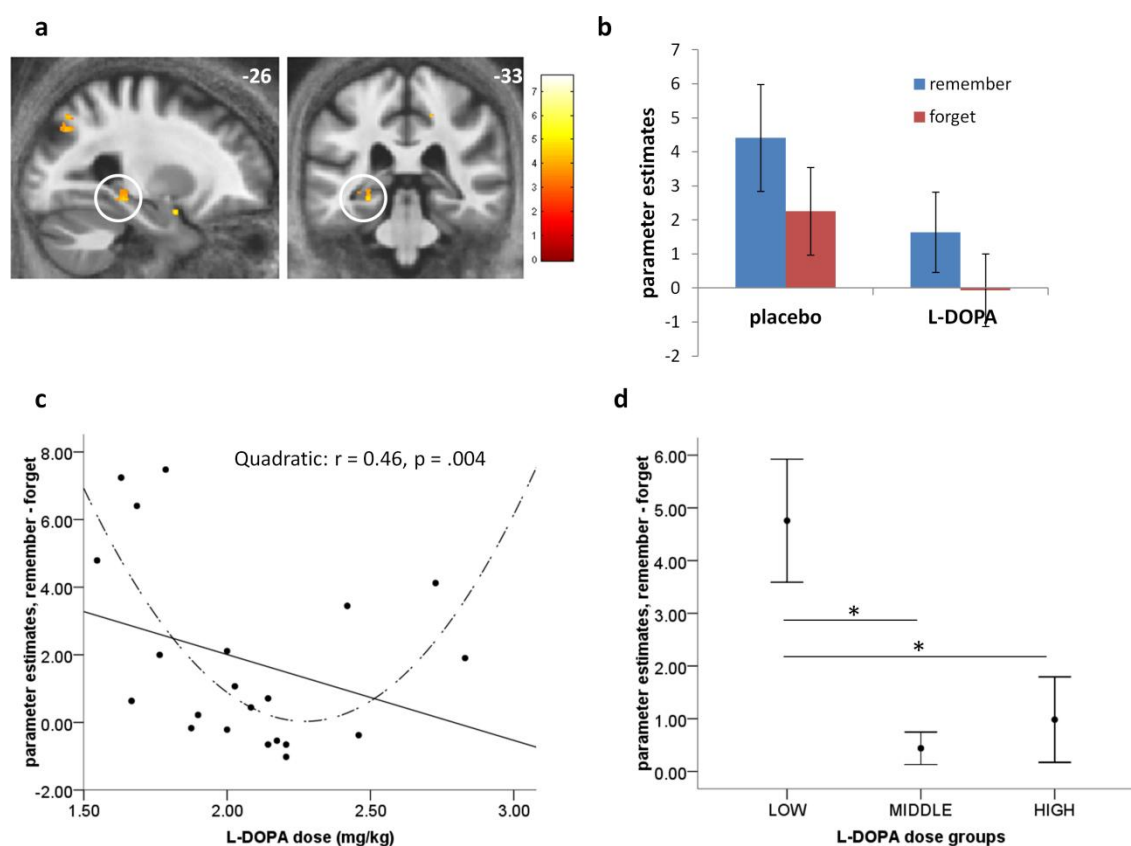


Figure 13. Dose-dependent ‘U-shaped’ modulation of hippocampal activity by L-DOPA.

(a,b) Left hippocampal activity for neutral items that were remembered compared to those that were forgotten.

(c) Parameter estimates from this left hippocampal region ($n=21$) for remembered minus forgotten items showed a non-linear (‘U-shape’) modulation by the weight-adjusted dose of L-DOPA (dashed line), indicating some participants showed no difference in encoding-related activity for subsequently remembered and forgotten items. Thus hippocampal activity at encoding did not predict an improvement in recollection seen in participants receiving the middle dose of L-DOPA (d). Bars represent mean \pm 1 SEM. * $p < 0.05$

No. voxels	T	Z	x	y	z	L/R	region
728	7.64	5.29	-34.5	-82.5	30	L	mid occipital*
41	6.03	4.58	18	-31.5	48	R	mid cingulum
58	5.41	4.27	30	-37.5	-12	R	fusiform
32	5.31	4.22	-42	-54	-10.5	L	fusiform
68	5.31	4.22	34.5	-73.5	34.5	R	mid occipital hippocampal/
217	5.05	4.07	-34.5	-39	-10.5	L	parahippocampal
31	4.93	4.00	-24	1.5	-19.5	L	amygdala
64	4.91	3.99	13.5	-54	21	R	precuneus
84	4.65	3.84	-48	-54	-1.5	L	mid temporal
22	4.31	3.63	0	-37.5	-21		cerebellar vermis
50	4.23	3.58	-9	-52.5	18	L	precuneus
13	4.17	3.54	24	-60	45	R	sup occipital
17	3.98	3.42	-19.5	-60	49.5	L	sup parietal
12	3.78	3.28	30	-79.5	12	R	mid occipital

Table 5. Remembered versus forgotten neutral items.

Uncorrected results $p < 0.001$, > 10 voxels (*whole brain FWE- $p < 0.05$)

No. voxels	T	Z	x	y	z	L/R	region
<u>L-DOPA > placebo</u>							
							ventricle /
214	7.10	5.07	19.5	-37.5	9	R	hippocampus
107	5.84	4.49	54	-25.5	37.5	R	supramarginal
55	5.82	4.48	4.5	-18	-19.5	R	SN/VTA
135	5.76	4.45	6	-60	48	R	precuneus
143	5.44	4.29	-9	-66	54	L	precuneus
200	5.44	4.28	-4.5	-55.5	-4.5	L	cerebellum
65	5.43	4.28	21	-70.5	55.5	R	superior parietal
89	5.32	4.22	9	-7.5	9	R	thalamus
23	4.81	3.94	-31.5	42	39	L	midfrontal
112	4.65	3.84	37.5	-49.5	40.5	R	inferior parietal
26	4.63	3.83	19.5	-58.5	69	R	superior parietal
106	4.56	3.78	31.5	43.5	31.5	R	midfrontal
77	4.44	3.71	-1.5	28.5	21	L	anterior cingulum
14	4.44	3.71	0	-66	15	L	calcarine
							supplementary
48	4.32	3.63	3	21	49.5	L	motor area
82	4.30	3.63	-39	12	1.5	L	insula
39	4.28	3.61	-33	33	31.5	L	mid frontal
26	4.15	3.53	24	-51	-18	R	cerebellum
21	4.12	3.51	0	-70.5	28.5	L	cuneus
39	4.11	3.50	-4.5	-40.5	51	L	mid cingulum
13	4.07	3.47	-1.5	-69	-12		vermis
31	4.02	3.45	-3	-25.5	43.5	L	mid cingulum
14	3.95	3.40	15	-79.5	40.5	R	cuneus
12	3.95	3.39	1.5	-33	40.5	R	mid cingulum
11	3.93	3.38	-7.5	-78	51	L	precuneus
17	3.93	3.38	-16.5	-48	-15	L	cerebellum
14	3.92	3.38	25.5	51	30	R	mid frontal
20	3.91	3.37	-43.5	-40.5	40.5	L	inferior parietal
15	3.82	3.31	-12	-13.5	9	L	thalamus
<u>placebo > L-DOPA</u>							
15	5.02	4.06	15	-31.5	49.5	R	paracentral
88	5.73	3.89	-40.5	-28.5	46.5	L	postcentral

Table 6. Interaction between memory for neutral items (remember > forgotten) and drug.

Uncorrected results, $p < 0.001$, > 10 voxels (no regions whole brain FWE- $p < 0.05$)

4.3.5 Dose-dependent modulation of encoding activity

Given the dose-dependent non-linear effect of L-DOPA on episodic memory performance for neutral events, I extracted parameter estimates from the functional hippocampal cluster for subsequent memory (remember minus forgotten responses for neutral events) on L-DOPA and used this measure in a regression analysis with the weight-adjusted dose of L-DOPA as the independent variable (as used for the behavioural regression analyses).

I found that L-DOPA modulated hippocampal activation for subsequent episodic memory for neutral items in a non-linear 'U-shape' pattern (regression with L-DOPA dose for $n=21$; quadratic: $F(2,18) = 7.68$, $p = .004$, $R^2 = .46$; linear regression: $F(1,19) = 2.27$, $p = .152$, $R^2 = .11$) (Figure 13c). Next, I explored how these parameter estimates related to the previously denoted weight-adjusted dose groups, where I previously identified behavioural enhancement of memory by L-DOPA in those who received the middle dose. Within this cohort of 21 subjects, six participants were from the 'low' dose group, eight from the 'middle' group and seven from the 'high' dose group. Hippocampal parameter estimates significantly differed between the three groups (one-way between-group ANOVA: $F(2,20) = 8.767$, $p = .002$; mean difference between low and middle dose groups = 4.32, $p = .003$; mean difference between low and high dose groups = 3.77, $p = .01$). Figure 13d illustrates that whilst the low dose group showed what could be considered a 'standard' pattern of activation (more activity for subsequently remembered than forgotten items), both the middle and high dose groups showed no difference in encoding-related activity. Thus, I show a dose-dependent reduction of the subsequent memory effect by L-

DOPA, evident in participants whose memory improved on L-DOPA (i.e. the middle dose group).

I found activation in both the left hippocampus [MNI -29,-34,-6; peak $Z = 4.38$, $p < 0.05$ FWE SVC] and right hippocampus [MNI 29,-33,-11; peak $Z = 4.27$, $p < 0.05$ FWE SVC] for items remembered more than forgotten when collapsing across both rewarded and neutral items (Figure 12b; uncorrected results available on request). However these parameter estimates ($n = 21$) were not robustly modulated by the weight-adjusted dose of L-DOPA (left hippocampus: quadratic model $F=3.01$, $p=.074$, linear model $F=1.79$, $p=.197$; right hippocampus: quadratic model $F=0.071$, $p=.932$, linear model $F=0.071$, $p=.793$), which, in keeping with the behavioural results, indicated a high degree of specificity of my neural findings for neutral items.

4.4. Discussion

I show that in healthy older adults, dopamine enhances recollection of neutral scenes in a dose-dependent inverted 'U-shape' pattern, where a dose of approximately 2 mg/kg bodyweight improved recollection in contrast to higher and lower doses which were ineffective. This pattern was not explained by encoding-related activity in the hippocampus, supporting a view that dopamine modulates a post-encoding consolidation process. In fact my data fit neatly with an influential model of molecular consolidation in the hippocampus, where encoding only leads to a short-lasting strengthening of synaptic connections. Dopamine-dependent protein synthesis is then necessary to stabilize and maintain these connections (Lisman et al., 2011). My behavioural data align with these findings in my demonstration that L-DOPA in comparison to placebo impacts primarily on delayed, but not early, recollection performance.

My neuroimaging data reveal whether the benefits of L-DOPA can be attributed to an enhancement in the hippocampal contribution to encoding. Molecular consolidation invokes effects on long-term plasticity as evident in animal models of long-term potentiation (LTP) (Frey and Morris, 1997; Smith et al., 2005; Bethus et al., 2010). There is behavioural evidence in rodents that dopamine antagonists at encoding do not impair hippocampus-dependent memories tested after short delays, but do cause an impairment after long delays (Bethus, Tse et al. 2010). According to the 'synaptic-tagging and capture model', the benefit of dopamine arises out of an effect on protein synthesis linked to consolidation (Frey and Morris 1997; Morris 2003). In fact, this post-encoding benefit of dopamine predicts that items which engender low levels of hippocampal activation at encoding, that may be classed as know or forgotten,

should be 'rescued' by subsequent protein-synthesis. This ability to later remember also weakly encoded events should lead to a decrease of encoding-related hippocampal subsequent memory activation under L-DOPA. My data shows this to be the case where there is a tight dose-response relationship between L-DOPA dose, behaviour and fMRI effects. An fMRI subsequent memory effect in the hippocampus was modulated in a dose-dependent non-linear 'U-shape' manner, whereby it was entirely abolished under an optimal dose of L-DOPA. Note that the combination of behavioural assessment after long-retention intervals and fMRI data from the time of encoding is a key strength of my study allowing, for the first time in humans, identification of a post-encoding mechanism that accounts for improved memory recollection following L-DOPA.

Evidence from molecular imaging studies using PET link dopamine receptor density to cognitive performance, whereby dopamine binding in the striatum and hippocampus correlate with standard neuropsychological measures of immediate recall (Takahashi et al., 2007; Cervenka et al., 2008). Importantly, dopamine loss with age of both D2 receptors and dopamine transporter mediate age-related episodic memory deficits (Bäckman et al., 2000; Erixon-Lindroth et al., 2005). Such studies have used immediate recall as a measure of episodic memory, which suggests that dopamine can modulate encoding processes. My study expands on this empirical molecular imaging evidence by using a functional measure of encoding in relation to subsequent memory tested after long retention intervals to infer dopaminergic modulation of post-encoding consolidation processes.

An inverted U-shape effect of dopamine on working memory performance, which is dependent on dopamine effects within the prefrontal cortex, is well recognised (Williams and Goldman-Rakic, 1995; Goldman-Rakic et al., 2000; Cools et al., 2001). In this model, an optimal dose of dopamine enhances function but higher doses are detrimental. My results show the same effect of dopamine on episodic memory performance, as well as a dose-dependent modulation of hippocampal activity. I suggest that the memory improvement from the optimal dose of L-DOPA results from increased hippocampal protein synthesis. Whilst higher doses of dopamine may increase protein synthesis in the hippocampus, other mechanisms are likely to account for a lack of improvement in recollection. At a molecular level, excess dopamine can induce a long-term depression through inhibition of NMDA receptors, thereby inhibiting memory consolidation (Thirugnanasambandam et al., 2011). At a systems level, a model that explains the physiology underlying the inverted U-shape phenomenon in working memory invokes moderate amounts of dopamine enhancing excitatory inputs to pyramidal cells, with higher levels associated with greater interneuron activity leading to inhibition of pyramidal cells and thus impaired cognitive performance (Goldman-Rakic et al., 2000). It should be noted that my fMRI data rule out an enhanced excitatory input to pyramidal cells as the mode of action through which dopamine boosted late memory under optimal doses. Such a mechanism would have been associated with increased hippocampal activation for subsequently recollected events under the optimal dose of L-DOPA. Finally, although I report the subsequent memory effects of L-DOPA in the SN/VTA for completeness, I did not entertain any specific hypothesis regarding the direction of effect of L-DOPA for this contrast due to

the potential complexity of the effect dopamine exerts in this region (for example, the effect of D2 autoreceptors on the firing rate of neurons as a consequence of manipulating the availability of dopamine). To determine if there is an optimal dose of L-DOPA for boosting the long-term persistence of episodic memories, future studies could combine my paradigm with a wide range of different dosages coupled with a measure of underlying dopamine reserve using molecular imaging methods (e.g. PET).

The dose-dependent effects of L-DOPA on both recollection and hippocampal activity were restricted to neutral items. SN/VTA activation in response to novelty has been previously demonstrated (Bunzeck and Duzel, 2006), suggesting that dopamine neurons are responsive to novelty even in the absence of apparent reward (Duzel et al., 2009a; Krebs et al., 2009; Krebs et al., 2011) . I anticipated L-DOPA would improve memory recollection for neutral items since a novelty induced dopamine release in response to these items would be expected. This is indeed what I found.

It is a well established observation that dopamine release is increased by reward-prediction (Schultz et al., 1997). This effect of reward has been associated with improved long-term memory in younger adults, where recollection was better for reward-predicting compared to neutral items when tested after a delay of three weeks (Wittmann et al., 2005). I included a reward component in my task as a way of manipulating endogenous dopamine release, so as to compare its effect to the exogenous manipulation through administration of L-DOPA. My hypothesis was that reward would shift the dose-response relationship between memory performance at the delayed test and L-DOPA to the left. However, I found no effect of reward on recollection at

delayed test or any interaction with L-DOPA. One possible reason for this is that reward-prediction in my task failed to elicit increased phasic dopamine release. Impaired reward processing, particularly in tasks with probabilistic reward, has been reported with increasing age (Marschner et al., 2005; Schott et al., 2007; Mell et al., 2009; Eppinger et al., 2011) and therefore the effects of reward-predicting cues in my task, both alone and in combination with L-DOPA, may have been more variable. I speculate that an interesting implication of my data is that L-DOPA administration in older adults does not reconstitute the known effects of reward-anticipation, i.e. even under L-DOPA there is no benefit of reward on memory suggesting that a lack of dopamine cannot account for the lack of a reward-related memory enhancement of memory in old age.

I took advantage of the inter-individual variation in body-weight to determine relative dose-dependent effects of L-DOPA, since the effective dose of L-DOPA is dependent on body-weight (Zappia et al., 2002). The enhancement of memory in the middle dose group at delayed test on L-DOPA compared to placebo suggests that memory performance differences were due to the drug rather than body-weight or other variables associated with body-weight. Furthermore, health-related measures and general cognitive performance did not differ between the three body-weight dose groups and therefore were unlikely to account for differences in memory performance. However I acknowledge a limitation of this study is that other unmeasured variables associated with body-weight may have influenced memory performance across participants (Volkow et al., 2012).

Since dopamine loss varies across older individuals, I cannot be certain that all participants responded to L-DOPA in a similar manner. Although I did not have

a true measure of intrinsic dopamine signalling, I obtained MT values of the SN/VTA. This demonstrated inter-individual variability in the structural integrity of dopaminergic midbrain but importantly, did not relate to differences in memory performance or body-weight. Thus MT is one measure that illustrates that although there was variable integrity of the dopaminergic midbrain amongst my cohort of older adults, this did not modulate memory performance or interact with L-DOPA. Hence, I do not have a strong reason to believe that participants showed markedly different physiological responses to L-DOPA. Molecular imaging methods such as PET would be required to characterize body-weight related responsivity to L-DOPA more fully.

The possibility of selectively influencing consolidation in humans, whilst not affecting encoding, has remained largely theoretical (with the exception of sleep-related studies) and to my knowledge my study is the first demonstration of this in conjunction with a measure of encoding activity. By combining behavioural and fMRI data with a pharmacological manipulation, I have identified a specific effect of dopamine on consolidation rather than encoding and could characterize its narrow dose-range. The research I report has wider implications given that an episodic memory decline with increasing age is both common and distressing. Thus far, research into post-encoding consolidation processes in old age has been largely neglected. My findings indicate that this may be an important area for research because by enhancing post-encoding consolidation, memory for weakly encoded events can be rescued. Hence an exogenous modification of consolidation can potentially compensate for hippocampal deficits in encoding, thereby providing a new therapeutic perspective to memory dysfunction.

One intriguing finding from this study was that reward anticipation in older adults did not improve memory, as has been demonstrated in younger adults (Wittmann et al., 2005) (Bialleck et al., 2011). As discussed, this may be related to reward processing deficits in old age. In the next two chapters, I explore this further by examining reward-based decision-making in older age and the effects of dopamine on reward prediction.

Chapter 5

Dopamine and reward prediction

5.1. Introduction

Aging is associated with a range of changes in cognition and behaviour in humans. For example, older adults are particularly poor at making decisions when faced with probabilistic rewards, possibly due to impaired learning of stimulus-outcome contingencies (Eppinger et al., 2011) (Mell et al., 2005). Such findings raise two fundamental questions, namely what are the substrates for learning in these circumstances and what accounts for this aberrant decision-making.

One function critical for such decisions is learning to predict rewards. There is ample evidence in animal experiments that the neuromodulator dopamine encodes the difference between actual and expected rewards (so-called 'reward prediction errors') (Schultz et al., 1997; Salamone et al., 2005). In humans there is now compelling evidence that functional activation patterns in the nucleus accumbens, a major target region of dopamine neurons (Haber et al., 2000), report rewarding outcomes and associated prediction errors (O'Doherty et al., 2003; O'Doherty et al., 2004; Daw et al., 2006; Knutson and Gibbs, 2007). A more direct link to dopamine is seen using pharmacological challenge with dopaminergic agents (Pessiglione et al., 2006; Rutledge et al., 2009).

In terms of what might go wrong an important clue is an age-related loss of dopamine neurons within the substantia nigra/ventral tegmental area (SN/VTA) (Bäckman et al., 2006) (Duzel et al., 2010), evident both in histology and when using diffusion tensor imaging (DTI) as a marker of structural degeneration (Fearnley and Lees, 1991) (Vaillancourt et al., 2012). However, the consequences of this decline in dopamine for decision-making are unclear because of functional interactions among the triplet of representations of the reward, representations of prediction errors associated with that reward, and the learning of predictions that underpins the expression of those prediction errors. In older age, abnormal activity in the nucleus accumbens has been associated with suboptimal decision-making and reduced reward anticipation but normal responses to rewarding outcomes (Samanez-Larkin et al., 2010) (Schott et al., 2007) (Cox et al., 2008). This has led to the suggestion that although older adults may maintain adequate representations of reward, they are unable to learn correctly from these representations. Interestingly, financial decision-making in older adults can be improved to match that of younger adults when additional value information is provided (Samanez-Larkin et al., 2011).

I studied the effect of probabilistic rewarding outcomes on the separate reward and prediction components of a prediction error signal (Behrens et al., 2008) in healthy older adults. To that end, I employed a simple probabilistic instrumental conditioning problem - the two armed bandit choice task (Figure 14A). Older adults underwent DTI and fMRI in combination with a pharmacological manipulation using the dopamine precursor levodopa (L-DOPA) in a within-subject double-blind placebo-controlled study. For behavioural comparison, I

tested younger adults using the same two armed bandit choice task without pharmacological manipulation. By using a reinforcement learning model I could determine which component of the prediction error (the actual and/or expected reward representation) was impaired in old age. DTI enabled us to examine nigro-striatal structural connectivity strength, based on a hypothesis that individual differences in this structural measure would predict inter-individual differences in baseline functional reward prediction error signalling. Crucial here is the fact that pharmacological enhancement of dopamine levels has been associated with greater prediction errors in younger adults (Pessiglione et al., 2006) and higher learning rates in patients with Parkinson's disease (Rutledge et al., 2009). I therefore predicted that boosting dopamine would increase the learning rate evident in behaviour as well as boost the representation of a reward prediction error in the nucleus accumbens of healthy older adults, specifically by increasing the component associated with the expected value.

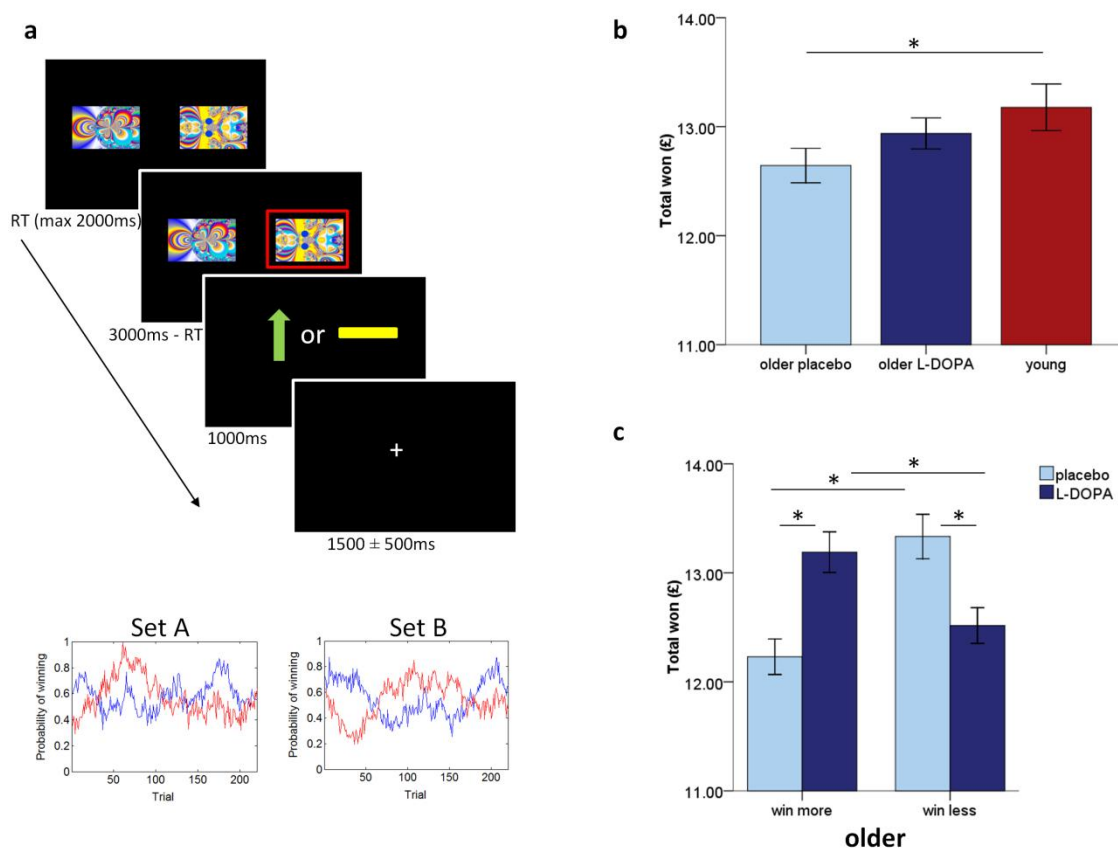


Figure 14. Task design and performance in young and older adults .

(a) On each trial, participants selected one of two fractal images which was then highlighted in a red frame. This was followed by an outcome where a green upward arrow indicated a win of 10 pence and a yellow horizontal bar indicated the absence of a win. The probability of obtaining a reward associated with each image varied on a trial-by-trial basis according to a Gaussian random walk. Two different sets of probability distributions (Set A and Set B) were used on the two testing days, counterbalanced across the order of L-DOPA/placebo administration.

(b) Older adults ($n = 32$) in the placebo condition won less money than younger adults ($n = 22$). When the same older adults ($n = 32$) received L-DOPA, performance was similar to younger adults.

(c) Older adults were divided into groups depending on whether they performed better on L-DOPA than placebo ('win more', $n = 15$) or performed worse on L-DOPA than placebo ('win less', $n = 17$). Baseline (i.e. placebo) performance was not equal in the two groups, resembling an 'inverted U-shape'.

* $p < 0.05$. Error bars indicate $\pm 1\text{SEM}$.

5.2. Methods

Older subjects

32 healthy older adults aged 65 – 75 years (see Table 7 for demographics) were recruited via advertisement in local public buildings, our departmental website and from a database of healthy volunteers held at King's College Hospital, London. Individuals were initially screened by telephone and excluded if they had any of the following: current or past history of neurological, psychiatric or endocrinological disorders (including diabetes mellitus and thyroid dysfunction), metallic implants, tinnitus, major visual impairment, history of drug addiction. To control for vascular risk factors, individuals known to have had a stroke or transient ischemic attack, myocardial infarction or require more than one anti-hypertensive medication were not eligible for participation. All participants had a Mini-Mental State Examination score ≥ 28 , Geriatric Depression Scale score ≤ 7 (a score > 11 would indicate depression) and a normal performance (within 1.5 SD of age-related norm) on a range of neuropsychological tests as follows: Rey Auditory and Verbal Learning Test (RAVLT) trials 1-5 (mean 50.2, SD 8.3), RAVLT trial 7 (mean 9.5, SD 2.3), D2 cancellation test of attention (mean 152.3, SD 33.5), Digit Span Forward (median 8, range 4 – 9), Digit Span Backward (median 5, range 3 – 8), Controlled Oral Word Association test (COWA) phonemic fluency (mean 58.0, SD 14.0), COWA semantic fluency (mean 26.5, SD 6.6) and Visual and Object Space Perception number location (median 10, range 8-10). All subjects had a normal neurological examination (performed by a neurologist R.C.) ensuring participants did not have concurrent undiagnosed neurological conditions.

Age (yrs)	70.00 (3.24)
Gender M:F	11:21
Education (yrs)	16.28 (2.88)
National Adults Reading Test IQ	121.72 (6.36)
Body mass index	26.6 (4.40)
Non-smoker	31 (97%)
Normotensive	30 (94%)
Mini-Mental State Examination	30 (28-30)
Geriatric Depression Scale	1 (0-7)

Table 7. Demographic details of 32 older adults.

Results are mean (SD), number (%) or median (range) for 32 participants.

Written informed consent was obtained from all participants. The study received ethical approval from the North West London Research Ethics Committee 2.

Participants in the current study were selected from a larger sample of 42 healthy older adults aged 65 – 75 years who had participated in a previous study within the preceding six months. Preselection was based on an assessment of magnetization transfer (MT) values of the SN/VTA in relation to another study performed by the same participants. MT values of the SN/VTA were normally distributed across the sample of 32 participants in the current study and MT did not correlate with any measures used in this study (behavioural, model parameters, functional parameter estimates or DTI metrics).

Four participants experienced side-effects (emesis) from L-DOPA administration. These participants remained in all analyses as they vomited more than 2.5 hours after L-DOPA ingestion, well after completion of the task and they did not feel unwell when performing the task in the scanner.

Younger subjects

In a control behavioural experiment, 22 healthy young adults (mean age 25.18 yrs, SD 3.85; 12 females) were recruited via the University College London subject pool and word of mouth. Participants were screened to ensure they were healthy with no history of neurological, psychiatric or other major health disorders, no medications, no recent illicit drug use and no recent participation in other research studies involving medication. These participants performed the same behavioural task on a laptop with no pharmacological manipulation and no MRI scanning.

Study procedure

This was a double-blind within-subject placebo controlled study. Older participants attended on two occasions, one week apart and performed the same task on both days, 60 minutes after ingestion of either levodopa (150mg levodopa + 37.5mg benserazide mixed in orange juice; L-DOPA) or placebo (orange juice alone), the order of which was counterbalanced. Benserazide promotes higher levels of dopamine in the brain whilst minimising peripheral side-effects such as nausea and vomiting. To achieve comparable drug absorption across individuals, subjects were instructed not to eat for up to two hours before commencing the study.

Repeated physiological measurements (blood pressure and heart rate) and subjective mood rating scales (Bond and Lader, 1974) were recorded on both days on arrival and just prior to task performance. For all measurements, I calculated the change from baseline to prior to performing the task, and compared these difference measures drug and placebo (paired t-tests, two-tailed). Heart rate was significantly lower following placebo compared to following L-DOPA (64 bpm and 68 bpm respectively, $t = -3.65$, $p = .001$). Systolic blood pressure was significantly lower following L-DOPA compared to placebo (141 and 152 respectively, $t(30) = 2.61$, $p = .014$) whereas diastolic blood pressure was unchanged (81 and 83 respectively, $t(30) = 1.632$, $p = .113$). There was no significant difference in how alert ($t = -0.68$, $p = .502$), content ($t = 1.24$, $p = .224$) or calm ($t = -0.11$, $p = .911$) participants rated themselves as feeling after receiving L-DOPA compared to placebo. After completing the task, on both days participants performed an unrelated episodic memory task and on one day had DTI scanning.

Task design

Figure 14A depicts the task. Participants were given both written and verbal instructions and undertook five practice trials before pharmacological manipulation. On each trial of this two armed bandit choice task, participants chose one of two stimuli (abstract fractal images; later I designate them as actions 0 and 1) within a 2 seconds time-window. The chosen image was then highlighted in a red frame (total duration image displayed = 3 seconds) and followed by an outcome of either a green upward-pointing arrow (indicating a win of 10 pence) or a yellow horizontal bar (indicating the absence of a win),

displayed for 1 second, followed by a jittered fixation cross (1 ± 0.5 seconds). If they did not choose a stimulus, the written message “you did not choose a picture” was displayed. The same pair of images was used throughout the task, although their position on the screen (left or right) varied. The task consisted of 220 trials separated into two sessions with a short break in between. Participants’ earnings were displayed at the end of the task and given to them at the end of the test day.

The probabilities of obtaining a reward for each stimulus were independent of each other and varied on a trial-to-trial basis according to a Gaussian random walk. Random walks were generated using an identical procedure to Daw et al., (2006) (Daw et al., 2006) briefly described here as follows. On choosing the i th image on trial t , the probability of receiving a reward varied between 0 and 1 and was drawn from a truncated Gaussian distribution (standard deviation $\sigma_o = 0.04$) around a mean $\mu_{i,t}$. At each timestep these means diffused in a decaying Gaussian random walk. The decay parameter was 0.9836, the decay centre θ was 0.50 and the diffusion noise v was zero-mean Gaussian (standard deviation $\sigma_d = 0.028$). Two sets of random walk distributions (Set A and Set B; see Figure 14A) were generated for the two days of testing, the order of which was counterbalanced across the group with regards to the order of pharmacological manipulation. Different pairs of fractal images were used on the two days of testing and randomly assigned amongst participants.

Reinforcement learning models

I fitted choice behaviour to a standard reinforcement learning model on a trial-by-trial basis. This involves $Q_a(t)$ -values for each action $a \in \{0,1\}$ on trial t , which are updated if the subject chooses action $a(t)$ as:

$$\begin{aligned} Q_{a(t)}(t+1) &= Q_{a(t)}(t) + \alpha\delta(t) \\ \delta(t) &= R(t) - Q_{a(t)}(t) \end{aligned}$$

Here, $Q_{a(t)}(t)$ is the expected value of the chosen option, which was set to zero at the beginning of the experiment. $\delta(t)$ is the reward prediction error which represents the difference between the actual outcome $R(t)$ and the expected outcome $Q_{a(t)}(t)$, where $R(t)$ was one (win) or zero (no win). The free parameter α defined subjects' learning rate, with higher values reflecting greater weight being given to more recent outcomes and leading to a more rapid updating of expected value.

As standard, I used a softmax rule to determine the probability of choosing between the two stimuli on trial t . If $m_a(t)$ are the propensities for doing action a on trial t , this uses

$$P(a(t) = a) = \frac{\exp(\beta m_a(t))}{\exp(\beta m_0(t)) + \exp(\beta m_1(t))}$$

in which the inverse temperature parameter β indexes how deterministic choices were. Larger β reflects less stochastic choices.

I consider two cases for $m_a(t)$. The simplest makes $m_a(t) = Q_a(t)$. However, it is often found that subjects have a tendency either to repeat or avoid doing the same action twice (Lau and Glimcher, 2005) (Schonberg et al., 2007). To account for this, I also consider a model in which $m_a(t) = Q_a(t) + b\chi_{a=a(t-1)}$ allowing an extra boost or suppression b associated with the action performed

on the previous trial. I fit all sessions (L-DOPA and placebo) for each participant using expectation-maximization in a hierarchical random effects model.

It has previously been noted that it can be hard to infer both α and β independently of each other (Schonberg et al., 2007) (Rutledge et al., 2009), since it is their product that dominates behaviour in certain regimes of learning. I therefore adopted the strategy of first fitting a full random effects model as if they are independent, and then clamping β to the mean of its posterior distribution and re-inferring α using the random effects model. Amongst other things, this implies that I do not make strong claims about having inferred differences in true learning rates.

In a second step, I used the mean posterior β parameter at the group level obtained on the preceding step (single fixed $\beta = 1.27$ for older adults; single fixed $\beta = 1.13$ for younger adults; note that data for young and older adults were analysed separately) as a fixed parameter in two, nested, RL models reflecting the two possibilities for $m_a(t)$. The first has one parameter, the learning rate, α . The second has the learning rate α and the perseveration/alternation parameter b .

For older adults only, I then repeated the two steps described above but instead estimated two separate β terms for the L-DOPA and placebo conditions. I then fixed each β at their respective posterior group means ($\beta = 1.43$; $\beta = 1.10$ for the L-DOPA and placebo respectively) and proceeded as before to test the two models outlined above.

Model fitting procedure and comparison

For older adults I compared the two RL models described above with a single fixed beta and the same two RL models with two fixed betas (four models in total; Table 8). For younger adults I compared the two RL models with a single fixed beta since younger adults did not undergo pharmacological manipulation. Procedures for fitting the models were identical to those used by Huys et al. (Huys et al., 2011) and by Guitart-Masip et al. (Guitart-Masip et al., 2012a) and are fully described there. For each subject and model I found the maximum a posteriori estimate of each parameter. I used the expectation-maximization algorithm to infer the maximum likelihood values of the parameters of the upper level prior over the parameters in the random effects model. This prior distribution on the parameters regularizes the inference and prevents parameters that are not well constrained from taking on extreme values. Before inference, all parameters were suitably transformed to enforce constraints (log and inverse sigmoid transforms). All model-fitting procedures were verified on surrogate data generated from a known decision process.

For Bayesian model comparison, I computed the model evidence, which was approximated in two steps. First, the integral over the hyperparameters was approximated via the Bayesian Information Criterion (BIC) at the *group* level (Kass and Raftery, 1995) using the integral over the individual parameters. This latter integral was approximated by sampling from the fitted priors. The BIC (which penalizes for model complexity) and pseudo- r^2 statistic (Camerer and Hua Ho, 1999) are reported in Table 8. A pseudo- r^2 statistic was defined as $(r - l)/r$ where l and r are the log likelihoods of the data under the model and under purely random choices respectively ($P = .50$ for all trials).

	single fixed beta		two fixed betas	
	alpha	alpha and perseveration	alpha	alpha and perseveration
pseudo-r²	0.3707	0.3752	0.3662	0.3705
BIC	12498	12464	12592	12560

Table 8. Quality of behavioural fits in older adults for four models.

Data were fit with a learning model with beta fixed either across all data ('single fixed beta') or fixed separately for placebo and L-DOPA ('two fixed betas'), and the free parameters alpha (learning rate) and choice perseveration. The winning model as determined by the lowest Bayesian information criterion (BIC) consisted of a single fixed beta, a learning rate and a choice perseveration parameter.

Behavioural analysis

I analysed task performance (amount of money won) using two-tailed paired t-tests (L-DOPA vs placebo in older adults) and independent t-tests (young vs old). Reinforcement learning model parameters (learning rate and perseveration) were not normally distributed (Shapiro-Wilk and Kolmogorov-Smirnov $p < 0.05$). Therefore I used two-tailed Wilcoxon Signed Ranks Tests to compare these parameters between the L-DOPA and placebo conditions. Two-tailed Pearson's and Spearman's correlations were used to analyse normally distributed and non-normally distributed data respectively.

Image acquisition

All MRI images were acquired using a 3.0T Trio MRI scanner (Siemens) using a 32-channel head coil.

Anatomical MRI acquisition

A structural multi-parameter map protocol employing a 3D multi-echo fast low angle shot (FLASH) sequence at 1mm isotropic resolution was used to acquire magnetization transfer (MT) weighted (echo time, TE, 2.2-14.70ms, repetition time, TR, 23.7ms, flip angle, FA, 6 degrees), proton density weighted (TE 2.2-19.7ms, TR 23.7ms, FA 6 degrees) and T1 weighted (TE 2.2-14.7ms, TR 18.7ms, FA 20 degrees) images (Helms et al., 2008b). B1 mapping (TE 37.06 and 55.59ms, TR 500ms, FA 230:-10:130 degrees, 4mm³ isotropic resolution) was acquired to correct the T1 maps for inhomogeneities in the transmit radiofrequency field (Lutti et al., 2010). A double-echo FLASH sequence (TE1 10ms, TE2 12.46ms, 3 x 3 x 2 mm resolution and 1mm gap) was used to

measure local field inhomogeneities and correct for the image distortions in the B1 mapping data. Using in-house code, a set of MT quantitative maps were extracted for each subject from the anatomical scans described above (Helms et al., 2008a).

fMRI data acquisition

Functional data using echo-planar imaging was acquired on two days. On each day, scanning consisted of two runs each containing 194 volumes (matrix 64 x 74; 48 slices per volume; image resolution= 3 x 3 x 3mm; TR 70ms, TE 30ms). The fMRI acquisition protocol was optimized to reduce susceptibility-induced BOLD (blood oxygen level dependent) response sensitivity losses in inferior frontal and temporal lobe regions (Weiskopf et al., 2006a). Six additional volumes at the beginning of each series were acquired to allow for steady state magnetization and were subsequently discarded. Individual field maps were recorded using a double echo FLASH sequence (matrix size = 64 x 64; 64 slices; spatial resolution = 3 x 3 x 2 mm; gap = 1 mm; short TE = 10 ms; long TE = 12.46 ms; TR = 1020 ms) for distortion correction of the acquired EPI images. Using the FieldMap toolbox, field maps were estimated from the phase difference between the images acquired at the short and long TE.

fMRI data preprocessing

Data were analysed using SPM8 (Wellcome Trust Centre for Neuroimaging, UCL, London). Pre-processing included bias correction, realignment, unwarping using individual fieldmaps, co-registration and spatial normalization to the Montreal Neurology Institute (MNI) space with spatial resolution after

normalization of 2 x 2 x 2mm. For the normalisation process, unified segmentation was used to classify anatomical T1w images into grey matter, white matter and cerebrospinal fluid. Using diffeomorphic registration algorithm (DARTEL), the flowfields required to warp T1w white and gray matter maps to MNI space were generated (Ashburner, 2007). These flowfields were then applied to the EPI images to normalise them to MNI space. Finally, data were smoothed with a 6mm FWHM Gaussian kernel. The fMRI time series data were high-pass filtered (cutoff = 128 s) and whitened using an AR(1)-model. For each subject a statistical model was computed by applying a canonical hemodynamic response function (HRF) combined with time and dispersion derivatives.

fMRI data analysis

My main aim was to determine the effects of L-DOPA on the components of the reward prediction error signal ($R(t)$; $Q_{a(t)}(t)$) in the nucleus accumbens. For this purpose, I fit a model using the group posterior mean α distribution from the winning model to determine the value of $Q_{a(t)}(t)$ on every trial. The general linear model for each subject at the 1st level consisted of regressors at the time of stimulus display separately for when a choice was made, when no choice was made and at the time of stimulus outcome. $R(t)$ and $Q_{a(t)}(t)$ were used as parametric modulators of outcome, as the prediction error at this time represents the difference between the received reward and the expected reward given the choice on that trial. Separate design matrices were calculated for the L-DOPA and placebo conditions. To capture residual movement-related artefacts, six covariates were included (the three rigid-body translation and three rotations resulting from realignment) as regressors of no interest. Finally I

also included 18 regressors for cardiac and respiratory phases in order to correct for physiological noise.

At the first level, I implemented a contrast for the prediction error i.e. $R(t) > Q_{a(t)}(t)$. At the second level, I examined the contrast $R(t) > Q_{a(t)}(t)$ collapsed across L-DOPA and placebo conditions. I used an uncorrected threshold of $p < 0.001$ to produce a whole-brain statistical parametric map of regions encoding prediction errors from which I identified a region in the right nucleus accumbens that responded to reward prediction errors. I used an anatomical mask (described below) to constrain this functional ROI. I used the Marsbar toolbox (Brett, 2002) to extract the parameter estimates from this region to enter into a two ($R/Q_{a(t)}$) by two (L-DOPA/placebo) repeated measures ANOVA to determine the effects of L-DOPA. I conducted post hoc tests to characterise the impairment in expected value representation (one-tailed one-sample t-tests for each condition to test the null hypothesis that they are not different from zero, and two-tailed paired t-tests to compare the effect of L-DOPA to placebo).

Nucleus accumbens mask: To define the nucleus accumbens in older subjects, I used a subject-derived mask for this region. I used Freesurfer's (version 4.5.0, <http://surfer.nmr.mgh.harvard.edu/>) automated recon-all pipeline to parcellate cortical and subcortical regions (Fischl et al., 2004). Each subjects' nucleus accumbens mask was visually inspected to ensure accurate segmentation. These nucleus accumbens masks were warped to MNI space using DARTEL flowfields as previously described and then group-averaged and

thresholded at 0.3. This mask (290 voxels) was then used to anatomically constrain the functional ROI.

Time course extraction

The main aim of this analysis was to visualise the effect of reward and expected value on the BOLD signal, at the time of the choice and at the time of the outcome, from the nucleus accumbens functional ROI over the course of a trial. In the fMRI SPM analysis it was not possible to simultaneously test for the effects of value expectation on the choice and the outcome phases. This is because the time of the choice and the time of the outcome were very close together in time (3s apart) and including the same parametric modulator on both time points would have resulted in highly correlated regressors. Thus, although the SPM model included regressors at the time of the choice and time of the outcome, I only included parametric modulators at the time of the outcome, so focussing on outcome prediction errors only.

Time courses were extracted from preprocessed data in MNI space. I upsampled the extracted BOLD signal to 100 ms. The signal was divided into trials and resampled to a duration of 15 s with the onset (presentation of the stimuli) occurring at 0s, the time of the choice occurring between 0-2s and the time of the outcome at 3s. I then estimated a general linear model across trials at every time point in each subject independently, where reward and expected value were the regressors of interest. These regressors were not orthogonalised and therefore competed for variance which is a particularly stringent test (Behrens et al., 2008). I calculated group mean effect sizes at

each time point and their standard errors, plotted separately for the placebo and L-DOPA conditions.

Diffusion tensor imaging acquisition

I acquired diffusion weighted images using a spin-echo echoplanar imaging (EPI) sequence, with twice refocused diffusion-encoding to reduce eddy-current-induced distortions (Reese et al., 2003). Amplitudes of diffusion-encoding gradients were calibrated for unbiased measurement of diffusion directions and improved fiber tracking (Nagy et al., 2007). I acquired 75 axial slices (whole brain to mid-pons) in an interleaved order [1.7 mm isotropic resolution; image matrix = 96×96 , field of view = 220×220 mm², slice thickness = 1.7 mm with no gap between slices, repetition time (TR) = 170 ms, echo time (TE) = 103 ms, asymmetric echo shifted forward by 24 phase-encoding (PE) lines, readout bandwidth (BW) = 2003 Hz/pixel] for 61 images with unique diffusion encoding directions. The first seven reference images were acquired with a b-value of 100 s/mm², the remaining 61 images with a b-value of 1000 s/mm² (Nagy et al., 2007). Two DTI sets were acquired with identical parameters except that the second was acquired with a reversed k-space readout direction to allow removal of susceptibility artefacts post-processing (Andersson et al., 2003). Since the SN/VTA was a major region of interest, I optimised the quality of my images by using pulse-gating to minimize pulsation artefact within the brainstem. The total data acquisition protocol lasted approximately 40 minutes depending on each individuals' heart rate. One participant was unable to tolerate scanning therefore DTI data was collected from 31 individuals.

DTI tractography

All tractography was performed in each individuals' native space. Tractography analysis was carried out from all voxels in each subject's anatomically-defined right SN/VTA ROI. I restricted my analysis to the right since this is where I determined my functional nucleus accumbens ROI. The medial and lateral boundaries of the SN/VTA were defined on each subjects' MT-weighted image where it is easily distinguishable from the surrounding tissues due to its bright grey colour in contrast to the adjacent cerebral peduncle. This region was manually defined by R.C. on every visible slice (between seven to ten slices) as per Düzel et al (Düzel et al., 2008) using MRICro (Rorden C, 2000). Ten randomly selected SN/VTA ROIs were segmented by a second trained individual and showed high inter-rater reliability (Intraclass correlation = 0.87, $p < 0.0005$). The single target mask of the right striatum was defined using the caudate and putamen masks from the AAL toolbox (Brett, 2002) (see Figure 17 for seed and target masks). This MNI-space mask was normalised to each individuals' native space using the inverse of the normalisation parameters. To avoid erroneous tractography results, I created individual subject exclusion masks using ITK-SNAP (Yushkevich et al., 2006). The ventricles and CSF spaces were automatically defined using the "snake" function, and particular attention was paid to manually refine the region surrounding the cerebral peduncle and medial wall of the temporal lobe.

FSL version 4.1.4 was used for DTI pre-processing. First, images were eddy current corrected. Correction for susceptibility artefacts was performed as previously described (Andersson et al., 2003). The low b images were averaged and used to generate a brain mask for skull stripping. Skull stripping was

performed manually for each subject using SPM8. Initial estimation of tensors was performed using dtifit allowing fractional anisotropy (FA) to be calculated, and all the results were visually checked prior to full estimation of the diffusion parameters. BEDPOSTX was used to estimate the probability distributions of two fiber populations at each voxel (Behrens et al., 2007). Finally, FSLs non-linear registration algorithm FNIRT was used to generate two warp fields to allow sampling between diffusion and structural space, and the results of these were manually checked for all individuals to ensure optimal alignment.

Tractography was run using FSL's probtrackX software (Behrens et al., 2007). Each voxel was sampled 5000 times with a burn in of 1000, curvature threshold of 0.2, modelling two fibers per voxel, utilising the previously calculated warp fields. I generated 'relative connectivity strength' maps as per Forstmann et al. (Forstmann et al., 2011) using the following steps. Here the probabilistic index of connectivity (PICO) between a seed and any other voxel in the brain is given by the number of traces arriving at the target site and is equivalent to the term "samples" used by other authors. **Step 1: Generate individual seed voxel PICO maps for every seed voxel.** In each map, the voxel values represents the number of samples (from 0 - 5000) originating from the seed passing through a voxel, using probtrackX. **Step 2: Generate individual ROI probability maps.** First I calculated the maximum PICO value that occurred within the ROI of interest across all seed PICO maps. I then thresholded the individual seed PICO maps at 0.02% of the maximum ROI PICO value, as per Aron et al. (Aron et al., 2007). The individual seed maps were combined so that the value at each ROI voxel then becomes the maximum PICO for that voxel across every seed map. **Step 3: Generate "Relative Connectivity Strength"**

maps. The ROI probability maps were divided by the sum of all PICO values within that specific map.

DTI analysis

The aim of my tractography analysis was to determine if inter-individual differences in nigro-striatal connectivity influenced the observed baseline variability in functional prediction error signalling. Figure 17 is a single-subject example demonstrating that the tractography target mask incorporated the functional ROI defined in the nucleus accumbens and that tracts from the SN/VTA targeted this region. I used Spearman's correlations to relate connectivity strength to prediction error signalling ($R(t)$ and $Q_{a(t)}(t)$ parameter estimates from the functional nucleus accumbens ROI) (Schwarzkopf et al., 2012). To identify outliers I converted connectivity strength to z-scores (conventionally defined as $z < -3$ or $z > 3$). Although none of the participants were outside this range, one participant had a z-score of 2.83 (equivalent to connectivity strength = 0.006) and was therefore excluded from the reported results. Even so, including this potential outlier in the analysis did not change the results. To take into account other potential contributing variables, I performed partial Spearman's correlations with the following covariates: age, gender, total intracranial volume and size of the manually defined seed (right SN/VTA) region. Note that the size of the target region was not included since this was the same for all participants. To determine if local structural organisation, determined by FA values of the SN/VTA seed and nucleus accumbens functional ROI also impacted expected value signalling I performed

additional Pearson's correlations (since FA values were normally distributed) between FA and $Q_{a(t)}(t)$ on placebo.

5.3. Results

5.3.1 Behavioural performance in young and older adults

32 older adults (mean age 70.00 years, SD 3.24; Table 7) on placebo and L-DOPA and 22 younger adults (mean age 25.18 years, SD 3.85) performed a two armed bandit choice task (Figure 14A). The amount of money won by older adults performing the task did not differ under L-DOPA (mean £12.94 SD 0.81) compared to placebo (mean £12.64 SD 0.89) (paired t test: $t(31) = 1.53$, $p = .137$). However, older adults on placebo won significantly less money than younger adults (independent samples t test: $t(52) = 2.05$, $p = .045$) whereas there was no difference in the amount won between older adults on L-DOPA and younger adults ($t(52) = 0.971$, $p = .336$) (Figure 14B).

Older adults completed a similar number of trials under both conditions (placebo: mean 218.16, SD 1.94; L-DOPA: mean 218.47, SD 1.74) as younger adults (mean 218.50, SD 2.44) (all $p > 0.4$). Older adults had similar choice reaction times on placebo (mean 796.81 ms, SD 152.89) and L-DOPA (mean 781.49 ms, SD 140.17) (paired t-test, $t(31) = 1.01$, $p = .321$), but overall were slower under both conditions compared to younger adults (mean 629.69 ms, SD 156.41) (independent t-tests, young vs. old-placebo: $t(52) = 3.91$; young vs old-L-DOPA: $t(52) = 3.73$; both $p < 0.0005$).

5.3.2 Reinforcement learning behaviour

I analysed trial-by-trial choice behaviour using a standard reinforcement learning model with a fixed β parameter (Figure 15A). A model with a single fixed $\beta = 1.27$ across drug and placebo conditions, one single learning rate and one choice perseveration parameter provided the best model fit of participants'

choices among the models that I compared, indexed by the lowest BIC values (Table 8). When calculating the BIC, the log evidence was penalized using the number of data points associated with each parameter.

In order to examine the effect of increasing dopamine levels on older participants' behaviour in the task, I used the Wilcoxon Signed Ranks Tests test to determine whether the learning rates (fitted using a single prior distribution including the drug and the placebo) differed between L-DOPA and placebo. I found that participants had a significantly higher learning rate under L-DOPA compared to placebo ($Z = -3.03$, $p = .002$; Figure 15B). In contrast, choice perseveration was unaffected by L-DOPA ($Z = -0.58$, $p = .562$). In younger adults, a model with a fixed $\beta = 1.13$ and single learning rate provided a better fit to participants' choices than when a choice perseveration parameter was added to the model (BIC 4348.15 and 4361.01 respectively). The learning rate in younger adults (median $\alpha = 0.62$, range 0.01 – 0.94) was intermediate between, and not significantly different from older adults either under the condition of placebo ($Z = -1.32$, $p = .187$) or L-DOPA ($Z = -1.25$, $p = .211$).

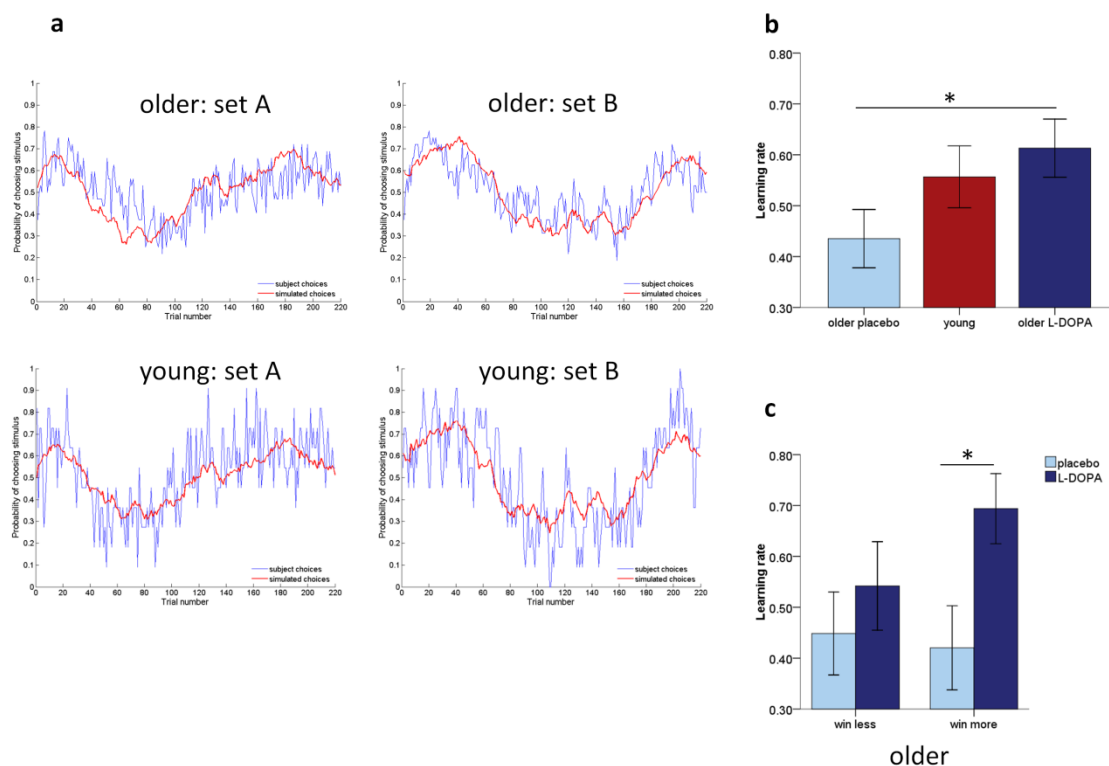


Figure 15. Reinforcement learning model and behaviour.

(a) Predicted choices from the learning model (red) closely matched subjects' observed choices (blue). The red lines show the same time-varying probabilities, but evaluated on choices sampled from the model. Plots are shown for older ($n = 32$) and young ($n = 22$) adults for the two different sets of probability distributions.

(b) Older adults ($n = 32$) had a higher learning rate under L-DOPA compared with placebo and did not differ from young adults ($n = 22$).

(c) Older adults who won more on L-DOPA than placebo ('win more', $n = 15$) had a significantly higher learning rate under L-DOPA than placebo, whereas learning rates did not differ between placebo and L-DOPA for older adults who won less on L-DOPA than placebo ('win less', $n = 17$). $*p < 0.05$. Error bars are ± 1 SEM.

5.3.3 L-DOPA and striatal prediction errors in older adults

I focussed my imaging analysis on reward predictions errors in the nucleus accumbens. Using a functional ROI approach I first defined reward sensitive voxels in the nucleus accumbens, namely voxels where there was an enhanced response at the time of outcome to actual rewards that was greater than that to expected rewards ($R(t) > Q_{a(t)}(t)$). Note that this is a liberal definition of reward prediction errors as voxels showing a significant effect with this contrast may not satisfy all the criteria to be considered for a canonical reward prediction error, namely both a positive effect of reward and a negative effect of expected value (Li and Daw, 2011) (Behrens et al., 2008). Using this approach I identified a cluster in the right nucleus accumbens [MNI x,y,z = 15, 11, -8; peak Z = 4.45, $p < 0.001$ uncorrected; 34 voxels] (Figure 16A).

Using this anatomically-constrained functional ROI I extracted the parameters estimates for $R(t)$ and $Q_{a(t)}(t)$ separately within these activated voxels. My two (placebo/L-DOPA) by two ($R(t)/Q_{a(t)}(t)$) repeated measures ANOVA revealed a main effect of L-DOPA ($F(1,31) = 5.712$, $p = .023$), suggesting that administration of L-DOPA had an impact on the representations associated with the two components of the reward prediction error (Figure 16A). Importantly, this signal was only compatible with a full prediction error signal (positive correlation between BOLD and $R(t)$ along with a negative correlation between BOLD and $Q_{a(t)}(t)$) when participants were under L-DOPA (one-tailed one-sample t-test: $R(t)$ placebo $t = 3.72$, $p < 0.001$; $Q_{a(t)}(t)$ placebo $t = -0.11$, $p = .455$; $R(t)$ L-DOPA $t = 1.92$, $p = .033$; $Q_{a(t)}(t)$ L-DOPA: $t = -1.73$, $p = .047$). This was due to a more negative representation of expected value on L-DOPA compared to placebo (paired t-test, $t(31) = 2.37$, $p = .024$) whereas there was

no difference in actual reward representation between L-DOPA and placebo ($t(31) = 1.38, p = .179$). These results show that the neural signature of reward predication errors were more strongly represented post administration of L-DOPA, and indeed only after L-DOPA was a full reward prediction error signal observed. I found no correlation between the total amount of money won during the task and the magnitude of the expected value on either placebo (Spearman's $\rho = -0.16, p = .379$) or L-DOPA ($\rho = -0.25, p = .166$).

To visualise the effects of L-DOPA on reward prediction over the course of a trial, I extracted the BOLD time course from the nucleus accumbens functional ROI and performed a regression of this fMRI signal against $R(t)$ and $Q_{a(t)}(t)$. Typically, I would expect to see a pattern of a reward 'prediction' (i.e. anticipation) at the time of the choice indicated by a positive effect of $Q_{a(t)}(t)$ and a reward 'prediction error' at the time of the outcome, indicated by both a positive effect of $R(t)$ and negative effect of $Q_{a(t)}(t)$, as indeed has been shown in younger adults (Behrens et al., 2008). As shown in Figure 16C, my time course analysis revealed exactly this expected pattern but only in the L-DOPA condition. Hence the abnormal response to the expected value observed on placebo (lack of reward anticipation at the time of the choice and absent negative expectation at the time of the outcome) was 'restored' when dopamine levels were enhanced. This analysis complements the aforementioned fMRI SPM analysis which showed that a full reward prediction error was only present on L-DOPA, by revealing abnormal expected value representations throughout the course of a trial.

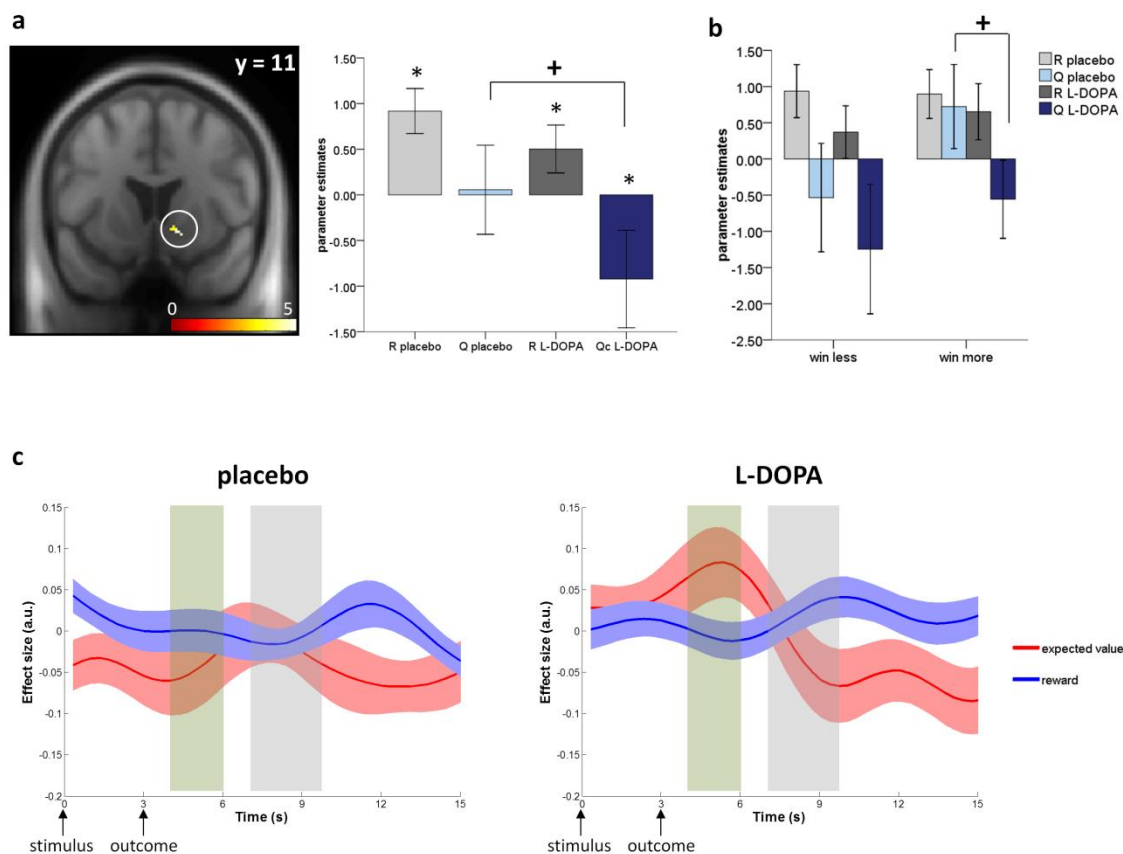


Figure 16. Reward prediction in the nucleus accumbens in 32 older adults

(a) A region in the right nucleus accumbens [peak voxel MNI co-ordinates: 15, 11, -8] showed greater BOLD activity for reward than for expected value ($R(t) > Q_{a(t)}(t)$) at the time of outcome. However, the lack of a negative effect of $Q_{a(t)}(t)$ under placebo meant that the prediction error signal was incomplete at baseline. L-DOPA increased the negative effect of $Q_{a(t)}(t)$ resulting in a full prediction error signal (i.e. both a positive effect of $R(t)$ and negative effect of $Q_{a(t)}(t)$). *one-tailed one sample t-test $p < 0.05$; †two-tailed paired t-test. Bars ± 1 SEM.

(b) L-DOPA only acted on parameter estimates for expected value ($Q_{a(t)}(t)$) in participants who won more on L-DOPA than placebo ('win more', $n = 15$) whereby these participants only demonstrated a negative effect of $Q_{a(t)}(t)$ under L-DOPA compared to placebo. Parameter estimates did not differ between L-DOPA and

placebo for participants who won less on L-DOPA ('win less', $n = 17$). [†]two-tailed paired t-test. Bars ± 1 SEM.

(c) Time course plots of the nucleus accumbens BOLD response to reward and expected value. Taking the typical BOLD haemodynamic response into account, the time window at 4-6 seconds approximately corresponds with the BOLD responses elicited at the time participants' made a choice (green box). The time window at 7-10 seconds approximately corresponds with the BOLD responses elicited when the outcomes were revealed (grey box). At baseline (i.e. under placebo) the only reliable signal observed was a response to reward (binary response to the outcomes: win/neutral). After boosting dopamine levels with L-DOPA, a full reward prediction error was observed, involving a positive expectation of value at the time of the choice together with a positive reward response and a negative expectation of value at the time of the outcome. Reward anticipation (positive effect of $Q_{a(t)}(t)$ at the time of the choice, red curve) was only observed on L-DOPA. Solid lines (blue = reward, red = expected value) are group means of the effect sizes, shaded areas represent ± 1 SEM.

5.3.4 Relationship between anatomical connectivity and prediction errors in older adults

My analysis identified substantial inter-individual variability in reward prediction error signals in the nucleus accumbens at baseline (i.e. under placebo). I hypothesised that this might be associated with the known variability in the age-related decline of dopamine neurons from the SN/VTA, and in principle indexed through anatomical nigro-striatal connectivity. Using DTI and probabilistic tractography, I defined a measure of connection strength between the right SN/VTA and right striatum (Figure 17A). Nigro-striatal tract connectivity strength measured with DTI correlated with the fMRI parameter estimate under placebo associated with the expected value $Q_{a(t)}(t)$ (Spearman's rho = -.46, p = .010) but not with that associated with the reward $R(t)$ (Spearman's rho = .12, p = .54) (Figure 17B & C). These correlations were significantly different from each other suggesting that individual functional activation differences of the representation of expected value but not reward were linked to anatomical connectivity strength between the SN/VTA and striatum (Fishers r-to-z transformation, $z = -2.32$, p = .002 two-tailed). This relationship between greater tract connectivity strength and more negative expected value parameter estimates remained significant after controlling for age, gender, total intracranial volume and size of the seed region from which tractography was performed (partial Spearman's rho = -0.40, p = .041). Neither the fractional anisotropy (FA) of SN/VTA nor nucleus accumbens functional ROI correlated with expected value (Pearson's $r = .26$ and $r = .17$, p = .16 and p = .38 respectively), suggesting that this correlation was related to circuit strength rather than local structural integrity as determined by FA.

If connectivity strength is a marker of structural integrity of the nigro-striatal dopamine circuit, then one prediction is that enhancement of dopamine levels could overcome the relationship between reduced anatomical connectivity and less robust representations of expected value. As predicted, I found that that connectivity strength and expected value parameter estimates under L-DOPA were no longer correlated (Spearman's $\rho = 0.04$, $p = .85$; Fishers r-to-z transformation comparing the correlation of connectivity strength with $Q_{a(t)}(t)$ on placebo and the correlation of connectivity strength with $Q_{a(t)}(t)$ on L-DOPA: $z = -2.02$, $p = .043$ two-tailed).

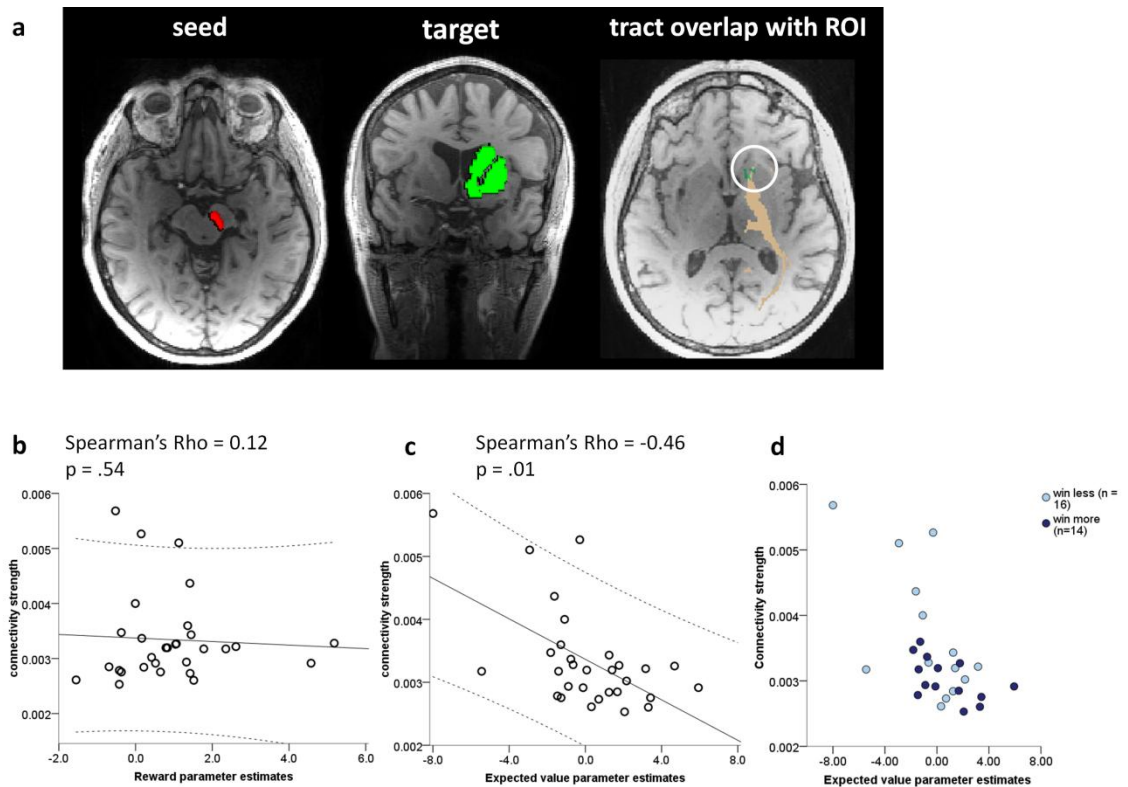


Figure 17. Anatomical connectivity and baseline functional prediction errors

(a) Single subject example of probabilistic tractography (gold = tract) from a seed in the right substantia nigra/ventral tegmental area (red) to the striatum target (green) which overlapped with the functional nucleus accumbens ROI (circled).

(b,c) Under placebo, older individuals with higher white matter nigro-striatal tract connectivity strength had a more negative effect of expected value $Q_{a(t)}$ whereas there was no correlation with reward $R(t)$. The solid line is the regression slope, dashed lines represent 95% confidence intervals. Both plots $n = 30$.

(d) A similar pattern was observed in both older participants who won less on L-DOPA ('win less', $n = 16$) and older participants who won more on L-DOPA ('win more').

Connectivity strength values are measured in arbitrary units.

5.3.5 Baseline individual differences

I assessed how baseline (i.e. placebo) performance across all 32 older individuals related to the computational model parameters and fMRI parameters. I found that individual differences in task performance (total won) correlated positively with the learning rate (α) (Spearman's Rho = 0.39, $p = .027$) but did not correlate with choice perseveration (Spearman's Rho = -0.07, $p = .704$). With regards to BOLD parameter estimates, task performance correlated negatively with expected value ($Q_{a(t)}(t)$) (Pearson's $r = -0.42$, $p = .016$) but did not correlate with reward ($R(t)$) (Pearson's $r = -0.07$, $p = .707$). Thus higher baseline performance was associated with a higher learning rate and more negative expected value representations in the nucleus accumbens. Task performance across all 32 older adults on L-DOPA did not correlate with α , $R(t)$ or $Q_{a(t)}(t)$ (Table 9).

	Total won (n = 32)	
	placebo	L-DOPA
Model parameter		
alpha placebo	Rho = 0.39, p = .027*	-
alpha L-DOPA	-	Rho = 0.06, p = .727
stickiness placebo	Rho = -0.07, p = .704	
stickiness L-DOPA	-	Rho = -0.33, p = .062
fMRI parameter estimates		
R(t)placebo	R = -0.07, p = .707	-
Q _{a(t)} (t) placebo	R = -0.42, p = .016*	-
R(t) L-DOPA	-	R = -0.21, p = .241
Q _{a(t)} (t) L-DOPA	-	R = -0.25, p = .171

Table 9. Individual differences on task performance and computation model and functional neuroimaging parameters.

Alpha = learning rate; Stickiness = choice perseveration. Rho = two-tailed Spearman correlations; R = two-tailed Pearson correlations; *p < 0.05

5.3.6 Post-hoc tests: performance in older adult subgroups

20 out of 32 individual older participants improved on L-DOPA compared to placebo (increase in the total amount won ranged from £0.10 to £3.00). 10 older participants performed worse on L-DOPA compared to placebo (decrease in the total amount won ranged from £0.50 to £1.50) and two participants won the same amount under both conditions. Overall, this suggests that L-DOPA improved performance in some older adults to the level of younger adults.

To explore this further, I defined two subgroups of older adults according to their difference in performance (total won on L-DOPA minus total won on placebo) and performed a median split, forming a 'win less' group (total won L-DOPA < placebo) and a 'win more' group (total won L-DOPA > placebo). Since the middle two participants had the same difference in performance and this amount was small (+ £0.30) I included them in the 'win less' rather than 'win more' group, such that the 'win more' group was a more robust representation of improved performance on L-DOPA. Therefore the 'win less' group consisted of 17 participants (performance L-DOPA vs placebo: $t(16) = -3.35$, $p = .004$) and the 'win more' group consisted of 15 participants (performance L-DOPA vs placebo: $t(14) = 6.68$, $p < 0.0005$) (Figure 14C).

First I examined the pattern of performance in these two subgroups which resembled an 'inverted U-shape' where rather than equivalent baseline levels of performance, participants with high baseline levels of performance on placebo performed worse on L-DOPA and participants with low baseline levels of performance improved on L-DOPA (repeated measures ANOVA with total won (L-DOPA/placebo) as the within-subject factor and group (win less/win more) as the between-subject factor; performance* group interaction: $F(1,30) = 53.53$, $p <$

0.0005; independent t test comparing performance in the placebo condition between the 'win less' and 'win more' group: $t(30) = 3.91$, $p = <0.0005$; comparing performance in the L-DOPA condition between the 'win less' and 'win more' group: $t(30) = -2.66$, $p = .012$) (Figure 14C).

In line with previously described non-linear effects of dopamine on cognition (for a recent review see (Cools and D'Esposito, 2011)), this pattern of performance may relate to the baseline integrity of an individuals 'dopaminergic status'. Thus participants with lower baseline dopamine levels ('win more' placebo) underperform at baseline and improve when dopamine levels are increased to a more optimal level for the task ('win more' L-DOPA). In contrast, participants with optimal underlying dopamine levels for the task exhibit high baseline performance ('win less' placebo) and perform when dopamine levels are further increased due to an 'overdose' effect ('win less' L-DOPA). Also of note is that young adults won £13.17 (SD 1.00) on this task, which was similar to winnings by older 'win less' adults on placebo and older 'win more' adults on L-DOPA. Overall, this interpretation is in keeping with a variable dopamine decline amongst older adults. I also confirm this was not an artefact of practice effects since the total won under L-DOPA and placebo did not interact with the order of drug administration (L-DOPA day 1/ L-DOPA day 2) (non-significant performance*order interaction: $F(1,30) = 0.20$, $p = .657$).

Second I assessed nigro-striatal DTI connectivity in these subgroups. Although I had no direct measurement of participants' baseline dopaminergic status, my DTI measure of nigro-striatal connectivity strength, a possible indirect marker of nigro-striatal structural integrity, was higher in participants with higher baseline performance ('win less' placebo vs. 'win more' placebo independent t-test: $t(29)$

= 2.40, $p = .023$). Reviewing the correlation between DTI connectivity strength and expected value representations under placebo, I found this correlation was significant for individuals in the 'win more' group ($Rho = -0.59$, $p = .035$; $n = 13$) but not in the 'win less' group ($Rho = -0.44$, $p = .076$; $n = 17$), although I note these correlations were performed with smaller sample sizes and both groups show a similar pattern of a negative association between expected value parameter estimates and connectivity strength (Figure 17D).

Third, I examined learning rate differences. Here I found that higher learning rates under L-DOPA compared to placebo were evident in the 'win more' group (Wilcoxon $z = -2.90$, $p = .004$) but not in the 'win less' group ($z = -0.97$, $p = .332$) (Figure 15C).

Finally, I examined the BOLD response within these subgroups. Critically, here I found that the only significant change of parameter estimates on placebo compared to L-DOPA was for expected value ($Q_{a(t)}(t)$) in the 'win more' group (Figure 16B) ($Q_{a(t)}(t)$ placebo vs. L-DOPA 'win more' group: $t = 2.26$, $p = .040$) (placebo vs. L-DOPA for $R(t)$ 'win less', $R(t)$ 'win more' and $Q_{a(t)}(t)$ 'win less', all $p > .14$). Thus for the participants who performed significantly better on L-DOPA than placebo, expected value representations in the nucleus accumbens were significantly more negative under L-DOPA than placebo.

I note that participants in this group also had a negative effect of $Q_{a(t)}(t)$ under L-DOPA even though their performance was worse on L-DOPA. One possible explanation is that for these participants, L-DOPA may have had adverse effects on prediction error signalling in other extra-striatal brain regions linked to worse task performance. Alternatively, L-DOPA may have had other adverse effects on unmeasured variables unrelated to prediction error signalling.

In summary, these post hoc tests link performance to neural correlates and provide a mechanism through which L-DOPA may improve performance, namely via an effect on higher learning rates and a more negative expected value representation in the nucleus accumbens.

5.4. Discussion

I used a probabilistic reinforcement learning task in combination with a pharmacological manipulation of dopamine, as well as structural and functional imaging, to probe reward-based decision-making in old age. Older adults performed less well than younger adults on this decision-making task, but performance improved to equivalent levels following enhancement of dopamine levels with L-DOPA in older adults. As a group, older adults had an incomplete prediction error signal in the nucleus accumbens at baseline (i.e. on placebo) consequent upon a lack of an expected neuronal response to expected reward value. Inter-individual variability of the expression of expected value was also evident and these baseline inter-individual differences in functional signalling were tightly coupled to nigro-striatal structural connectivity strength, determined using DTI. In older adults, L-DOPA increased the task-based learning rate and modified the BOLD correlates of both reward anticipation and the reward prediction error signal in the nucleus accumbens. Critically, increasing dopamine levels led to a more complete prediction error signal by restoring the representation of expected value in the nucleus accumbens.

Previous studies have shown that older adults perform worse on probabilistic learning tasks than their younger counterparts (Mell et al., 2005) (Eppinger et al., 2008) (Samanez-Larkin et al., 2011). Since it is widely held that dopamine neurons encode a reward prediction error signal, it is conceivable that dopamine decline that occurs as part of the normal aging process could account for these behavioural deficits. Indeed this was a prime motivation for the use of pharmacological manipulation with L-DOPA in this study. Whilst there was no significant difference in task performance in older adults on placebo versus L-

DOPA, a difference between older and younger adults on placebo was abolished when the older adults were subject to treatment with L-DOPA. Using a reinforcement-learning model, I also found that older adults had a higher learning rate on L-DOPA compared to placebo, consistent with findings in patients with Parkinson's Disease (a dopamine deficit disorder) whose learning rates when on dopaminergic medication were higher than when off their medication, albeit in that instance no difference was noted in overall performance (Rutledge et al., 2009). As in that study (Rutledge et al., 2009), it is impossible to make a definitive distinction between learning rate, magnitude of the prediction error that arises from learning, and the stochastic way that learning leads to choice.

There are two important points in each trial at which a temporal difference (TD) error type signal can be anticipated namely at the time of choice, when the TD error is the expected value of the chosen option, and at the time of outcome when the TD error is the difference between the reward actually provided and the expected value. Decomposing the outcome signal into these separate positive and negative components is important because the response to reward is highly correlated with the full prediction error, potentially readily confusing the two (Behrens et al., 2008) (Li and Daw, 2011) (Guitart-Masip et al., 2012a). In my experiment, under placebo, although the representation of the actual reward appeared normal, neither of the components of the expected value signal at choice or outcome was present in nucleus accumbens BOLD signal. This absence is consistent with the few behavioural (Samanez-Larkin et al., 2011) and neuroimaging studies (Schott et al., 2007; Samanez-Larkin et al., 2010) that have suggested that older adults have abnormal expected value

representations, although it is important to note that I did not find a substantial behavioural impairment. Most critically, I show that under L-DOPA, both components of the expected value signal were restored.

There are at least two possible explanations for the absence of the expected value signal. One is that a putative model-free decision-making system, most closely associated with neuromodulatory effects (Schultz et al., 1997) (Dickinson, 2002) is impaired. This would render behaviour subject to the operation of a model-based system, which is thought to be less dependent on dopaminergic transmission (Dickinson et al., 2000). This possibility is supported by evidence that older adults perform better than younger adults in tasks requiring a model of the environment (e.g. where future outcomes are dependent on previous choices) (Worthy et al., 2011). Reconciling it with the observations that suppressing (de Wit et al., 2012) or boosting (Wunderlich et al., 2012) dopamine in healthy young volunteers respectively suppresses or boosts model-based over model-free control is more of a challenge.

The other possibility for the absence of the model-free expected value signal is that it is still calculated normally, but that when dopamine levels are low, it is not apparent in nucleus accumbens BOLD signal. One can certainly expect that dopamine levels will have an impact on the state of striatal neurons (Nicola et al., 2000), but the impact on the BOLD signal of cortical and dopaminergic input to, and local activity within the striatum, remain unclear. In future studies, it would be interesting to use paradigms based on recent reports (e.g. (Daw et al., 2011; Simon and Daw, 2011)) in older participants with and without L-DOPA to investigate the balance of model-free and model-based control.

Enriching the above picture are recent studies in healthy young participants showing that at least some aspects of the representation in striatal BOLD of the expected value component of the TD error are conditional on a requirement for action (Guitart-Masip et al., 2012b). In Guitart-Masip et al (2012a) the representation of expected value was not modulated by L-DOPA; however, it is not clear whether this is an effect of the more extensive training provided there (which can render behaviours insensitive to dopamine manipulations (Choi et al., 2005)), or the fact that the expected value did not fluctuate in a way that was relevant for choice. My current study raises an interesting possibility that dopamine might only modulate the neural representation of expected value when it is behaviourally relevant for the task at hand.

My DTI connectivity analysis provides support for the notion that neuronal representations of expected value, and hence appropriate reward prediction error signalling, rely on the integrity of the dopaminergic system. The connectivity strength of tracts is one DTI metric reported to predict age-related performance differences (Coxon et al., 2012; Forstmann et al., 2012). I found that individuals with stronger connectivity between SN/VTA and striatum had more robust value representations in the nucleus accumbens. Although my findings can be interpreted within the context of the well-defined decline of nigro-striatal dopamine neurons with increasing age, I acknowledge that DTI measures of connectivity are not a direct mapping of dopamine neurons, but rather reflect white matter tract strength between the SN/VTA and striatum. Also, the direction of information flow cannot be inferred from DTI-based tractography (Le Bihan and Johansen-Berg, 2012). Interestingly, I did not observe a relationship between fractional anisotropy (FA) of either the SN/VTA

or striatum with functional activity in the accumbens. FA values characterise the extent of water diffusion, so providing an indirect measure of myelin, axons and the structural organisation of both grey and white matter (Vaillancourt et al., 2012) (Draganski et al., 2011). My results are therefore an indication that inter-individual anatomical differences at the level of nigro-striatal circuit-strength rather than local grey-matter integrity within SN/VTA or striatum determine the success of prediction error signalling in healthy older adults.

In summary, my results pinpoint structural and functional mechanisms that underpin the variable expression of reward-based decision-making in older adults. By establishing a link between dopaminergic signalling in the nucleus accumbens and the representations of expected value in the brain my results provide a potential therapeutic route towards tackling age-related impairments in decision-making.

In the next chapter I present a study which further explores individual structural anatomical differences, this time focussing on integrity of the SN/VTA, in relation to the flexibility of reward-based learning.

Chapter 6

Midbrain structural integrity and flexible learning

6.1. Introduction

To efficiently harvest reward and avoid punishment, humans need to learn appropriate instrumental responses (Dickinson, 2002) (O'Doherty et al., 2004). Recent data suggest that this basic form of behavioural adaption is surprisingly inflexible in humans (Guitart-Masip et al., 2012a). While healthy young human adults readily learn to act ('go') in order to obtain a reward or not to act ('no-go') in order to avoid a punishment, they have difficulties learning to act in order to avoid a punishment and not to act to obtain a reward (Guitart-Masip et al., 2012a). This inflexibility in learning suggests that signals that predict rewards are prepotently associated with behavioural activation promoting approach behaviour whereas signals associated with punishments are intrinsically coupled to behavioural inhibition promoting avoidance. These behavioural tendencies can be described as Pavlovian biases that corrupt the flexibility of instrumental learning (Gray, 2000; Dayan et al., 2006). Computational modelling in younger adults has shown that the observed pattern of behaviour is captured by a model incorporating a Pavlovian bias, where the strength of this bias is

related to failure to learn the conflicting conditions: no-go to obtain reward and go to avoid punishment (Guitart-Masip et al., 2012a).

Dopamine neurons, which project from the substantia nigra/ventral tegmental area (SN/VTA) of the midbrain, are important for instrumental learning (Schultz et al., 1997; Salamone et al., 2005) including signalling reward predictions errors (Schultz et al., 1997), energizing actions (Niv et al., 2007) and driving novelty-related exploratory behaviour (Düzel et al., 2010; Lisman et al., 2011). In humans, dopaminergic medication after learning influences the brain responses to action and reward anticipation (Guitart-Masip et al., 2012b). Importantly, the SN/VTA undergoes degeneration with aging (Fearnley and Lees, 1991; Bäckman et al., 2006; Vaillancourt et al., 2012). Age-differences in instrumental learning have been linked to functional activity in dopaminergic target regions including the striatum and prefrontal cortex (Samanez-Larkin et al., 2010) (Mell et al., 2009) (Fera et al., 2005) (Aizenstein et al., 2006). Structural degeneration of the SN/VTA and associated circuits may be indexed *in vivo* by magnetization transfer (MT) imaging, where lower MT values reflect decreased structural integrity (Eckert et al., 2004; Düzel et al., 2008; Tambasco et al., 2011).

The primary goal of this study was to relate individual differences of SN/VTA integrity in old age to flexible instrumental learning for competing responses (“to act” or “not to act”) to rewards and punishments. I hypothesized that older adults with higher SN/VTA integrity would show greater learning flexibility. Thus instrumentally learning to act in order to avoid a punishment and not to act to obtain a reward would be equivalent to learning to act in order to obtain a reward or not to act in order to avoid a punishment, the latter two behaviours

being Pavlovian response biases that tend to dominate learning. I obtained trait measures of novelty seeking to test the relationship with instrumental learning and structural integrity. Separate data was obtained from younger adults to explore age-group comparisons of learning and structural integrity of SN/VTA.

6.2. Methods

Older subjects: 42 healthy older adults aged 64-75 years (mean 69.12 yrs SD 3.44; 29 females; 40 right-handed) were recruited via the departmental website, advertisement in local public buildings and by word of mouth. Individuals were initially screened by telephone and excluded if they had any of the following: current or past history of neurological, psychiatric conditions or endocrinological disorders, metallic implants, tinnitus, major visual impairment, history of drug addiction. To control for vascular risk factors, individuals known to have had a stroke or transient ischemic attack, myocardial infarction or other significant cardiovascular history, diabetes mellitus or hypertension requiring more than one anti-hypertensive medication were not eligible for participation. All participants undertook a neuropsychological test battery to ensure normal global cognitive performance (Table 10). On the basis of this no subjects were excluded from the analysis (all participants scored within 1.5 SDs of the age-related norm for each test). All subjects had a normal neurological examination (performed by myself) ensuring participants did not have concurrent undiagnosed neurological conditions. MRI scans were visually inspected to ensure no participants had severe white matter changes or other major lesions. Clinical examination, neuropsychological testing, the go/no-go task and structural MRI scanning were all performed in a single four hour session. Written informed consent was obtained from all participants. The study received ethical approval from the North West London Research Ethics Committee 2.

Test	Cognitive domain	Score
MMSE	Global cognitive screen	30 (28-30)
GDS	Subjective depression rating scale	1 (0-7)
NART IQ	Predicted IQ	120.31 (7.21)
RAVLT total score trials 1-5	Declarative memory, immediate free recall	49.71 (8.55)
RAVLT trial 7*	Declarative memory, delayed free recall	9.54 (2.66)
D2 cancellation score	Visuo-motor speed & attention	150.38 (35.11)
Digit span forward	Working memory	7 (4-9)
Digit span backward	Working memory	5 (3-8)
COWA FAS total score	Phonemic fluency	57.24 (13.23)
COWA category total score	Semantic fluency	25.40 (6.61)
VOSP number location	Visuo-spatial perception	10 (8-10)
TPQ Novelty seeking score	Novelty seeking personality	15.29 (5.23)
TPQ Harm avoidance score	Harm avoidance personality	9.57 (6.45)
TPQ Reward dependence score	Reward dependence personality	18.52 (3.88)

Table 10. Neuropsychological test scores in older adults.

Scores are either mean (SD) or median (range). * n=41, one subject missing data; MMSE: Mini-Mental State Examination; GDS: Geriatric Depression Scale; NART IQ: National Adult Reading Test Intelligence Quotient; RAVLT: Rey Auditory and Verbal Learning Test; WAIS: Wechsler Adult Intelligence Scale; COWA: Controlled Oral Word Association test; VOSP: Visual and Object Space Perception; TPQ: Tridimensional Personality Questionnaire

Young subjects: Data from two previously published experiments performed at the host institution were obtained to enable separate age-comparisons of behavioural data and MRI data. In one, behavioural data from 47 healthy young adults (28 female; mean age 23.1 years, SD 4.1) performing the same go/no-go task was obtained allowing comparisons of behavioural performance between young and older adults (Guitart-Masip et al., 2012a). Structural neuroimaging including MT imaging was available for 30 of these young adults, which I used to examine the correlation between SN/VTA integrity and task performance. These scans were obtained on a different MRI scanner (3-T Siemens Allegra) using a different acquisition protocol that did not include B1 correction (see (Guitart-Masip et al., 2012a) for details), thus direct age-comparisons of MT values could not be made with this dataset and mine.

Therefore in the second study, neuroimaging data from 12 healthy young adults (6 females; mean age 33.8, SD 12.84) using the same MRI scanner and imaging sequence was obtained to allow comparison of MT values of SN/VTA between young and older adults (Lambert et al., 2012).

2.2 Go/no-go task

Participants performed a probabilistic monetary go/no-go task as described in Guitart-Masip et al., (2012) (Guitart-Masip et al., 2012a) (Figure 18). The correct response (to execute or withhold an action) to four cues (abstract fractal images) had to be learnt through trial and error, in order to win or avoid losing money. Participants were told that at the start of the task they would not know the correct responses (to press or not press a button) for each image but that

these would become clear through trial and error. After seeing an image (1000ms), there was a variable interval (250-2000 ms) after which participants were presented with a circle (target detection, 1500ms), at which point they had to either press a button (go) with their dominant hand to indicate the target side within 1000ms or not press a button (no-go) . Following this, the outcome was depicted for 1000ms by a green up-pointing arrow (indicating a win of £1), a red down-pointing arrow (indicating a loss of £1) or a yellow horizontal bar (neither win nor lose). The outcome was probabilistic, whereby in the win conditions 80% of correct choices and 20% of incorrect choices were rewarded (the remaining 20% of correct and 80% of incorrect choices leading to a neutral outcome). In the lose conditions, 80% of correct choices and 20% of incorrect choices avoided punishment. The probabilistic nature of the task was made clear to participants in the written and verbal instructions prior to the task. Thus, the task consisted of four trial types depending on the nature of the fractal cue presented at the beginning of the trials:

- Press the correct button in the target detection task to gain a reward (go to win, GW)
- Press the correct button in the target detection task to avoid punishment (go to avoid losing, GAL)
- Do not press a button in the target detection task to gain a reward (no-go to win, NGW)
- Do not press a button in the target detection task to avoid punishment (no-go to avoid losing, NGAL)

The task consisted of 240 trials (60 trials for each of the four conditions, presented in a randomised fashion) and lasted approximately 35 minutes. At the

beginning of the task, participants were told they could win between £5 to £15 and were given their earnings on task completion. Prior to the actual task, participants undertook a brief training session of ten practice trials in which only the target detection circles were presented. Subjects were instructed to press the corresponding button for every target (left arrow key on the keyboard if the target appeared on the left of the screen and visa versa for right). This allowed participants to familiarise themselves with the appropriate buttons on the computer keyboard and obtain an overall feel for the speed of the task without exposure to any of the cues used in the main task.

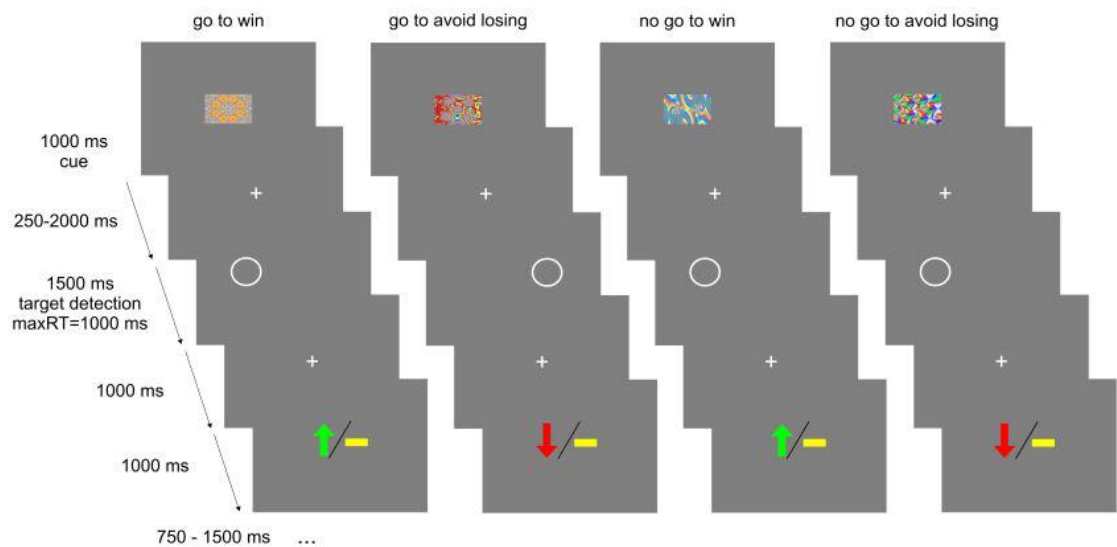


Figure 18. Probabilistic monetary go/no-go task

Tridimensional Personality Questionnaire

Each participant completed the Tridimensional Personality Questionnaire (TPQ) (Cloninger, 1987a). This self-report questionnaire consists of 100 true-false items measuring three personality traits: novelty-seeking, harm-avoidance and reward-dependence.

MRI scanning

A high-resolution structural MRI dataset for each participant was obtained on a 3.0T MRI scanner (Magnetom TIM Trio, Siemens Healthcare, Erlangen, Germany) using a 32-channel head coil. A structural multi-parameter map protocol employing a 3D multi-echo fast low angle shot (FLASH) sequence at 1mm isotropic resolution was used to acquire MT weighted (echo time, TE, 2.2-14.70ms, repetition time, TR, 23.7ms, flip angle, FA, 6 degrees), proton density weighted (TE 2.2-19.7ms, TR 23.7ms, FA 6 degrees) and T1 weighted (TE 2.2-14.7ms, TR 18.7ms, FA 20 degrees) images (Helms et al., 2008b). B1 mapping (TE 37.06 and 55.59ms, TR 500ms, FA 230:-10:130 degrees, 4mm³ isotropic resolution) was acquired to correct the T1 maps for inhomogeneities in the transmit radiofrequency field (Lutti et al., 2010). A double-echo FLASH sequence (TE1 10ms, TE2 12.46ms, 3 x 3 x 2 mm resolution and 1mm gap) was used to measure local field inhomogeneities and correct for the image distortions in the B1 mapping data. Using in-house code, the MT, T1 and R2* (1/T2*) quantitative maps were extracted for each subject from the anatomical scans described above. Proton density scans were not used for any analyses but were acquired as they are crucial for estimating MT and T1 parameters (for

full details regarding the generation of quantitative maps see (Helms et al., 2008b)). MT, T1 and R2* values reflect structural integrity (Wolff and Balaban, 1989; Eckert et al., 2004; Düzel et al., 2008; Tambasco et al., 2011), myelin and iron content respectively (Martin et al., 2008; Martin, 2009; Draganski et al., 2011).

Imaging analysis

Data processing and analysis was performed using Statistical Parametric Mapping software (SPM8; Wellcome Trust Centre for Neuroimaging, London, UK) and MATLAB 7.8 (Mathworks, Sherborn, MA, USA). Two independent analyses were conducted with the structural MRI data from older adults. The first was a region-of-interest analysis (ROI) of the SN/VTA. The second was a whole-brain voxel-based analysis.

Definition of regions of interest

Substantia nigra/ventral tegmental area (SN/VTA): The medial and lateral boundaries of the SN/VTA were defined on each subjects' MT-weighted image where it is easily distinguishable from the surrounding tissues due to its bright grey colour in contrast to the adjacent cerebral peduncle. For each subject, this region was manually defined on every visible slice, usually between seven to ten slices as per Düzel et al (Düzel et al., 2008) using MRICro (Rorden C, 2000). Figure 19 is an example of all slices from a single subject. For each subject, their ROI was projected as an overlay on their MT, T1 and R2* maps to obtain a

mean value for the region. Bilateral SN/VTA values in older adults, calculated by averaging right and left SN/VTA values, were as follows (values are in arbitrary units): MT mean 0.93 (SD 0.070), T1 mean 1129.31 (SD 51.23), R2* mean 0.028 (SD 0.0048).

Subthalamic nucleus (STN): The STN was manually segmented for each subject using the software package ITK-SNAP (Yushkevich et al., 2006) as described in Lambert et al (2012) (Lambert et al., 2012). Briefly, using R2* maps, it appears as a hyperintense region. The borders of the STN were defined as the zona incerta superiorly and immediately medially; prelemniscal radiations, posterior-lateral hypothalamus and red nucleus further medially and cerebral peduncle laterally. The inferior tip lies on the superior aspect of the substantia nigra at the level of the optic tract. See Figure 19 for a single subject example.

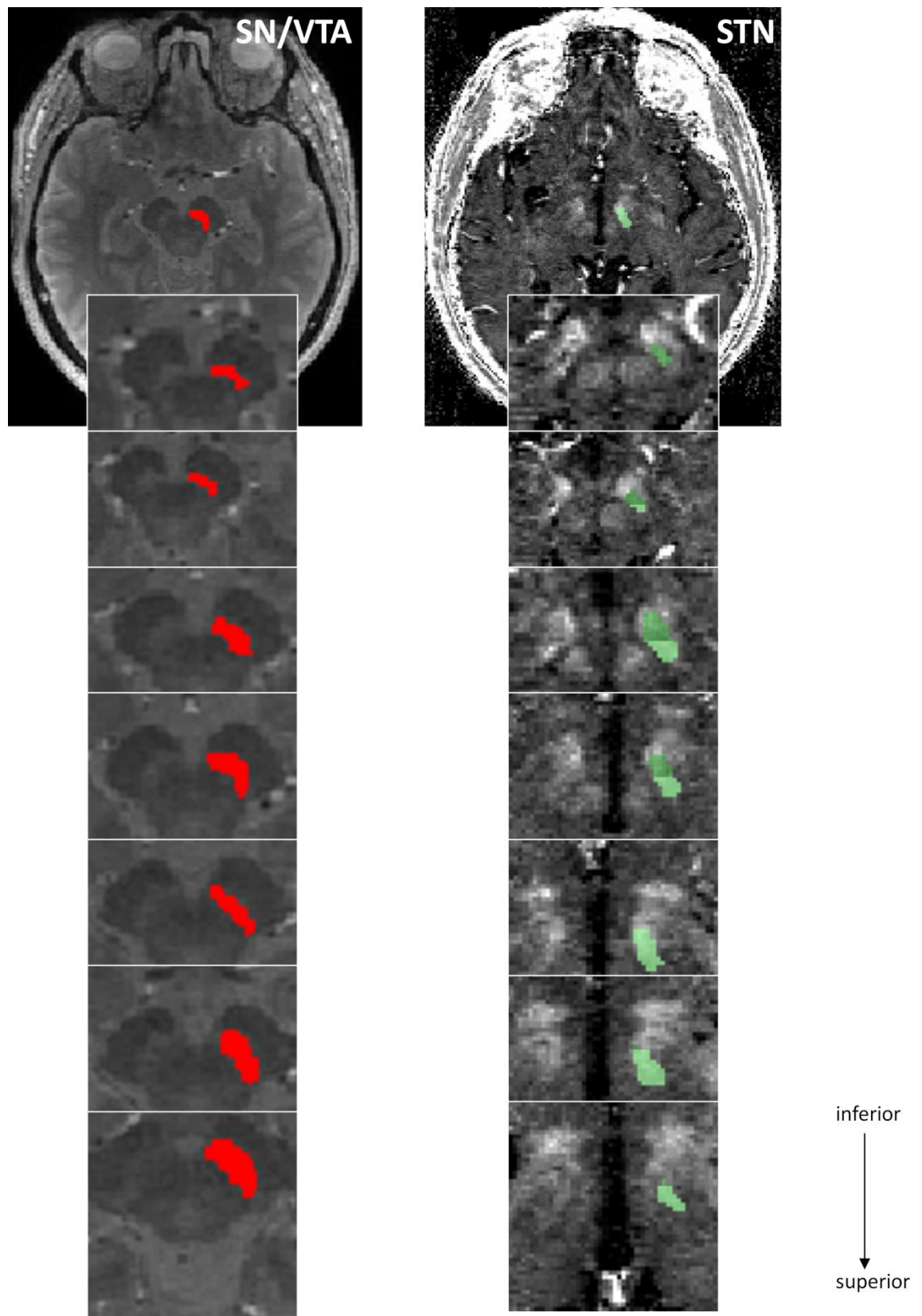


Figure 19. Manually-defined regions of interest. Single-subject example of right substantia nigra/ventral tegmental area (red) and subthalamic nucleus (green).

Ten randomly selected SN/VTA and STN ROIs were segmented by a second trained individual, showing high inter-rater reliability (SN/VTA: Intraclass correlation = 0.87, $p=.000$; STN: Intraclass correlation = .98, $p=.000$).

Magnetization transfer (MT) subgroups

I obtained MT data for 12 young adults (mean age 33.8 years SD 12.84, 6 females) from a separate published experiment (Lambert et al., 2012). For comparison I formed two subgroups each consisting of 12 elderly adults matched for age and gender (10 females per group), that differed significantly in MT values of the right SN/VTA (independent samples t-test, 2-tailed: $t(22) = -9.93$, $p < 0.0001$). For these subgroups, 12 elderly adults with the highest and lowest MT values of the right SN/VTA were selected to form a 'high MT' group (MT (mean, SD): 0.98, 0.038; age (mean, SD): 69.33 years, 2.74) and 'low MT' group respectively (MT (mean, SD): 0.84, 0.023; age (mean, SD): 70.08 years, 3.34). I used right SN/VTA for post hoc tests of the MT subgroups based on the major VBQ finding of a correlation between right SN/VTA integrity and NGW performance. I used these subgroups for three analyses: first, to further explore the relationship between MT and behaviour within older adults only; second, to compare MT values of the SN/VTA between young and older adults; and third to compare novelty seeking scores within older adults only.

Voxel based quantification

To explore the regional specificity of the correlation between SN/VTA integrity and task performance, a method recently termed Voxel Based Quantification (VBQ) was used (Draganski et al., 2011). This allows whole brain statistical analysis of quantitative MRI parameters such as MT. The methodology was adapted from Draganski *et al.*, (2011) with a few adjustments specific to the current cohort summarised as follows. In brief, unified segmentation was used to classify MT maps into grey matter, white matter and cerebrospinal fluid (Ashburner and Friston, 2005). Whilst better segmentation of subcortical regions can be attained using MT rather than T1 maps (Helms et al., 2009), visual inspection revealed that the SN/VTA region was often incomplete and misclassified as white matter. Therefore, in subject space the manually defined SN/VTA ROI was added to each un-modulated grey matter mask and subtracted from the white matter. These maps were adjusted to ensure that all voxels remained in the range from zero to one. Using a diffeomorphic registration algorithm (DARTEL) the MT white and gray matter maps were warped to a common template (Ashburner, 2007). Modulation was achieved by multiplying these warped images with their Jacobian determinants. Finally, weighted average MT maps were created as previously described (Draganski et al., 2011) and smoothed with an isotropic Gaussian kernel of 6mm full width at half maximum.

Statistical analysis

Performance in each of the four task conditions was calculated as the percentage of correct responses and analysed using a repeated measures ANOVA with action (go/no-go) and valence (win/avoid loss) as the within-subjects factors. To compare performance between elderly MT subgroups, MT-group (low/high) was added as a between-subjects factor. To compare performance between all young and all older adults, age-group (young/old) was added as a between-subjects factor. To further explore behavioural response biases in go/no-go task performance in old age, I calculated the following measures using the total number of correct trials per condition: main effect of action (GW+GAL-NGW-NGAL), main effect of valence (GW+NGW-GAL-NGAL) and an interaction between action and valence (GW+NGAL-NGW-GAL). Partial Pearson's correlations (controlling for age and SN/VTA volume) were used to correlate response biases with SN/VTA MT values (significance level set at $p < 0.017$ after Bonferonni correction for three tests) and to assess the relationship between the behavioural interaction and personality measures of novelty seeking, reward dependence and harm avoidance (significance level set at $p < 0.017$ after Bonferonni correction for three tests). All reported significance values are two-tailed.

For structural imaging parameters of SN/VTA, linear multiple regression analyses were performed using Statistical Package for the Social Sciences (SPSS, Version 17.0). I used a backwards model to conduct a separate analysis for each of the four task conditions (GW, GAL, NGW, NGAL) where performance (percentage of total correct responses) in these conditions was used as the dependent variable. The five independent variables in each model

were the three imaging parameter values of bilateral SN/VTA (MT, T1 and R2* values), volume of the SN/VTA and age. The significance level for each model was set at $p < 0.0125$ (Bonferroni correction for four models). All reported significance values are two-tailed.

To address co-variance between MT and T1 values (Table 11) I also show the same results are obtained from separate correlations between neuroimaging parameters and task performance (Table 12).

	MT	T1	R2*
MT	-	$r = -0.36, p = .020$	$r = -0.11, p = .473$
T1	$r = -0.36, p = .020$	-	$r = 0.01, p = .949$
R2*	$r = -0.11, p = .473$	$r = 0.01, p = .949$	-

Table 11. Co-variance between neuroimaging parameters

r = Pearson's correlation coefficient (two-tailed); MT = magnetization transfer

	No-go to win	
	r	p
MT	0.48	.002
T1	-0.18	.251
R2*	0.02	.890

Table 12. Separate correlations between neuroimaging parameters and no-go to win

Separate correlations for each of the imaging parameter values showed the same results as the region-of-interest regression models, namely that MT but not T1 or R2* values of the SN/VTA correlated with no-go to win performance. r = partial Pearson's correlations with age as a covariate (two-tailed).

The VBQ analysis was only performed for the significant task condition (no-go to win) and image type (MT) from the behavioural regression analyses to minimise the number of voxel-based analyses. The calculated weighted average MT maps were analysed in a multiple regression model in SPM8. A single analysis was performed using a design matrix containing performance in all four task conditions (GW, GAL, NGW, NGAL) as separate covariates and age, gender and total intracranial volume (sum of grey matter, white matter and CSF) as regressors of no interest. I included performance in all four task conditions in a single model as a more stringent test to identify the unique variance associated with NGW performance over and above performance in the other conditions (Table 13) shows no significant covariance between these measures). An explicit mask created from the grey matter probability maps thresholded at 0.2 was applied. Uncorrected whole brain p-values <0.001 for clusters greater than 10 voxels are reported. I created SN/VTA and STN masks for small volume correction using individual subjects' manually defined ROI's, normalised to MNI space using DARTEL and group-averaged. A statistical threshold of $p < 0.05$ after family-wise error correction was used for the hypothesis-based small volume correction analyses.

	GW	GAL	NGW	NGAL
GW	-	$r = 0.24, p = .124$	$r = -0.28, p = .071$	$r = -0.01, p = .975$
GAL	$r = 0.24, p = .124$	-	$r = 0.08, p = .613$	$r = 0.13, p = .418$
NGW	$r = -0.28, p = .071$	$r = 0.08, p = .613$	-	$r = 0.20, p = .198$
NGAL	$r = -0.01, p = .975$	$r = 0.13, p = .418$	$r = 0.20, p = .198$	-

Table 13. Co-variance between performance in different task conditions.

Non-significant cross-correlations between performance in the four conditions of the task. r = Pearson's correlation coefficient (two-tailed); GW = go to win; GAL = go to avoid losing; NGW = no-go to win; NGAL = no-go to avoid losing

6.3. Results

6.3.1 Go/no-go task performance in older adults

Older participants were, on average, more accurate at go choices when the outcome was a reward (GW) and at no-go choices when the outcome was avoidance of losses (NGAL) (two (go/no-go) by two (win/avoid loss) repeated measures ANOVA: action by valence interaction: $F(1,41) = 12.55$, $p=.001$; GW versus GAL: $t(41) = 2.26$, $p=.029$; NGW versus NGAL: $t(41) = -3.20$, $p=.003$; Figure 20A). I also found a main effect of action indicating participants were better at learning go compared to no-go choices ($F(1,41) = 7.29$, $p=.01$). There was no main effect of valence ($F(1,41) = 1.87$, $p=.18$). These results demonstrate that older adults had a marked asymmetry in their learning behaviour (Figure 20A).

Older adults showed a preponderant initial bias towards go responses (Figure 20A) (one sample t-test for performance in the first 10 trials: GW $t(41) = 6.578$, $p = .000$; GAL $t(41) = 2.249$, $p = .030$). In contrast, performance in the first ten trials was at chance for the NGAL condition ($t(41) = 0.638$, $p = .527$) and significantly below chance for NGW ($t(41) = -4.365$, $p = .000$). This suggests a persisting action bias in the reward condition, whereas with loss a bias towards no-go responses emerged during learning.

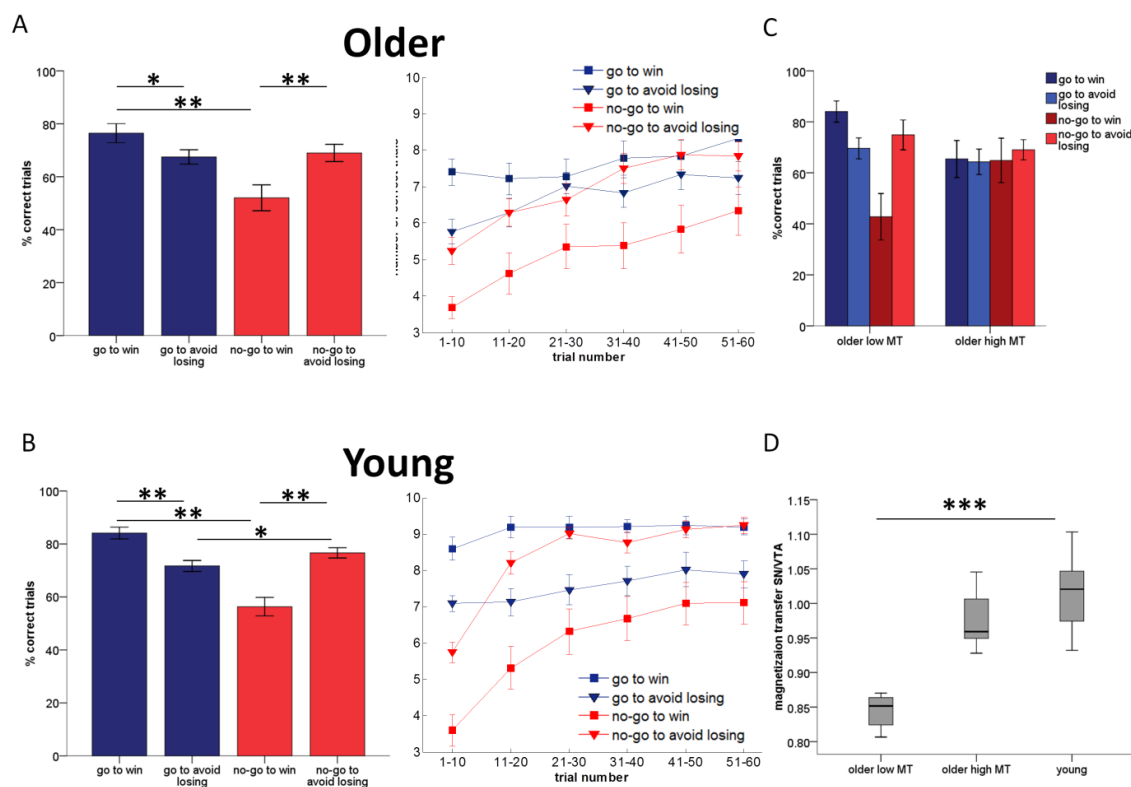


Figure 20. Go/no-go task performance in older and younger adults

(A, left): Older participants ($n = 42$) had an asymmetry in action-valence learning, such that they were better at learning to act for a reward ('go to win') than to avoid punishment ('go to avoid losing'), whereas they were better at learning to not act to avoid punishment ('no-go to avoid losing') than for reward ('no-go to win').

(A, right): Older adults began the task with a bias towards choosing an action ('go'). Learning occurred in all conditions over the course of the task.

(B, left & right) A similar overall pattern of behaviour was evident in 47 younger adults.

(C): A subgroup of 12 older individuals with higher SN/VTA integrity ('high MT') could overcome response biases to acquire competing responses for reward, compared to a subgroup of 12 older adults with lower SN/VTA integrity ('low MT').

(D): This 'low MT' subgroup of older adults had significantly lower MT values of SN/VTA than 12 young adults whereas the 'high MT' subgroup of older adults had similar MT values to younger adults. Note the young group here is a different set of participants from those whose behaviour is shown in B. Magnetization transfer values are in arbitrary units.

Error bars represent ± 1 SEM. * $0.01 < p < 0.05$, ** $p < 0.01$, *** $p < 0.0005$.

6.3.2 Structural neuroimaging in older adults

Region-of-interest analysis: For each experimental condition amongst older adults, I constructed a multiple regression model with task performance as the dependent variable and SN/VTA imaging parameter values (MT, T1, R2*), age and SN/VTA volume as independent variables. These models only explained variance in NGW performance where the best model contained MT as the only explanatory variable (standardised Beta MT = 0.46, $p = .002$, R square = 0.21). The additional variables did not add explanatory power Table 14. Thus, higher SN/VTA integrity predicted an ability to learn to inhibit an action to obtain reward. Figure 21A plots this correlation, which remained significant after controlling for both total intracranial volume and size of the SN/VTA (partial Pearson's $r = 0.39$, $p = .014$). Regression models for the remaining task conditions were not significant suggesting that neither structural integrity, iron or myelin content of SN/VTA were associated with learning the GW, GAL or NGAL conditions (Table 15).

	predictor variable(s)	β	p
<u>Model 1</u>	T1	-0.07	0.66
	R2*	0.08	0.59
	age	0.20	0.18
	vol	0.26	0.10
	MT	0.38	0.02
<u>Model 2</u>	R2*	0.08	0.57
	age	0.20	0.19
	vol	0.24	0.10
	MT	0.41	0.07
<u>Model 3</u>	age	0.22	0.12
	vol	0.24	0.10
	MT	0.40	0.007
<u>Model 4</u>	vol	0.21	0.17
	MT	0.40	0.01
<u>Model 5</u>	MT	0.46	0.002

Table 14. Multiple regression results for each predictor variable for no-go to win performance.

The magnetization transfer (MT) value of the SN/VTA was the only significant contributing variable to no-go to win performance in each model. Vol = SN/VTA volume.

	predictor variable(s)	F	p
<u>Go to win</u>			
Model 1	MT, vol, age, T1, R2*	1.25	0.31
Model 2	MT, vol, age, T1	1.56	0.21
Model 3	MT, vol, age	2.05	0.12
Model 4	MT, vol	2.80	0.073
Model 5	MT	4.01	0.052
<u>Go to avoid losing</u>			
Model 1	vol, MT, T1, age, R2*	0.97	0.45
Model 2	vol, MT, T1, age	1.25	0.31
Model 3	vol, MT, T1	1.68	0.19
Model 4	vol, MT	1.57	0.22
Model 5	vol	1.73	0.20
<u>No-go to win</u>			
Model 1	MT, vol, age, R2*, T1	3.14	0.02
Model 2	MT, vol, age, R2*	3.97	0.01
Model 3	MT, vol, age	5.28	0.004
Model 4	MT, vol	6.40	0.004
Model 5	MT	10.55	0.002
<u>No-go to avoid losing</u>			
Model 1	Age, T1, vol, MT, R2*	0.62	0.68
Model 2	Age, T1, vol, MT	0.79	0.54
Model 3	Age, T1, vol	1.05	0.38
Model 4	Age, T1	1.28	0.29
Model 5	Age	1.64	0.21

Table 15. Multiple regression models relating imaging parameter values to go/no-go performance in each of the four task conditions

Multiple regression models using a 'backwards method' shows magnetization transfer (MT) values of SN/VTA was the strongest predictor for no-go to win performance. Vol = SN/VTA volume.

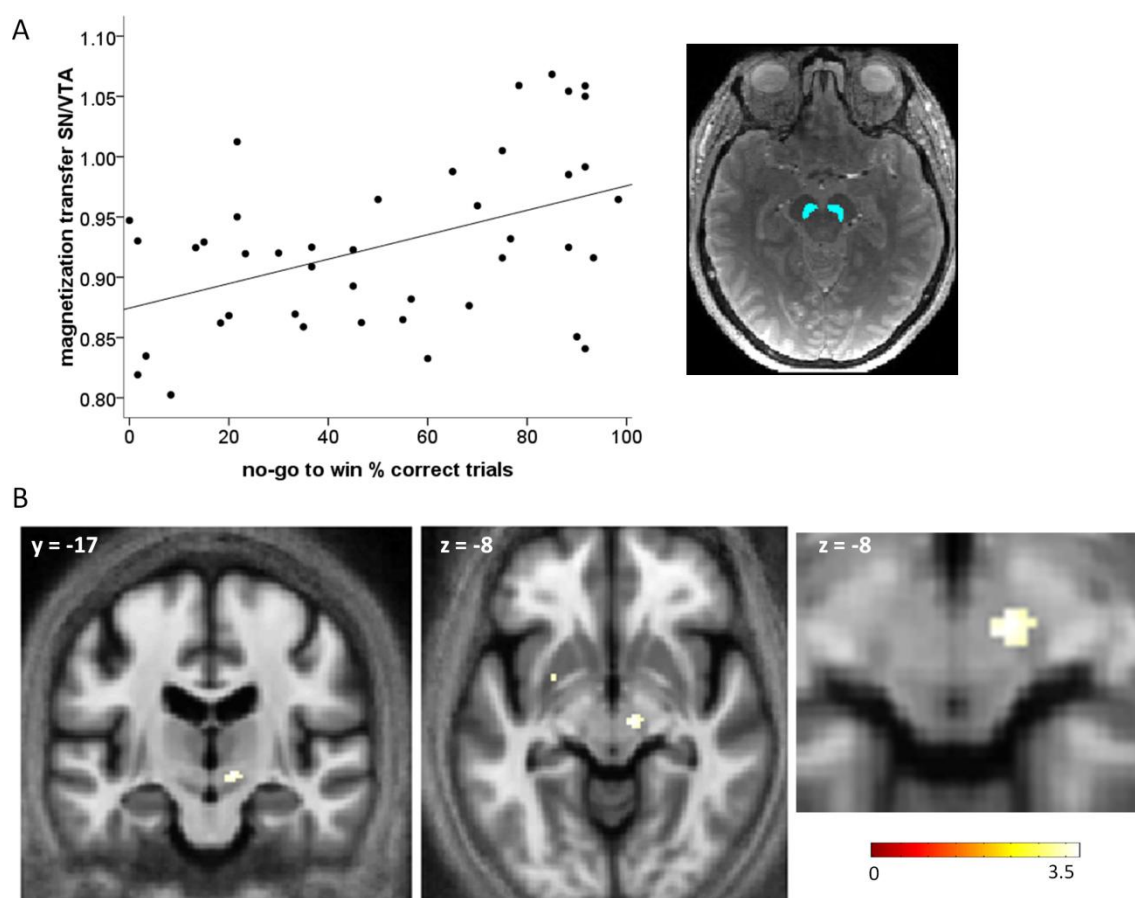


Figure 21. Higher no-go to win performance is associated with higher structural integrity of SN/VTA and STN

(A): Region-of-interest analysis of the SN/VTA (single subject single slice illustration of the bilateral SN/VTA ROI, blue). Plot shows older individuals with higher SN/VTA integrity, indexed by higher magnetization transfer (MT) values, performed better in the no-go to win condition of the task. Magnetization transfer values on y-axis of plot are measured in arbitrary units.

(B): An independent whole-brain voxel-based analysis of MT maps confirmed the association between higher MT values and no-go to win learning, localising to a region overlapping with the right SN/VTA and right STN. Displayed on group-averaged MT image, uncorrected threshold $p < 0.001$.

I next analysed how SN/VTA integrity related to the ability to overcome response biases. The action bias (go > no-go performance for both wins and losses) was negatively correlated with SN/VTA integrity ($r = -0.45$, $p = 0.003$, Figure 22A) suggesting that only those individuals with high SN/VTA integrity were able to overcome this action bias. Moreover, the negative correlation between the interaction in task performance (go to win and no-go to avoid losing > no-go to win and go to avoid losing performance) and SN/VTA integrity suggests the action-valence learning asymmetry could also be overcome with higher SN/VTA integrity ($r = -0.42$, $p = 0.006$; Figure 22B). There was no correlation between SN/TA integrity and the main effect of valence ($r = -0.22$, $p = .155$).

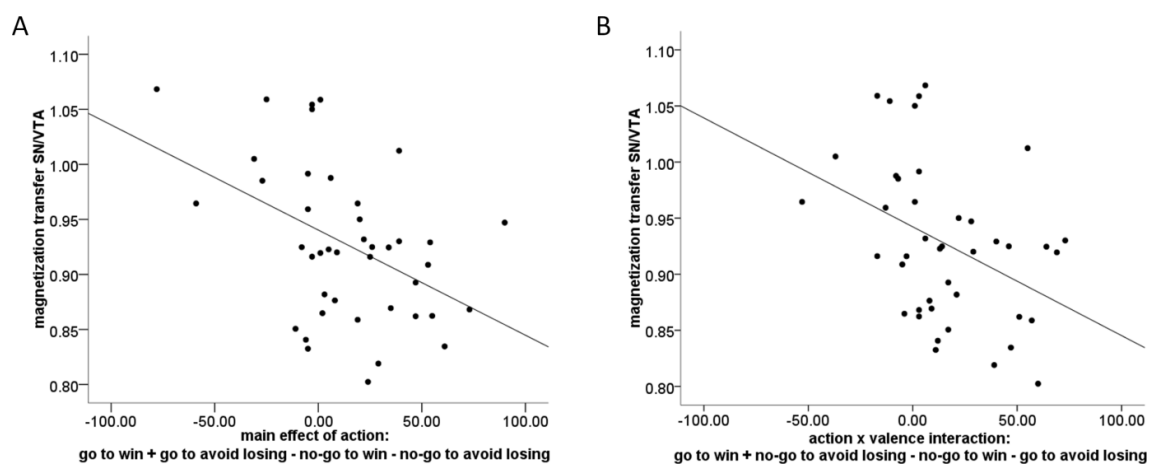


Figure 22. Relationship between SN/VTA structural integrity and flexibility of instrumental learning

Scatter plots, where each dot represents an individual, showing that higher SN/VTA integrity in older adults correlated with both a reduced action bias (A) and reduced interaction between action and valence learning (B). Magnetization transfer values on y-axis of both plots are measured in arbitrary units.

These results were also reflected in the elderly MT subgroup analyses, whereby I formed two gender-matched groups of older adults with the highest and lowest MT values of SN/VTA. I performed a repeated measures ANOVA as before with action (go/ no-go) and valence (win/ avoid loss) as within-subjects factors but additionally included MT group (low/ high) as a between-subjects factor. Figure 20C shows the striking behavioural asymmetry between action and valence learning was present in the low MT group but not in the high MT group (3-way action by valence by MT-group interaction: $F(1,22) = 5.25, p = .032$).

Older individuals with low SN/VTA integrity were inflexible in learning the reward conditions: they readily learned the GW condition but were less able to concurrently learn the NGW condition. In contrast, older individuals with high SN/TA integrity were instrumentally more flexible, i.e. acquired both go and no-go responses concurrently to obtain rewards. However, higher flexibility in the high MT group came at a cost for GW performance (trend towards a negative correlation between GW and NGW performance ($r = -0.28, p = 0.071$) but not between GAL and NGAL ($r = 0.13, p = 0.42$). This suggests a trade-off between the ability to learn competing responses in the reward conditions. Similar to the assessment of behaviour across all 42 older adults, this analysis of the MT-subgroups also demonstrated a trend towards a main effect of action ($F(1,22) = 3.16, p = .089$), a significant action by valence interaction ($F(1,22) = 8.28, p = .009$) and no main effect of valence ($F(1,22) = 1.47, p = .24$). Overall, these results suggest that amongst older individuals, those with higher integrity of the SN/VTA were able to overcome their initial response biases leading to more flexible instrumental learning, evidenced by a more even performance across the different action-valence contingencies. Since the behavioural interaction

was mostly driven by GW and NGW learning, these correlations also show that higher SN/VTA integrity confers flexibility by an improvement in NGW learning but with a concurrent slight decline in GW learning.

6.3.3 Voxel-based quantification

To address potential bias from a ROI-analysis, and assess the anatomical specificity in the relationship between NGW performance and SN/VTA, I used a whole brain voxel-based quantification (VBQ) analysis. This showed that positive correlations between NGW performance and MT values were restricted to a region that included the right SN/VTA and STN (Figure 21B), with smaller clusters in the left cerebellum and left putamen only (Table 16). For the SN/VTA and STN cluster, I quantified the percentage of overlap with probability maps of each anatomical region and found that 17.4% of the cluster overlapped with the STN, compared to 47.6% overlap with the SN/VTA. Using these probability maps, the multiple regression VBQ analysis of NGW performance and MT values of the right SN/VTA survived a hypothesis-based small volume correction ($p < 0.05$, FWE-corrected, $Z_{\max} = 3.39$, $x = 9$, $y = -17$, $z = -8$). The same was true for the right STN ($p < 0.05$, FWE-corrected, $Z_{\max} = 3.33$, $x = 11$, $y = -17$, $z = -8$).

Region	No. voxels	MNI co-ordinates			T	Z
		X (mm)	Y (mm)	Z (mm)		
right SN/VTA & STN	33	9	-17	-8	3.73	3.39
left cerebellum	16	-38	-65	-39	3.57	3.27
left putamen	13	-27	3	-5	3.51	3.22

Table 16. Voxel-based quantification results for no-go to win positive correlation with grey matter MT images.

Peak level results are shown for all clusters greater than 10 voxels, p-value <0.001 uncorrected at the whole brain level. SN/VTA = substantia nigra/ventral tegmental area; STN = subthalamic nucleus

6.3.4 Age-comparison of task performance

To contextualise behavioural performance of older adults, I obtained data from a separate experiment in which the same behavioural task was performed by 47 younger adults, of which 30 underwent MT imaging (a detailed description of behaviour amongst these younger adults can be found in (Guitart-Masip et al., 2012a)). A two by two repeated measures ANOVA with action (go/no-go) and valence (win/avoid loss) as within subjects factors, and age group (young/old) as between subjects factor showed a main effect of action ($F(1,87) = 21.75, p = .000$), main effect of valence ($F(1,87)=4.17, p = .044$) and significant action by valence interaction ($F(1,87) = 47.23, p = .000$) but no significant interaction of any factors with age group. Thus the overall pattern of performance showing a marked behavioural asymmetry was present in both young and older adults (Figure 20B). Performance averaged over all task conditions was worse in older adults (main effect of age $F(1,88) = 15.15, p < 0.0005$).

Performance heterogeneity in these young adults has previously been described, where some individuals performed well in all conditions of the task (so-called 'learners', 19/30 participants) and others in whom instrumental learning was unsuccessful (so-called 'non-learners', 11/30 participants), where these differences were related to stronger Pavlovian biases in non-learners. (see (Guitart-Masip et al., 2012a)). I found that performance in older adults in the low MT subgroup resembled that of young non-learners whereby Pavlovian response biases dominated performance (Figure 23). In contrast, performance in older adults in the high MT subgroup more closely resembled that of young adult learners. However, whilst overall performance levels were higher in young learners compared to non-learners (89% vs 66% respectively, independent

samples t-test $t(28) = 10.79, p < 0.0005$), older adults in the high MT subgroup demonstrated a trade-off between Pavlovian biases (in this case, GW) and instrumental learning (in this case, NGW) such that overall performance levels did not differ between the older groups (66% vs 68% respectively, independent samples t-test $t(22) = 0.41, p = .685$).

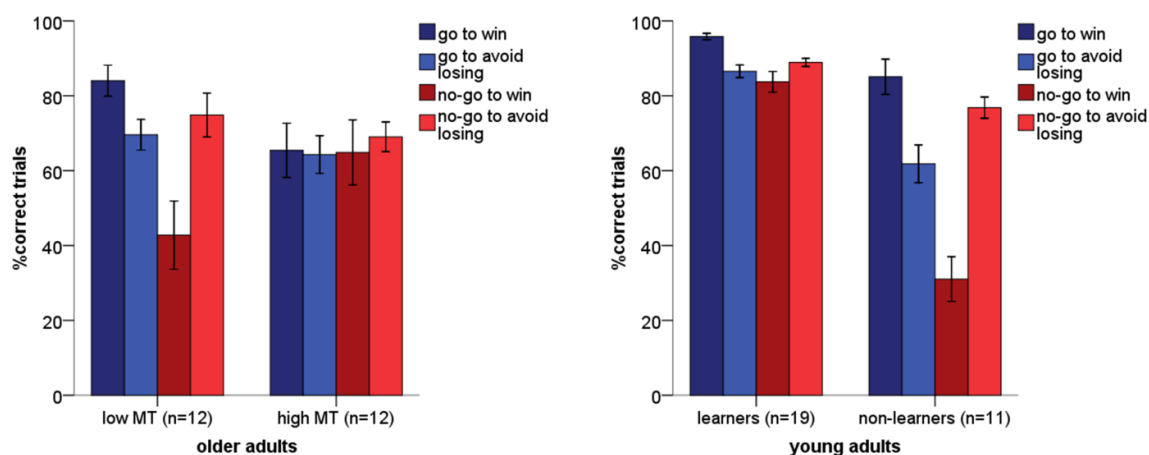


Figure 23. Illustration of performance in older subgroups (low/high MT) and younger subgroups (leaners/non-learners)

The same action-valence asymmetry (indicating unsuccessful instrumental learning) was present in older adults with low MT values of SN/VTA ($n = 12$) and young adult non-learners ($n = 11$). Elimination of an action-valence asymmetry (indicating successful instrumental learning) was present in older adults with high MT values of SN/VTA ($n = 12$) and young adult learners ($n = 19$). However, in contrast to young adult learners vs non-learners, higher NGW learning was accompanied by lower GW learning in older adults with high MT compared to older adults with low MT, meaning that more flexible instrumental learning in older age did not equate to higher performance levels overall.

6.3.5 Age differences of SN/VTA structural integrity and relationship with performance

In contrast to the strong relationship between higher NGW performance and higher SN/VTA structural integrity in older adults, no such correlation existed in young adults ($n = 30$), nor indeed with any of the task conditions (partial Pearson's correlations with age and SN/VTA volume as covariates: GW, $r = -0.12$, $p = .543$; GAL, $r = 0.01$, $p = .970$; NGW $r = -0.04$, $p = .859$; NGAL, $r = 0.07$, $p = .743$). Thus SN/VTA integrity predicted individual differences in flexible learning amongst older but not younger adults (Fisher's r -to- z transformation comparing partial correlation strengths of NGW with MT SN/VTA between young and older adults, with age and SN/VTA volume as covariates: $z = -1.93$, $p = .05$ two-tailed).

To examine age-group differences in SN/VTA integrity, I obtained comparable MT imaging (obtained on the same MRI scanner and using the same acquisition and reconstruction protocols) from a separate cohort of 12 younger adults. Here I found significantly higher MT values of SN/VTA in young adults than in older adults, suggesting that older adults had age-related structural decline of the SN/VTA (independent t -test, $t(52) = 4.13$, $p < 0.0005$). Further analysis of the older MT subgroups with younger adults using a one-way ANOVA with MT values of the right SN/VTA as the dependent variable and age-group as the between subjects factor confirmed a significant between group difference ($F(2,33) = 60.23$, $p < 0.0001$). Post hoc tests between the three groups with Bonferroni correction for multiple comparisons showed that there was a significant difference between MT values in the young group and low MT group in older adults ($p < 0.0005$) but not between the young group and high MT

group in older adults ($p = .081$) (Figure 20D). This suggests inter-individual variability of MT values of the right SN/VTA across this older cohort.

6.3.6 Instrumental learning and novelty seeking in older adults

Finally, using a Tridimensional Personality Questionnaire I assessed the impact of a novelty seeking personality trait on the success of instrumental learning in old age, specifically the ability to overcome the behavioural action-valence interaction. I observed an almost significant trend towards a negative correlation between the behavioural interaction (GW and NGAL > GAL and NGW) and novelty seeking (partial Pearson's correlations controlling for age: $r = -0.37$, $p = .019$) whereas no correlation was observed with the other measured personality traits of harm avoidance ($r = 0.008$, $p = .959$) or reward dependence ($r = 0.09$, $p = .560$) (Figure 24). This suggests that older adults with a more novelty seeking personality had greater flexible instrumental learning. Interestingly, older participants in the high MT subgroup, that is participants who showed greater flexibility of instrumental learning, also had higher novelty seeking scores than older participants in the low MT group (independent samples t-test: $t(22) = -2.74$, $p = .012$) (Figure 24).

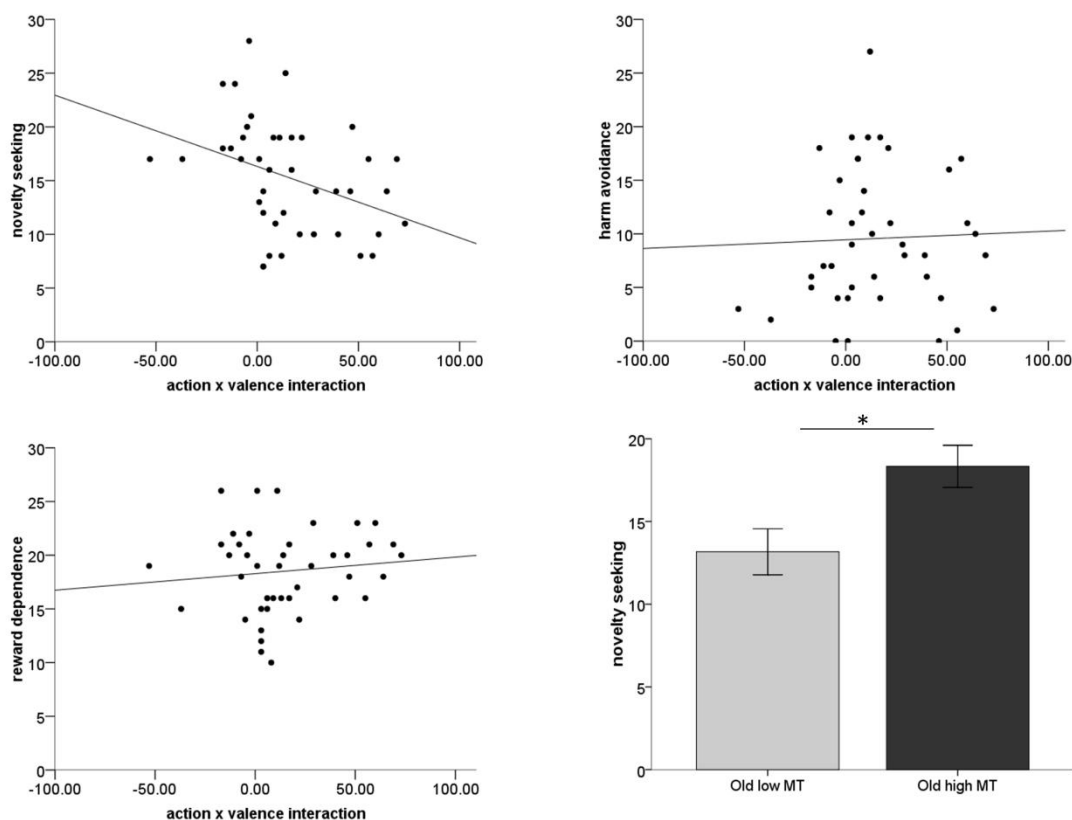


Figure 24. Correlation between novelty seeking and the interaction in go/no-go task performance.

Higher novelty seeking, but not harm avoidance or reward dependence, personality trait scores correlated with a reduced behavioural interaction in task performance (action x valence interaction represents $GW + NGAL > NGW + GAL$). A subgroup of older adults with high magnetization transfer values (MT) values of the SN/VTA had higher novelty seeking scores than older adults with low MT values (n=12 per MT group). * $p < 0.05$

6.4. Discussion

My results reveal that some healthy older adults are unable to flexibly learn two responses (go and no-go) for reward within a single task. Through the use of high resolution quantitative MT imaging I show that this ability to flexibly learn competing choices for reward is predicted by structural integrity of the SN/VTA and STN. Although I hypothesized that integrity in the SN/VTA would correlate with instrumental learning as demonstrated by my ROI analysis, the additional level of specificity in the whole-brain analysis is remarkable and suggests that the dopaminergic system may arbitrate between go and no-go choices for reward.

This striking relationship between higher NGW performance and higher SN/VTA integrity was surprising given previous reports that dopamine promotes 'go' and impairs 'no-go' learning, for example in patients with Parkinson's disease (Frank et al., 2004). However such studies have tended to explore behavior in two conditions, GW and NGAL. Here, using a task which orthogonalises action (go and no-go) and valence (reward and punishment), I can demonstrate a more precise contribution of the dopaminergic system to this behavioural inflexibility in healthy older individuals. Previous research in patients with Parkinson's disease suggested that loss of dopaminergic neurotransmission should primarily impair the ability to learn go responses towards rewards (Frank et al., 2004). My data are not necessarily in opposition with these findings. First of all, in my task rewards may be harvested by go and no-go choices generating a competition between both responses, whereas in most previous experiments rewards are harvested through go choices and punishment avoided through no-go choices (e.g. (Frank et al., 2004; Cools et al., 2009)). Second, older adults

were healthy and did not have any neurological impairment suggestive of clinically apparent basal ganglia dysfunction. Hence, the low integrity of SN/VTA indexed by MT imaging can be viewed as being mild. Thus, in the early stages of SN/VTA degeneration, dopaminergic neurotransmission may be sufficiently intact to enable go learning for rewards. Instead, the earliest behavioural sign of SN/VTA degeneration may be an impairment to learn competing instrumental responses for rewarding outcomes. Individuals with early SN/VTA degeneration still exhibit a prepotent bias for behavioural activation towards rewards during instrumental learning (go to win) but are impaired in concurrently learning competing no-go responses for the same outcome. Those with high SN/VTA integrity are able to flexibly learn both, the prepotent (biased) 'go' response and the competing 'no-go' response. However, this flexibility to learn both responses appears to come at a cost for overall performance, with the result that performance in the go for rewards condition suffers from the inability to concurrently also learn no-go responses to rewards.

It has been suggested that age-related dopamine decline has an impact on the relationship between novelty processing and motivational behavior (Duzel et al., 2010). I found that older participants with less of an asymmetry in action-valence learning had higher novelty seeking personality scores and older adults with higher SN/VTA integrity were more novelty seeking than those with low integrity. These findings may be in keeping with the so-called 'exploration bonus' hypothesis that dopamine neurons originating in the SN/VTA can modulate motivational behaviour by signalling novel and reward-predicting events (Kakade and Dayan, 2002). It has been reported that novelty seeking individuals show heightened prediction error signalling in the nucleus

accumbens (Abler et al., 2006), as well as increased dopaminergic responses to novelty in the ventral striatum (Zald et al., 2008). Thus whilst one possible explanation for my findings is that variations in SN/VTA integrity may confer different sensitivities to reward and punishments, the link I identify with novelty seeking could suggest that SN/VTA integrity modulates motivational behaviour in this task. Inflexible behaviour can arise if participants stick to go choices after receiving a reward for a go choice early in the task. In contrast, higher novelty seeking individuals may be more likely to explore alternative responses (i.e. sample no-go responses) allowing them to successfully instrumentally learn. However, I acknowledge that a novelty seeking personality trait is not a direct measurement of exploratory behaviour. Alternatively, novelty seeking may be a marker of greater dopaminergic integrity rather than a mechanism related to instrumental learning in the task per se.

Differences in reward sensitivity alone could not fully explain my finding of an interaction between action and valence. If SN/VTA degeneration mainly affected reward sensitivity, then both reward conditions in the task (GW and NGW) would be equally affected, rather than the pattern I observe of better performance in one condition (NGW) at the expense of the other (GW) in individuals with greater SN/VTA integrity. I consider this ability to acquire competing responses for rewards as a marker of flexible learning, although I acknowledge this does not translate to overall higher performance levels but rather a more even performance across the different contingencies of the task. Future studies relating midbrain structural integrity to other behavioural indices of flexibility, such as reversal learning, could help to further address the nature of this relationship.

In addition to the SN/VTA, the other structure implicated in modulating NGW performance in older adults was the STN. The STN is a biconvex structure that lies superior to the SN/VTA (Dormont et al., 2004). Along with other basal ganglia structures, it too is innervated by dopaminergic fibres from the SN/VTA (Hamani et al., 2004). The STN plays a critical role in action inhibition by relaying a stopping signal (Aron and Poldrack, 2006) (Frank et al., 2007) (Fleming et al., 2010) . This inhibitory network depends on interactions between the STN, inferior frontal gyrus and supplementary motor area (Coxon et al., 2012) (Duann et al., 2009) (Aron and Poldrack, 2006; Aron et al., 2007) (Jahfari et al., 2011; Swann et al., 2012). Previous work by from the host institution using the same go/no-go task has shown that inferior frontal gyrus activity is associated with no-go learning and successful instrumental control (Guitart-Masip et al., 2012a). The current structural SN/VTA and STN findings are therefore compatible with a literature relating functional activity in the post-synaptic targets of midbrain nuclei and their related circuits to both response inhibition and instrumental learning. It is also notable that my VBQ analysis localised NGW learning to structural integrity of the right SN/VTA and STN since inhibitory processing has been reported to evoke a right-lateralised network (Garavan et al., 1999; Aron et al., 2003; Zheng et al., 2008; Coxon et al., 2012).

Although overall patterns of performance were similar in young and older adults (as shown in Figure 20), some differences emerged which I speculate are linked to age-related neural differences. At a group level, older adults with the lowest MT values of SN/VTA displayed a behavioural inflexibility particularly for

rewards. These same adults had significantly lower MT values of SN/VTA than younger adults, which might mean they had age-related degeneration of the SN/VTA. Although significantly lower overall performance was observed in the older group, performance in these older individuals was markedly similar to young adults who were unable to learn this task in terms of the observed action by valence interaction during learning. In contrast, performance in older adults with similar midbrain integrity to younger adults resembled performance seen in young adult 'learners'. However it was notable that these older adults who learned to overcome pre-potent response biases did so at the cost of overall task performance. This trade-off between instrumental and Pavlovian systems was not evident in young adults who successfully instrumentally learned. One possible explanation for this is the involvement of other brain regions in young adults performing this task. For example, it has been shown that young adults who are able to instrumentally learn in this task show heightened activity in the inferior frontal gyrus (Guitart-Masip et al., 2012a). Future studies designed to directly test age-differences in this structure-function relationship could elucidate this further.

An advantage of my study was the use of high quality MT images to accurately identify the SN/VTA and R2* images to define the STN. The MT contrast is particularly suited to visualising brainstem structures as it provides better grey/white matter contrast than the standard T1w MRI contrast (Helms et al., 2009). MT measures macromolecule concentration and thus reflect the properties of bound protons in structures such as myelin (Tofts, 2003), axons (Klistorner et al., 2011), cell membrane proteins and phospholipids (Bruno et al.,

2004) (Wolff and Balaban, 1989). Moreover, reduced MT in the SN/VTA has been described in Parkinson's disease and is proposed to reflect the loss of dopamine neurons (Eckert et al., 2004) (Tambasco et al., 2011). I found that some but not all older adults had lower structural integrity of the SN/VTA than younger adults. This suggests inter-individual variability of SN/VTA structural integrity amongst older adults and possibly relates to variable dopamine decline as a function of age, although I acknowledge that the exact pathology underlying alterations in the MT signal in normal aging remains unknown. Future studies combining MT imaging with other imaging modalities (e.g. Positron Emission Tomography) and histological evidence will help to provide greater insight into the interpretation of MT values of dopaminergic brainstem structures.

In summary, the new perspective highlighted here is that individual differences of SN/VTA integrity contribute to learning flexibility by allowing older individuals to overcome response biases. In contrast, structural integrity of SN/VTA did not predict instrumental learning in younger adults, suggesting that instrumental learning in older age is sensitive to structural changes of the dopaminergic midbrain.

In this study I have shown that action and valence bias the flexibility of learning. Other forms of decision-making, such as affective processing, are also influenced by the aging process and may also be susceptible to asymmetrical valence processing. In the next chapter, I study the effect of age on valence relating to positive and negative information about the future, within a different context: optimism.

Chapter 7

Optimism in older age

7.1. Introduction

Increasing age heralds an array of negative life events including bereavement, reduced social networks, a decline in physical health and cognitive function, together with the inevitable foreshortening of ones time horizon (Rowe and Kahn, 1987) (Hedden and Gabrieli, 2004). Viewed from the perspective of young adulthood, one might reasonably infer that this should portend an increasing pessimism. Yet surprisingly, older adults have higher levels of emotional well-being than their younger counterparts, including a decline in their experience of negative emotions (Blanchflower and Oswald, 2008; Stone et al., 2010; Carstensen et al., 2011).

Optimism has been associated with greater well-being and therefore provides one explanatory account for enhanced well-being in older age (Scheier and Carver, 1993). However, few studies have addressed the effect of age on optimism and the results are inconsistent. One such study showed older adults had a more optimistic style when explaining life events (Isaacowitz, 2005) whereas another study found that younger rather than older adults had a more optimistic outlook about the future (Lachman et al., 2008). Many studies have focussed on the related concept of an age-related 'positivity effect' on cognitive

processing (for reviews see (Mather and Carstensen, 2005) and (Isaacowitz and Blanchard-Fields, 2012)). For example, in comparison to their younger counterparts older adults remember faces displaying positive emotions more than negative emotions (Mather and Carstensen, 2003), have less rich autobiographical memory for negative events (Comblain et al., 2005) and experience less negative arousal when anticipating monetary loss (Samanez-Larkin et al., 2007). Such findings have been interpreted within the framework of socioemotional selectivity theory, whereby changing time horizons may lead to modification and prioritization of emotionally relevant goals (Carstensen et al., 1999) (Charles and Carstensen, 2010).

Optimism, defined by the tendency to underestimate the likelihood of future negative events, has been related to an asymmetry in updating beliefs when faced with desirable and undesirable information (Fischer and Chalmers, 2008) (Sharot et al., 2011) (Sharot et al., 2012a) (Sharot et al., 2012b). Optimism in younger adults seems to be, at least in part, mediated via functional activity of inferior frontal gyrus (Sharot et al., 2011) and anterior cingulate cortex (ACC) (Sharot et al., 2007). Importantly, a large body of literature links age-related functional magnetic resonance imaging (MRI) differences in ACC to a positivity effect on cognitive processing and greater emotion regulation with age (Kensinger and Schacter, 2008; Leclerc and Kensinger, 2008; Brassens et al., 2011; Samanez-Larkin and Carstensen, 2011; Brassens et al., 2012). Structural abnormalities of the ACC, in particular dorsal ACC, have been identified in clinical depression, where pessimism is a core feature (Vasic et al., 2008) (Pizzagalli, 2011). Higher volume of this dorsal as opposed to ventral subregion

has been found in healthy individuals who show greater cognitive reappraisal, a mechanism through which emotions may be regulated (Giuliani et al., 2011).

To determine whether or not optimism is enhanced in old age, and the underlying mechanisms, I tested young and older healthy adults using a modified version of a previously described belief updating paradigm (Sharot et al., 2011) (Figure 25). I also obtained a measure of trait optimism. To determine if the volume of the ACC was related to age-related differences in the update bias, I used structural neuroimaging and a region-of-interest analysis of the dorsal and ventral subregions together with an independent whole brain analysis to identify the neural correlates of updating beliefs.

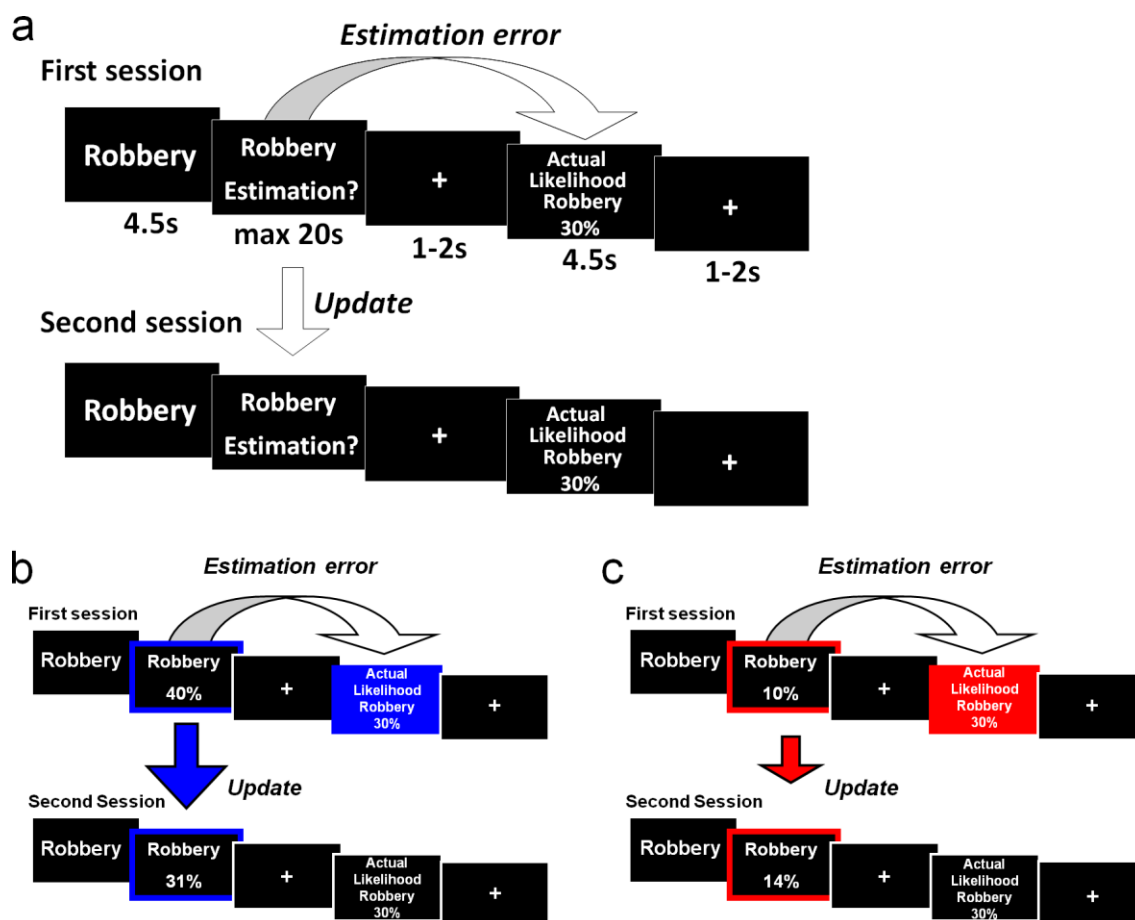


Figure 25. Optimism task design.

(a) On each trial, participants were presented with one of 45 adverse life events and asked to estimate how likely this event was to occur to them in the next 5 years. They were then presented with the average probability of that event occurring to a person similar to themselves in the same socio-cultural environment. For each event an estimation error was calculated as the difference between the participants' estimation and the actual probability provided. The second session was the same as the first session.

(b) For each event, an update was calculated as the difference between the participants' first and second estimations. If the participants' first estimate was higher than the actual probability provided, that trial was classified as 'desirable' since the

information presented was better than expected, calling for an adjustment in an optimistic direction.

(c) If the participants' first estimate was lower than the actual probability provided, that trial was classified as 'undesirable' since the information presented was worse than expected, calling for an adjustment in a pessimistic direction.

7.2. Methods

Participants

18 younger adults (mean age = 22 years, range = 20 - 29) and 18 older adults (mean age = 66 years, range = 57 - 76), all of whom were healthy and not depressed, participated in this study (see Table 17 for demographics). Participants were recruited through an advertisement placed in a local newspaper and word of mouth. Written informed consent was obtained from all participants. The study received ethical approval from the UCL research ethics committee. To ensure participants were healthy, they were initially screened by telephone and excluded if they had any of the following: current or past history of neurological, psychiatric or endocrinological disorders (including diabetes mellitus and thyroid dysfunction), major visual or hearing impairment, history of drug addiction and current illicit drug use. To control for vascular risk factors, individuals known to have had a stroke or transient ischemic attack, myocardial infarction or require more than one anti-hypertensive medication were not eligible for participation. Participants with any contraindications to MRI scanning were not eligible for participation.

	Young	Old	t / Z	p
Age (yrs)	22.22 (2.29)	66.00 (5.62)	30.63	<0.0005
Gender (M:F)	8:10	7:11	0.33	.791
Yrs education	17.11 (1.18)	16.83 (2.01)	0.51	.616
IQ	110.72 (7.88)	123.83 (6.19)	5.55	<0.0005
MMSE	30 (29 – 30)	30 (29 – 30)	0.81	.613
BDI	3.06 (2.10)	4.00 (2.30)	1.26	.216

Table 17. Demographic details.

Mean (SD) or median (range). Independent t-tests for parametric variables, Mann-Whitney U test for non-parametric variables. IQ estimated using the National Adult Reading Test; MMSE: Mini-Mental State Examination; BDI: Beck Depression Inventory. n = 18 per group.

Cognitive screening: All participants had a Mini-Mental State Examination (MMSE) score ≥ 28 . Since the MMSE alone is not a sensitive marker of pathology, in older adults I administered additional standardised neuropsychological tests to screen for deficits in declarative memory (Rey Auditory Verbal Learning Test, RAVLT immediate and delayed recall), visuo-motor speed (Digit Symbol Substitution Test, DSST), attention and set-shifting (Trail-making A & B). I excluded participants who scored $>1SD$ outside the age-related norms for the cognitive tests to ensure I had a cognitively intact sample of older adults. This resulted in the exclusion of two participants based on their RAVLT delayed free recall score, where low scores may be an early indicator of pathology (Estévez-González et al., 2003). For the remaining elderly participants, mean (SD) cognitive scores were as follows: RAVLT immediate recall 55.50 (6.33), RAVLT delayed recall 11.33 (2.23), DSST score 56.67 (8.22), Trail-Making A time 29.55 sec (6.19), Trail-Making B time 58.51 sec (20.04).

Mood screening: I measured depressive symptoms in all participants using the Beck Depression Inventory (Beck et al., 1961). BDI scores > 10 indicate depression, therefore I excluded one young and three old participants (note one of these older adults was also excluded on the basis of their low RAVLT score as described above).

Optimism task

As shown in Figure 25, I used a modified version of the task by Sharot et al. (2011) (Sharot et al., 2011). The task structure remained the same and was as follows: participants viewed 45 negative events, such as robbery (4.5s) (see Table 18 for a list of all stimuli) and were asked to type on a keyboard their estimate of how likely the event was to occur to them in the next five years (20s). After a brief fixation cross (1-2s) they were presented with the average probability of this event happening to someone in the general population (4.5s), followed by a further fixation cross (1-2s). Immediately after this first session, participants performed the same task again. The order of the presentation of events was randomised between the first and second sessions and across participants. I adapted the task to make it applicable to both young and older adults as follows. First, all participants were given longer to input their responses than on previously run versions of this task. I note reaction times did not differ between young and older adults (Table 19). Second, I only included events that had an equal likelihood for both groups thus no health-related questions were included. Third, participants were asked to rate how likely events were to occur to them in the next 5 years to account for differences between time perspectives in the two groups. At the end of the study I asked participants to estimate their lifespan; all participants thought they would live longer than 5 years, ensuring that they could imagine the events occurring in their lifetime.

As previously described by Sharot et al (2011), the average probability of each event occurring to a person living in the same socio-cultural environment was determined using online resources and additionally in this study, using a small

number of events from a previously validated set of events likely to occur to the general population (Strunk et al., 2006). Very rare and very common events were not included thus all event probabilities lay between 10% and 70%. Participants were told the range of probabilities was between 3% and 77% to ensure the ranges of possible overestimation and underestimation were equal.

Trials in which the estimation error was zero or participants did not respond were discarded. On average, both young and old adults completed most trials (mean 44.8, SD 0.73 and mean 44.1, SD 1.48 respectively).

fraud when buying something on the internet	victim of violence at home
theft from vehicle	having fleas/lice
card fraud	severe injury due to accident (traffic or house)
victim of violence with need to go to A&E	victim of mugging
sport related accident	holiday cancelled due to natural disaster
household accident	public transport delay causing you to be late
mouse/rat in house	identity fraud
victim of violence by acquaintance	insect infestation (e.g. ants) in your home
being cheated by husband/wife/partner	roof leak
more than £30000 debts	spill difficult-to-remove substance (e.g. red wine) on carpet
miss a flight	short-changed in a shop
witness a traumatising accident	passenger in a car accident
domestic burglary	lose your house keys
victim of violence by stranger	heating system in your house breaks down
car/bicycle stolen	stung by a bee
being convicted of crime	accidentally break something at a guests house
house vandalised	car vandalised
computer crash with loss of important data	burn something you are cooking
skin burn	serious disagreement with a good friend
theft from person	receive unwanted call from telemarketer
shouted at by a stranger	have a serious family argument
more than 15 minutes late for an important meeting	get a parking or speeding ticket
bounce a cheque/payment	

Table 18. List of 45 stimuli presented to participants.

	Young	Old	Group average
First session			
Desirable trials	3.60 (0.83)	4.17 (1.19)	3.89 (1.05)
Undesirable trials	3.94 (0.78)	4.28 (1.62)	4.11 (1.27)
Second session			
Desirable trials	3.94 (0.57)	3.50 (0.78)	3.49 (0.67)
Undesirable trials	3.37 (0.62)	3.55 (0.88)	3.46 (0.75)

Table 19. Optimism task reaction times.

Mean reaction times in seconds, SD in parentheses.

Main behavioural analysis

Optimism task: By comparing participants' own initial estimates to the average probabilities presented ('first estimation error'), I could determine whether older adults had a greater tendency to underestimate negative events relative to young adults. The more negative the first estimation error relative to the average probability, the more participants underestimated the likelihood of the events occurring to them, suggesting they were more optimistic at the outset of the task. An independent t-test was used to compare the first estimation error between young and older adults.

The key test in this study was to determine differences between young and older adults pertaining to changing their beliefs after being presented with information that was better or worse than expected. For each subject, each trial was classified as 'desirable' or 'undesirable' depending on whether their initial estimate was higher or lower than the average statistic respectively. Thus, whilst all trials involved negative events, participants could receive desirable (better than expected) or undesirable (worse than expected) information for each event. I then calculated their change in beliefs ('update') as the difference between their first and second estimation (first estimation – second estimation for desirable trials; second estimation – first estimation for undesirable trials). I could then examine whether the update differed between desirable and undesirable trials, indicating an 'update bias', and whether age affected this bias. For this analysis of update, I used a repeated-measures ANOVA with valence (desirable/undesirable) as the within-subjects measure and age group (young/old) as the between-subjects measure. To account for potential confounding variables, differences on subjective rating scales, memory errors

and demographic variables were included as covariates in this analysis (see below).

Memory test and subjective rating scales: After the task, participants completed a self-paced memory test in which they were asked to recall the average probabilities that were previously presented for all events. Memory errors were calculated as the absolute difference between the average probability previously presented and the participants' recollection of that statistical number. Participants also rated all 45 events on the following subjective measures using a Likert scale from 1 (not at all) to 6 (very): vividness, familiarity, personal experience, emotional arousal and negativity. Subjective ratings for each measure and memory errors were analysed using a repeated measures ANOVA with valence (desirable/undesirable) as the within-subjects factor and age group (young/old) as the between-subjects factor. I also calculated a difference measure between subjective rating scores for desirable and undesirable trials to include as covariates in the main behavioural analysis.

Trait optimism: Participants completed the Life Orientation Test-Revised (LOT-R) which provides a measure of trait optimism (Scheier et al., 1994). Scores range from 0 (pessimistic) to 24 (optimistic). Between age-group differences in trait optimism were compared using an independent t-test.

Behavioural Statistical Analysis

All analyses were conducted using SPSS Version 17.0. The significance level for ANOVAs was set at $p < 0.05$, two-tailed. I did not perform corrections for multiple comparisons when testing for post hoc for differences in memory performance and subjective ratings since the aim of these analyses was to identify potential confounding factors that could be added as covariates to my main behavioural analysis, thus by not using Bonferroni corrections here my analyses were more stringent.

Neuroimaging acquisition

A high resolution structural MRI data set was acquired on a 3.0T Trio MRI scanner (Siemens) using a 32-channel head coil. Two sets of a multiparameter map protocol at 0.8mm isotropic resolution were acquired for each subject and averaged into a single data set to improve the signal-to-noise ratio. This 3D multi-echo fast low angle shot (FLASH) sequence was used to acquire T1-weighted images (TE 2.2-9.85ms, TR 23.7ms, FA 28 degrees) (Helms et al., 2008b). B1 mapping (TE 39.38 and 19.69ms, TR 500ms, FA 270:10-180 degrees, 4mm³ isotropic resolution) was acquired to correct the T1 maps for inhomogeneities in the transmit radiofrequency field (Lutti et al., 2010). A double-echo FLASH sequence (TE1 10ms, TE2 12.46ms, 3 x 3 x 2 mm resolution and 1mm gap) was used to measure local field inhomogeneities and correct for the image distortions in the B1 mapping data.

T1w images were segmented into grey matter, white matter and cerebrospinal fluid (Ashburner and Friston, 2005) using the New Segment toolbox in SPM8. Using a diffeomorphic registration algorithm (DARTEL) the grey matter maps

were warped to a common template (Ashburner, 2007). Grey matter maps were modulated, warped to MNI space and smoothed with an isotropic Gaussian kernel of 8mm full width at half maximum using the DARTEL toolbox 'Normalise to MNI' procedure. These smoothed, warped, modulated T1w images were used in independent region-of-interest and whole-brain voxel-based morphometry (VBM) analyses.

Neuroimaging analysis

Region-of-interest analysis: To directly compare the relationship between ACC grey matter volume and belief updating between young and old adults, I used a region-of-interest approach. I used a bilateral ACC atlas mask, obtained from the AAL toolbox (Tzourio-Mazoyer et al., 2002). Manual segmentation of this ACC atlas mask into dorsal and ventral subregions was achieved using ITK-SNAP (Yushkevich et al., 2006) using established guidelines where the ventral portion was defined by drawing a line in the coronal plane at the tip of corpus callosum (Killiany et al., 2000) (Giuliani et al., 2011). I performed correlations between grey matter volume of dorsal and ventral ACC and task measures in both age groups (two-tailed Pearson's correlations and partial Pearson's correlations with age, gender and total intracranial volume as covariates). I focussed on the update bias (desirable update minus undesirable update) since this summary measure best captured the behavioural difference between age-groups and minimised the number of statistical tests. The significance level for these correlations was $p < 0.0125$ (Bonferoni correction for four tests). Follow-up post hoc tests for dorsal ACC were performed using the

components of the update bias (i.e. desirable update and undesirable update). For significant correlations in older age, I tested if these were significantly stronger in older than younger adults using Fisher's r-to-z transformation (one-tailed).

Based on a previous study of the functional correlates of optimism (Sharot et al., 2011), I used a right inferior frontal gyrus atlas mask, also obtained from the AAL toolbox (Tzourio-Mazoyer et al., 2002), to test a specific correlation between grey matter volume of this region and undesirable update.

Voxel-based morphometry, VBM: I performed three exploratory VBM analyses. For all these analyses, no regions survived a statistical threshold of $p < 0.05$ after whole brain peak-level family-wise error correction but for completeness I report the uncorrected results in Table 23, Table 24, Table 25 and Table 26 at the end of the results section. Since no previous studies have reported the structural correlates of optimism, for the first analysis I performed whole-brain VBM analyses across all participants. Regressors in this multiple regression model included update for desirable information, update for undesirable information, and age, gender and total intracranial volume (TIV, sum of grey matter, white matter and CSF) as covariates of no interest. In a second analysis I used update bias (desirable update minus undesirable update) and age, gender and IV as covariates of no interest in a full factorial design to identify age-interactions of the update bias (contrasts: update bias young > old and update bias old > young). In the third analysis I performed a conjunction analysis to identify regions that atrophied with age (contrast: young

> old) and correlated positively with undesirable update in young adults (contrast: young undesirable update > older undesirable update) to address the specific hypotheses that an enhanced update bias may emerge in older age due to age-related volume reduction of a region implicated in updating undesirable information (hence gender and TIV but not age were used as covariates of no interest in this model).

SN/VTA structural integrity and optimism: I performed an exploratory analysis to determine if structural integrity of the SN/VTA, indexed by MT values, was related to optimism. The left and right SN/VTA was manually defined on every visible slice as per Düzel et al (Düzel et al., 2008) using ITK-SNAP (Yushkevich et al., 2006). For each subject, this ROI was projected as an overlay on their MT maps to obtain a mean value for the region. These values were then compared between high and low optimists within each age group using an independent t-test. I defined high and low optimists using a median split of LOT-R values within each age group, resulting in 9 participants per group. Mean (SD) LOT-R values per group were as follows: young low optimists 14.1 (2.2), young high optimists 19 (2.1), old low optimists 17.8 (1.9), old high optimists 22.6 (1.1).

7.3. Results

7.3.1 Age-comparison of optimistic behaviour

18 young and 18 older healthy adults completed the optimism task (Figure 25).

My results showed both an asymmetry between updating beliefs for desirable and undesirable information and a marked age-related difference in this update bias. Older adults had a greater asymmetry in belief updating than younger adults (update valence*age group $F(1,34) = 17.75, p < 0.0005$). Strikingly, older adults updated their beliefs for undesirable information even less than younger adults ($t(34) = 3.01, p = .005$), whereas both groups updated their beliefs for desirable information to a similar extent ($t(34) = 1.65, p = .109$), resulting in a greater update bias amongst older adults (Figure 26a). Both young and older subjects displayed an update bias. In other words participants of all ages updated their beliefs more for desirable information than undesirable information (main effect of update valence $F(1,34) = 58.29, p < 0.0005$). This pattern was evident in 72% of younger adults and 94% of older adults. Older adults also had a greater tendency to underestimate the likelihood of negative events, indicated by a more negative first estimation error ($t(34) = 3.60, p = .001$; Figure 26 b).

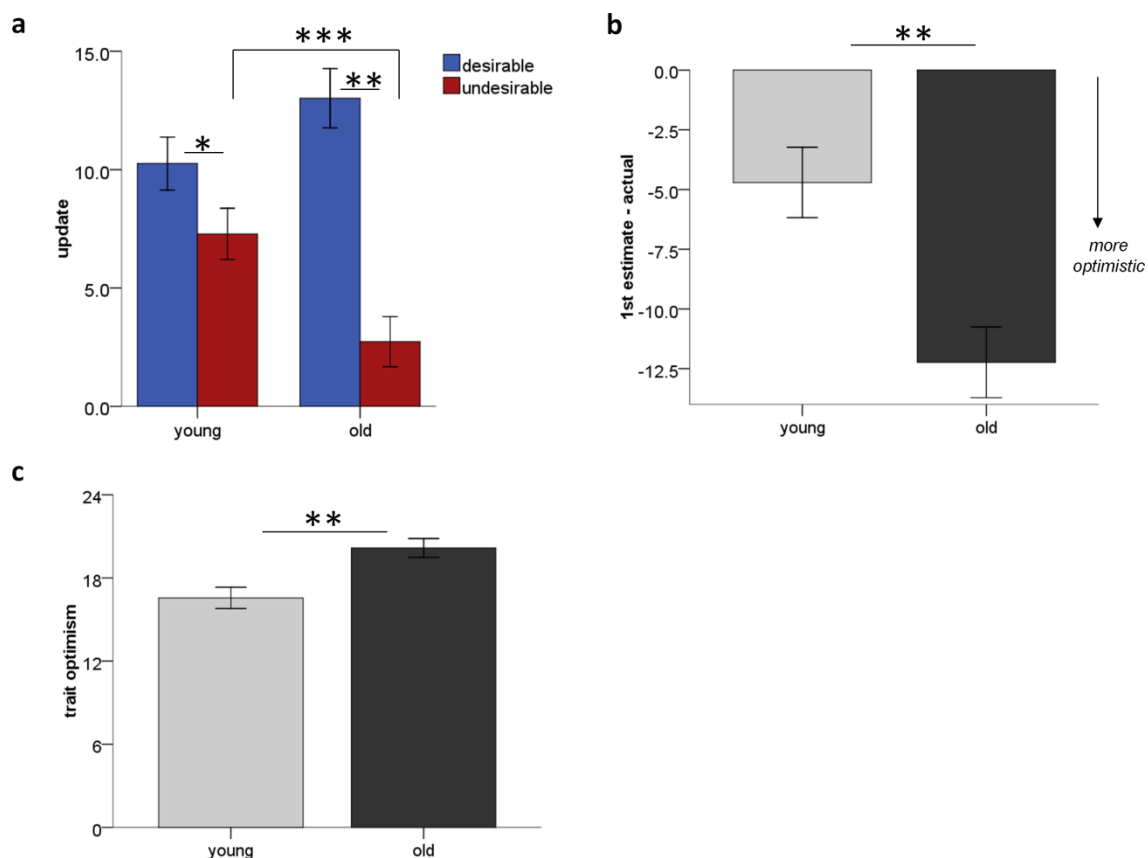


Figure 26. Older adults are even more optimistic than younger adults

(a) Both young and older adults updated their beliefs (difference between 1st and 2nd estimate) more when faced with desirable than undesirable information, but this update bias was larger in older adults due to reduced updating of undesirable information.

(b) Older adults had a larger first estimation error (1st estimation minus the actual probability of the event) indicating a greater tendency to underestimate the likelihood of negative events.

(c) Trait optimism scores, measured by the LOT-R, were higher in older adults compared to younger adults.

Bars \pm 1 SEM. * $p < 0.05$, ** $p < 0.01$, *** $p < 0.0005$

To determine if other variables contributed to this age-related difference in update bias, I obtained measures of reaction time (Table 19), memory performance and subjective ratings of the task events (Table 20). Reaction times did not differ between age-groups (session*valence*age interaction: $F(1,34) = 2.73$, $p = .108$). All participants had slower reaction times when entering their first estimate compared to the second (main effect of session: $F(1,34) = 16.14$, $p < 0.0005$). For the first session alone all participants were slower on undesirable compared to desirable trials (session*valence interaction: $F(1,34) = 4.70$, $p = .037$). This was due to faster responses for desirable trials compared to undesirable trials on the 1st session ($t(35) = -2.13$, $p = .040$), whereas there was no difference between desirable and undesirable trials on the 2nd session ($t(35) = 0.51$, $p = .617$).

	Vivid	Familiar	Experience	Arousal	Negative	Memory errors
All (n = 36)						
Desirable	4.38 (0.81)	4.08 (0.81)	2.64 (0.55)	3.62 (0.81)	3.72 (0.88)	9.79 (4.19)
Undesirable	3.52 (0.83)	3.48 (0.93)	1.82 (0.29)	3.95 (0.79)	4.09 (0.77)	10.67 (3.38)
Young (n = 18)						
Desirable	4.03 (0.52)	3.84 (0.78)	2.50 (0.51)	3.30 (0.71)	3.71 (0.49)	8.08 (2.98)
Undesirable	3.32 (0.66)	3.49 (0.86)	1.79 (0.30)	3.46 (0.78)	4.15 (0.59)	9.49 (3.18)
Old (n = 18)						
Desirable	4.73 (0.91)	4.32 (0.78)	2.79 (0.56)	3.95 (0.79)	3.74 (0.12)	11.51 (4.59)
Undesirable	3.52 (0.83)	3.46 (0.10)	1.84 (2.87)	4.34 (0.58)	4.03 (0.93)	11.86 (3.24)

Table 20. Subjective ratings and memory performance.

Subjective ratings are scores measured using a Likert scale ranging from 1 (not at all) to 6 (very) for all 45 task events. Memory errors are the absolute difference between the actual probability presented for each adverse event and the participants' recollection of those actual probabilities. Scores are mean, SD in parentheses.

All participants rated trials where they received desirable information as more vivid, more familiar and indicated greater past experience of these events compared to trials where they received undesirable information (main effect of valence: Vivid $F(1,34) = 86.98$; Familiar $F(1,34) = 44.74$; Experience ($F(1,34) = 87.84$; all $p < 0.0005$). All participants rated trials where they received undesirable information as more arousing and more negative than trials where they received desirable information (main effect of valence: Arousal $F(1,34) = 16.55$; Negative $F(1,34) = 20.12$; all $p < 0.0005$). An age-related difference was only present for ratings of arousal (main effect of age: $F(1,34) = 13.89$, $p = .001$; all other main effects of age $p > 0.1$) and familiarity (valence*age interaction: $F(1,34) = 7.49$, $p = .010$; all other valence*age interactions $p > 0.1$). In fact, older adults rated all events as more emotionally arousing than younger adults. This would suggest that the greater update bias in older adults was not due to participants being less engaged in the task or finding the stimuli less relevant than younger adults did. Familiarity ratings indicated how familiar participants were with each event regardless of their personal experience. Here I found that although there was a trend towards older adults rating desirable events as more familiar than younger adults ($t(34) = 1.82$, $p = .078$), there was no age-group difference for familiarity with undesirable trials ($t(34) = 0.08$, $p = .939$).

Overall, these subjective ratings analyses suggest the task events were just as salient for old as for young adults and the relative lack of interactions with age-group make it highly unlikely these variables accounted the age-related difference in the update bias. Nonetheless, to fully account for this possibility I added the following measures as covariates to the analysis of the update bias: IQ, first estimation error, difference measures of all subjective ratings, difference

measures of reaction times and average memory errors. Importantly, the significantly greater update bias in older adults persisted (ANCOVA update valence*age interaction $F(1,34) = 6.15, p = .021$) and no covariates interacted with the update bias (covariates*update valence interactions all $p > 0.2$).

Two further measures confirmed greater optimism in my sample of healthy older adults. Firstly, older adults also had a greater tendency than young adults to underestimate the likelihood of negative events, indicated by a more negative first estimation error ($t(34) = 3.60, p = .001$; Figure 26b). Secondly I used the LOT-R self-rating personality scale as an independent measure of optimism and found that older adults had higher trait optimism scores than young adults ($t(34) = 3.53, p = .001$) (Figure 26c).

In summary, I show that older adults are more optimistic than younger adults as indicated by both a greater tendency to underestimate the likelihood of negative events and higher trait optimism scores. Furthermore, I show an enhanced update bias in older age with a selective reduction in update when older adults were faced with undesirable information.

7.3.2 Structural neuroimaging: ACC and biased updating

I performed a structural neuroimaging analysis in relation to my *a priori* region of interest, associated in previous studies with a positivity effect in old age, namely the ACC. I parcellated an anatomically defined bilateral mask of this region to obtain grey matter volume of dorsal and ventral ACC subregions and examined the correlation with updating beliefs and age-group differences. I found that volume of both the dorsal and ventral ACC correlated positively with the update

bias in older adults whereas neither region correlated with update bias in younger adults (Table 21). The dorsal ACC correlation in older adults was significantly greater than in young adults (Fishers r-to-z, $z = -1.78$, $p = .036$), in contrast to the non-significant age-group difference for the ventral ACC ($z = -1.42$, $p = .078$) (Figure 27). Greater dorsal ACC volume also correlated with higher desirable update in older adults, although this association was less robust than with update bias after controlling for age, gender and TIV (Table 22). Thus amongst older but not younger adults, the correlation between dorsal ACC structure and update bias suggests this region arbitrated between desirable and undesirable update (Figure 28; Fishers r-to-z comparing the correlation with volume and desirable update to the correlation with volume and undesirable update, $z = -2.13$, $p = 0.017$).

	Older		Young	
	r	p	r	p
Dorsal ACC	.649, .526	.004*, .044	.122, .057	.631, .841
Ventral ACC	.626, .504	.005*, .056	.213, .262	.395, .345

Table 21. Correlation between ACC subregions and update bias.

Correlation coefficients (Pearson's correlations) for the correlation between dorsal & ventral subregions of anterior cingulate cortex (ACC) grey matter volume and update bias (desirable update minus undesirable update). Partial correlations controlling for age, gender and TIV are given in the same cell of the table. * $p < 0.0125$ (significance level after Bonferroni correction for four tests).

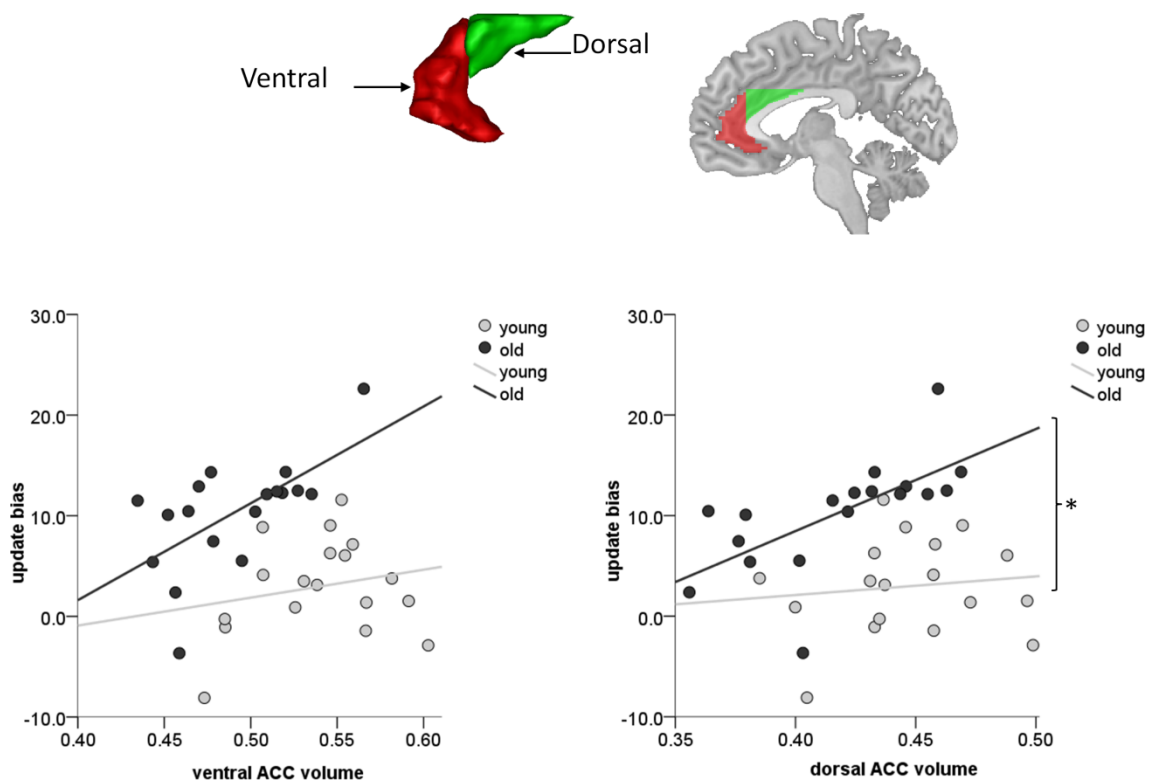


Figure 27. Region of interest analysis of the anterior cingulate cortex (ACC).

Scatter plots showing higher volume of dorsal anterior cingulate cortex (green mask) and ventral anterior cingulate cortex (red mask) in older adults correlated with higher update bias (desirable update minus undesirable update) in older adults. No significant correlations were observed in young adults. $N=18$ per age group. * Fisher's r -to- z transformation comparing correlation strengths $p < 0.05$. ACC volume measurements on x-axis of both plots measured in arbitrary units.

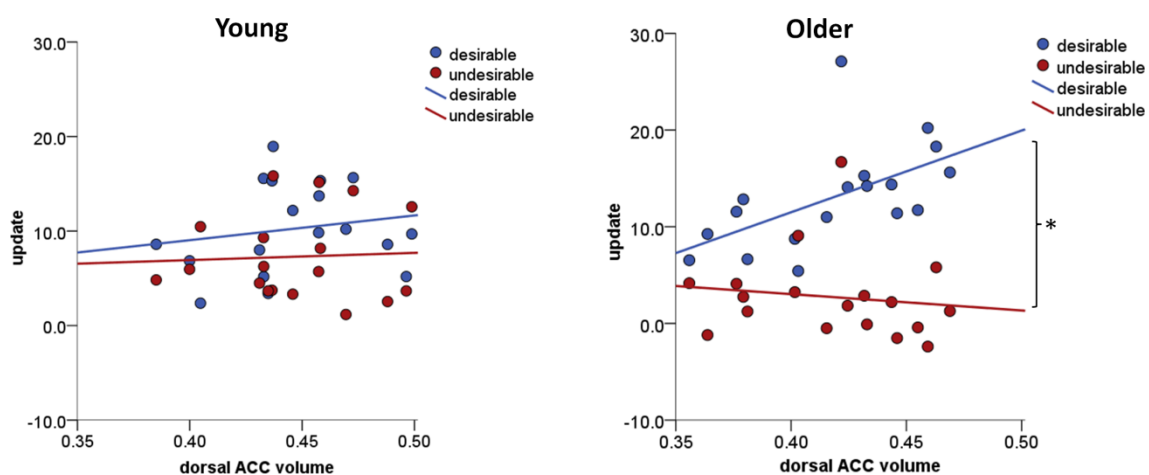


Figure 28. Dorsal ACC volume and update.

Scatter plots showing associations between dorsal anterior cingulate cortex (ACC) volume and desirable and undesirable update in young and older adults. * Fisher's r -to- z transformation comparing correlation strengths $p < 0.05$. ACC volume measurements on x-axis of both plots measured in arbitrary units.

	young		old	
	r	p	r	p
Desirable	.175, .229	.488, .412	.567, .415	.014, .124
Undesirable	.053, .258	.836, .354	-.134, -.178	.596, .527

Table 22. Correlation between dorsal ACC volume and update.

Correlation coefficients (Pearson's correlations) for the correlation between dorsal anterior cingulate cortex grey matter volume and desirable update and undesirable update. Partial correlations controlling for age, gender and TIV are given in the same cell of the table.

The volume of both dorsal ACC (young mean 0.45 SD 0.032; older mean 0.42 SD 0.036) and ventral ACC (young mean 0.54 SD 0.037; older mean 0.49 SD 0.036) were reduced overall in older age (dorsal: $t(34) = -2.55$ $p = .015$; ventral $t(34) = -4.08$ $p < 0.0005$). To further assess whether the association between volumes of ACC subregions and update bias differed between age-groups because of the range of volume values, I formed age-groups matched for volume. I excluded young adults with dorsal ACC volumes higher than volumes in older adults ($n = 3$) and excluded older adults with lower dorsal ACC volumes than young adults ($n = 4$). This did not change the pattern of results, whereby a strong correlation remained in older adults ($r = 0.72$, $p = .004$) and there remained no correlation amongst young adults ($r = 0.34$, $p = .209$). Using the same approach for the ventral ACC, I excluded young adults with higher ventral ACC volumes than older adults ($n = 3$) and older adults with lower ventral ACC volumes than young adults ($n = 7$). Here, despite the small sample size, the significant correlation persisted in older adults ($r = 0.72$, $p = .013$). Additionally, an almost significant correlation emerged in young adults ($r = 0.51$, $p = .051$). These results indicate that whilst the ventral ACC may play a general role in mediating the update bias, individual differences of dorsal ACC volume contributed more to the update bias in older adults compared to young adults despite age-related volume differences.

An additional potential explanation for the enhanced update bias in older age is that the greater failure to update undesirable information occurs as a consequence of age-related atrophy. In younger adults, functional activity of the right inferior frontal gyrus has been associated with tracking undesirable information. However in this cohort, volume of this region was similar in young

and older adults (independent t-test, $t(34) = -1.08$, $p = .287$ two-tailed) and did not correlate with undesirable update in either age group (both $p > 0.3$). A further exploratory whole-brain VBM conjunction analysis identified clusters in the superior and middle temporal lobe, superior frontal gyrus and cerebellum, indicating regions that were both reduced in volume in older adults and correlated with undesirable update more in younger than older adults, yet none of these regions survived whole brain correction for multiple comparisons (Table 27).

7.3.3 SN/VTA integrity and trait optimism

Amongst older adults, high optimists ($n = 9$) had greater SN/VTA structural integrity than low optimists ($n = 9$) ($t(16) = 2.54$, $p = .022$). Amongst younger adults there was no difference between low optimists ($n = 9$) and high optimists ($n = 9$) ($t(16) = 1.42$, $p = .17$).

No. voxels	T	Z	x	y	z	L/R	region
3219	4.99	4.23	-16	-43	-47	L	cerebellum
1294	4.88	4.16	36	-35	62	R	postcentral inferior
1706	4.48	3.89	49	-14	-30	R	temporal
293	4.27	3.74	-38	-30	-22	L	fusiform
1146	4.24	3.72	-62	-18	26	L	postcentral inferior
398	4.06	3.60	-49	-13	-28	L	temporal
261	4.04	3.58	41	-63	12	R	mid temporal anterior
449	3.97	3.53	10	50	12	R	cingulate inferior frontal gyrus
487	3.92	3.49	-50	8	32	L	superior frontal
1071	3.90	3.48	22	7	53	R	hippocampus
587	3.87	3.46	-30	-3	-22	L	insula
320	3.81	3.41	-34	2	2	L	mid frontal supplementary
83	3.75	3.37	23	46	28	R	motor area
150	3.74	3.36	-6	1	70	L	postcentral superior
89	3.69	3.32	42	-25	47	R	occipital
37	3.61	3.27	-20	-82	26	L	mid cingulum superior
100	3.60	3.25	2	-13	31	R	occipital
28	3.57	3.23	29	-78	22	R	cerebellum
39	3.54	3.21	29	-51	-53	R	mid frontal inferior
29	3.53	3.21	28	17	42	R	temporal
18	3.53	3.20	56	-33	-21	R	mid temporal
10	3.50	3.18	56	-54	19	R	mid temporal interior frontal gyrus
14	3.48	3.16	46	-50	18	R	supplementary motor area
12	3.45	3.14	44	22	9	R	
17	3.43	3.13	-6	16	62	L	

Table 23. Positive correlation with desirable update across all participants.

No regions correlated negatively with desirable update. Uncorrected threshold $p < 0.001$, > 10 voxels.

No. voxels	T	Z	x	y	z	L/R	region
<u>Undesirable negative</u>							
368	4.00	3.55	58	-12	30	R	postcentral
<u>Undesirable positive</u>							
118	3.96	3.52	-16	-80	22	L	superior occipital
175	3.74	3.36	-7	-83	-23	L	cerebellum

Table 24. Correlations with undesirable update across all participants.

Uncorrected threshold $p < 0.001$, > 10 voxels.

No. voxels	T	Z	x	y	z	L/R	region
339	4.34	3.79	-17	-80	23	L	superior occipital
899	4.27	3.75	59	-13	29	R	supramarginal
871	3.97	3.53	37	-29	60	R	postcentral inferior
57	3.85	3.44	-38	-29	-22	L	temporal
52	3.77	3.39	34	-58	-53	R	cerebellum
88	3.72	3.35	-14	-58	-53	L	cerebellum
74	3.71	3.34	-29	-1	-18	L	amygdala supplementary
223	3.67	3.31	-13	-4	69	L	motor area
59	3.60	3.26	-18	-42	-46	L	cerebellum
96	3.58	3.24	23	8	54	R	superior frontal inferior frontal
24	3.53	3.20	45	23	11	R	gyrus
71	3.53	3.20	-61	-18	26	L	postcentral
13	3.44	3.13	46	-62	18	R	mid temporal

Table 25. Correlations with update bias across all participants.

Desirable update > undesirable update. Uncorrected threshold $p < 0.001$, > 10 voxels.

No. voxels	T	Z	x	y	z	L/R	region
<u>old > young</u>							
357	4.17	3.66	20	-58	50	R	superior parietal
649	4.12	3.63	26	-1	-8	R	putamen
764	3.86	3.44	-25	-7	-8	L	putamen supplementary
13	3.74	3.35	14	-16	59	R	motor area
20	3.49	3.16	38	-54	35	R	angular gyrus
<u>young > old</u>							
1087	4.44	3.85	22	-64	-9	R	lingual
562	3.95	3.51	-4	-22	39	L	mid cingulum inferior frontal
217	3.86	3.44	-54	15	26	L	gyrus
113	3.86	3.44	-23	-67	-14	L	fusiform
205	3.83	3.42	9	-98	21	R	superior occipital
102	3.72	3.33	4	-80	-26		cerebellum
53	3.69	3.31	-8	-99	21	L	superior occipital superior temporal
28	3.63	3.27	-27	25	-34	L	pole
62	3.60	3.24	-2	-68	20	L	calcarine
113	3.50	3.17	42	-46	-17	R	fusiform

Table 26. Age-comparison of update bias (desirable update > undesirable update).

Uncorrected threshold $p < 0.001$, > 10 voxels.

No.							
voxels	T	Z	x	y	z	L/R	region
							superior
514	4.21	3.70	62	-38	22	R	temporal
356	3.96	3.52	-7	38	45	L	superior frontal
76	3.64	3.29	54	-59	21	R	mid temporal
16	3.63	3.28	19	-43	-21	R	cerebellum

Table 27. Conjunction analysis.

Conjunction analysis of young > old and update undesirable young > update undesirable old. Uncorrected threshold $p < 0.001$, > 10 voxels.

7.4. Discussion

I provide evidence showing healthy older adults display greater optimism compared to younger adults, manifest as an enhanced tendency to underestimate the likelihood of negative events and higher trait optimism scores. Moreover I show that older adults are less likely than younger adults to change their beliefs when faced with undesirable information about their future. This greater asymmetry in belief updating was present despite older adults experiencing greater subjective feelings of emotional arousal for all the task events. This enhanced update bias was not related to poorer memory amongst older adults and was independent of non-age related valence differences in subjective ratings of the task stimuli including the sense of personal experience, vividness, familiarity, and negativity.

My study provides the first demonstration that greater asymmetry in belief updating in older adults is tightly coupled to volume of the dorsal ACC. Previous studies report a critical role of the ACC as a cognitive-emotional interface (for reviews see (Bush et al., 2000) and (Ochsner and Gross, 2005)) and greater functional ACC activity has been associated with more emotional regulation in old age (Brassen et al., 2011; Brassen et al., 2012) (Samanez-Larkin and Carstensen, 2011). My study showed that the dorsal subregion of ACC played a stronger role in mediating the update bias in older than younger age. Moreover, even after accounting for age-related atrophy by matching the volume of ACC subregions across age-groups, no correlation emerged in younger adults between update bias and volume of the dorsal subregion suggesting this localised relationship was exclusive to older adults. Volume of the dorsal as opposed to ventral ACC, often dubbed 'cognitive' and affective'

regions respectively (Devinsky et al., 1995) (Bush et al., 2000) has been linked to greater cognitive reappraisal strategies in healthy adults (Giuliani et al., 2011) and volume of this subregion is reduced in patients with depression where emotional dysregulation and pessimism are highly characteristic (Vasic et al., 2008). Thus I speculate that my findings linking dorsal ACC to an enhanced update bias in older adults suggests that the enhanced optimism bias and the well-documented positivity bias in older age may share a similar 'cognitive control' mechanism. In contrast I found some evidence that the ventral ACC may be associated with updating beliefs irrespective of age when I matched age-groups for volume of this subregion. Indeed a previous study in younger adults showed functional activation in a similar region was associated with an optimistic bias when imagining future events (Sharot et al., 2007).

Importantly I found a positive correlation, such that older adults with greater dorsal ACC volume had an enhanced update bias. This seems to indicate that older adults have additional resources which they are able to deploy when processing negative events, whereas younger adults do not rely on this region during task performance. This interpretation is in keeping with the socioemotional selectivity theory, whereby enhanced optimism in old age may be viewed as a positive phenomenon rather than a 'side-effect' of age-related structural decline. To investigate the latter alternative explanation, I also performed a whole brain VBM analysis to determine whether age-related decline of any other brain regions was associated with a failure of undesirable update in older age, yet I did not find any strong evidence for this. However I acknowledge this may have been due to sample size and I do not exclude this

as an additional mechanism contributing to the enhanced update bias in older age.

Functional activation of the inferior frontal gyrus has previously been linked to an optimism bias in younger adults (Sharot et al., 2011). Although I identified the left inferior frontal gyrus in my whole-brain VBM analysis as showing an age-interaction (young > old) for the update bias, no grey matter regions in this analysis survived whole brain correction for multiple comparisons. Therefore I remain cautious about interpreting this as an age-specific effect. Additionally, I also found no age-related decline or any structural association between right inferior frontal gyrus volume and undesirable update.

I speculate that my findings may be in line with a recent study showing that pharmacological enhancement of dopamine levels in younger adults also increased the optimism bias due to a reduction of updating undesirable information (Sharot et al., 2012a). Dopamine neurons, including mesocortical projections from the SN/VTA, and dopamine receptors in the ACC variably decline as a consequence of aging (Fearnley and Lees, 1991; Volkow et al., 2000; Bäckman et al., 2010). I found greater structural integrity of the SN/VTA, indexed by MT imaging, was associated with higher trait optimism in older adults. Although a preliminary analysis based on small group numbers, this suggestion of a link between structural integrity of the dopaminergic midbrain and optimism in old age warrants further study, since dopaminergic manipulation, either exogenously by pharmacological means, or endogenously for example through reward and novelty processing, may influence optimism in old age.

I acknowledge other socio-cultural factors specific to this cohort could account for the differences I find in optimism between young and older participants. These are necessarily harder to determine with a cross-sectional design, but large-scale longitudinal studies have demonstrated less negative emotions in old age across multiple generations (Charles et al., 2001) (Carstensen et al., 2011).

In summary, I show healthy older adults are even more optimistic and display an enhanced update bias compared to younger adults, an effect that correlates with the grey matter volume of the ACC. My findings relate to healthy individuals and a logical extension of my study would be to examine whether age-associated diseases (e.g. cardiovascular, orthopaedic, neurodegenerative and metabolic disorders) impact upon this update bias. In our aging society, I provide a timely demonstration of an age-related enhancement of the update bias that has important implications for healthy aging. This enhanced bias, and an exaggerated failure to adjust beliefs in the face of undesirable information, may influence other economic, personal and health-related decisions. For example, older adults may make inappropriate insurance purchases based on a false optimism in relation to their future. My findings point towards a need for in-depth examination of 'real-world' decision-making processes in healthy aging.

Chapter 8

Discussion

The work presented in this thesis uses a multi-modal approach to study the role of dopamine in learning and memory in healthy older age. Specifically I combined pharmacological manipulation with behavioural testing and fMRI to determine whether pharmacological manipulation to enhance dopamine levels improved long-term episodic memory (Chapter 4) and reinforcement learning (Chapter 5). I used quantitative structural MRI and DTI to study how anatomical differences of dopaminergic regions of the brain and their projection areas relate to reward-based learning (functional reward prediction error signalling in Chapter 5 and flexible learning in Chapter 6) and belief updating (Chapter 7).

In this final chapter, I will discuss the implications of these studies, limitations and ideas for future study.

8.1. Memory

In Chapter 4 I showed that delayed episodic memory in older adults improved with L-DOPA administration in a dose-dependent non-linear manner. The pattern of BOLD activity in the hippocampus suggested this effect was mediated through consolidation rather than encoding.

This is the first study to provide empirical evidence for two effects – the first is the non-linear ‘inverted U-shape’ effect of dopamine on episodic memory which has previously been reported in the context of working memory (Cools and D’Esposito, 2011) and a similar effect on episodic memory has been suggested by computational simulations (Li and Sikström, 2002). The second is human evidence for the role of dopamine in memory consolidation which has previously been elegantly described in animal studies of episodic-like memory (Bethus et al., 2010). These findings are relevant to healthy aging since a decline in episodic memory is well-recognised with age and can be a source of considerable distress. Manipulations of dopamine may therefore provide a mechanism to overcome encoding-related deficits. Future studies could determine whether the memory benefit I found persists beyond 6 hours (testing memory at 6 hours was a limitation of my study which was due to the practicalities of testing older individuals and balancing the use of a within-subject design with an acceptable number of test days for older volunteers). It would also be interesting to determine the effects of repeated drug doses on long-term memory since such a schedule has been associated with better verbal learning in younger adults (Knecht et al., 2004). It is worth being mindful that potential side-effects from long-term use of drugs such as L-DOPA are unknown in healthy individuals. My study may feed into the debate over the use of pharmacological interventions, so-called ‘cognitive enhancers’, in healthy populations (Sahakian and Morein-Zamir, 2007). Interestingly, one study found that community physicians would be more comfortable prescribing a hypothetical cognitive enhancer to older rather than younger adults (Banjo et al., 2010). Presumably this partly relates to what is defined as ‘healthy’ as

physicians in that particular study felt that younger adults were less needful of cognitive enhancement and ran a greater risk of misuse, whereas they saw more benefits in older adults in terms of well-being and overall health.

My findings also raise the intriguing possibility that manipulating dopamine by non-pharmacological means may enhance memory. For example, a study could be conducted in which drug administration is replaced by exposure to novelty to determine whether this had similar effects. This could have major real-life consequences by providing a simple means of memory enhancement in older age. However, my study raised one problem with this non-pharmacological approach since I found that reward anticipation did not enhance long-term memory. This may have been due to age-differences underlying reward processing, which I demonstrate in other chapters in this thesis (Chapters 5 & 6). A limitation of my study in Chapter 4 is that the design was not optimised to analyse the effects of reward but rather focussed on episodic memory. Therefore a future study combining implicit encoding and a subsequent memory test embedded within a probabilistic reinforcement learning task could help to tease this apart further. Such a study could include varying magnitudes of reward to assess whether reward also has a 'dose-dependent' effect. It is also possible that I may have observed reward-effects on memory if memory was tested after a longer delay. Ultimately, some way of quantifying dopamine levels associated with reward anticipation would provide a more complete analysis, particularly since my data already highlight that a complex dose-response relationship exists. Without such a measure, it could be even harder to interpret the effects of non-pharmacological dopaminergic manipulations on the background of variable age-related dopamine decline. Thus human studies with

PET and animal studies with voltammetry may be fruitful ways of exploring this further.

In general, the results of this study speak to a growing body of research seeking to understand the interaction between motivation and memory (Shohamy and Adcock, 2010) (Duzel et al., 2010). This may not only be relevant to healthy aging but also disease states in which episodic memory is impaired, such as Mild Cognitive Impairment (MCI) and Alzheimer's disease. In these conditions, dopamine manipulation has not traditionally been considered given the prominent role of another neurotransmitter - acetylcholine. Nonetheless, milder dopaminergic deficits may co-exist and thus my results may provide an alternative means for investigating memory deficits in these illnesses. Indeed there is a close interaction between acetylcholine release and the firing of dopaminergic neurons in the SN/VTA (Picciotto et al., 2012). Even though underlying pathologies between normal aging and MCI may differ, there has been limited success from the use of acetylcholine-based medications in MCI (Salloway et al., 2004; Petersen et al., 2005). Therefore it may be worth investigating whether dopaminergic modulation may provide some symptomatic benefit with regards to delayed episodic memory deficits.

8.2. Reinforcement learning

In Chapter 6 I show that a marked asymmetry between learning different action-valence contingencies in some older adults. Individual differences in this behavioural inflexibility were linked to the structural integrity of SN/VTA indexed by MT imaging in older but not younger adults. It has been suggested that

valence may influence learning in old age through different sensitivities to reward and punishment (for a review see (Eppinger et al., 2011)). My study uses a well-designed task that allows us to tease apart the contribution of action and valence to learning, and better understand the interaction between motivational tendencies and the ability to learn to execute 'incongruent' responses. My results suggest that it is not necessarily learning-related valence biases that change with age but rather changes in the flexibility of instrumental learning, mediated by midbrain integrity that may account for these effects. The wider implication of this study, as already alluded to, is how these motivational biases relate to other aspects of cognition and how this can be exploited to improve age-related cognitive decline.

One limitation of the study in Chapter 6 was that I performed indirect comparisons with two separate younger control groups – one group for whom I had task performance and MT imaging that was not directly comparable with MT imaging performed in older adults (Guitart-Masip et al., 2012a), and a second smaller group of young individuals who had comparable MT imaging but no behavioural data (Lambert et al., 2012). The reason for this was that the primary aim of the study was to examine individual differences in the structure-function relationship amongst healthy older adults. Also, the interpretation of MT values in younger adults, as opposed to old age and various disease states, is less clear given the myelination changes that occur in the maturing brain (Düzel et al., 2008). Nonetheless, comparison with these other data sets provided some interesting albeit indirect observations about the age-specific nature of my findings. A future study could assess both young and older adults and combine MT imaging with fMRI. This would be particularly interesting to examine

dopamine target regions, such as potential age differences in prefrontal cortex activation within the context of flexible learning, since instrumental learning in younger adults is associated with inferior frontal gyrus activity (Guitart-Masip et al., 2012a).

One strength of my study was the use of quantitative imaging as a proxy marker for dopaminergic integrity. Traditionally, the standard T1 MRI contrast has been used to measure grey matter volume, but historically due to inaccurate segmentation algorithms, the SN/VTA may be misclassified as white matter and therefore not assessed in a standard VBM study. However with the advent of multiparameter mapping, an array of MRI sequences can be employed to better visualise subcortical structures and exploit different tissue properties, providing insight into other underlying biological properties such as macromolecular structural integrity (MT), iron content ($R2^*$), myelin (T1), water content (MD) and fibre organisation (FA). This has allowed me to make rich inferences from structural imaging data throughout this thesis. However, a notable limitation is that the histological correlates of many of these imaging parameters are not yet known. Thus, whilst I suggest the study in Chapter 6 provides evidence that dopamine mediates learning flexibility, the imaging markers do not provide direct evidence for this. In the first instance, animal studies would be useful to provide these much needed histological correlates for neuroimaging markers.

Chapter 5 details the results of a pharmacological reinforcement learning fMRI study in which I show that some healthy older adults have absent reward prediction errors in the nucleus accumbens. L-DOPA restored the appropriate functional activation pattern via a more positive effect of expected value when participants made a choice ('reward prediction') and a more negative effect of

expected value at the time of the outcome ('reward prediction error'). Abnormal striatal activity during reward anticipation with normal representations of rewarding outcomes have previously been identified in old age (Samanez-Larkin et al., 2010) (Schott et al., 2007). The novel contribution of my study is first, to characterise the expected value component of this deficit and secondly, to show that it can be modified by enhancing dopamine levels. I also show that individual differences in baseline functional signalling of reward prediction errors correlated with anatomical nigro-striatal connectivity strength, perhaps explaining some of the observed inter-individual functional variability. This study identifies a neural structural and functional basis for abnormal reward prediction error signalling in healthy old age. This is important given the well documented difficulties that older adults have on probabilistic learning tasks (Eppinger et al., 2011) although I acknowledge that in my study, L-DOPA resulted in only a slight increase in performance in comparison to placebo. The mild improvement in behaviour and emergence of a normal pattern of reward prediction error signalling in the nucleus accumbens again highlights the potential role of dopamine as a therapeutic means for tackling age-related instrumental learning dysfunction.

Some older adults did improve following L-DOPA to win similar amounts of money on the task as young people did. One possible explanation for this is that behaviour in this task relies on the reward component more than expected value. If that were true, then a future study may observe a direct link between prediction errors and task performance if the numbers of bandits were increased such that accurate value representations would be required to guide behaviour. In such a task (e.g. a four-arm bandit task) the effect of L-DOPA on

additional measures such as the exploration-exploitation trade-off could also be measured (Daw et al., 2006). It may also be interesting for future studies to try a bandit task which incorporates different magnitudes of reward since it is unknown how this may affect the reward prediction error signal in old age.

As discussed in Section 5.4, my data may suggest that older adults have an impaired system and thus adopt a more model-based approach when performing reinforcement learning tasks. There is some evidence that older adults are more 'model-based', where learning occurs by building a structure of the reward environment, compared to their younger counterparts who adopt a 'model-free' approach where the value of each choice is learned without constructing an explicit cognitive map (Glaescher J et al., 2010) (Worthy DA et al., 2011). Although older adults often perform worse than younger adults on probabilistic learning tasks, there is also evidence that learning does not universally decline with increasing age, but rather learning strategies change – hence the adage 'older and wiser' (Grossmann et al., 2010) (Worthy et al., 2011), coupled with variability in performance levels. The results I report in Chapter 6 are also in keeping with this, whereby older adults may have been able to overcome Pavlovian response biases because of a more model-based approach. This could explain why older and younger adults with similar MT values of SN/VTA displayed different patterns of learning. Yet this model-based system may fail in older age when dopaminergic integrity is compromised, in keeping with evidence that enhancing dopamine levels promotes the model-based over model-free learning (Wunderlich K et al., 2012). Also, there is differential development of the various dopaminergic pathways with age, where late development of the mesocortical system in adolescent rats has been linked

to maturation of goal-directed behaviour (Naneix et al., 2012). Hence one interpretation of the results in Chapter 6 is that older adults with impaired dopamine integrity (low MT values of SN/VTA) could not utilise a model-based approach and were therefore unsuccessful at instrumentally learning to overcome their response biases, in effect 'reverting' to showing a similar pattern of learning as younger adults. Taken together, the results in Chapters 5 and 6 hint at a possible mechanism underlying the change in learning strategies with increasing age (a switch from model-free to model-based learning) and reasons this may fail (consequent upon dopamine decline). To test this would require direct testing of changes in the Pavlovian bias across age-groups, and the use of a model-free and model-based paradigm such as that used by Wunderlich et al. (Wunderlich et al., 2012), ideally using a longitudinal study design.

Combining the two-arm bandit task in Chapter 5 with DTI provided new insight into the structure-function relationship underlying reward processing. A further extension of this would be to test the relationship between anatomical and functional connectivity (e.g. using a psychophysiological interaction). An important focus would be on effective connectivity of striatal-prefrontal circuits since these regions are subject to age-related structural decline (Raz et al., 2003; Raz and Rodrigue, 2006) and implicated in reinforcement learning, as well as being a feasible pathway to characterise using probabilistic tractography (Samanez-Larkin et al., 2012).

8.3. Optimism

In Chapter 7 I show that a group of healthy older adults were more optimistic than younger adults, indexed by three measures. The first was a greater tendency to underestimate the likelihood of negative events occurring in the future. The second was an enhanced update bias, whereby older adults changed their beliefs for undesirable information even less than younger adults did, whilst changing their beliefs for desirable information to a similar extent. The third was using the LOT-R trait personality scale on which older adults scored higher than younger adults. The enhanced update bias was associated with greater grey matter volume of the dorsal ACC in older but not younger adults. This suggests that at least one mechanism underlying greater optimism in older age was not secondary to age-related neurodegeneration. .

There are many reasons to study optimism and affective processing in old age. Optimism is associated with health benefits and general well-being (Scheier and Carver, 1993) raising the possibility of sharing mechanisms with successful aging. In our continually aging society where late-life depression is common, associated with high morbidity (Alexopoulos, 2005), and characterised in part by pessimism, a clearer understanding of optimistic behaviour may offer new therapeutic contributions. The optimism bias could also have disadvantageous effects in old age since a valence asymmetry in belief updating could bias everyday decisions such as choosing an appropriate insurance policy. It would therefore be useful for future studies to combine this optimism task with other decision-making tasks, for example a financial risk-taking task, to determine the impact of the update bias on other decision-making processes.

One limitation of my study is that the results may be confounded by cohort effects, such as exposure to different socio-environmental factors for adults growing up in 1950s compared to those growing up in the 1990s. This is a long-standing concern of cross-sectional studies of aging. To address this issue, a longitudinal study could be performed to ascertain whether the same individuals become more optimistic as they age. Measures of physical health and well-being could also be collected to see whether optimism had a causal effect on an individuals' physical and mental health.

One original hypothesis for this study was based on the observation that pharmacological enhancement of dopamine levels enhances the optimism bias by selectively reducing belief updating from undesirable information (Sharot et al., 2012a). Therefore I hypothesised that old age may be associated with less optimism due to declining dopamine levels. Resolving this question was one motivation for undertaking this study, since at face value this neurobiological account is at odds with socio-emotional studies which suggest greater well-being and fewer negative emotions with increasing age. My study found that older adults were more optimistic than younger adults, although a further exploratory analysis revealed this does not necessarily conflict with an age-related dopamine decline. I explored the link with dopamine by obtaining quantitative MT imaging of the SN/VTA. Using trait optimistic personality ratings to divide my cohort into high and low optimists, this exploratory analysis revealed that older 'high optimists' had higher MT values of the SN/VTA than older 'low optimists' whereas there was no difference amongst younger adults. These pilot results may link dopamine and optimism in old age, since both mesocortical dopamine projections from the SN/VTA and dopamine receptors in

the ACC variably decline as a consequence of aging (Fearnley and Lees, 1991; Volkow et al., 2000; Bäckman et al., 2010). This raises the possibility that variable dopamine decline with age could be linked to the expression of optimism. A larger study with additional measures of dopamine could explore this further.

To better understand the role of the ACC in optimism in old age, fMRI could be used to identify networks associated with the ACC and whether these networks differ for updating desirable and undesirable information. The functional circuits associated with 'cognitive' and 'affective' subregions of the ACC could be inspected for dissociation with regards to the update bias. The ACC also plays a role in avoidance learning, error detection and conflict monitoring to guide decision-making (Botvinick, 2007). This could relate to my findings if undesirable information is perceived as more conflicting than desirable information so driving cognitive control, akin to the association of greater ACC activation with feelings of regret in older adults (Brassen et al., 2012).

8.4. Other considerations

8.4.1 Aging as a model of dopamine decline

Health older age provides the opportunity to study features associated with dopamine decline. For this purpose, aging is perhaps a better model than Parkinson's disease since the latter is accompanied by more widespread pathological changes in the brain, occurring before involvement of the substantia nigra (Braak et al., 2004). However other neurotransmitters including serotonin, acetylcholine and noradrenaline, also decline with age (see (Eppinger

et al., 2011) for a review). Aging is therefore not a 'pure' model of dopamine decline and the actions of other neurotransmitters may well play a role in the results presented in this thesis.

8.4.2 Generalisability

One critical feature highlighted by the studies in this thesis is the heterogeneity of the aging process. This, together with recruitment bias ('healthy volunteers') and environmental cohort effects, limit the generalisability of my results to the elderly population as a whole. The participants in the studies I have presented were all screened to ensure they were healthy and free of other risk factors for cognitive dysfunction (e.g. vascular risk factors). It would be interesting for future studies to utilise the paradigms in this thesis in larger samples, where a more representative cohort of the general population could be examined, whilst also taking the effects of potential confounding factors which would occur as a consequence of having less stringent exclusion criteria, into account.

8.4.3 Final remarks

The research I have conducted provides a novel perspective on the critical contribution of dopamine to individual differences in learning and memory performance in older age. Bringing together these previous somewhat disparate strands of neuroscience research converge on the idea that motivation interacts with learning and memory (Duzel et al., 2009a) (Shohamy and Adcock, 2010) and motivational changes with age are both a key component of age-related

changes in these behaviors as well as potential targets for improving behavioral deficits (Carstensen et al., 1999; Carstensen, 2006).

Many unasked and unanswered questions remain in the exciting field of the neuroscience of aging. The studies I have presented in this thesis are somewhat analogous to the 'rule of thirds', showing that as we age: some things get worse (Chapters 4 & 5), some things stay the same (Chapter 6) and some things get better (Chapter 7). My hope is that the work presented here sheds some new light on how the brain mediates these diverse rises and falls that accompany us with the passing of time.

References

- Abler B, Walter H, Erk S, Kammerer H, Spitzer M (2006) Prediction error as a linear function of reward probability is coded in human nucleus accumbens. *Neuroimage* 31:790-795.
- Adcock RA, Thangavel A, Whitfield-Gabrieli S, Knutson B, Gabrieli JDE (2006) Reward-Motivated Learning: Mesolimbic Activation Precedes Memory Formation. *Neuron* 50:507-517.
- Aizenstein HJ, Butters MA, Clark KA, Figurski JL, Andrew Stenger V, Nebes RD, Reynolds lii CF, Carter CS (2006) Prefrontal and striatal activation in elderly subjects during concurrent implicit and explicit sequence learning. *Neurobiology of Aging* 27:741-751.
- Alexander GE, DeLong MR, Strick PL (1986) Parallel Organization of Functionally Segregated Circuits Linking Basal Ganglia and Cortex. *Annual Review of Neuroscience* 9:357-381.
- Alexopoulos GS (2005) Depression in the elderly. *The Lancet* 365:1961-1970.
- Ances BM, Liang CL, Leontiev O, Perthen JE, Fleisher AS, Lansing AE, Buxton RB (2009) Effects of aging on cerebral blood flow, oxygen metabolism, and blood oxygenation level dependent responses to visual stimulation. *Human Brain Mapping* 30:1120-1132.
- Andersson JLR, Skare S, Ashburner J (2003) How to correct susceptibility distortions in spin-echo echo-planar images: application to diffusion tensor imaging. *Neuroimage* 20:870-888.

- Andersson JLR, Hutton C, Ashburner J, Turner R, Friston K (2001) Modeling Geometric Deformations in EPI Time Series. *Neuroimage* 13:903-919.
- Aron AR, Poldrack RA (2006) Cortical and Subcortical Contributions to Stop Signal Response Inhibition: Role of the Subthalamic Nucleus. *The Journal of Neuroscience* 26:2424-2433.
- Aron AR, Fletcher PC, Bullmore ET, Sahakian BJ, Robbins TW (2003) Stop-signal inhibition disrupted by damage to right inferior frontal gyrus in humans. *Nat Neurosci* 6:115-116.
- Aron AR, Behrens TE, Smith S, Frank MJ, Poldrack RA (2007) Triangulating a Cognitive Control Network Using Diffusion-Weighted Magnetic Resonance Imaging (MRI) and Functional MRI. *The Journal of Neuroscience* 27:3743-3752.
- Ashburner J (2007) A fast diffeomorphic image registration algorithm. *Neuroimage* 38:95-113.
- Ashburner J, Friston KJ (2000) Voxel-Based Morphometry--The Methods. *Neuroimage* 11:805-821.
- Ashburner J, Friston KJ (2001) Why Voxel-Based Morphometry Should Be Used. *Neuroimage* 14:1238-1243.
- Ashburner J, Friston KJ (2005) Unified segmentation. *Neuroimage* 26:839-851.
- Bäckman L, Lindenberger U, Li S-C, Nyberg L (2010) Linking cognitive aging to alterations in dopamine neurotransmitter functioning: Recent data and future avenues. *Neuroscience & Biobehavioral Reviews* 34:670-677.
- Bäckman L, Nyberg L, Lindenberger U, Li S-C, Farde L (2006) The correlative triad among aging, dopamine, and cognition: Current status and future prospects. *Neuroscience & Biobehavioral Reviews* 30:791-807.

- Bäckman L, Ginovart N, Dixon RA, Wahlin T-BR, Wahlin Å, Halldin C, Farde L (2000) Age-Related Cognitive Deficits Mediated by Changes in the Striatal Dopamine System. *Am J Psychiatry* 157:635-637.
- Banjo OC, Nadler R, Reiner PB (2010) Physician Attitudes towards Pharmacological Cognitive Enhancement: Safety Concerns Are Paramount. *PLoS ONE* 5:e14322.
- Beck AT, Ward CH, Mendelson M, Mock J, Erbaugh J (1961) An Inventory for Measuring Depression. *Arch Gen Psychiatry* 4:561-571.
- Behrens TEJ, Johansen-Berg H (2005) Relating connective architecture to grey matter function using diffusion imaging. *Philosophical Transactions of the Royal Society B: Biological Sciences* 360:903-911.
- Behrens TEJ, Hunt LT, Rushworth MFS (2009) The Computation of Social Behavior. *Science* 324:1160-1164.
- Behrens TEJ, Hunt LT, Woolrich MW, Rushworth MFS (2008) Associative learning of social value. *Nature* 456:245-249.
- Behrens TEJ, Berg HJ, Jbabdi S, Rushworth MFS, Woolrich MW (2007) Probabilistic diffusion tractography with multiple fibre orientations: What can we gain? *Neuroimage* 34:144-155.
- Behrens TEJ, Johansen-Berg H, Woolrich MW, Smith SM, Wheeler-Kingshott CAM, Boulby PA, Barker GJ, Sillery EL, Sheehan K, Ciccarelli O, Thompson AJ, Brady JM, Matthews PM (2003) Non-invasive mapping of connections between human thalamus and cortex using diffusion imaging. *Nat Neurosci* 6:750-757.
- Benton AL (1967) Problems of test construction in the field of aphasia. *Cortex* 3:32-58.

- Bethus I, Tse D, Morris RGM (2010) Dopamine and Memory: Modulation of the Persistence of Memory for Novel Hippocampal NMDA Receptor-Dependent Paired Associates. *J Neurosci* 30:1610-1618.
- Bialleck KA, Schaal H-P, Kranz TA, Fell J, Elger CE, Axmacher N (2011) Ventromedial Prefrontal Cortex Activation Is Associated with Memory Formation for Predictable Rewards. *PLoS ONE* 6:e16695.
- Birn RM, Diamond JB, Smith MA, Bandettini PA (2006) Separating respiratory-variation-related fluctuations from neuronal-activity-related fluctuations in fMRI. *Neuroimage* 31:1536-1548.
- Blanchflower DG, Oswald AJ (2008) Is well-being U-shaped over the life cycle? *Social Science & Medicine* 66:1733-1749.
- Bliss TVP, Gardner-Medwin AR (1973) Long-lasting potentiation of synaptic transmission in the dentate area of the unanaesthetized rabbit following stimulation of the perforant path. *The Journal of Physiology* 232:357-374.
- Bond A, Lader M (1974) The use of analogue scales in rating subjective feelings. *British Journal of Medical Psychology* 47:211-218.
- Botvinick MM (2007) Conflict monitoring and decision making: Reconciling two perspectives on anterior cingulate function. *Cognitive, Affective, & Behavioral Neuroscience* 7:356-366.
- Braak H, Ghebremedhin E, Rüb U, Bratzke H, Del Tredici K (2004) Stages in the development of Parkinson's disease-related pathology. *Cell and Tissue Research* 318:121-134.
- Brassen S, Gamer M, Buchel C (2011) Anterior Cingulate Activation Is Related to a Positivity Bias and Emotional Stability in Successful Aging. *Biological Psychiatry* 70:131-137.

- Brassen S, Gamer M, Peters J, Gluth S, Buchel C (2012) Don't Look Back in Anger! Responsiveness to Missed Chances in Successful and Nonsuccessful Aging. *Science* 336:612-614.
- Breitenstein C, Korsukewitz C, Floel A, Kretzschmar T, Diederich K, Knecht S (2006) Tonic Dopaminergic Stimulation Impairs Associative Learning in Healthy Subjects. *Neuropsychopharmacology* 31:2552-2564.
- Brett M, Anton, J.-L., Valabregue, R., and Poline, J.-B. (2002) Region of interest analysis using an SPM toolbox. 8th International Conference on Functional Mapping of the Human Brain (Sendai, Japan).
- Bruno SD, Barker GJ, Cercignani M, Symms M, Ron MA (2004) A study of bipolar disorder using magnetization transfer imaging and voxel-based morphometry. *Brain* 127:2433-2440.
- Buckner RL (2004) Memory and Executive Function in Aging and AD: Multiple Factors that Cause Decline and Reserve Factors that Compensate. *Neuron* 44:195-208.
- Bunzeck N, Duzel E (2006) Absolute coding of stimulus novelty in the human substantia nigra/VTA. *Neuron* 51:369-379.
- Bush G, Luu P, Posner MI (2000) Cognitive and emotional influences in anterior cingulate cortex. *Trends in Cognitive Sciences* 4:215-222.
- Cabeza R, Anderson ND, Locantore JK, McIntosh AR (2002) Aging Gracefully: Compensatory Brain Activity in High-Performing Older Adults. *Neuroimage* 17:1394-1402.
- Camerer C, Hua Ho T (1999) Experience-weighted Attraction Learning in Normal Form Games. *Econometrica* 67:827-874.

- Carstensen LL (2006) The Influence of a Sense of Time on Human Development. *Science* 312:1913-1915.
- Carstensen LL, Isaacowitz D, Charles ST (1999) Taking time seriously. A theory of socioemotional selectivity. *American Psychologist* 54:165-181.
- Carstensen LL, Turan B, Scheibe S, Ram N, Ersner-Hershfield H, Samanez-Larkin GR, Brooks KP, Nesselroade JR (2011) Emotional experience improves with age: evidence based on over 10 years of experience sampling. *Psychol Aging* 26:21-33.
- Cervenka S, Bäckman L, Cselenyi Z, Halldin C, Farde L (2008) Associations between dopamine D2-receptor binding and cognitive performance indicate functional compartmentalization of the human striatum. *Neuroimage* 40:1287-1295.
- Charles ST, Carstensen LL (2010) Social and Emotional Aging. *Annual Review of Psychology* 61:383-409.
- Charles ST, Reynolds CA, Gatz M (2001) Age-related differences and change in positive and negative affect over 23 years. *Journal of Personality and Social Psychology* 80:136-151.
- Chételat G, Fouquet M, Kalpouzos G, Denghien I, De la Sayette V, Viader F, Mézenge F, Landeau B, Baron JC, Eustache F, Desgranges B (2008) Three-dimensional surface mapping of hippocampal atrophy progression from MCI to AD and over normal aging as assessed using voxel-based morphometry. *Neuropsychologia* 46:1721-1731.
- Choi WY, Balsam PD, Horvitz JC (2005) Extended Habit Training Reduces Dopamine Mediation of Appetitive Response Expression. *The Journal of Neuroscience* 25:6729-6733.

- Chowdhury R, Guitart-Masip M, Bunzeck N, Dolan RJ, Duzel E (2012) Dopamine Modulates Episodic Memory Persistence in Old Age. *The Journal of Neuroscience* 32:14193-14204.
- Clayton NS, Dickinson A (1998) Episodic-like memory during cache recovery by scrub jays. *Nature* 395:272-274.
- Cloninger CR (1987a) The tridimensional personality questionnaire. Version IV. St Louis, MO: Department of Psychiatry, Washington University School of Medicine.
- Cloninger CR (1987b) A Systematic Method for Clinical Description and Classification of Personality Variants: A Proposal. *Arch Gen Psychiatry* 44:573-588.
- Cohen MX, Frank MJ (2009) Neurocomputational models of basal ganglia function in learning, memory and choice. *Behavioural Brain Research* 199:141-156.
- Cohen MX, Schoene-Bake J-C, Elger CE, Weber B (2009) Connectivity-based segregation of the human striatum predicts personality characteristics. *Nat Neurosci* 12:32-34.
- Comblain C, D'Argembeau A, Van der Linden M (2005) Phenomenal characteristics of autobiographical memories for emotional and neutral events in older and younger adult. *Experimental Aging Research* 31:173-189.
- Cools R, D'Esposito M (2011) Inverted-U Shaped Dopamine Actions on Human Working Memory and Cognitive Control. *Biological Psychiatry* 69:e113-e125.

- Cools R, Barker RA, Sahakian BJ, Robbins TW (2001) Enhanced or Impaired Cognitive Function in Parkinson's Disease as a Function of Dopaminergic Medication and Task Demands. *Cereb Cortex* 11:1136-1143.
- Cools R, Frank MJ, Gibbs SE, Miyakawa A, Jagust W, D'Esposito M (2009) Striatal Dopamine Predicts Outcome-Specific Reversal Learning and Its Sensitivity to Dopaminergic Drug Administration. *The Journal of Neuroscience* 29:1538-1543.
- Cox KM, Aizenstein HJ, Fiez JA (2008) Striatal outcome processing in healthy aging. *Cogn Affect Behav Neurosci* 8:304-317.
- Coxon JP, Van Impe A, Wenderoth N, Swinnen SP (2012) Aging and Inhibitory Control of Action: Cortico-Subthalamic Connection Strength Predicts Stopping Performance. *The Journal of Neuroscience* 32:8401-8412.
- Craik FIM, Rose NS (2012) Memory encoding and aging: A neurocognitive perspective. *Neuroscience & Biobehavioral Reviews* 36:1729-1739.
- D'Esposito M, Deouell LY, Gazzaley A (2003) Alterations in the BOLD fMRI signal with ageing and disease: a challenge for neuroimaging. *Nat Rev Neurosci* 4:863-872.
- Daw ND, Niv Y, Dayan P (2005) Uncertainty-based competition between prefrontal and dorsolateral striatal systems for behavioral control. *Nat Neurosci* 8:1704-1711.
- Daw ND, O'Doherty JP, Dayan P, Seymour B, Dolan RJ (2006) Cortical substrates for exploratory decisions in humans. *Nature* 441:876-879.

- Daw Nathaniel D, Gershman Samuel J, Seymour B, Dayan P, Dolan Raymond J (2011) Model-Based Influences on Humans' Choices and Striatal Prediction Errors. *Neuron* 69:1204-1215.
- Dayan P, Niv Y, Seymour B, Daw N (2006) The misbehavior of value and the discipline of the will. *Neural Networks* 19:1153-1160.
- de Wit S, Standing H, Devito E, Robinson O, Ridderinkhof K, Robbins T, Sahakian B (2012) Reliance on habits at the expense of goal-directed control following dopamine precursor depletion. *Psychopharmacology (Berl)* 219:621-631.
- Devinsky O, Morrell MJ, Vogt BA (1995) REVIEW ARTICLE: Contributions of anterior cingulate cortex to behaviour. *Brain* 118:279-306.
- Dickinson A, Smith J, Mirenowicz J (2000) Dissociation of Pavlovian and instrumental incentive learning under dopamine antagonists. *Behav Neurosci* 114:468-483.
- Dickinson A, & Balleine, B (2002) The role of learning in the operation of motivational systems, Third Edition. New York: John Wiley & Sons.
- Dormont D, Ricciardi KG, Tande D, Parain K, Menuel C, Galanaud D, Navarro S, Cornu P, Agid Y, Yelnik J (2004) Is the Subthalamic Nucleus Hypointense on T2-Weighted Images? A Correlation Study Using MR Imaging and Stereotactic Atlas Data. *AJNR Am J Neuroradiol* 25:1516-1523.
- Draganski B, Ashburner J, Hutton C, Kherif F, Frackowiak RSJ, Helms G, Weiskopf N (2011) Regional specificity of MRI contrast parameter changes in normal ageing revealed by voxel-based quantification (VBQ). *Neuroimage* 55:1423-1434.

- Duann J-R, Ide JS, Luo X, Li C-sR (2009) Functional Connectivity Delineates Distinct Roles of the Inferior Frontal Cortex and Presupplementary Motor Area in Stop Signal Inhibition. *The Journal of Neuroscience* 29:10171-10179.
- Duarte A, Graham KS, Henson RN (2010) Age-related changes in neural activity associated with familiarity, recollection and false recognition. *Neurobiology of Aging* 31:1814-1830.
- Düzel E, Schütze H, Yonelinas AP, Heinze H-J (2011) Functional phenotyping of successful aging in long-term memory: Preserved performance in the absence of neural compensation. *Hippocampus* 21:803-814.
- Düzel S, Schütze H, Stallforth S, Kaufmann J, Bodammer N, Bunzeck N, Munte TF, Lindenberger U, Heinze HJ, Düzel E (2008) A close relationship between verbal memory and SN/VTA integrity in young and older adults. *Neuropsychologia* 46:3042-3052.
- Düzel E, Bunzeck N, Guitart-Masip M, Düzel S (2009a) NOvelty-related Motivation of Anticipation and exploration by Dopamine (NOMAD): Implications for healthy aging. *Neurosci Biobehav Rev*.
- Düzel E, Bunzeck N, Guitart-Masip M, Düzel S (2010) NOvelty-related Motivation of Anticipation and exploration by Dopamine (NOMAD): Implications for healthy aging. *Neuroscience & Biobehavioral Reviews* 34:660-669.
- Düzel E, Bunzeck N, Guitart-Masip M, Wittmann B, Schott BH, Tobler PN (2009b) Functional imaging of the human dopaminergic midbrain. *Trends Neurosci* 32:321-328.

- Duzel S, Schutze H, Stallforth S, Kaufmann J, Bodammer N, Bunzeck N, Munte TF, Lindenberger U, Heinze HJ, Duzel E (2008) A close relationship between verbal memory and SN/VTA integrity in young and older adults. *Neuropsychologia* 46:3042-3052.
- Dyrby TB, Sogaard LV, Parker GJ, Alexander DC, Lind NM, BaarÃ© WFC, Hay-Schmidt A, Eriksen N, Pakkenberg B, Paulson OB, Jelsing J (2007) Validation of in vitro probabilistic tractography. *Neuroimage* 37:1267-1277.
- Eckert T, Sailer M, Kaufmann J, Schrader C, Peschel T, Bodammer N, Heinze H-J, Schoenfeld MA (2004) Differentiation of idiopathic Parkinson's disease, multiple system atrophy, progressive supranuclear palsy, and healthy controls using magnetization transfer imaging. *Neuroimage* 21:229-235.
- Eppinger B, Hammerer D, Li S-C (2011) Neuromodulation of reward-based learning and decision making in human aging. *Annals of the New York Academy of Sciences* 1235:1-17.
- Eppinger B, Kray J, Mock B, Mecklinger A (2008) Better or worse than expected? Aging, learning, and the ERN. *Neuropsychologia* 46:521-539.
- Erixon-Lindroth N, Farde L, Robins Wahlin T-B, Sovago J, Halldin C, Backman L (2005) The role of the striatal dopamine transporter in cognitive aging. *Psychiatry Research: Neuroimaging* 138:1-12.
- Esteviz-Gonzalez A, Kulisevsky J, Boltes A, Otermın P, Garcıa-Sanchez C (2003) Rey verbal learning test is a useful tool for differential diagnosis in the preclinical phase of Alzheimer's disease: comparison with mild

cognitive impairment and normal aging. *International Journal of Geriatric Psychiatry* 18:1021-1028.

Fearnley JM, Lees AJ (1991) Ageing and Parkinson's Disease: substantia nigra regional selectivity. *Brain* 114:2283-2301.

Fera F, Weickert TW, Goldberg TE, Tessitore A, Hariri A, Das S, Lee S, Zolnick B, Meeter M, Myers CE, Gluck MA, Weinberger DR, Mattay VS (2005) Neural Mechanisms Underlying Probabilistic Category Learning in Normal Aging. *The Journal of Neuroscience* 25:11340-11348.

Filippi M, Campi A, Dousset V, Baratti C, Martinelli V, Canal N, Scotti G, Comi G (1995) A Magnetization Transfer Imaging Study of Normal-Appearing White Matter in Multiple Sclerosis. *Neurology* 45:478-482.

Fischer R, Chalmers A (2008) Is optimism universal? A meta-analytical investigation of optimism levels across 22 nations. *Personality and Individual Differences* 45:378-382.

Fischl B, van der Kouwe A, Destrieux C, Halgren E, Ségonne F, Salat DH, Busa E, Seidman LJ, Goldstein J, Kennedy D, Caviness V, Makris N, Rosen B, Dale AM (2004) Automatically Parcellating the Human Cerebral Cortex. *Cerebral Cortex* 14:11-22.

Flandin G, Friston K (2008) *Statistical Parametric Mapping*.

Fleming SM, Thomas CL, Dolan RJ (2010) Overcoming status quo bias in the human brain. *Proceedings of the National Academy of Sciences* 107:6005-6009.

Floel A, Vomhof P, Lorenzen A, Roesser N, Breitenstein C, Knecht S (2008) Levodopa improves skilled hand functions in the elderly. *European Journal of Neuroscience* 27:1301-1307.

- Floresco SB, West AR, Ash B, Moore H, Grace AA (2003) Afferent modulation of dopamine neuron firing differentially regulates tonic and phasic dopamine transmission. *Nat Neurosci* 6:968-973.
- Flugel D, Cercignani M, Symms MR, Koepp MJ, Foong J (2006) A Magnetization Transfer Imaging Study in Patients with Temporal Lobe Epilepsy and Interictal Psychosis. *Biological Psychiatry* 59:560-567.
- Folstein MF, Folstein SE, McHugh PR (1975) "Mini-mental state" : A practical method for grading the cognitive state of patients for the clinician. *Journal of Psychiatric Research* 12:189-198.
- Forstmann BU, Tittgemeyer M, Wagenmakers E-J, Derrfuss J, Imperati D, Brown S (2011) The Speed-Accuracy Tradeoff in the Elderly Brain: A Structural Model-Based Approach. *The Journal of Neuroscience* 31:17242-17249.
- Forstmann BU, Keuken MC, Jahfari S, Bazin P-L, Neumann J, Schäfer A, Anwander A, Turner R (2012) Cortico-subthalamic white matter tract strength predicts interindividual efficacy in stopping a motor response. *Neuroimage* 60:370-375.
- Frank MJ, Kong L (2008) Learning to avoid in older age. *Psychology and Aging* 23:392-398.
- Frank MJ, Seeberger LC, O'Reilly RC (2004) By Carrot or by Stick: Cognitive Reinforcement Learning in Parkinsonism. *Science* 306:1940-1943.
- Frank MJ, Samanta J, Moustafa AA, Sherman SJ (2007) Hold Your Horses: Impulsivity, Deep Brain Stimulation, and Medication in Parkinsonism. *Science* 318:1309-1312.

- Frey U, Morris RGM (1997) Synaptic tagging and long-term potentiation. *Nature* 385:533-536.
- Friston K, Ashburner J, Kiebel S, Nicols T, Penny WD (2006) *Statistical Parametric Mapping: The Analysis of Functional Brain Images* 1st Edition: Academic Press Inc.
- Friston KJ, Dolan RJ (2010) Computational and dynamic models in neuroimaging. *Neuroimage* 52:752-765.
- Friston KJ, Stephan KE, Lund TE, Morcom A, Kiebel S (2005) Mixed-effects and fMRI studies. *Neuroimage* 24:244-252.
- Garavan H, Ross TJ, Stein EA (1999) Right hemispheric dominance of inhibitory control: An event-related functional MRI study. *Proceedings of the National Academy of Sciences* 96:8301-8306.
- Gardini S, Cloninger CR, Venneri A (2009) Individual differences in personality traits reflect structural variance in specific brain regions. *Brain Research Bulletin* 79:265-270.
- Giuliani NR, Drabant EM, Gross JJ (2011) Anterior cingulate cortex volume and emotion regulation: Is bigger better? *Biological Psychology* 86:379-382.
- Glover GH, Li TQ, Ress D (2000) Image-based method for retrospective correction of physiological motion effects in fMRI: RETROICOR. *Magn Reson Med* 44:162-167.
- Goldman-Rakic PS, Muly IEC, Williams GV (2000) D1 receptors in prefrontal cells and circuits. *Brain Research Reviews* 31:295-301.
- Good CD, Johnsrude IS, Ashburner J, Henson RNA, Friston KJ, Frackowiak RSJ (2001) A Voxel-Based Morphometric Study of Ageing in 465 Normal Adult Human Brains. *Neuroimage* 14:21-36.

- Gray JA, and McNaughton, M. (2000) The neuropsychology of anxiety: an inquiry into the function of the septohippocampal system, 2nd Edition: Oxford University Press.
- Grossmann I, Na J, Varnum MEW, Park DC, Kitayama S, Nisbett RE (2010) Reasoning about social conflicts improves into old age. *Proceedings of the National Academy of Sciences* 107:7246-7250.
- Guitart-Masip M, Huys QJM, Fuentemilla L, Dayan P, Duzel E, Dolan RJ (2012a) Go and no-go learning in reward and punishment: Interactions between affect and effect. *Neuroimage* 62:154-166.
- Guitart-Masip M, Chowdhury R, Sharot T, Dayan P, Duzel E, Dolan RJ (2012b) Action controls dopaminergic enhancement of reward representations. *Proceedings of the National Academy of Sciences* 109:7511-7516.
- Guitart-Masip M, Fuentemilla L, Bach DR, Huys QJM, Dayan P, Dolan RJ, Duzel E (2011) Action Dominates Valence in Anticipatory Representations in the Human Striatum and Dopaminergic Midbrain. *The Journal of Neuroscience* 31:7867-7875.
- Haber SN, Knutson B (2009) The Reward Circuit: Linking Primate Anatomy and Human Imaging. *Neuropsychopharmacology* 35:4-26.
- Haber SN, Fudge JL, McFarland NR (2000) Striatonigrostriatal Pathways in Primates Form an Ascending Spiral from the Shell to the Dorsolateral Striatum. *J Neurosci* 20:2369-2382.
- Hamani C, Saint-Cyr JA, Fraser J, Kaplitt M, Lozano AM (2004) The subthalamic nucleus in the context of movement disorders. *Brain* 127:4-20.

- Hanyu H, Asano T, Iwamoto T, Takasaki M, Shindo H, Abe K (2000) Magnetization Transfer Measurements of the Hippocampus in Patients with Alzheimer's Disease, Vascular Dementia, and Other Types of Dementia. *AJNR Am J Neuroradiol* 21:1235-1242.
- Hayasaka S, Phan KL, Liberzon I, Worsley KJ, Nichols TE (2004) Nonstationary cluster-size inference with random field and permutation methods. *Neuroimage* 22:676-687.
- Hayton T, Furby J, Smith K, Altmann D, Brenner R, Chataway J, Hughes R, Hunter K, Tozer D, Miller D, Kapoor R (2009) Grey matter magnetization transfer ratio independently correlates with neurological deficit in secondary progressive multiple sclerosis. *Journal of Neurology* 256:427-435.
- Head D, Buckner RL, Shimony JS, Williams LE, Akbudak E, Conturo TE, McAvoy M, Morris JC, Snyder AZ (2004) Differential Vulnerability of Anterior White Matter in Nondemented Aging with Minimal Acceleration in Dementia of the Alzheimer Type: Evidence from Diffusion Tensor Imaging. *Cerebral Cortex* 14:410-423.
- Hebb DO (1949) *The Organisation of Behaviour: A Neuropsychological Theory*: John Wiley and Sons.
- Hedden T, Gabrieli JDE (2004) Insights into the ageing mind: a view from cognitive neuroscience. *Nat Rev Neurosci* 5:87-96.
- Heeger DJ, Ress D (2002) What does fMRI tell us about neuronal activity? *Nat Rev Neurosci* 3:142-151.

- Helms G, Dathe H, Dechent P (2008a) Quantitative FLASH MRI at 3T using a rational approximation of the Ernst equation. *Magnetic Resonance in Medicine* 59:667-672.
- Helms G, Dathe H, Kallenberg K, Dechent P (2008b) High-resolution maps of magnetization transfer with inherent correction for RF inhomogeneity and T1 relaxation obtained from 3D FLASH MRI. *Magnetic Resonance in Medicine* 60:1396-1407.
- Helms G, Draganski B, Frackowiak R, Ashburner J, Weiskopf N (2009) Improved segmentation of deep brain grey matter structures using magnetization transfer (MT) parameter maps. *Neuroimage* 47:194-198.
- Henkelman RM, Stanisz GJ, Graham SJ (2001) Magnetization transfer in MRI: a review. *NMR in Biomedicine* 14:57-64.
- Huettel S (2004) *Functional Magnetic Resonance Imaging*, 2nd Edition: Sinauer Associates.
- Hutton C, Draganski B, Ashburner J, Weiskopf N (2009) A comparison between voxel-based cortical thickness and voxel-based morphometry in normal aging. *Neuroimage* 48:371-380.
- Huys QJM, Cools R, Gámez M, Friedel E, Heinz A, Dolan RJ, Dayan P (2011) Disentangling the Roles of Approach, Activation and Valence in Instrumental and Pavlovian Responding. *PLoS Comput Biol* 7:e1002028.
- Inoue M, Suhara T, Sudo Y, Okubo Y, Yasuno F, Kishimoto T, Yoshikawa K, Tanada S (2001) Age-related reduction of extrastriatal dopamine D2 receptor measured by PET. *Life Sciences* 69:1079-1084.
- Isaacowitz D (2005) Correlates of well-being in adulthood and old age: A tale of two optimisms *Journal of Research in Personality* 39:224-244.

- Isaacowitz DM, Blanchard-Fields F (2012) Linking Process and Outcome in the Study of Emotion and Aging. *Perspectives on Psychological Science* 7:3-17.
- Jahfari S, Waldorp L, van den Wildenberg WPM, Scholte HS, Ridderinkhof KR, Forstmann BU (2011) Effective Connectivity Reveals Important Roles for Both the Hyperdirect (Fronto-Subthalamic) and the Indirect (Fronto-Striatal-Pallidal) Fronto-Basal Ganglia Pathways during Response Inhibition. *The Journal of Neuroscience* 31:6891-6899.
- Johansen-Berg H (2010) Behavioural relevance of variation in white matter microstructure. *Current Opinion in Neurology* 23:351-358.
- Kaasinen V, Rinne JO (2002) Functional imaging studies of dopamine system and cognition in normal aging and Parkinson's disease. *Neuroscience & Biobehavioral Reviews* 26:785-793.
- Kakade S, Dayan P (2002) Dopamine: generalization and bonuses. *Neural Networks* 15:549-559.
- Kass R, Raftery A (1995) Bayes factors. *Journal of the American Statistical Association* 90.
- Kensinger EA, Schacter DL (2008) Neural Processes Supporting Young and Older Adults' Emotional Memories. *Journal of Cognitive Neuroscience* 20:1161-1173.
- Killiany R, Gomez-Isla T, Moss M, Kikinis R, Sandor T, Jolesz F, Tanzi R, Jones K, Hyman B, Albert M (2000) Use of structural magnetic resonance imaging to predict who will get Alzheimer's disease. *Ann Neurol* 47:430-439.

- Kimberg D, D'Esposito M, Farah M (1997) Effects of bromocriptine on human subjects depend on working memory capacity. *Neuroreport* 8:3581-3585.
- Klein A, Andersson J, Ardekani BA, Ashburner J, Avants B, Chiang M-C, Christensen GE, Collins DL, Gee J, Hellier P, Song JH, Jenkinson M, Lepage C, Rueckert D, Thompson P, Vercauteren T, Woods RP, Mann JJ, Parsey RV (2009) Evaluation of 14 nonlinear deformation algorithms applied to human brain MRI registration. *Neuroimage* 46:786-802.
- Klein JC, Behrens TEJ, Robson MD, Mackay CE, Higham DJ, Johansen-Berg H (2007) Connectivity-based parcellation of human cortex using diffusion MRI: Establishing reproducibility, validity and observer independence in BA 44/45 and SMA/pre-SMA. *Neuroimage* 34:204-211.
- Klistorner A, Chaganti J, Garrick R, Moffat K, Yiannikas C (2011) Magnetisation transfer ratio in optic neuritis is associated with axonal loss, but not with demyelination. *Neuroimage* 56:21-26.
- Knecht S, Breitenstein C, Bushuven S, Wailke S, Kamping S, Flöel A, Zwitserlood P, Ringelstein EB (2004) Levodopa: Faster and better word learning in normal humans. *Annals of Neurology* 56:20-26.
- Knutson B, Gibbs S (2007) Linking nucleus accumbens dopamine and blood oxygenation. *Psychopharmacology* 191:813-822.
- Koller W, Melamed E (2007) *Parkinson's disease and related disorders*: Elsevier.
- Koller WC, Rueda MG (1998) Mechanism of action of dopaminergic agents in Parkinson's disease. *Neurology* 50:S11-S14.

- Kravitz AV, Freeze BS, Parker PRL, Kay K, Thwin MT, Deisseroth K, Kreitzer AC (2010) Regulation of parkinsonian motor behaviours by optogenetic control of basal ganglia circuitry. *Nature* 466:622-626.
- Krebs RM, Schott BH, Duzel E (2009) Personality traits are differentially associated with patterns of reward and novelty processing in the human substantia nigra/ventral tegmental area. *Biol Psychiatry* 65:103-110.
- Krebs RM, Heipertz D, Schuetze H, Duzel E (2011) Novelty increases the mesolimbic functional connectivity of the substantia nigra/ventral tegmental area (SN/VTA) during reward anticipation: Evidence from high-resolution fMRI. *Neuroimage* 58:647-655.
- Lachman ME, Rocke C, Rosnick C, Ryff CD (2008) Realism and Illusion in Americans' Temporal Views of Their Life Satisfaction. *Psychological Science* 19:889-897.
- Lambert C, Zrinzo L, Nagy Z, Lutti A, Hariz M, Foltynie T, Draganski B, Ashburner J, Frackowiak R (2012) Confirmation of functional zones within the human subthalamic nucleus: Patterns of connectivity and sub-parcellation using diffusion weighted imaging. *Neuroimage* 60:83-94.
- Lau B, Glimcher PW (2005) Dynamic response-by-response models of matching behavior in rhesus monkeys. *J Exp Anal Behav* 84:555-579.
- Le Bihan D, Johansen-Berg H (2012) Diffusion MRI at 25: Exploring brain tissue structure and function. *Neuroimage* 61:324-341.
- Leclerc CM, Kensinger EA (2008) Age-related differences in medial prefrontal activation in response to emotional images. *Cogn Affect Behav Neurosci* 8:153-164.

- Lewis S (2012) Learning and memory: Dopamine boosts ageing memories. *Nat Rev Neurosci* 13:812-813.
- Lezak MD, Howieson DB, Loring DW, Hannay HJ, Fischer JS (2004) *Neuropsychological Assessment*, 4th Edition. Oxford: Oxford University Press.
- Li J, Daw ND (2011) Signals in Human Striatum Are Appropriate for Policy Update Rather than Value Prediction. *The Journal of Neuroscience* 31:5504-5511.
- Li S-C, Sikström S (2002) Integrative neurocomputational perspectives on cognitive aging, neuromodulation, and representation. *Neuroscience & Biobehavioral Reviews* 26:795-808.
- Li S-C, Naveh-Benjamin M, Lindenberger U (2005) Aging Neuromodulation Impairs Associative Binding. *Psychological Science* 16:445-450.
- Light LL (1991) Memory and Aging: Four Hypotheses in Search of Data. *Annual Review of Psychology* 42:333-376.
- Lisman J, Grace AA, Duzel E (2011) A neoHebbian framework for episodic memory; role of dopamine-dependent late LTP. *Trends in Neurosciences* 34:536-547.
- Lisman JE, Grace AA (2005) The Hippocampal-VTA Loop: Controlling the Entry of Information into Long-Term Memory. *Neuron* 46:703-713.
- Logothetis NK, Pauls J, Augath M, Trinath T, Oeltermann A (2001) Neurophysiological investigation of the basis of the fMRI signal. *Nature* 412:150-157.

- Luo AH, Tahsili-Fahadan P, Wise RA, Lupica CR, Aston-Jones G (2011) Linking Context with Reward: A Functional Circuit from Hippocampal CA3 to Ventral Tegmental Area. *Science* 333:353-357.
- Lutti A, Hutton C, Finsterbusch J, Helms G, Weiskopf N (2010) Optimization and validation of methods for mapping of the radiofrequency transmit field at 3T. *Magnetic Resonance in Medicine* 64:229-238.
- Marschner A, Mell T, Wartenburger I, Villringer A, Reischies FM, Heekeren HR (2005) Reward-based decision-making and aging. *Brain Research Bulletin* 67:382-390.
- Martin WRW (2009) Quantitative estimation of regional brain iron with magnetic resonance imaging. *Parkinsonism & Related Disorders* 15:S215-S218.
- Martin WRW, Wieler M, Gee M (2008) Midbrain iron content in early Parkinson disease. *Neurology* 70:1411-1417.
- Mather M, Carstensen LL (2003) Aging and Attentional Biases for Emotional Faces. *Psychological Science* 14:409-415.
- Mather M, Carstensen LL (2005) Aging and motivated cognition: the positivity effect in attention and memory. *Trends in Cognitive Sciences* 9:496-502.
- McKenzie S, Eichenbaum H (2011) Consolidation and Reconsolidation: Two Lives of Memories? *Neuron* 71:224-233.
- Mell T, Heekeren HR, Marschner A, Wartenburger I, Villringer A, Reischies FM (2005) Effect of aging on stimulus-reward association learning. *Neuropsychologia* 43:554-563.
- Mell T, Wartenburger I, Marschner A, Villringer A, Reischies FM, Heekeren HR (2009) Altered function of ventral striatum during reward-based decision making in old age. *Frontiers in Human Neuroscience* 3.

- Missale C, Nash SR, Robinson SW, Jaber M, Caron MG (1998) Dopamine Receptors: From Structure to Function. *Physiol Rev* 78:189-225.
- Mohr PNC, Li S-C, Heekeren HR (2010) Neuroeconomics and aging: Neuromodulation of economic decision making in old age. *Neuroscience & Biobehavioral Reviews* 34:678-688.
- Monte-Silva K, Liebetanz D, Grundey J, Paulus W, Nitsche MA (2010) Dosage-dependent non-linear effect of l-dopa on human motor cortex plasticity. *The Journal of Physiology* 588:3415-3424.
- Morcom AM, Good CD, Frackowiak RSJ, Rugg MD (2003) Age effects on the neural correlates of successful memory encoding. *Brain* 126:213-229.
- Morcom AM, Bullmore ET, Huppert FA, Lennox B, Praseedom A, Linnington H, Fletcher PC (2009) Memory Encoding and Dopamine in the Aging Brain: A Psychopharmacological Neuroimaging Study. *Cereb Cortex*:bhp139.
- Nader K, Hardt O (2009) A single standard for memory: the case for reconsolidation. *Nat Rev Neurosci* 10:224-234.
- Nagy Z, Weiskopf N, Alexander DC, Deichmann R (2007) A method for improving the performance of gradient systems for diffusion-weighted MRI. *Magnetic Resonance in Medicine* 58:763-768.
- Naneix F, Marchand AR, Di Scala G, Pape J-Rm, Coutureau E (2012) Parallel Maturation of Goal-Directed Behavior and Dopaminergic Systems during Adolescence. *The Journal of Neuroscience* 32:16223-16232.
- Nelson HE (1982) National Adult Reading Test: Test Manual: Windsor.
- Nicola SM, Surmeier DJ, Malenka RC (2000) Dopaminergic Modulation of Neuronal Excitability in the Striatum and Nucleus Accumbens. *Annual Review of Neuroscience* 23:185-215.

- Niv Y, Daw N, Joel D, Dayan P (2007) Tonic dopamine: opportunity costs and the control of response vigor. *Psychopharmacology* 191:507-520.
- Nutt JG (2008) Pharmacokinetics and pharmacodynamics of levodopa. *Movement Disorders* 23:S580-S584.
- Nyberg L, Lovden M, Riklund K, Lindenberger U, Backman L (2012) Memory aging and brain maintenance. *Trends in Cognitive Sciences* 16:292-305.
- O'Carroll CM, Martin SJ, Sandin J, Frenguelli B, Morris RGM (2006) Dopaminergic modulation of the persistence of one-trial hippocampus-dependent memory. *Learning & Memory* 13:760-769.
- O'Doherty J, Dayan P, Schultz J, Deichmann R, Friston K, Dolan RJ (2004) Dissociable Roles of Ventral and Dorsal Striatum in Instrumental Conditioning. *Science* 304:452-454.
- O'Doherty JP, Hampton A, Kim H (2007) Model-Based fMRI and Its Application to Reward Learning and Decision Making. *Annals of the New York Academy of Sciences* 1104:35-53.
- O'Doherty JP, Dayan P, Friston K, Critchley H, Dolan RJ (2003) Temporal Difference Models and Reward-Related Learning in the Human Brain. *Neuron* 38:329-337.
- Ochsner KN, Gross JJ (2005) The cognitive control of emotion. *Trends in Cognitive Sciences* 9:242-249.
- Ogawa S, Lee TM, Kay AR, Tank DW (1990) Brain magnetic resonance imaging with contrast dependent on blood oxygenation. *Proceedings of the National Academy of Sciences* 87:9868-9872.
- Ogawa S, Tank DW, Menon R, Ellermann JM, Kim SG, Merkle H, Ugurbil K (1992) Intrinsic signal changes accompanying sensory stimulation:

functional brain mapping with magnetic resonance imaging. *Proceedings of the National Academy of Sciences* 89:5951-5955.

Pessiglione M, Seymour B, Flandin G, Dolan RJ, Frith CD (2006) Dopamine-dependent prediction errors underpin reward-seeking behaviour in humans. *Nature* 442:1042-1045.

Petersen RC, Thomas RG, Grundman M, Bennett D, Doody R, Ferris S, Galasko D, Jin S, Kaye J, Levey A, Pfeiffer E, Sano M, van Dyck CH, Thal LJ (2005) Vitamin E and Donepezil for the Treatment of Mild Cognitive Impairment. *New England Journal of Medicine* 352:2379-2388.

Picciotto Marina R, Higley Michael J, Mineur Yann S (2012) Acetylcholine as a Neuromodulator: Cholinergic Signaling Shapes Nervous System Function and Behavior. *Neuron* 76:116-129.

Pizzagalli DA (2011) Frontocingulate Dysfunction in Depression: Toward Biomarkers of Treatment Response. *Neuropsychopharmacology* 36:183-206.

Randy L B (2004) Memory and Executive Function in Aging and AD: Multiple Factors that Cause Decline and Reserve Factors that Compensate. *Neuron* 44:195-208.

Raz N, Rodrigue KM (2006) Differential aging of the brain: Patterns, cognitive correlates and modifiers. *Neuroscience & Biobehavioral Reviews* 30:730-748.

Raz N, Rodrigue KM, Kennedy KM, Head D, Gunning-Dixon F, Acker JD (2003) Differential Aging of the Human Striatum: Longitudinal Evidence. *American Journal of Neuroradiology* 24:1849-1856.

- Redondo RL, Morris RGM (2011) Making memories last: the synaptic tagging and capture hypothesis. *Nat Rev Neurosci* 12:17-30.
- Reese TG, Heid O, Weisskoff RM, Wedeen VJ (2003) Reduction of eddy-current-induced distortion in diffusion MRI using a twice-refocused spin echo. *Magnetic Resonance in Medicine* 49:177-182.
- Reitan RM (1955) The relation of the trail making test to organic brain damage. *J Consult Psychol* 19:393-394.
- Rescorla RA, Wagner AD (1972) A theory of Pavlovian conditioning: variations in the effectiveness of reinforcement and nonreinforcement: Appleton-Century-Crofts.
- Reuter-Lorenz PA, Lustig C (2005) Brain aging: reorganizing discoveries about the aging mind. *Current Opinion in Neurobiology* 15:245-251.
- Ridha BH, Tozer DJ, Symms MR, Stockton KC, Lewis EB, Siddique MM, MacManus DG, Rossor MN, Fox NC, Tofts PS (2007) Quantitative Magnetization Transfer Imaging in Alzheimer Disease¹. *Radiology* 244:832-837.
- Rieckmann A, Karlsson S, Karlsson P, Brehmer Y, Fischer Hk, Farde L, Nyberg L, Bäckman L (2011) Dopamine D1 Receptor Associations within and between Dopaminergic Pathways in Younger and Elderly Adults: Links to Cognitive Performance. *Cerebral Cortex*.
- Robbins TW, Arnsten AFT (2009) The Neuropsychopharmacology of Fronto-Executive Function: Monoaminergic Modulation. *Annual Review of Neuroscience* 32:267-287.
- Rorden C BM (2000) Stereotaxic display of brain lesions. *Behavioral Neurology* 12:191-200.

- Rowe JW, Kahn RL (1987) Human aging: usual and successful. *Science* 237:143-149.
- Rutledge RB, Lazzaro SC, Lau B, Myers CE, Gluck MA, Glimcher PW (2009) Dopaminergic Drugs Modulate Learning Rates and Perseveration in Parkinson's Patients in a Dynamic Foraging Task. *The Journal of Neuroscience* 29:15104-15114.
- Sahakian B, Morein-Zamir S (2007) Professor's little helper. *Nature* 450:1157-1159.
- Salamone JD, Correa M, Mingote SM, Weber SM (2005) Beyond the reward hypothesis: alternative functions of nucleus accumbens dopamine. *Current Opinion in Pharmacology* 5:34-41.
- Salloway S, Ferris S, Kluger A, Goldman R, Griesing T, Kumar D, Richardson S, Group FT (2004) Efficacy of donepezil in mild cognitive impairment. *Neurology* 63:651-657.
- Samanez-Larkin GR, Carstensen LL (2011) *Socioemotional functioning and the aging brain*. New York: Oxford University Press.
- Samanez-Larkin GR, Wagner AD, Knutson B (2011) Expected value information improves financial risk taking across the adult life span. *Social Cognitive and Affective Neuroscience* 6:207-217.
- Samanez-Larkin GR, Kuhnen CM, Yoo DJ, Knutson B (2010) Variability in Nucleus Accumbens Activity Mediates Age-Related Suboptimal Financial Risk Taking. *J Neurosci* 30:1426-1434.
- Samanez-Larkin GR, Levens SM, Perry LM, Dougherty RF, Knutson B (2012) Frontostriatal White Matter Integrity Mediates Adult Age Differences in

Probabilistic Reward Learning. *The Journal of Neuroscience* 32:5333-5337.

Samanez-Larkin GR, Gibbs SE, Khanna K, Nielsen L, Carstensen LL, Knutson B (2007) Anticipation of monetary gain but not loss in healthy older adults. *Nat Neurosci* 10:787-791.

Scatton B, Simon H, Le Moal M, Bischoff S (1980) Origin of dopaminergic innervation of the rat hippocampal formation. *Neuroscience Letters* 18:125-131.

Scheier MF, Carver CS (1993) On the Power of Positive Thinking: The Benefits of Being Optimistic. *Current Directions in Psychological Science* 2:26-30.

Scheier MF, Carver CS, Bridges MW (1994) Distinguishing optimism from neuroticism (and trait anxiety, self-mastery, and self-esteem): A reevaluation of the Life Orientation Test. *Journal of Personality and Social Psychology* 67:1063-1078.

Schonberg T, Daw ND, Joel D, O'Doherty JP (2007) Reinforcement Learning Signals in the Human Striatum Distinguish Learners from Nonlearners during Reward-Based Decision Making. *The Journal of Neuroscience* 27:12860-12867.

Schott BH, Niehaus L, Wittmann BC, Schutze H, Seidenbecher CI, Heinze HJ, Duzel E (2007) Ageing and early-stage Parkinson's disease affect separable neural mechanisms of mesolimbic reward processing. *Brain* 130:2412-2424.

Schultz W (1998) Predictive Reward Signal of Dopamine Neurons. *Journal of Neurophysiology* 80:1-27.

- Schultz W, Dayan P, Montague PR (1997) A neural substrate of prediction and reward. *Science* 275:1593-1599.
- Schwarzkopf DS, de Haas B, Rees G (2012) Better ways to improve standards in brain-behavior correlation analysis. *Frontiers in Human Neuroscience* 6.
- Seehaus AK, Roebroek A, Chiry O, Kim D-S, Ronen I, Bratzke Hr, Goebel R, Galuske RAW (2012) Histological Validation of DW-MRI Tractography in Human Postmortem Tissue. *Cerebral Cortex*.
- Sharot T, Korn CW, Dolan RJ (2011) How unrealistic optimism is maintained in the face of reality. *Nat Neurosci* 14:1475-1479.
- Sharot T, Riccardi AM, Raio CM, Phelps EA (2007) Neural mechanisms mediating optimism bias. *Nature* 450:102-105.
- Sharot T, Guitart-Masip M, Korn Christoph W, Chowdhury R, Dolan Raymond J (2012a) How Dopamine Enhances an Optimism Bias in Humans. *Current Biology* 22:1477-1481.
- Sharot T, Kanai R, Marston D, Korn CW, Rees G, Dolan RJ (2012b) Selectively altering belief formation in the human brain. *Proceedings of the National Academy of Sciences* 109:17058-17062.
- Shohamy D, Adcock RA (2010) Dopamine and adaptive memory. *Trends in Cognitive Sciences* 14:464-472.
- Simon DA, Daw ND (2011) Neural Correlates of Forward Planning in a Spatial Decision Task in Humans. *The Journal of Neuroscience* 31:5526-5539.
- Small SA, Schobel SA, Buxton RB, Witter MP, Barnes CA (2011) A pathophysiological framework of hippocampal dysfunction in ageing and disease. *Nat Rev Neurosci* 12:585-601.

- Smith WB, Starck SR, Roberts RW, Schuman EM (2005) Dopaminergic Stimulation of Local Protein Synthesis Enhances Surface Expression of GluR1 and Synaptic Transmission in Hippocampal Neurons. *Neuron* 45:765-779.
- Stanislaw H, N. T (1999) Calculation of signal detection theory measures. *Behav Res Methods Instrum Comput* 31:137-149.
- Stone AA, Schwartz JE, Broderick JE, Deaton A (2010) A snapshot of the age distribution of psychological well-being in the United States. *Proceedings of the National Academy of Sciences* 107:9985-9990.
- Strunk DR, Lopez H, DeRubeis RJ (2006) Depressive symptoms are associated with unrealistic negative predictions of future life events. *Behaviour Research and Therapy* 44:861-882.
- Sutton RS, Barton AG (1998) *Reinforcement Learning: An Introduction*. Cambridge, MA: MIT Press.
- Swann NC, Cai W, Conner CR, Pieters TA, Claffey MP, George JS, Aron AR, Tandon N (2012) Roles for the pre-supplementary motor area and the right inferior frontal gyrus in stopping action: Electrophysiological responses and functional and structural connectivity. *Neuroimage* 59:2860-2870.
- Takahashi H, Kato M, Hayashi M, Okubo Y, Takano A, Ito H, Suhara T (2007) Memory and frontal lobe functions; possible relations with dopamine D2 receptors in the hippocampus. *Neuroimage* 34:1643-1649.
- Takahashi H, Kato M, Takano H, Arakawa R, Okumura M, Otsuka T, Kodaka F, Hayashi M, Okubo Y, Ito H, Suhara T (2008) Differential Contributions of

- Prefrontal and Hippocampal Dopamine D1 and D2 Receptors in Human Cognitive Functions. *The Journal of Neuroscience* 28:12032-12038.
- Tambasco N, Belcastro V, Sarchielli P, Floridi P, Pierguidi L, Menichetti C, Castrioto A, Chiarini P, Parnetti L, Eusebi P, Calabresi P, Rossi A (2011) A magnetization transfer study of mild and advanced Parkinson's disease. *European Journal of Neurology* 18:471-477.
- Thirugnanasambandam N, Grundey J, Paulus W, Nitsche MA (2011) Dose-Dependent Nonlinear Effect of L-DOPA on Paired Associative Stimulation-Induced Neuroplasticity in Humans. *The Journal of Neuroscience* 31:5294-5299.
- Tofts P (2003) *Quantitative MRI of the Brain: Measuring Changes Caused by Disease* Wiley.
- Tulving E (1985) Memory and consciousness. *Canadian Psychology* 26:1-12.
- Tzourio-Mazoyer N, Landeau B, Papathanassiou D, Crivello F, Etard O, Delcroix N, Mazoyer B, Joliot M (2002) Automated Anatomical Labeling of Activations in SPM Using a Macroscopic Anatomical Parcellation of the MNI MRI Single-Subject Brain. *Neuroimage* 15:273-289.
- Vaillancourt DE, Spraker MB, Prodoehl J, Zhou XJ, Little DM (2012) Effects of aging on the ventral and dorsal substantia nigra using diffusion tensor imaging. *Neurobiology of Aging* 33:35-42.
- Van Petten C (2004) Relationship between hippocampal volume and memory ability in healthy individuals across the lifespan: review and meta-analysis. *Neuropsychologia* 42:1394-1413.
- Vasic N, Walter H, Hose A, Wolf RC (2008) Gray matter reduction associated with psychopathology and cognitive dysfunction in unipolar depression: A

- voxel-based morphometry study. *Journal of Affective Disorders* 109:107-116.
- Volkow ND, Wang GJ, Fowler JS, Tomasi D, Baler R (2012) Food and Drug Reward: Overlapping Circuits in Human Obesity and Addiction. *Current Topics in Behavioral Neurosciences* 11:1-24.
- Volkow ND, Logan J, Fowler JS, Wang G-J, Gur RC, Wong C, Felder C, Gatley SJ, Ding Y-S, Hitzemann R, Pappas N (2000) Association Between Age-Related Decline in Brain Dopamine Activity and Impairment in Frontal and Cingulate Metabolism. *Am J Psychiatry* 157:75-80.
- Wang S-H, Morris RGM (2010) Hippocampal-Neocortical Interactions in Memory Formation, Consolidation, and Reconsolidation. *Annual Review of Psychology* 61:49-79.
- Warrington E, James M (1991) *The Visual Object and Space Perception Battery*. Suffolk, England: Thames Valley Test Company.
- Weiskopf N, Hutton C, Josephs O, Deichmann R (2006a) Optimal EPI parameters for reduction of susceptibility-induced BOLD sensitivity losses: a whole-brain analysis at 3 T and 1.5 T. *Neuroimage* 33:493-504.
- Weiskopf N, Hutton C, Josephs O, Deichmann R (2006b) Optimal EPI parameters for reduction of susceptibility-induced BOLD sensitivity losses: A whole-brain analysis at 3 T and 1.5 T. *Neuroimage* 33:493-504.
- Williams GV, Goldman-Rakic PS (1995) Modulation of memory fields by dopamine D1 receptors in prefrontal cortex. *Nature* 376:572-575.
- Wittmann BC, Daw ND, Seymour B, Dolan RJ (2008) Striatal Activity Underlies Novelty-Based Choice in Humans. *Neuron* 58:967-973.

- Wittmann BC, Schott BH, Guderian S, Frey JU, Heinze HJ, Duzel E (2005) Reward-related fMRI activation of dopaminergic midbrain is associated with enhanced hippocampus-dependent long-term memory formation. *Neuron* 45:459-467.
- Wolff SD, Balaban RS (1989) Magnetization transfer contrast (MTC) and tissue water proton relaxation in vivo. *Magnetic Resonance in Medicine* 10:135-144.
- Worthy DA, Gorlick MA, Pacheco JL, Schnyer DM, Maddox WT (2011) With Age Comes Wisdom. *Psychological Science* 22:1375-1380.
- Wunderlich K, Smittenaar P, Dolan Raymond J (2012) Dopamine Enhances Model-Based over Model-Free Choice Behavior. *Neuron* 75:418-424.
- Yesavage J, Brink T, Rose T, Lum O, Huang V, Adey M, Leirer V (1982) Development and validation of a geriatric depression screening scale: a preliminary report. *J Psychiatr Res* 17:37-49.
- Yonelinas AP (2002) The Nature of Recollection and Familiarity: A Review of 30 Years of Research. *Journal of Memory and Language* 46:441-517.
- Yonelinas AP, Kroll NEA, Quamme JR, Lazzara MM, Sauve M-J, Widaman KF, Knight RT (2002) Effects of extensive temporal lobe damage or mild hypoxia on recollection and familiarity. *Nat Neurosci* 5:1236-1241.
- Yushkevich PA, Piven J, Hazlett HC, Smith RG, Ho S, Gee JC, Gerig G (2006) User-guided 3D active contour segmentation of anatomical structures: Significantly improved efficiency and reliability. *Neuroimage* 31:1116-1128.
- Zald DH, Cowan RL, Riccardi P, Baldwin RM, Ansari MS, Li R, Shelby ES, Smith CE, McHugo M, Kessler RM (2008) Midbrain Dopamine Receptor

Availability Is Inversely Associated with Novelty-Seeking Traits in Humans. *The Journal of Neuroscience* 28:14372-14378.

Zappia M, Crescibene L, Arabia G, Nicoletti G, Bagala A, Bastone L, Caracciolo M, Bonavita S, Di Costanzo A, Scornaienchi M, Gambardella A, Quattrone A (2002) Body Weight Influences Pharmacokinetics of Levodopa in Parkinson's Disease. *Clinical Neuropharmacology* March/April 25:79-82.

Zheng D, Oka T, Bokura H, Yamaguchi S (2008) The Key Locus of Common Response Inhibition Network for No-go and Stop Signals. *Journal of Cognitive Neuroscience* 20:1434-1442.